Old and Young. Can they coexist?

Oud en Jong. Kunnen ze samen voorkomen?
(met een samenvatting in het Nederlands)

PROEFSCHRIFT

ter verkrijging van de graad van doctor aan de Universiteit Utrecht, op gezag van de Rector Magnificus, Prof.dr. W. H. Gispen, ingevolge het besluit van het College voor Promoties in het openbaar te verdedigen op woensdag 14 januari 2004 des middags te 12.45 uur

door

Natalia Victorovna Davydova

geboren op 30 september 1975 te Moskou, Rusland

Promotor: Prof.dr. O. Diekmann

Faculteit der Wiskunde en Informatica
Universiteit Utrecht

On the front cover one can see cartoons illustrating competition between age classes: cannibalism as an example of high sensitivity of the young and large impact of the old; and high sensitivity of the old to the lack of the resource. On the back cover there are numerical bifurcation diagrams discussed in detail in Section 5.8.

Printed in The Netherlands by PrintPartners Ipskamp.

ISBN: 90-393-3592-3

Mathematics Subject Classification (2000) : 92D25, 37N25, 37E05 (Ch. 5)

We struggle with complexities
and avoid simplicities.

Norman Vincent Peale

Contents

Chapter 1

Introduction

Have you ever seen this relation, dear Reader?

$$x_{n+1} = \lambda\, x_n\, (1 - x_n).$$

I doubt no minute that the answer is *Yes*. One of you would call it *logistic equation*, another the *quadratic family*. In any case you recognize if not a basic stone, then a picturesque tower of the Nonlinear Dynamics castle. In the tower you follow staircases ending by cobwebs, simple, spiraling to a center or keeping winding around you or so tangled that many travelers got into them trying to understand the structure. From the tower you see cascades of doublings entering chaos, still magic and attracting, and only really devoted knights could understand the notion of it. This tower is situated near the gates leading to the land of Population Dynamics. Part of it was even built by people coming from this area for their own purposes [May & Oster], but most of it by inhabitants of the castle which are from the Kingdom of Mathematics.

Why have I begun with this fairy–tale, Reader? A fact is that I too was caught by the beauty of the dynamics produced by the above and similar relations. And the appearance of Chapter 5 is mostly due to this fact. In other words Nonlinear Dynamics and its attractions served as one of the two substrates for an exothermic reaction which warmed my interest. Another ingredient was the desire to capture infinitely dimensional, multi–level complicated Nature in the know–how–to–deal–with language of mathematics and then back, with the aid of simple (well, sometimes...) calculations to organize the picture, which Nature shows us, and possibly to find hidden aspects of it.

But now, after this short prelude, let me be consistent. My story is not about the logistic equation. It serves as a symbol and it was indeed one of the first models of Population Dynamics. Now I want to discuss a main goal and a main object of this work. The questions were

- how to introduce an age structure in a discrete model of population dynamics;
- which difference does it make for the dynamics.

The simplest possible way was to divide a population into cohorts: *old and young.* Then a question arose (which became a title to this thesis)

WHETHER A COEXISTENCE IS POSSIBLE OF OLD AND YOUNG.

The problem of *Parents and Children* appeared to be relevant in the animal world as well as for humans. Though I speak about coexistence of old and young, we consider two cohorts only in Chapter 3 of the thesis. In the rest of the thesis the number of cohorts varies. Whenever possible we keep it general $k \in \mathbb{Z},\ k \geq 2$.

Let me mention also a third source of energy which feeds an interest of a researcher. It is indeed a puzzle, an open question. Such a source of inspiration became for us *cicada.* Magicicada intrigues scientists for more than fifty years, and the last thirty years not only biologists but also mathematicians struggle with this phenomenon. Magicicada are known by their rare, sudden and perfectly synchronized emergences in huge numbers. But what is especially unusual is that these emergences occur once in thirteen or seventeen years. These large prime numbers attracted much attention, but still there is no satisfactory explanation for this fact. In the last Chapter 6 of this thesis I try to solve the riddle. And I believe that age-structured competition models can help with this.

The rest of this introduction is divided into sections. In Section 1.1 we introduce the main object of this work. We build up an age-structured discrete-time model for population dynamics of semelparous species. A short interlude within this section is devoted especially to the notion of an environmental variable. In Section 1.2 we summarize results and give their interpretation. In Section 1.3 we discuss models for prime cicada periods.

1.1 What is it all about? The model formulation.

The largest part of this thesis (apart from the last chapter) is devoted to analysis of the same model. So I have decided to introduce it here. This is a model of semelparous species dynamics. *Semelparous species are those whose individuals reproduce only once in their lives and die afterwards.* Examples are annual and biennial plants, fishes (salmon), many insects.

If reproduction is restricted to a small time window in the year and life span has a fixed length of, say, k years, a population splits into year classes according to the year of birth (counted modulo k) or, equivalently, the year of reproduction $(\bmod k)$. (Note the terminology: an individual belongs to the same *year class* throughout its life, whereas the *age class* to which it

belongs is determined by its age and therefore increases by one each year.) As a year class is reproductively isolated from the other year classes, it forms a population by itself.

Yet year classes are likely to interact, for instance by competition for food. It may then happen that a year class is driven to extinction. Bulmer [Bulmer] calls an insect *periodical* if it consists of a single year class, i.e. if all but one year classes are missing. Famous example is the cicada species with 13 and 17 year life cycles.

We shall describe interaction (i.e. density dependence) as *feedback via the environment* (see below *Interlude about the environmental variable* and [DGHKMT, DGM] for the general philosophy). The phenomenon of periodical insects then leads to the following questions in the context of a model: *can one year class tune the environmental conditions such that the other year classes are driven to extinction when rare? Or can missing year classes invade successfully? Do we get coexistence or competitive exclusion?*

Let us begin the modelling procedure from the most important event in the life of a semelparous individual: from a reproduction of adults and a birth of the youngest. We assume that *a year ends by the reproduction event.* Let $N_k(t)$ be the number of adults (k-years old individuals) in the end of year t. If $E(t)$ is the average number of eggs per individual, $E(t)\,N_k(t)$ will be eggs produced. Let $p_e(t)$ be the probability for an egg to survive and to hatch. Both E and p_e can vary from year to year. Then the number of newborns $N_0(t+1)$ *in the beginning of year* $t+1$ is

$$N_0(t+1) = p_e(t)\,E(t)\,N_k(t).$$

On the other hand the number $N_k(t)$ is determined by the number of $(k-1)$-years old individuals N_{k-1} in the beginning of the year t

$$N_k(t) = p_{k-1}(t)\,N_{k-1}(t),$$

where $p_{k-1}(t)$ is the survival probability of a $(k-1)$-year old individual during the year t. Finally,

$$N_0(t+1) = N_{k-1}(t)\,h_{k-1}(t) \tag{1.1}$$

with

$$h_{k-1}(t) = p_{k-1}(t)\,p_e(t)\,E(t),$$

i.e. $h_{k-1}(t)$ is the *expected number of offspring* of a $(k-1)$-year old individual *after one year.*

The equation (1.1) is the most difficult to derive in our model. And misinterpretations of it are, unfortunately, rather common. That is why we

explained it in detail. The other equations are simple to interpret:

$$N_{i+1}(t+1) = h_i(t)\, N_i(t), \qquad i = 0, ..., k-2 \tag{1.2}$$

The quantity $N_i(t)$ is the number of i-years old individuals in the beginning of a year t and $h_i(t)$ is a survival probability during this year.

For shortness we can rewrite relations (1.1) and (1.2) as a k-dimensional recursion:

$$N(t+1) = L(h(t))N(t) \tag{1.3}$$

with vectors $N = (N_0, ..., N_{k-1})^T$ and $h = (h_0, ..., h_{k-1})^T$. We use $L(h)$ to denote the Leslie matrix corresponding to h. So, explicitly, we have

$$L(h) = \begin{pmatrix} 0 & 0 & ... & 0 & h_{k-1} \\ h_0 & 0 & ... & 0 & 0 \\ 0 & h_1 & ... & 0 & 0 \\ ... & & & & \\ 0 & 0 & ... & h_{k-2} & 0 \end{pmatrix}.$$

Now we concentrate on the vector $h(t)$. A first wish is to make it independent of time, i.e., to assume that the expected number of offspring and the survival probabilities do not change. Then the recursion relation (1.3) becomes *linear*. This case is trivial. It is considered in Section 2.2 of this thesis.

In principle, the dependence of h on time t can be arbitrary; in fact, $h(t)$ can be a random variable. But in this work we prefer to deal with *an autonomous system*. This means that h does not directly depend on time, but rather it depends on $N(t)$, i.e., we assume

$$h(t) = \hat{h}(N(t)).$$

So, we should provide a feedback from the phase variables N to themselves. This is probably the most interesting part of the modelling procedure.

Interlude about the environmental variable.

This approach was proposed by a group of people in [DGHKMT, DGM] where it is explained in detail. Here I try to give an idea of what is an *environmental variable*.

Any population consists of individuals. We *define the environment so that all individuals are independent from one another when the environment is prescribed*. For example, if there is competition between plants for nutrients, then the environment at some moment in time is fully determined by the

amount of the nutrients available at that time. The population then consists of individuals who have no *direct* influence on each other. Yet, since plants consume the nutrients, they do interact by feedback to the environmental variable which is in this case the amount of nutrients available.

We denote an environmental variable by the symbol I. The letter "I" stems from the word "input" and means environmental input to behaviour of individuals. In the above example I is a scalar quantity. But it is not always the case, for plants we can consider light as a second environmental variable, water as a third etc.

Each scalar component of the environmental variable is *a linear combination of population numbers* $I = \sum c_i N_i$ (or a linear functional of densities). We emphasize that it is *not* an assumption. As individuals are independent in a given environment, their *impacts on the environment are also independent.* So that the environmental variable is a sum of all impacts. We divide a population into classes where individuals have the same impact. Then I is a weighted sum of the numbers of individuals in all classes, and the weights c_i are the impacts. Also note that many earlier authors [Silva & Hallam, Wikan, Bergh, Cushing & Li] introduced density dependence in their models by way of weighted population numbers.

We explain with the aid of the plant example what impact is. Higher plants have a larger impact on the light variable than lower ones. Plants with larger roots have a larger impact on water and nutrients variables. Etc.

Different classes differ not only by impacts on the environment but also by their *sensitivity* to the environment. The notion of sensitivity is much less well-defined than the notion of impact. I try to describe here my own understanding. Again revisiting the plant example, a lack of water can kill some plants in a couple of days while our office plants can stay without water two to three weeks and even then they do not show that they are suffering.

The term "sensitivity" is already used in the literature on matrix population models [Caswell]. The sensitivity of a quantity $f(x)$ to x is just the derivative $f'(x)$. But it is more convenient for our purposes to call the functions $h_i(I)$ *sensitivity functions.* This reflects the fact that the survival probabilities and/or fecundity depend on the environment or, in other words, they are *sensitive* to the environment.

This is all right but we want sensitivity to be a parameter (as in the case of impact), not a function. In some cases this is possible. For example, if the sensitivity functions $h_i(I)$ belong to the same family of functions $\sigma H(gI)$ with g as a parameter and different population classes have different parameters g, we can call g as sensitivity of a population class to the environment (the parameter σ is of minor importance and can be scaled out).

Summarizing this interlude, we will use the notion of the environmental variable to make a feedback from phase variables N, which are age class numbers, to themselves. We assume that the age classes differ by their impact on, and sensitivity to, the environment. In addition, and this is a very restrictive assumption, we assume that I *is one-dimensional* in our case. One can interpret this as a *competition for one resource.* Finally,

$$I = \sum_{i=0}^{k-1} c_i N_i$$

and for $i = 0, ..., k-1$

$$h_i(t) = \tilde{h}_i(I(N(t))).$$

Whenever useful, we shall choose the functions $h_i(I)$ from the same two–parameter family, i.e.

$$\tilde{h}_i(I) = \sigma_i \, H(g_i I) \tag{1.4}$$

(for a more precise formulation see Section 2.3), but we do not put this restriction generally in our model. If we need some particular form of function, we use one of our favorites: exponential function (or, Ricker type of) density dependence:

$$h_i(I) = \sigma_i \, e^{-g_i I} \tag{1.5}$$

or Beverton-Holt density dependence

$$h_i(I) = \sigma_i \, \frac{1}{1 + g_i I}. \tag{1.6}$$

We call a parameter g_i *sensitivity* of the i-th age class to the environment.

Now, omiting tildes, I rewrite the *autonomous discrete-time age-structured model for semelparous species dynamics with one-dimensional environmental variable.*

$$N(t+1) = L\Big(h(I(t))\Big) \; N(t) \tag{1.7}$$

with

$$L(h) = \begin{pmatrix} 0 & 0 & ... & 0 & h_{k-1} \\ h_0 & 0 & ... & 0 & 0 \\ 0 & h_1 & ... & 0 & 0 \\ ... & & & & \\ 0 & 0 & ... & h_{k-2} & 0 \end{pmatrix}.$$

and

$$I = c \cdot N \tag{1.8}$$

with the impact vector $c = (c_0, ..., c_{k-1})^T$.

1.2 Analysis of the model and results.

The system (1.7) with general k is analyzed in Chapter 2 of this thesis while in Chapter 3 and Chapter 4 the particular cases of biennials $k = 2$ and triennials $k = 3$ are considered respectively. In Chapter 5 we consider Single Year Class dynamics in detail (see below).

Chapter 3 is a modified version of the published paper [DDvG1] in Journal of Mathematical Biology; more precisely, in [DDvG1] we dealt only with the Ricker type density dependence (1.5), while in Chapter 3 we keep the sensitivity functions general whenever possible. Section 3.11 of this chapter is a part of another paper [DDvG2], which is submitted in a special issue of Journal of Linear Algebra and Applications. The main part of [DDvG2] is Chapter 2 and Chapter 4 of the thesis. Chapter 5 is a paper which is at the moment under revision for SIAM Journal of Applied Dynamical Systems.

A clever rescaling.

We start the analysis of the system (1.7) with a rescaling. Though just an intermediate step of calculation, we find our rescaling procedure an achievement. It allows to simplify the calculations and the presentation of the results a lot. It can probably be used in other models, because the idea of the rescaling has its roots in biology.

Here we give just an intuitive explanation of the idea. Mathematical details can be found in Section 2.3. The number of newborns are always much larger (sometimes orders of magnitude) than the number of adults. More precisely, the number of individuals in an older age class is less than in a younger because individuals die. Contributions from different age classes to the environmental quantity is comparable only if impacts of older individuals are larger. In other words, a difference in abundance of age classes should be compensated by a difference in impacts. The rescaling we propose makes age class numbers and impacts comparable. More precisely, age class numbers become even exactly equal in a coexistence equilibrium (see below). And instead of considering real impacts, we deal with *expected impacts*, i.e. impacts multiplied by a survival probability from the birth till a given age.

Of course, when we interpret results, we should scale back, so the biological conclusions are formulated in terms of the unscaled impacts. If we nevertheless use expected impacts we state it explicitly.

On circulant populations. Symmetry.

Lemma 2.3 says: the recursion (1.7) is invariant under the transformation $N \mapsto SN, h \mapsto Sh, c \mapsto Sc$, where S is a shift, given by

$$S = \begin{pmatrix} 0 & ... & 0 & 1 \\ 1 & ... & 0 & 0 \\ & ... & & \\ 0 & ... & 1 & 0 \end{pmatrix}.$$

If we have this property for a model of population dynamics, we call such a population *circulant*. This is where the name of Chapter 2 comes from. The symmetry expresses that for semelparous organisms life is indeed a *cycle*.

Eigenvalues and eigenvectors of the shift S play a special role in the analysis of a circulant population (Sections 2.5, 2.6, 2.8). They are given, for $n \in \mathbb{Z}$ by

$$\lambda_{n,k} = e^{i\frac{2\pi n}{k}}, \qquad \xi_{n,k} = \begin{pmatrix} 1 \\ \lambda_{n,k}^{-1} \\ ... \\ \lambda_{n,k}^{-k+1} \end{pmatrix}. \tag{1.9}$$

The eigenvalues are the roots of unity. Below we explain the usefulness of these characteristics in the analysis.

Coexistence equilibrium.

The model (1.7) has a unique equilibrium with all year classes present. In Section 2.8 we derive a characteristic equation corresponding to the coexistence equilibrium. Though the equation has a nice and rather simple form, it does not allow to derive stability conditions for the steady state for general k. But for $k = 2$ and $k = 3$ this is possible. In Section 3.3 we do this in the case of biennials and in Section 4.3 in the case of triennials.

There is an important conclusion formulated in Corollary 2.37 that the eigenvalues of the shift $\lambda_{n,k}$ (1.9) can be roots of the characteristic equation if, in particular,

$$c \cdot \xi_{n,k} = 0, \tag{1.10}$$

where c is a vector of impacts (see (1.8)) and $\xi_{n,k}$ are the eigenvectors of the shift (1.9). Since the roots of unity are situated on the unit circle, they correspond to bifurcations of the coexistence equilibrium. But the most interesting is that the bifurcations are not generic, but *vertical*.

Vertical bifurcation.

If a dynamical system possesses, for some parameter values, an invariant manifold in the phase space filled with periodic points, we call this phenomenon a *vertical bifurcation.* In the end of Section 2.4 we explain this as follows. "Imagine a standard bifurcation diagram for a period-doubling (Figure 2.2). For a particular value of a bifurcation parameter a fixed point branches into two period-2 points. In the case of the vertical bifurcation the whole family of 2-cycles occurs for one particular (bifurcation) value of the parameter, so that we see a *vertical* line of periodic points on the bifurcation diagram."

Vertical bifurcations are key-points in the dynamics of (1.7): we claim that *vertical bifurcations serve as a switch between coexistence and competitive exclusion.* In Section 2.10 one finds comments on this. For $k = 2$ we prove it rigorously (Section 3.10).

There are two situations in which we encounter vertical bifurcations. The first one corresponds to a case of a singular circulant matrix (Sections 2.5-2.6). We show that if a matrix

$$C = \begin{pmatrix} c_0 & c_1 & \dots & c_{k-1} \\ c_{k-1} & c_0 & \dots & c_{k-2} \\ \dots & & & \\ c_1 & c_2 & \dots & c_0 \end{pmatrix}$$

is singular, there is an invariant manifold (a line or a plane) in the phase space filled with k–periodic points. We show also that the circulant C is singular if the identity (1.10) is satisfied for some n. Therefore *(1.10) gives us precise conditions on age class impacts for which we can expect a switch from coexistence to exclusion.* In Section 2.5 we give a table where we rewrite this identity in more explicit form for different k.

Another case of the vertical bifurcation is not so simple. It corresponds to the situation when a *nonlinear circulant* system, composed of sensitivity functions,

$$\begin{array}{lllllll} h_0 & (I_0) & h_1 & (I_1) & \dots & h_{k-1} & (I_{k-1}) & = 1 \\ h_{k-1} & (I_0) & h_0 & (I_1) & \dots & h_{k-2} & (I_{k-1}) & = 1 \\ \dots & & & & & & & \\ h_1 & (I_0) & h_2 & (I_1) & \dots & h_0 & (I_{k-1}) & = 1 \end{array} \tag{1.11}$$

has a family of solutions (i.e., when the system is degenerate).

In Section 2.7 we find sufficient conditions for this system to have a uniform solution $I_0 = \dots = I_{k-1}$ only (Theorem 2.27). In particular, if, for $k = 2$ and $k = 3$, the ratios $\frac{h_i}{h_j}(I)$, $i \neq j$ are monotone, this is indeed the case. If the functions h_i are from the same parameter family (1.4)–(1.6), it is possible that for, say, $g_0 < g_1$ a ratio $\frac{h_0}{h_1}(I)$ is increasing, for $g_1 < g_0$ it

is decreasing and for $g_0 = g_1$ $\frac{h_0}{h_1}(I) \equiv 1$. In this last case the system (1.11) can have a family of solutions. Hence, *if the sensitivity functions are equal we expect a switch from coexistence to exclusion.* In Section 2.7 we find also invariant manifolds corresponding to a family of solutions of (1.11) for different forms of degeneracy, see also Section 3.6 for $k = 2$. Again we expect switches from coexistence to exclusion in these cases.

Single Year Class points. Transversal stability.

The notion of Single Year Class dynamics (SYC-dynamics) was first introduced in [Solberg] and independently by us in [DDvG1]. Another name for this phenomenon is *synchronization.* This corresponds to the situation when we observe, at a given moment, only individuals of exactly the same age in the population (as in the case of cicada mentioned in the beginning).

Mathematically the phenomenon of possibly missing year classes is showing up as *invariance* of coordinate axes and (hyper)planes for the *Full-Life-Cycle map* of looking k years ahead (or the k-th iterate of the original map). For each invariant subspace we can discuss/investigate the dynamics within it, as well as the *transversal stability*, by which we mean the attraction or repulsion in the transverse direction, or, in more biological terms, the decline or growth of a missing year class which is introduced in small numbers.

SYC-points are equilibria of the Full-Life-Cycle map situated on the axes in the phase space. In Section 2.9 we consider *transversal stability* of the SYC-points, that is stability with respect to the invasion of missing year classes. For the original map a SYC-point corresponds to a SYC k-periodic cycle taking its values successively on the axes. The values of the environmental quantity I corresponding to this cycle also perform a k-cycle with values $I_0, ..., I_{k-1}$. In terms of these quantities we have a simple invasibility test: the year class which is j years older than the ruling year class can grow when

$$\prod_{i=0}^{k-1} h_{j+i}(I_i) > 1. \tag{1.12}$$

But we were unable to translate this test into an inequality for parameters of the model for general k. Again we succeeded in the case $k = 2$ (Section 3.8) and partially for $k = 3$ (Section 4.4). However in Section 2.9 we give some monotonicity conditions on the impacts c and survival functions h which guarantee transversal (in)stability of the SYC-points. In particular, if h_i are from the same parameter-family (1.4), we reach the following biological conclusion: *if the sensitivity g increases with age, while the impact c decreases with age, the SYC-points are transversally stable (i.e. we can observe synchronization in the population).*

Single Year Class dynamics.

As well as transversal (in)stability we can consider *internal* (in)stability of the SYC-points. Chapter 5 is devoted to this. First we introduce a notion of Single Year Class map which is a composition of the functions $x \mapsto xh_i(x)$.

We consider different classes of SYC-maps. In particular, if a SYC-map is composed of monotone functions (as in the case of Beverton-Holt nonlinearity (1.6)), the dynamics is extremely simple. The SYC-map has a unique nontrivial fixed point which is globally stable (within the SYC-dynamics, of course).

Here I want to make a general remark on modelling. If one constructs a discrete-time model of population dynamics and one does not want to struggle with the extreme complexities of strange and chaotic attractors, one better chooses the Beverton-Holt density dependence (or another type of monotone response). Such an approach allows to find the essential features of the dynamics and to avoid excessive details on structure of attractors. We follow this principle in Chapter 6. If later one decides to generalize the model, one can include nonmonotone density dependencies as well. But, in general, this results in complifications of attractors, already found for monotone density dependence, for large values of the basic reproduction ratio R_0.

However, to come to this conclusion, we had to learn from our own experience of going through many complexities of the discrete-time dynamics. A great deal of Chapter 5 is devoted to the case $k = 2$ and the Ricker type of density dependence (1.5). We perform a rather detailed bifurcation analysis and construct various bifurcation diagrams. We choose R_0 as one of the bifurcation parameters and see destabilization of dynamics for large R_0.

In Section 5.9 we mention also another interesting feature of the SYC-dynamics. The interval of values of R_0, for which a SYC-point can be stable, grows with k. We cite from the section: "This has a very interesting (and counter-paradigmal) biological interpretation: *the introduction of age-structure in the population model can result in more stable dynamics than in the corresponding unstructured model.* We must say that a stable SYC fixed point corresponds to a k-year cycle with a single year class present, i.e., the population exhibits cyclic and not steady behaviour. However we consider this behaviour as "stable" comparing with (almost) irregular behaviour which corresponds to high-periods and chaotic attractors which one observes in the building block map for large values of R_0." (A "building block" corresponds to the unstructured model.)

Biennials.

Chapter 3 is devoted to $k = 2$ and, especially, to the case of the Ricker nonlinearity (1.5). We make a local bifurcation analysis of the coexistence equilibrium and find two bifurcations: a period-doubling and a Neimark-Sacker (Hopf bifurcation for maps). The Neimark-Sacker bifurcation can occur only for rather large values of R_0. For even larger values, the coexistence equilibrium can not be stable. This demonstrates the Paradox of Enrichment again. However, if we choose the Beverton-Holt nonlinearity (1.6) the Neimark-Sacker bifurcation is impossible, and the equilibrium can be stable even for very large R_0.

The period-doubling bifurcation can occur for all values of R_0. It can be degenerate, it can be exactly the vertical bifurcation which we discussed above. It can happen in two cases: either the impacts of both age classes are equal (uniform impact) or the sensitivities are equal (uniform sensitivity). Under each of these conditions we observe a curve (or even a line) in the phase space filled with 2-cycles. For other values of parameters, if the ratio $\frac{h_0}{h_1}(I)$ is monotone, a 2-cycle with both year classes present can not exist in the interior of the phase space, only on the axes. Then this is a 2-periodic Single Year Class cycle.

We prove the strict dichotomy (Theorem 3.17) for not very large values of R_0: either the coexistence steady state is stable and the SYC-cycle is transversally unstable, or vice versa. Or, in biological terms (Theorem 3.18 and its corollaries): "Competitive exclusion occurs if sensitivity increases with age, while expected impact decreases with age. It also occurs if sensitivity decreases with age while expected impact increases with age". (Expected impact includes survival of the older age class during the first year.)

We show by means of an example that if the ratio $\frac{h_0}{h_1}(I)$ is not monotone, we can have a general period-doubling bifurcation and a 2-cycle with both year classes present can exist. I.e., the switch from coexistence to exclusion does not occur.

Triennials.

In Chapter 4 we consider the case $k = 3$. We perform a local stability analysis of the coexistence steady state and find again a period-doubling and a Neimark-Sacker bifurcation. But they exchange their roles. This time the Neimark-Sacker bifurcation exists for all values of R_0 and the period-doubling can occur for larger R_0 (but not in the Beverton-Holt case!). Both bifurcations are generic, but there is a special case of the Neimark-Sacker bifurcation when it becomes vertical. It corresponds again to the cases of uniform impact or uniform sensitivity.

The reason, why the vertical bifurcation is period-doubling for $k = 2$ and Neimark-Sacker for $k = 3$, is very simple. It has to do with roots of unity which are -1 in the first case and $e^{\pm i\frac{2\pi}{3}}$ in the second. Actually, in the latter case we have formally a so-called 1:3 resonance but again it is degenerate.

The vertical bifurcation is less important for $k = 3$ than for $k = 2$ because it has codimension 2. There is a more generic route from coexistence to competitive exclusion. One can trace it on the bifurcation diagram (Fig. 4.7). This diagram is made for a special case, when only the youngest age class is sensitive to competition, and for the Beverton-Holt nonlinearity. On this diagram we combine the information about local stability of Single Year Class equilibria and existence of Multiple Year Class equilibria with two year classes present with the information about the local stability of the internal steady state. Also we describe a type of dynamics which is impossible for $k = 2$, but found for $k = 3$. This is a heteroclinic cycle which can be an attractor under the Full-Life-Cycle map for rather wide intervals of parameter values. It can be interpreted as dynamics with sudden switches of year class dominance (see Section 4.5 and, in particular, Figure 4.8).

1.3 Magical cicada.

Here we outline briefly the results of the last Chapter 6 concerning the modelling attempts to explain prime number periods. (This is on-going work, which is not yet submitted.) We cite from Section 6.1: "There was only one mechanism proposed to produce this behaviour. Cicada "do not want" to be in resonance with a 2–3-years periodic parasite or a predator. The only problem was that there was no such a periodic parasite or a predator found." The main idea of our work is that we propose short–living cicadas as a candidate for the "periodic parasite". In other words, *because of competition with short-living periodic cicada, only a mutant with a prime period of the life cycle can invade.*

First we introduce a minimal model producing the desired behaviour. This is a competition model of three species biennials, triennials and k-ennials on a shared resource. We consider only *nursery competition*, i.e. competition between newborns. The model does not explain many features of the Magicicada dynamics (e.g., synchronization), but it demonstrates what is potentially the main mechanism behind prime periods occurrence.

Then we put more details into the model. In particular, we make the environment two–dimensional. Indeed, coexistence of several species on one resource is unprobable. We include also impacts of older age classes into

the environmental variable. We show that short–living cicadas which exhibit coexistence of year classes at the present can be periodical during Ice Ages, when the species of cicadas were formed. We were able to obtain the exclusion of non-prime periods in this model as well as for the minimal one but as a consequence of competition of the youngest age class of k-ennials with older age classes of biennials and triennials.

***

To conclude the Introduction we answer the question which is in the title to this thesis: can old and young coexist? The answer is *Yes*. But the condition for this is that neither old nor young should suffer too much from the other. If you create the environment around you, you should be responsive to it. If you are dominating, you should be sensitive and sympathetic.

Dear Reader, I wish you pleasure in reading the thesis.

Sincerely yours, the author.

Chapter 2

On Circulant Populations. Algebra of Semelparity.

2.1 Introduction.

The structure of this chapter is as follows. In Section 2.2 we introduce notation and formulate a *linear* Leslie matrix model. In this case survival probabilities and the number of offspring are density independent. We introduce a compound parameter R_0, called the *basic reproduction ratio*. The dynamics of the model is fully characterized by R_0: the population grows if $R_0 > 1$ and declines if $R_0 < 1$, while the relative proportions of the age classes cycle with period k.

We also notice that the linear model possesses a cyclic symmetry which extends to a nonlinear model which we introduce in Section 2.3. The density dependence is incorporated via an *environmental quantity* I, which we assume to be one-dimensional (it is a linear combination of age class numbers). We define the impact of age classes on the environment and the sensitivity to it. Furthermore, we perform a scaling of the nonlinear model which simplifies the further investigations and the presentation of results. Also in Section 2.3 we find a unique steady state with all year classes present (to which we refer both as the coexistence steady state/equilibrium and as the internal steady state/equilibrium).

In Section 2.4 we begin the analysis of the nonlinear model. We look for k-periodic orbits. Under certain assumptions on the sensitivity functions $h_i(I)$ a cycle of period k with all year classes present can exist only for some particular parameter combinations which form sets of measure zero in the parameter space. But still we are interested in this because these parameter combinations correspond to *bifurcations*, i.e., they point out where the qualitative behaviour of the system changes. The corresponding environmental quantity I is then also k-periodic and takes values $I_0, ..., I_{k-1}$

This chapter is a main part of [DDvG2]

which should be solutions of a *nonlinear circulant* system. In the case with all I_i equal, the relation between I and the age class numbers N_i is given by a *linear circulant* system. If the corresponding circulant matrix is singular, there is a whole family of k-cycles with all year classes present. In this section we consider the most degenerate situation when all impacts are equal (*uniform impact* case). An analogue of that, but for the nonlinear circulant, is when all sensitivity functions are the same. In that case we speak about *uniform sensitivity.* In both cases there is a manifold in the phase space filled with periodic orbits. If such a phenomenon is observed for some particular parameter combination in a model, we call it a *vertical bifurcation.*

In Section 2.5 we derive a detailed list of conditions for the singularity of a circulant matrix, as a generalization of the uniform impact case described in Section 2.4. In Section 2.6 we describe manifolds (which are just simplices) filled with k-cycles corresponding to different cases of singularity of the circulant.

In Section 2.7 we look for families of k-cycles if the environmental quantity is not constant, i.e. the nonlinear circulant system has nonuniform solutions. In fact, we try to generalize the uniform sensitivity case of Section 2.4.

In Section 2.8 we write down a characteristic equation corresponding to the internal steady state. Though we are not able to perform a full linear stability analysis, we show that eigenvalues of the internal steady state are on the unit circle under the conditions for the vertical bifurcations found in Sections 2.5 and 2.7. It leads us to conjecture that the vertical bifurcations can serve as a switch between the stability of the internal steady state and the stability of a cycle with some year classes missing.

In Section 2.9 we consider the other extreme, a k-cycle with only one year class present. We call this case Single Year Class (SYC) dynamics [DDvG1, Wikan]. We show, in particular, that a SYC-cycle is stable in a special case when the impact on the environment is a decreasing function of age while the sensitivity increases with age.

2.2 The linear model

In this section we consider a k-dimensional linear recursion

$$N(t+1) = L(h)N(t). \tag{2.1}$$

We number the *age classes* from 0 to $k-1$. A component $N_i(t)$ of the vector $N(t)$ denotes the number of individuals in the i-th age class. Time is measured in years, $t \in \mathbb{Z}$. The symbol h denotes the k-vector with components $h_i > 0$ where, for $i = 0, ..., k-2$, h_i is the *survival probability*

of an i-years old individual in some year to an $(i+1)$-years old individual in the next year, and h_{k-1} is the *expected number of offspring* of a $(k-1)$-years old individual *in the next year*. We use $L(h)$ to denote the Leslie matrix corresponding to h. So, explicitly we have

$$L(h) = \begin{pmatrix} 0 & 0 & \dots & 0 & h_{k-1} \\ h_0 & 0 & \dots & 0 & 0 \\ 0 & h_1 & \dots & 0 & 0 \\ \dots & & & & \\ 0 & 0 & \dots & h_{k-2} & 0 \end{pmatrix}. \tag{2.2}$$

Adopting (throughout the thesis!) the convention that indices are considered modulo k, we can express the solution to (2.1) explicitly in terms of the initial condition by the formula

$$N_i(t) = \left(\prod_{j=0}^{t-1} h_{i-t+j} \right) N_{i-t}(0).$$

Putting $t = k$ we find in particular

$$N_i(k) = R_0 \, N_i(0) \tag{2.3}$$

with R_0 the so-called *basic reproduction ratio* defined by

$$R_0 = \prod_{i=0}^{k-1} h_i. \tag{2.4}$$

So the dynamics is a superposition of a cyclic shift and growth (if $R_0 > 1$) or decline (if $R_0 < 1$). Under the constant (by assumption) environmental conditions all year classes have the same per generation growth factor R_0 and the relative proportions in which they occur return to the initial values after every k years.

Thus we obtained a complete description of the dynamics in the case of independent year classes, but we add some observations for future use. The matrix $L(h)$ with positive components h_i is irreducible but not primitive. In fact it has period k [Seneta], which is reflected in the characteristic equation

$$\lambda^k = R_0$$

and its roots, which are the $R_0^{\frac{1}{k}}$ multiples of the k-th roots of unity.

Let $\mathbf{1}$ denote the k-vector with all components equal to 1, then

$$S = L(\mathbf{1}) = \begin{pmatrix} 0 & \dots & 0 & 1 \\ 1 & \dots & 0 & 0 \\ & \dots & & \\ 0 & \dots & 1 & 0 \end{pmatrix} \tag{2.5}$$

is the cyclic forward shift on $\mathbb{R}^k$

$$S : \begin{pmatrix} x_0 \\ x_1 \\ \dots \\ x_{k-1} \end{pmatrix} \mapsto \begin{pmatrix} x_{k-1} \\ x_0 \\ \dots \\ x_{k-2} \end{pmatrix}.$$

The transpose S^T equals the inverse S^{-1}, which is the cyclic backward shift. Moreover, as a straightforward calculation shows, one has the following two results.

Lemma 2.1. $SL(h)S^{-1} = L(Sh)$.

Corollary 2.2. *The recursion (2.1) is invariant under the transformation* $N \mapsto SN$, $h \mapsto Sh$.

2.3 Formulation and scaling of the nonlinear model.

We next introduce density dependence (nonlinearity) in a two step procedure. First, we assume that the positive quantities h_i, defined in the previous section, depend on a variable I describing the *environmental condition*. We restrict ourselves to the case that I is one-dimensional. The functions $h_i(I)$ are decreasing and, in addition, smooth enough, so if we deal with derivatives $h_i'(I)$, we choose these functions to be C^1 etc. Typical examples of the kind of dependence are provided by the Ricker family

$$h_i(I) = \sigma_i \, e^{-g_i I} \tag{2.6}$$

and the Beverton-Holt family

$$h_i(I) = \frac{\sigma_i}{1 + g_i I}. \tag{2.7}$$

In the second step of the model construction, we formulate a feedback law that relates the environmental condition I to the population size and composition N.

$$I = c \cdot N = \sum_{i=0}^{k-1} c_i N_i.$$

The underlying idea is that I should be such that individuals are independent from one another when I is given (prescribed) and that this independence extends to the feedback. More details on the notion of I and on the general

modelling philosophy can be found in Chapter 1 and also in [DGHKMT, DGM].

We shall use the following terminology: c_i is the age-specific *impact* on the environmental condition, and the functions $h_i(I)$ are the age-specific *sensitivity to the environment*, in cases like (2.6) and (2.7), the parameters g_i are also called the sensitivity to the environment. (The quantities σ_i featuring in (2.6) and (2.7) are of minor importance, as we will show below that they can be eliminated by an appropriate scaling.)

We note that quite often the functions $h_i(I)$ are chosen from the same two–parameter family $\sigma H(gI)$, as indeed in the Ricker (2.6) and Beverton-Holt (2.7) cases. So, $h_i(I)$ can be written in the form

$$h_i(I) = \sigma_i H(g_i I), \tag{2.8}$$

where the function H is normalized so that

$$H(0) = |H'(0)| = 1. \tag{2.9}$$

(These equalities are indeed satisfied for the Ricker and Beverton-Holt families.) But, in general, we do not put this restriction on the functions h_i and only use it whenever useful.

So, the object of our study is the dynamical system generated by the nonlinear recursion

$$\begin{aligned} N(t+1) &= L\Big(h(I(t))\Big)\ N(t) \\ I(t) &= c \cdot N(t). \end{aligned} \tag{2.10}$$

Since $c \cdot N = Sc \cdot SN$ (recall that $S^T = S^{-1}$!) there is an analogue to Corollary 2.2:

Lemma 2.3. *The recursion (2.10) is invariant under the transformation* $N \mapsto SN, h \mapsto Sh, c \mapsto Sc$.

(Here we take the notational freedom of denoting the "lift" of S from $\mathbb{R}^k$ to $\mathbb{R}^k$ –valued functions by the same symbol; in cases like (2.6) and (2.7) one can work with $g \mapsto Sg$ instead.)

When I is constant we are back to the linear setting of the preceding section. Motivated by (2.3) and (2.4) we notice that $N_i(k) = N_i(0)$ if

$$\Pi(I) = 1 \tag{2.11}$$

with

$$\Pi(I) := \prod_{i=0}^{k-1} h_i(I) \tag{2.12}$$

The basic reproduction ratio in the virgin environment is, by definition,

$$R_0 = \Pi(0) = \prod_{i=0}^{k-1} h_i(0). \tag{2.13}$$

We assume that

i) $R_0 > 1$;

ii) Π is a strictly decreasing continuous function of I (and each of the functions h_i is decreasing);

iii) $\lim_{I\to\infty} \Pi(I) < 1$.

The consequence is that (2.11) has a unique positive solution, which we denote by $\bar{I}$. So the *steady environmental condition* $\bar{I}$ is such that under this condition the population will neither grow nor decline, but just cycle with period k. Technically we have

$$\Pi(\bar{I}) = 1, \tag{2.14}$$

where $\Pi(I)$ is given by (2.12).

Even though $\bar{I}$ is only implicitly determined, we use it to perform a scaling of N, h and c. We stress that this scaling has miraculous effects in simplifying the subsequent analysis (having struggled a lot with messy calculations before discovering this scaling, we feel entitled to do so)!

Theorem 2.4. *Consider the system (2.10). By scaling one can achieve that*

$$\begin{aligned} &h_i(\bar{I}) = 1 \quad \text{for } i = 0, ..., k-1, && \text{(a)} \\ &\sum_{i=0}^{k-1} c_i = 1. && \text{(b)} \end{aligned} \tag{2.15}$$

Proof. Below the upper index "s" denotes "scaled" variables and "u" denotes "unscaled" variables. Let for $i = 0, ..., k-1$

$$\begin{aligned} N_i^s &= \theta_i^{-1} N_i^u \\ h_i^s(I) &= \tfrac{\theta_i}{\theta_{i+1}} h_i^u(I) \\ c_i^s &= \theta_i c_i^u, \end{aligned} \tag{2.16}$$

where

$$\theta_{i+1} = \theta_i \, h_i^u(\bar{I}) = \theta_0 \prod_{j=0}^{i} h_j^u(\bar{I}),$$

$$\theta_0 = \left(\sum_{i=0}^{k-1} c_i^u \prod_{j=0}^{i-1} h_j^u(\bar{I}) \right)^{-1}$$

The system (2.10) is invariant under this transformation and the properties (2.15) are satisfied for h_i^s and c_i^s. □

Remark. Under the scaling (2.16)

$$h_i^s(I) = \frac{h_i^u(I)}{h_i^u(\bar{I})}.$$

In particular, if the functions $h_i^u(I)$ belong to a two–parameter family (2.8), we have for the new functions

$$h_i^s(I) = \frac{H(g_i I)}{H(g_i \bar{I})}. \tag{2.17}$$

Under the scaling the Ricker family and the Beverton-Holt family look, respectively, as follows

$$h_i(I) = e^{-g_i(I-\bar{I})}, \tag{2.18}$$

$$h_i(I) = \frac{1 + g_i \bar{I}}{1 + g_i I}. \tag{2.19}$$

Remark. The quantity $\bar{I}$ can be considered as a new parameter of the model instead of the basic reproduction ratio R_0 given by (2.13). There is a one-to-one correspondence between $\bar{I}$ and R_0, given functions h_i. Let $\Pi(I) = R_0 \, \pi(I)$ with $\pi(0) = 1$. Then $R_0 = \frac{1}{\pi(\bar{I})}$ and R_0 can be considered as an increasing function of $\bar{I}$. In particular, $\bar{I} > 0$ if and only if $R_0 > 1$.

One can notice that the scaling (2.16) is not complete, there is still some freedom, as we haven't scaled I.

Theorem 2.5. *If the scaled functions $h_i(I)$ belong to the family (2.17), by another scaling one can achieve that*

$$\sum_{i=0}^{k-1} g_i = 1 \tag{2.20}$$

without destroying the properties (2.15) and (2.17).

Proof. The scaling is given by

$$N^{ss} = N^s \sum_{i=0}^{k-1} g_i^u$$

$$g_i^s = \frac{g_i^u}{\sum_{i=0}^{k-1} g_i^u},$$

where the index "ss" denotes doubly scaled N. Then the properties (2.20) and (2.15) hold. Since

$$I^s = I^u \sum_{i=0}^{k-1} g_i^u$$

we notice that $g_i I$ is invariant under the scaling for all i. Hence the functions $h_i^s(I)$ do not change and still have the form (2.17). □

Remark. The parameter $\bar{I}$ changes also according to the above formula so that

$$\bar{I}^s = \bar{I}^u \sum_{i=0}^{k-1} g_i^u.$$

Since the scaling (2.16) depends on $\bar{I}$, the rescaling of this parameter implies that we choose another absolute scale for N.

In the rest of the chapter we consider the situation after scaling, i.e., we deal with N^{ss}, $\bar{I}^s$, c^s, g^s and h^s, but still use the symbols N, $\bar{I}$, c, g and h without "s", just like we did in (2.10). If (2.17) does not apply, we do not perform the second scaling and deal with N^s (or adopt the convention $N^{ss} = N^s$).

A first advantage of the proposed scaling is demonstrated by the very simple form in which the unique coexistence steady state of (2.10) appears.

Corollary 2.6.

$$L(h(\bar{I})) = L(\mathbf{1}) = S$$

Theorem 2.7. *The nonlinear recursion (2.10) has a unique nontrivial steady state*

$$\bar{N} = \mathbf{1}\bar{I}. \tag{2.21}$$

Proof. In a steady state I is constant and, in view of (2.3), (2.4) and (2.14), must be equal to $\bar{I}$. Corollary 2.6 tells us that under such conditions all orbits are periodic with period k. If, and only if, N is actually a multiple

of the positive eigenvector $\mathbf{1}$ of S, do we obtain a degenerate periodic orbit consisting of one point. Consistency with the feedback condition $\bar{I} = c \cdot \bar{N}$ then yields, in view of (2.15 b), the formule (2.21) as the only possibility. $\square$

2.4 In search for k-periodic orbits with all year classes present.

As k-periodicity is inherent in the life cycle, it is natural to look for k-periodic orbits of (2.10). We first look for conditions on the values I_i that the environmental condition takes. So assume $t \mapsto N(t)$ is k-periodic and define $I_i = c \cdot N(i)$ then necessarily

$$N_j(k) = \left(\prod_{i=0}^{k-1} h_{j+i}(I_i) \right) N_j(0) \tag{2.22}$$

(this is just the time-inhomogeneous analogue of (2.3).) So either the j-th year class is missing or we need to have that

$$\prod_{i=0}^{k-1} h_{j+i}(I_i) = 1. \tag{2.23}$$

If we want all of the year classes to be present we therefore need to solve the system of k equations:

$$\begin{array}{lllllll} h_0 & (I_0) & h_1 & (I_1) & ... & h_{k-1} & (I_{k-1}) & = 1 \\ h_{k-1} & (I_0) & h_0 & (I_1) & ... & h_{k-2} & (I_{k-1}) & = 1 \\ ... & & & & & & & \\ h_1 & (I_0) & h_2 & (I_1) & ... & h_0 & (I_{k-1}) & = 1 \end{array} \tag{2.24}$$

for the k unknowns $I_0, I_1, ..., I_{k-1}$. By analogy with a circulant matrix (see Section 2.5), we call the left hand side of (2.24) a *nonlinear circulant* (and (2.24) itself a nonlinear circulant (system of) equation(s)). Let us introduce a vector $\mathbf{I} = (I_0, I_1, ..., I_{k-1})$ (we write it in bold in order to distinguish from the environmental quantity I itself which is one-dimensional). The relation between $\mathbf{I}$ and N is given implicitly by the equation:

$$\begin{pmatrix} c_0 & ... & c_{k-1} \\ c_1 h_0(I_0) & ... & c_0 h_{k-1}(I_0) \\ ... & ... & ... \\ c_{k-1} h_{k-2}(I_{k-1}) ... h_0(I_0) & ... & c_{k-2} h_{k-3}(I_{k-1}) ... h_0(I_1) h_{k-1}(I_0) \end{pmatrix} N = \mathbf{I}. \tag{2.25}$$

When $I_i = \bar{I}$ for $i = 0, ..., k-1$, then (2.24) is just a k-fold repetition of (2.14) and therefore satisfied. So we know already one solution of (2.24); we call this solution *uniform*, and before embarking on the question whether there are any other (*nonuniform*) solutions, we consider the second step of the construction of k-periodic orbits, which consists of determining one or more initial conditions that yield the correct sequence of I-values. When $I_i = \bar{I}$ we can exploit Corollary 2.6 to deduce that our task is to determine $N \in \mathbb{R}^k$ such that

$$\bar{I} = c \cdot S^i N = S^{-i} c \cdot N \quad \text{for } i = 0, ..., k-1$$

or, written out in detail,

$$\begin{array}{llllll} c_0 & N_0 + c_1 N_1 + & ... & + c_{k-1} & N_{k-1} & = \bar{I} \\ c_{k-1} & N_0 + c_0 N_1 + & ... & + c_{k-2} & N_{k-1} & = \bar{I} \\ ... & & & & & \\ c_1 & N_0 + c_2 N_1 + & ... & + c_0 & N_{k-1} & = \bar{I} \end{array} \tag{2.26}$$

and, in more symbolic form,

$$CN = \mathbf{1}\bar{I}, \tag{2.27}$$

where C is the *circulant matrix* [Davis] generated by the vector c (see Section 2.5):

$$C = \begin{pmatrix} c_0 & c_1 & ... & c_{k-1} \\ c_{k-1} & c_0 & ... & c_{k-2} \\ ... & & & \\ c_1 & c_2 & ... & c_0 \end{pmatrix} \tag{2.28}$$

Again we already know a solution, viz. (2.21). But is it the only solution? It is if C is non-singular and it is not if C is singular, so we reformulate the question as: *when is a nonnegative circulant matrix singular?* The next section is devoted to answering this question. But before being systematic we study the most singular case, which obviously corresponds to all c_i being equal. In that case (2.26) is simply the k-fold repetition of the equation $c \cdot N = \bar{I}$. In combination with Corollary 2.6 this observation immediately leads to

Theorem 2.8. (uniform impact) *If* $c = \mathbf{1}\frac{1}{k}$ *the simplex*

$$\left\{ N : c \cdot N = \frac{1}{k} \sum_{i=0}^{k-1} N_i = \bar{I} \right\} \tag{2.29}$$

is invariant under the nonlinear recursion (2.10) and every point on this simplex is k*-periodic.*

So under a rather restrictive condition on c we find a plenitude of k-periodic orbits, filling a $(k-1)$-dimensional "flat" subset of the positive cone. Inspired by this result we now return to the nonlinear circulant equation (2.24). What if the analogue of constant c_i holds, i.e., what if $h_i(I)$ is independent of i?

Theorem 2.9. (uniform sensitivity) *If*

$$h(I) = \mathbf{1}\phi(I)$$

(and, in particular, in the case (2.17) with $g = \mathbf{1}\frac{1}{k}$ *) any positive half-line*

$$X_\sigma = \{N = A\sigma : A \geq 0\}$$

with $\sigma \in \mathbb{R}^k, \sigma_i \geq 0, \sum_{i=0}^{k-1} \sigma_i = 1$ *, is invariant under the* k*-th iterate of the nonlinear recursion (2.10).*

Proof. If $h(I) = \mathbf{1}\phi(I)$ the recursion (2.10) takes the form

$$N(t+1) = \phi(c \cdot N(t))\, SN(t)$$

(we say that there is a *scalar nonlinearity*). Now put

$$N(t) = A(t)\sigma(t)$$

with $A(t) \in \mathbb{R}^+$ and $|\sigma(t)| = \sum_{i=0}^{k-1} \sigma_i(t) = 1$, so that σ specifies the direction and A the magnitude. Then

$$\sigma(t+1) = S\sigma(t)$$

and

$$A(t+1) = \phi(A(t)c \cdot \sigma(t))\, A(t). \tag{2.30}$$

Hence $\sigma(t+k) = \sigma(t)$ or, in words, the positive cone decomposes into a collection of invariant k-tuples of half-lines which are cyclically mapped into each other.

□

Note that the coordinate axes form the outer extreme of these k-tuples and that these are mapped cyclically into each other even if sensitivity is non-uniform. In the "middle" there is the invariant half-line spanned by $\mathbf{1}$, which forms a degenerate k-tuple.

Proposition 2.10. *Let $R_0 > 1$ (R_0 is given by (2.13)) and let the matrix C, given by (2.28), be non-singular. Assume uniform sensitivity, then the one-dimensional map $A(t) \mapsto A(t+k)$ generated by (2.30) has at least one fixed point for any given σ, if ϕ is a decreasing function with $\lim_{I\to\infty} \phi(I) = 0$.*

Proof. To a fixed point of the map $A(t) \mapsto A(t+k)$ corresponds a fixed point of the k-th iterate of the original map (1.7), which is a solution of the system (2.25), provided I satisfies (2.24). In the case of uniform sensitivity (2.25) can be rewritten as a linear system

$$C\,N = \begin{pmatrix} I_0 \\ \frac{I_{k-1}}{\phi(I_0)...\phi(I_{k-2})} \\ ... \\ \frac{I_1}{\phi(I_0)} \end{pmatrix}$$

with C given by (2.28). Clearly, this system has a unique solution for a given combination $(I_0, ..., I_{k-1})$ if C is non-singular. So we should prove that there exists a $(I_0, ..., I_{k-1})$ combination corresponding to any σ. We substitute $N = A\sigma$ in the system above and obtain, by eliminating A via the first equation,

$$I_j = I_0\phi(I_0)...\phi(I_{j-1})\,\frac{c \cdot S^j\sigma}{c \cdot \sigma}, \qquad j = 1, ..., k-1.$$

Therefore we have a one-dimensional set of candidate vectors $(I_0, ..., I_{k-1})$ with I_0 as a free parameter (if $c \cdot \sigma = 0$ we can write similar relations, but choose I_1 as a free parameter etc.). In addition, we should have

$$\phi(I_0)...\phi(I_{k-1}) = 1$$

in order to satisfy (2.24). This is an equation for I_0. It can be rewritten as

$$R_0 H(I_0)...H(I_{k-1}) = 1, \tag{2.31}$$

where $H(I) = \frac{\phi(I)}{\phi(0)} < 1 \,\forall I > 0$. The left-hand side is equal to $R_0 > 1$ if $I_0 = 0$ and

$$R_0 H(I_0)...H(I_{k-1}) \le R_0 H(I_0).$$

The right-hand side of this inequality tends to zero as $I_0 \to \infty$, so the left-hand side tends to zero as well and the equation (2.31) has at least one solution which is positive. □

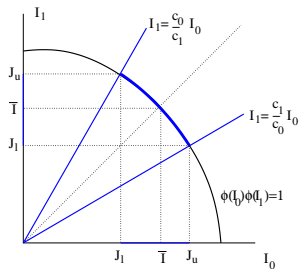

Figure 2.1: The region of the (related) parameters I_0 and I_1 which define, for $k = 2$, the family of fixed points of the second iterate of the map (1.7) (see Proposition 2.12). We assume $c_0 > c_1$.

Corollary 2.11. *Fixed points of the k-th iterate of the map (2.30) form a $(k-1)$-parameter family of k-periodic points of the original map (1.7) parameterized by σ ($\sum_{j=0}^{k-1} \sigma_j = 1$).*

This family is a nonlinear analogue of the simplex (2.29). Chapter 5 is devoted to a more systematic study of the map $A(t) \mapsto A(t+k)$. As an illustration of the results above let us give an explicit expression for the family of 2-periodic points in the case $k = 2$ and uniform sensitivity.

Proposition 2.12. *Let $k = 2$ and $h_0(I) = h_1(I) = \phi(I)\ \forall I \geq 0$. Let, in addition, $c_0 \neq c_1$. Then there exists a one-parameter family of fixed points of the second iterate of the map (1.7) given explicitly by*

$$\begin{pmatrix} N_0 \\ N_1 \end{pmatrix} = \frac{1}{c_0^2 - c_1^2} \begin{pmatrix} c_0 I_0 - c_1 \frac{I_1}{\phi(I_0)} \\ c_0 \frac{I_1}{\phi(I_0)} - c_1 I_0 \end{pmatrix}$$

with I_0 and I_1 related by

$$\phi(I_0)\phi(I_1) = 1.$$

This implicit relation is symmetric w.r.t. the diagonal $I_0 = I_1$ (Figure 2.1). Moreover, I_1 can be viewed as a decreasing function of I_0 or vice versa, and

$$(I_0, I_1) \in J,$$

where J is a symmetric region $[J_l, J_u] \times [J_l, J_u]$ containing $(\bar{I}, \bar{I})$ and given implicitly by

$$\phi(J_l)\phi(J_u) = 1 \text{ with } J_u = J_l \max\{\tfrac{c_0}{c_1}, \tfrac{c_1}{c_0}\}.$$

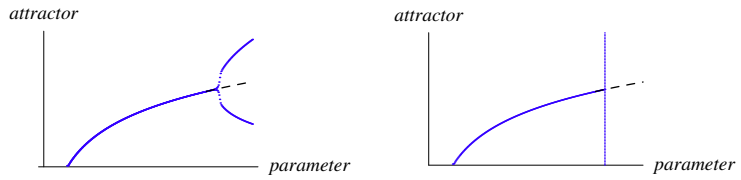

Figure 2.2: A standard bifurcation diagram with a period doubling and a vertical bifurcation, in which a family of 2-cycles occurs for one particular (bifurcation) value of the parameter.

This proposition can be obtained by straightforward computation of solutions of the linear system (2.25) (compare (3.53) below). Values of the environmental quantities I_j which are a family of solutions of the nonlinear circulant, serve themselves as parameters of the family of the fixed points. The boundaries of the regions J correspond to the case when one of the components N_i is zero, inside the region all the components are positive. We notice that in the case $k = 2$ the interval $[J_l, J_u]$ is largest if one of the parameters c_0 or c_1 is zero and that this interval degenerates to the point $\bar{I}$ if $c_0 = c_1$. So in the case of uniform impact there exists only one biologically relevant solution of the nonlinear circulant which is in fact the uniform solution. But a whole family of fixed points of the second iterate of the map corresponds to this solution (see Theorem 2.8).

If a dynamical system possesses, for special parameter values, an invariant manifold in the phase space filled with periodic points, we call this phenomenon a *vertical bifurcation*. The motivation for that is the following. Imagine a standard bifurcation diagram for a period-doubling (Figure 2.2). For a particular value of a bifurcation parameter a fixed point branches into two period-2 points. In the case of the vertical bifurcation the whole family of 2-cycles occurs for one particular (bifurcation) value of the parameter, so that we see a *vertical* line of periodic points on the bifurcation diagram. In the system (2.10) we indeed have such a situation: in Section 2.8 we show that eigenvalues of the internal steady state are on the unit circle under the parameter conditions for a vertical bifurcation.

2.5 Singular circulants.

Now we come back to the question formulated in the previous section: when is a circulant matrix singular? Answering this question we find conditions

for vertical bifurcations which generalize those of the *uniform impact* case of Theorem 2.8.

First, we need a couple of formal definitions and lemmas which we have taken from [Davis].

Definition 2.13. *A matrix*

$$C = \mathrm{circ}\,(c_0, ..., c_{k-1}) = \begin{pmatrix} c_0 & c_1 & ... & c_{k-1} \\ c_{k-1} & c_0 & ... & c_{k-2} \\ ... & & & \\ c_1 & c_2 & ... & c_0 \end{pmatrix} \tag{2.32}$$

is called a circulant matrix of order k *or a* circulant *of order* k *.*

A matrix is called *uniform* if all its entries are equal. A uniform matrix is, of course, circulant.

Lemma 2.14. *A circulant* C *can be represented as*

$$C = c_0 E + c_1 S^{-1} + ... + c_{k-1} S^{-(k-1)},$$

where S *is the shift defined in (2.5) and* E *is the identity matrix of order* k *.*

Proof. Notice that $S^{-1} = \mathrm{circ}(0, 1, 0..., 0)$, $S^{-k} = E = \mathrm{circ}(1, 0, ..., 0)$ and

$$S^i = \mathrm{circ}(\underset{\substack{\uparrow \\ 0\mathrm{th}}}{0, ...0,} \underset{\substack{\uparrow \\ i\mathrm{th}}}{1, 0, ...,} \underset{\substack{\uparrow \\ (k-1)\mathrm{th}}}{0})$$

□

Definition 2.15. *The polynomial*

$$p(z) = c_0 + c_1 z + ... + c_{k-1} z^{k-1} \tag{2.33}$$

is called the representer of the circulant C *.*

The eigenvalues of the shift S are the k-th roots of unity

$$\lambda_{n,k} = e^{n\frac{2\pi i}{k}}, \qquad n = 0, 1, ..., k-1$$

and the corresponding eigenvectors are

$$\xi_{n,k} = \begin{pmatrix} 1 \\ \lambda_{n,k}^{-1} \\ ... \\ \lambda_{n,k}^{-k+1} \end{pmatrix}. \tag{2.34}$$

From Lemma 2.14 one can see that

$$C\xi_{n,k} = p(\lambda_{n,k}^{-1})\xi_{n,k}, \tag{2.35}$$

i.e. $\xi_{n,k}$ are also eigenvectors of C with corresponding eigenvalues $p(\lambda_{n,k}^{-1})$. Hence we have the following lemma, which gives the answer to the question in the beginning of the section.

Lemma 2.16. *A circulant C is singular if and only if a k-th root of unity is a zero of its representer $p(z)$, i.e. there exists an n such that*

$$p(\lambda_{n,k}^{-1}) = 0, \tag{2.36}$$

or, in other words,

$$c \cdot \xi_{n,k} = 0 \tag{2.37}$$

Remark. Without loss of generality we can consider n in the interval $[0, \frac{k}{2}]$, because all other values of n give the same or complex conjugated roots.

To illustrate the lemma, we consider a couple of special cases of singular circulants and then formulate a general theorem.

Proposition 2.17. *If the sum of the entries $c_0 + ... + c_{k-1}$ of a circulant is zero, the circulant is singular.*

Proof. The equality $c_0 + ... + c_{k-1} = 0$ implies that $\mu = 1$ is a zero of the representer. Hence C is singular. □

This is the most simple case which, however, is uninteresting for us because we deal with nonnegative circulants. If the sum of all entries is zero, we have just a matrix consisting of all zeros, which we call a *trivial circulant.*

Proposition 2.18. *A nontrivial nonnegative circulant of order 2 or 3 is singular if and only if it is uniform.*

Proof. In the case of a circulant of order 2 this can be checked by straightforward computation. But use of Lemma 2.16 is also possible. If a circulant of order 2 is singular, either 1 or -1 is a zero of its representer. In the first case the circulant is trivial, in the second $c_0 - c_1 = 0$.

Consider a circulant of order 3. It is singular if either 1 or $e^{\pm i\frac{2\pi}{3}}$ are zeros of the representer. The first possibility gives again a trivial circulant. In the second case $p(z) = c_1(z - e^{i\frac{2\pi}{3}})(z - e^{-i\frac{2\pi}{3}}) = c_1(z^2 + z + 1)$. Hence all entries are equal. □

Therefore, if the system (2.10) is low-dimensional ($k = 2$ or 3), it possesses a k-cycle, with all year-classes present and constant environmental condition $\bar{I}$, only in the case of *uniform impact* (cf. Theorem 2.8).

Proposition 2.19. *Let C be a circulant of an even order. It is singular if the sum of its even components is equal to the sum of its odd components, i.e.*

$$\sum_{i=0}^{\frac{k-2}{2}} c_{2i} = \sum_{i=0}^{\frac{k-2}{2}} c_{2i+1}. \tag{2.38}$$

Proof. The condition of the proposition implies that -1 is a zero of the representer. □

Now we formulate the main theorem.

Theorem 2.20. *For any k there exist $\left[\frac{k}{2}\right]$ different families of nontrivial nonnegative singular circulants C of order k, where*

$$\left[\frac{k}{2}\right] = \begin{cases} \frac{k}{2} & k \text{ even} \\ \frac{k-1}{2} & k \text{ odd} \end{cases}$$

Here is the list of these families.

i) $k = 2, 3$. *A one-parameter family of uniform matrices.*

ii) $k > 3$ *and* k *is even. A* $(k-1)$*-parameter family of circulants such that the sum of the even entries is equal to the sum of the odd entries (2.38).*

iii) $k > 3$. *There are* $\left[\frac{k-1}{2}\right]$ *different* $(k-2)$*-parameter families of singular circulants enumerated by* $0 < n < \frac{k}{2}$ *such that*

$$\mathbf{f}_{k,n}(c_0, ..., c_{k-1}) = 0 \tag{2.39}$$

where $\mathbf{f}_{k,n}(c_0, ..., c_{k-1})$ *is a linear function* $\mathbb{R}^k \to \mathbb{R}^2$ *given by the*

following relation

$$\mathbf{f}_{k,n}(c_0,...,c_k) =$$
$$\begin{cases} c_0 + (c_1 + c_{k-1})\cos\frac{2\pi n}{k} + (c_2 + c_{k-2})\cos\frac{4\pi n}{k} + \\ \qquad ... + \left[\begin{array}{ll} (c_{\frac{k-1}{2}} + c_{\frac{k+1}{2}})\cos\frac{\pi(k-1)n}{k}, & k \text{ odd} \\ (-1)^n c_{\frac{k}{2}}, & k \text{ even} \end{array} \right. \\ (c_1 - c_{k-1})\sin\frac{2\pi n}{k} + (c_2 - c_{k-2})\sin\frac{4\pi n}{k} + \\ \qquad ... + \left[\begin{array}{ll} (c_{\frac{k-1}{2}} + c_{\frac{k+1}{2}})\sin\frac{\pi(k-1)n}{k}, & k \text{ odd} \\ (c_{\frac{k-2}{2}} + c_{\frac{k+2}{2}})\sin\frac{\pi(k-2)n}{k}, & k \text{ even} \end{array} \right. \end{cases} \tag{2.40}$$

Proof. Proposition 2.18 gives the statement (i) for $k = 2, 3$.

Let $k > 3$. Lemma 2.16 says that a circulant is singular if (2.36) holds. We can rewrite this condition in the form (2.39) for $0 \le n \le \frac{k}{2}$. There are three different cases possible:

- $n = 0$ corresponds to 1 being a root of the representer. In this case the circulant is trivial.
- k is even, $n = \frac{k}{2}$. A root of the representer is -1. The statement (ii) is given by Proposition 2.19. The second condition of (2.39)–(2.40) vanishes and the family of such singular circulants has $(k-1)$ free parameters.
- $0 < n < \frac{k}{2}$. The expressions (2.39)–(2.40) give two different conditions on c. Hence for any n we have $k-2$ free parameters. Moreover, the families given by the different values of n are also different. There are $\left[\frac{k-1}{2}\right]$ such families.

□

In some cases it is possible to rewrite the condition (2.37) using functions with lower values of k and sums of c's as arguments.

Proposition 2.21. *Let $\frac{n}{k} = \frac{l}{m}$, where $l, m \in \mathbb{Z}$, $m < k$. Then the condition (2.37) can be rewritten as*

$$c_\Sigma \cdot \xi_{l,m} = 0,$$

where

$$c_\Sigma = \begin{pmatrix} c_0 + c_m + ... + c_{k-m} \\ c_1 + c_{m+1} + ... + c_{k-m+1} \\ ... \\ c_{m-1} + c_{2m-1} + ... + c_{k-1} \end{pmatrix}$$

Proof. Noticing that $\lambda_{n,k} = \lambda_{l,m}$ and that $\xi_{n,k}$ is a compound of l copies of $\xi_{l,m}$, i.e. $\xi_{n,k} = (\xi_{l,m}, \xi_{l,m}, ..., \xi_{l,m})^T$, the proof is straightforward. □

This proposition is illustrated in Table 2.1. For example, let $k = 6$ and $n = 2$. Then a common divisor is $m = 2$ and a condition on the c's has the same form as for $k' = 6/2 = 3$ and $n' = 2/2 = 1$, namely $c_0 = c_1 = c_2$, but instead of c_0, c_1 and c_2 we have sums: $c_0 + c_3$, $c_1 + c_4$ and $c_2 + c_5$ respectively. The same analogy we observe for $k = 4$ and $n = 2$, for $k = 6$ and $n = 3$ etc.

Table 2.1 gives a complete list of families of nontrivial nonnegative singular circulants of order $k = 2, ..., 9, 12$. It can be extended to other orders without much difficulty. 'Divisor' is a divisor of k. The number $n = \frac{k}{\text{divisor}} \bmod k$. μ is the corresponding root of the representer, $\mu = e^{i\frac{2\pi n}{k}}$. The function $\mathbf{f}_{k,n}(c_0, ..., c_k)$ is given by (5.2). The parameter *dim* is the dimension of the family, i.e. the number of free components c_i of the circulant (since $\sum_{i=0}^{k-1} c_i = 1$ we have *dim* is $k-2$ if $\mu = -1$ and $k-3$ otherwise).

2.6 k-cycles on affine subsets.

In the case of uniform impact we have found a simplex filled with k-cycles (Theorem 2.8). The aim of this section is to find, in each case of a singular circulant, a geometrical object in $\mathbb{R}^k_+$ filled with a family of k-cycles. We show that these are the intersection of either a line or a plane with the positive cone.

Theorem 2.22. *Let $\lambda_{n,k} = e^{i\frac{2\pi n}{k}}$ be a root of the representer of a nonnegative singular circulant C of order k with $\sum_{i=0}^{k-1} c_i = 1$.*

i) If $\lambda_{n,k} = -1$ (i.e., k is even and $n = \frac{k}{2}$), the line segment $\mathcal{L}_k$ defined by

$$\mathcal{L}_k = \{N : \begin{matrix} N_{2j} & = \bar{I}(1+p) \\ N_{2j+1} & = \bar{I}(1-p) \end{matrix}, j = 0, 1, ... \tfrac{k}{2} - 1;\ -1 \le p \le 1\}$$

k	divisor	n	μ	dim	family description
2	2	1	-1	0	$c_0 = c_1 = \frac{1}{2}$
3	3	1	$e^{i\frac{2\pi}{3}}$	0	$c_0 = c_1 = c_2 = \frac{1}{3}$
4	2	2	-1	2	$c_0 + c_2 = c_1 + c_3 = \frac{1}{2}$
	4	1	$e^{i\frac{\pi}{2}}$	1	$c_0 = c_2$ $c_1 = c_3 = \frac{1}{2} - c_0$
5	5	1	$e^{i\frac{2\pi}{5}}$	2	$c_0 + (c_1 + c_4)\cos\frac{2\pi}{5} - (c_2 + c_3)\cos\frac{\pi}{5} = 0$ $(c_1 - c_4)\sin\frac{2\pi}{5} + (c_2 - c_3)\sin\frac{\pi}{5} = 0$
	5	2	$e^{i\frac{4\pi}{5}}$	2	$c_0 - (c_1 + c_4)\cos\frac{\pi}{5} + (c_2 + c_3)\cos\frac{2\pi}{5} = 0$ $(c_1 - c_4)\sin\frac{\pi}{5} - (c_2 - c_3)\sin\frac{2\pi}{5} = 0$
6	2	3	-1	4	$\sum c_{2i} = \sum c_{2i+1} = \frac{1}{2}$
	3	2	$e^{i\frac{2\pi}{3}}$	3	$c_0 + c_3 = c_1 + c_4 = c_2 + c_5 = \frac{1}{3}$
	6	1	$e^{i\frac{\pi}{3}}$	3	$(c_0 - c_3) + \frac{1}{2}(c_1 + c_5) - \frac{1}{2}(c_2 + c_4) = 0$ $c_1 + c_2 = c_4 + c_5$
7	7	1	$e^{i\frac{2\pi}{7}}$	4	$c_0 + (c_1 + c_6)\cos\frac{2\pi}{7} - (c_2 + c_5)\cos\frac{3\pi}{7} - (c_3 + c_4)\cos\frac{\pi}{7} = 0$ $(c_1 - c_6)\sin\frac{2\pi}{7} + (c_2 - c_5)\sin\frac{3\pi}{7} + (c_3 - c_4)\sin\frac{\pi}{7} = 0$
	7	2	$e^{i\frac{4\pi}{7}}$	4	$c_0 - (c_1 + c_6)\cos\frac{3\pi}{7} - (c_2 + c_5)\cos\frac{\pi}{7} + (c_3 + c_4)\cos\frac{2\pi}{7} = 0$ $(c_1 - c_6)\sin\frac{3\pi}{7} - (c_2 - c_5)\sin\frac{\pi}{7} - (c_3 - c_4)\sin\frac{2\pi}{7} = 0$
	7	3	$e^{i\frac{6\pi}{7}}$	4	$c_0 - (c_1 + c_6)\cos\frac{\pi}{7} + (c_2 + c_5)\cos\frac{2\pi}{7} - (c_3 + c_4)\cos\frac{3\pi}{7} = 0$ $(c_1 - c_6)\sin\frac{\pi}{7} - (c_2 - c_5)\sin\frac{2\pi}{7} + (c_3 - c_4)\sin\frac{3\pi}{7} = 0$
8	2	4	-1	6	$\sum c_{2i} = \sum c_{2i+1} = \frac{1}{2}$
	4	2	$e^{i\frac{\pi}{2}}$	5	$c_0 + c_4 = c_2 + c_5$ $c_1 + c_6 = c_3 + c_7$
	8	1	$e^{i\frac{\pi}{4}}$	5	$(c_0 - c_4) + \frac{1}{\sqrt{2}}((c_1 + c_7) - (c_3 + c_5)) = 0$ $(c_2 - c_6) + \frac{1}{\sqrt{2}}((c_1 - c_7) + (c_3 - c_5)) = 0$
	8	3	$e^{i\frac{3\pi}{8}}$	5	$c_0 + (c_1 + c_7)\cos\frac{3\pi}{8} - \frac{1}{\sqrt{2}}(c_2 + c_6) - (c_3 + c_5)\cos\frac{\pi}{8} = 0$ $-c_4 + (c_1 - c_7)\sin\frac{3\pi}{8} + \frac{1}{\sqrt{2}}(c_2 - c_6) - (c_3 - c_5)\sin\frac{\pi}{8} = 0$
9	3	3	$e^{i\frac{2\pi}{3}}$	6	$c_0 + c_3 + c_6 = c_1 + c_4 + c_7 = c_2 + c_5 + c_8 = \frac{1}{3}$
	9	1	$e^{i\frac{2\pi}{9}}$	6	$\mathbf{f}_{9,1}(c_0, ..., c_8) = 0$
	9	2	$e^{i\frac{4\pi}{9}}$	6	$\mathbf{f}_{9,2}(c_0, ..., c_8) = 0$
	9	4	$e^{i\frac{8\pi}{9}}$	6	$\mathbf{f}_{9,4}(c_0, ..., c_8) = 0$
12	2	6	-1	10	$\sum c_{2i} = \sum c_{2i+1} = \frac{1}{2}$
	3	4	$e^{i\frac{2\pi}{3}}$	9	$\sum c_{3i} = \sum c_{3i+1} = \sum c_{3i+2} = \frac{1}{3}$
	4	3	$e^{i\frac{\pi}{2}}$	9	$\sum c_{4i} = \sum c_{4i+2}$ $\sum c_{4i+1} = \sum c_{4i+3}$
	6	2	$e^{i\frac{\pi}{3}}$	9	$\mathbf{f}_{6,1}(c_0 + c_6, ..., c_5 + c_{11}) = 0$
	12	1	$e^{i\frac{\pi}{6}}$	9	$\mathbf{f}_{12,1}(c_0, ..., c_{11}) = 0$
	12	5	$e^{i\frac{5\pi}{6}}$	9	$\mathbf{f}_{12,5}(c_0, ..., c_{11}) = 0$

Table 2.1: A list of conditions for a nontrivial nonnegative circulant of order k to be singular. See explanations in the text.

is both contained in the set $\{N : CN = \mathbf{1}\bar{I}\}$ *(i.e.* $\mathcal{L}_k$ *is a one-parameter family of solutions of the system (2.26)) and invariant under* S *.*

ii) In all other cases the set $\mathcal{P}_{n,k}$ *defined by*

$$\begin{aligned}\mathcal{P}_{n,k} = \quad & \{N : \ N = \bar{I}(\mathbf{1} + p \operatorname{Re} \xi_{n,k} + q \operatorname{Im} \xi_{n,k}), \\ & \textit{where } p \textit{ and } q \textit{ are real numbers such that } N \textit{ is nonnegative}\},\end{aligned}$$

(with $\xi_{n,k}$ *given by (2.34)), is both contained in* $\{N : CN = \mathbf{1}\bar{I}\}$ *and invariant under* S *.*

Proof. We begin with the second assertion. The condition for singularity of the circulant is (2.37)

$$c \cdot \xi_{n,k} = 0.$$

It is invariant under S , i.e.,

$$S^m c \cdot \xi_{n,k} = 0, \quad m = 0, 1, ..., k-1.$$

The equation $CN = \mathbf{1}\bar{I}$ we can write as

$$\begin{aligned} c \cdot N \quad &= \bar{I} \\ Sc \cdot N \quad &= \bar{I} \\ &\dots \\ S^{k-1} c \cdot N \quad &= \bar{I}. \end{aligned}$$

We substitute $N \in \mathcal{P}_{n,k}$ in each of the equations above and get

$$S^m c \cdot \mathbf{1}\bar{I} + p\, S^m c \cdot \operatorname{Re} \xi_{n,k} + q\, S^m c \cdot \operatorname{Im} \xi_{n,k} = \bar{I}.$$

The last two terms vanish and, since the sum of c_i is one, this is indeed a true identity for all m . Hence $\mathcal{P}_{n,k}$ is contained in $\{N : CN = \mathbf{1}\bar{I}\}$.

To show that $\mathcal{P}_{n,k}$ is invariant under S , rewrite the expression for N as

$$N = \bar{I}(\mathbf{1} + \operatorname{Re}(a\, \xi_{n,k})), \tag{2.41}$$

where $a = p - iq$ is a complex number such that N is nonnegative. This is indeed the case if

$$1 + \operatorname{Re}(a\, \lambda_{n,k}^{-j}) \geq 0 \quad \text{for all } j = 0, 1, ..., k-1. \tag{2.42}$$

Since $\xi_{n,k}$ is the eigenvector of S and $\lambda_{n,k}$ is the corresponding eigenvalue

$$SN = \bar{I}(\mathbf{1} + \operatorname{Re}(b\, \xi_{n,k}))$$

with $b = \lambda_{n,k}\, a$. Clearly, if the conditions (2.42) are satisfied for a, they are also satisfied for b, because we just apply the shift to the system of inequalities (2.42). Indeed,

$$1 + \mathrm{Re}\,(b\,\lambda_{n,k}^{-j}) = 1 + \mathrm{Re}\,(a\,\lambda_{n,k}^{-(j-1)}) \geq 0.$$

And hence $\mathcal{P}_{n,k}$ is invariant under the shift.

Let now k be even and consider the eigenvalue $\lambda_{k/2,k} = -1$. Then $\mathrm{Im}\,\xi_{k/2} = 0$ and $\mathcal{P}_{n,k}$ reduces to the line segment $\mathcal{L}_k$. □

Corollary 2.23. *Every point on the line segment $\mathcal{L}_k$ is 2-periodic.*

It is rather simple to visualize the line segment $\mathcal{L}_k$. The end points of this segment are two points with coordinates $(0, 2\bar{I}, 0, 2\bar{I}, ..., 0, 2\bar{I})$ and $(2\bar{I}, 0, 2\bar{I}, 0, ..., 2\bar{I}, 0)$, so each of them lies in a $\frac{k}{2}$-dimensional coordinate hyperplane. We now try to develop a geometric "feeling" concerning the invariant sets $\mathcal{P}_{n,k}$ and the dynamics on them. We can rewrite $\mathcal{P}_{n,k}$ as follows:

$$\begin{aligned}\mathcal{P}_{n,k} := \quad & \{N :\ N = \bar{I}(\mathbf{1} + \mathrm{Re}\,(a\,\xi_{n,k})),\\ & \text{with } a \in \mathbb{C} \text{ such that } N \geq 0, \text{ i.e. such that (2.42) holds.}\},\end{aligned} \tag{2.43}$$

Corollary 2.24. *Let $\frac{n}{k} = \frac{l}{m}$, where $\frac{l}{m}$ is the irreducible fraction. Every point N on $\mathcal{P}_{n,k}$ is m-periodic (with m as minimal period). And if we join points $\{N, SN, ..., S^{m-1}N, N\}$ successively by line segments, we obtain a regular (simple or star-shaped) polygon with m vertices (a so-called m-gon).*

Proof. We have $S^m N = \bar{I}(\mathbf{1} + \mathrm{Re}\, a\, S^m \xi_{n,k})$ and $S^m \xi_{n,k} = \lambda_{n,k}^m \xi_{n,k} = e^{i\frac{2\pi n}{k}m}\xi_{n,k} = e^{i\frac{2\pi l}{m}m}\xi_{n,k} = \xi_{n,k}$. Hence $S^m N = N$.

We notice that the distance between two successive points from $\{N, SN, ..., S^{m-1}N, N\}$ is determined by differences $|N_i - N_{i+1}|$, with $i = 0, ..., k-1$, and thus the same for all pairs $\{S^j N, S^{j+1}N\}$, $j = 0, ..., m-1$. The same for the angles between $S^{j+1}N - S^j N$ and $S^{j-1}N - S^j N$. □

Corollary 2.25. *Let $\frac{n}{k} = \frac{l}{m}$, where $\frac{l}{m}$ is the irreducible fraction. The set $\mathcal{P}_{n,k}$ is a regular filled m-gon with the vertices given by $a = \frac{1}{\cos(\pi/m)} e^{i(\pi + \frac{\pi + 2\pi j}{m})}$, $j = 0, ..., m-1$.*

Proof. If $\frac{n}{k} = \frac{l}{m}$, where $\frac{l}{m}$ is the irreducible fraction, the number of independent inequalities in (2.42) is m. Let us define a set $\mathcal{P}_{n,k}^{\mathbb{C}}$ of all possible

values of a:

$$\mathcal{P}^{\mathbb{C}}_{n,k} := \{a \in \mathbb{C} : \ 1 + \mathrm{Re}\,(a\, e^{i\frac{2\pi j}{m}}) \geq 0 \quad \text{for all } j = 0, 1, ..., m-1, \tfrac{l}{m} = \tfrac{n}{k}\}. \tag{2.44}$$

This set is a filled regular m-gon in the complex plane. To see we notice that for $\phi \in (\pi - \frac{\pi}{m}, \pi + \frac{\pi}{m})$ with $a = re^{i\phi}$

$$\min_{j=0,...,m-1} \mathrm{Re}\,(a\, e^{i\frac{2\pi j}{m}}) = 1 + r\cos\phi$$

and hence for these values of ϕ $r \leq \left|\frac{1}{\cos\phi}\right|$. This inequality and the restrictions on ϕ define a filled triangle in the complex plane with vertices 0 and $\frac{1}{\cos(\pi/m)} e^{i(\pi \pm \frac{\pi}{m})}$. This consideration remains valid if we replace ϕ by $\phi + \frac{2\pi j}{m}$, $m = 0, ..., j-1$. Therefore we obtain m equal filled triangles by the rotation over $\frac{2\pi j}{m}$, which form the regular m-gon.

The set $\mathcal{P}_{n,k}$ (consisting of k-dimensional vectors) can be obtained by the linear transformation (given in (2.43)) from the set $\mathcal{P}^{\mathbb{C}}_{n,k}$ of complex numbers. We notice also that the distance between any two points on $\mathcal{P}_{n,k}$ is determined only by the difference between the corresponding a's, and that therefore angles and ratios are preserved under the transformation from $\mathcal{P}^{\mathbb{C}}_{n,k}$ to $\mathcal{P}_{n,k}$. So, we conclude that $\mathcal{P}_{n,k}$ is a filled regular m-gon too. □

The boundary of the filled polygon is determined by the fact that at least one or at most two inequalities in (2.44) turn to be equalities. The first case corresponds to an edge of the polygon and the latter to a vertex.

If $\frac{n}{k}$ is irreducible, this translates to the fact that the vertices of the polygon $\mathcal{P}_{n,k}$ lie in coordinate hyperplanes of codimension 2, in other words, points of $\mathcal{P}_{n,k}$ corresponding to the vertices have two zero components, and the edges of $\mathcal{P}_{n,k}$ lie in hyperplanes of codimension 1, i.e., have one zero component. In particular in the case $k = 3$ the vertices of the equilateral triangle, which $\mathcal{P}_{1,3} = \mathcal{P}_{2,3} = \{N_0 + N_1 + N_2 = \bar{I},\}$ is in this case, lie on coordinate axes and the edges on coordinate planes.

If, on the contrary, $\frac{n}{k}$ is reducible and $\frac{n}{k} = \frac{l}{m}$ with $m < k$, then for a point N on the edge of the polygon, there are $\frac{k}{m}$ different components of N which are equal to zero, and $\frac{2k}{m}$ zero components for a vertex. For example, let $k = 6$ and $n = 2$. The set $\mathcal{P}_{2,6}$ is given explicitly by

$$\mathcal{P}_{2,6} = \{N_0 = N_3, N_1 = N_4, N_2 = N_5, N_0 + N_1 + N_2 = \bar{I}\}.$$

Clearly, e.g., one of the vertices of the polygon lies in the coordinate plane $N_0 = N_3 = N_1 = N_4 = 0$.

If the representer of the circulant C has several roots which are different (and not complex conjugate) roots of unity, we have a result similar to Theorem 2.22. A family of k-periodic points is not (a part of) a line or a plane, but a simplex of dimension equal to the number of such roots, counting complex conjugate roots as different and not counting multiplicity of the roots of the representer. (The last remark follows from the fact that C has always k *different* eigenvectors $\xi_{n,k}, n = 0, ..., k-1$ because of (2.35); hence the dimension of its null-space (which is also the dimension of the family of k-periodic points of (1.7)) is equal to the number of *different* $\lambda_{n,k}$ which are roots of the representer.

Theorem 2.26. *Let* $\lambda_{n_j,k} = e^{i\frac{2\pi n_j}{k}}$ *, for* $j = 1, ..., q$ *and* $1 \le n_1 < n_2 < ... < n_q \le \frac{k}{2}$ *, be roots of the representer of a nonnegative singular circulant* C *of order* k *with* $\sum_{i=0}^{k-1} c_i = 1$ *. The set* $\mathcal{P}_{\mathbf{n},k}$ *with* $\mathbf{n} = (n_1, ..., n_q)^T$ *defined by*

$$\begin{aligned}\mathcal{P}_{\mathbf{n},k} = \quad & \{N : \ N = \bar{I}(\mathbf{1} + \sum_{j=1}^{q} \mathrm{Re}\,(a_j\, \xi_{n_j,k})), \\ & \textit{where } a_j \in \mathbb{C} \textit{ are such that } N \textit{ is nonnegative}\},\end{aligned}$$

(with $\xi_{n,k}$ *given by (2.34)), is both contained in* $\{N : CN = \mathbf{1}\bar{I}\}$ *and invariant under* S *.*

The proof of this theorem is completely similar to the proof of Theorem 2.22.

2.7 Nonlinear circulant.

In Section 2.4 we have observed that the system (2.24) has a uniform solution $I_0 = ... = I_{k-1} = \bar{I}$. And for this solution we have found, in Section 2.5, conditions on the parameters c_i , under which the recursion (1.7) possesses families of cycles with all year classes present. Now we ask whether (2.24) can have a nonuniform solution or even a family of solutions. We are especially interested in this last possibility because this is exactly what happens in the case of vertical bifurcation.

Theorem 2.27. *If* $k-1$ *ratios* $\frac{h_i}{h_{i+1}}(I)$ *are all monotone increasing/decreasing (with one strictly increasing/decreasing), the system (2.24) has only* $I_0 = ... = I_{k-1} = \bar{I}$ *as a solution.*

Proof. Denote the ratios $\frac{h_i}{h_{i+1}}(I)$ by $h_{i\,i+1}$. We divide the second equation in (2.24) by the first, the third by the second etc. and the first by the last.

In this way we obtain

$$\begin{aligned}
&h_{01}(I_1)\, h_{12}(I_2)...h_{k-2\,k-1}(I_{k-1}) &&= h_{01}(I_0)\, h_{12}(I_0)...h_{k-2\,k-1}(I_0)\\
&h_{01}(I_2)\, h_{12}(I_3)...h_{k-2\,k-1}(I_0) &&= h_{01}(I_1)\, h_{12}(I_1)...h_{k-2\,k-1}(I_1)\\
&... \\
&h_{01}(I_0)\, h_{12}(I_1)...h_{k-2\,k-1}(I_{k-2}) &&= h_{01}(I_{k-1})\, h_{12}(I_{k-1})...h_{k-2\,k-1}(I_{k-1}).
\end{aligned}$$

If I_0 is the largest or the smallest of all I_i, the first identity can not be satisfied. The same can be said about I_j and the $j+1$-th identity above. Thus none of the values I_i can be the largest or the smallest, hence they are all equal. □

For $k=2$ we have the following corollary.

Corollary 2.28. *If $\frac{h_0}{h_1}(I)$ is strictly monotone, the system*

$$\begin{aligned}
h_0(I_0)\, h_1(I_1) &= 1\\
h_1(I_0)\, h_0(I_1) &= 1
\end{aligned} \tag{2.45}$$

has only $I_0 = I_1 = \bar{I}$ as a solution.

For $k=3$ we can relax the assumption of Theorem 2.27, i.e., we can also deal with the case in which two (necessarily successive) ratios are monotone in opposite directions.

Theorem 2.29. *If two ratios $\frac{h_i}{h_j}(I)$, $i,j=0,...,2$, $i \neq j$ are monotone (and at least one of them is strictly monotone), the system*

$$\begin{aligned}
h_0(I_0)\, h_1(I_1)\, h_2(I_2) &= 1\\
h_2(I_0)\, h_0(I_1)\, h_1(I_2) &= 1\\
h_1(I_0)\, h_2(I_1)\, h_0(I_2) &= 1
\end{aligned} \tag{2.46}$$

has only $I_0 = I_1 = I_2 = \bar{I}$ as a solution.

Proof. If the two successive ratios $h_{i\,i+1}, i=0,1$ are monotone in the same manner, then the result is a special case of Theorem 2.27. Let now h_{01} be increasing and h_{12} decreasing (or h_{01} decreasing and h_{12} increasing). Then dividing the first equation of (2.46) by the third and the second by the first we have

$$\begin{aligned}
h_{01}(I_0)h_{21}(I_2) &= h_{01}(I_2)h_{21}(I_1)\\
h_{01}(I_1)h_{21}(I_0) &= h_{01}(I_0)h_{21}(I_2)
\end{aligned}$$

If I_2 lies between I_0 and I_1, the first identity can not be satisfied. The same can be said about I_0 and the second identity. Hence $I_0 = I_1 = I_2$. When h_{20} and h_{01} are monotone in opposite ways the same conclusion can be derived in the same way. □

Notice that for the families (2.18) and (2.19) we have that the ratios of the sensitivity functions are strictly monotone if the corresponding parameters g_i are not equal. Hence we have the following corollary of the results above.

Corollary 2.30. *Consider the Ricker family (2.18) or the Beverton-Holt family (2.19).*

i) Let $k = 2$. If $g_0 \neq g_1$ and $c_0 \neq c_1$ there can exist no cycle with minimal period 2 in the interior of the phase space. If $g_0 = g_1$ there exists a one-parameter family of 2-cycles in (the interior of) the phase space.

ii) Let $k = 3$. If not all g's are equal and not all c's are equal there can exist no cycle with minimal period 3 in the interior of the phase space. If $g_0 = g_1 = g_2$ there exists a two-parameter family of 3-cycles in (the interior of) the phase space.

In other words we have "all or nothing": either there is an whole family of cycles or there is no cycle at all. The first case corresponds to the vertical bifurcation. In each case the second assertion follows directly from Corollary 2.11. The first assertion of i) is also given (in a slightly different form) in Section 3.4.

Notice that the ratio of two functions h_0 and h_1 from the same parameter family (2.17) is not necessarily monotone if $g_0 \neq g_1$. Indeed,

$$\begin{aligned} \operatorname{sign}\left(\tfrac{d}{dI}\,\tfrac{h_0(I)}{h_1(I)}\right) &= \operatorname{sign}\left(\tfrac{h_0'(I)}{h_0(I)} - \tfrac{h_1'(I)}{h_1(I)}\right) \\ &= \operatorname{sign}\left(\tfrac{g_0 I\, H'(g_0 I)}{H(g_0 I)} - \tfrac{g_1 I\, H'(g_1 I)}{H(g_0 I)}\right). \end{aligned}$$

I.e. $\frac{h_0}{h_1}(I)$ is monotone in this case if and only if $\frac{IH'(I)}{H(I)}$ is monotone. This last function is called *elasticity* [Caswell]. Let us give an example of a function with nonmonotone elasticity (which, in addition, satisfies the normalization assumptions (2.9))

$$H(I) = \tfrac{1}{3}(2 + \cos I)\, e^{-I}.$$

And indeed, the ratio

$$\frac{h_0}{h_1}(I) = \frac{2 + \cos g_0 I}{2 + \cos g_1 I}\, e^{(g_1 - g_0)x}$$

is nonmonotone, for example, for $g_0 = .4$ and $g_1 = .6$.

In Section 3.11 we consider the case $k = 2$ and a nonmonotone ratio of sensitivity functions. We show that in this case an isolated 2-cycle can exist

in the interior of the phase space and that we can have a normal period-doubling bifurcation instead of the vertical one.

Let us now consider general $k > 3$. As we have already said, the system (2.24) has always the uniform solution $I_0 = ... = I_{k-1} = \bar{I}$. From the Implicit Function Theorem it follows that there are no other solutions in a neighbourhood of it, if the derivative of the left-hand side of (2.24) at the point $I_0 = ... = I_{k-1} = \bar{I}$ is non-singular. Of particular interest is the case when the derivative is singular. Indeed, new solution branches can appear in the neighbourhood of the uniform solution in this case. The Jacobian of the left-hand side of (2.24) at the point $I_0 = ... = I_{k-1} = \bar{I}$ is

$$\begin{pmatrix} h'_0 & (\bar{I}) & h'_1 & (\bar{I}) & ... & h'_{k-1} & (\bar{I}) \\ h'_{k-1} & (\bar{I}) & h'_0 & (\bar{I}) & ... & h'_{k-2} & (\bar{I}) \\ ... & & & & & & \\ h'_1 & (\bar{I}) & h'_2 & (\bar{I}) & ... & h'_0 & (\bar{I}) \end{pmatrix}$$

(recall that $\forall j \; h_j(\bar{I}) = 1$). This is again a circulant matrix. Hence the condition for its degeneracy is

$$h'(\bar{I}) \cdot \xi_{n,k} = 0. \tag{2.47}$$

Of course, it is not guaranteed that a system with a zero Jacobian possesses a family of solutions. The question, what further conditions on the functions h_i are required to guarantee this, we leave open.

To train our intuition we first consider a specific example. Let all the functions h_i be of Ricker type (2.18). Then the nonlinear circulant in the left hand side of (2.24) reduces to a linear circulant and (2.24) can be rewritten as

$$\begin{array}{llllll} g_0 & I_0 + & g_1 I_1 + & ... & + g_{k-1} & I_{k-1} & = \bar{I} \\ g_{k-1} & I_0 + & g_0 I_1 + & ... & + g_{k-2} & I_{k-1} & = \bar{I} \\ ... & & & & & & \\ g_1 & I_0 + & g_2 I_1 + & ... & + g_0 & I_{k-1} & = \bar{I} \end{array}$$

(noticing that $\sum g_i = 1$) or

$$G\,\mathbf{I} = \mathbf{1}\bar{I}, \tag{2.48}$$

where $\mathbf{I}$ is the vector $(I_0, I_1, ..., I_{k-1})$. This system has a family of solutions if the circulant G (generated by the vector g) is singular. So all the results of Section 2.5 are once again relevant.

If G is singular, we can find a family of solutions of the circulant system above in the way of Section 2.6. By doing that we find a line or a plane but no longer in the phase space with points $\{N_0, ..., N_{k-1}\}$, but in the space of

environmental conditions with points $\{I_0, ..., I_{k-1}\}$.

The desire is now to reduce somehow the nonlinear circulant to a linear one and use the knowledge we have about linear circulants. The trick is to transform the multiplicative structure into additive structure introducing the functions

$$g_i(I) := \ln h_i(I).$$

Then

$$h_i(I) = \exp g_i(I)$$

and the system (2.24) becomes

$$\begin{array}{llllll} g_0 & (I_0) & + & g_1(I_1)+ & ... & + g_{k-1} & (I_{k-1}) & = 0 \\ g_{k-1} & (I_0) & + & g_0(I_1)+ & ... & + g_{k-2} & (I_{k-1}) & = 0 \\ ... & & & & & & & \\ g_1 & (I_0) & + & g_2(I_1)+ & ... & + g_0 & (I_{k-1}) & = 0, \end{array} \tag{2.49}$$

which we rewrite in a symbolic form (analogous to (2.48)) as

$$G(g, \mathbf{I}) = 0. \tag{2.50}$$

We look for vertical bifurcations, i.e. we ask the question: when does the system (2.50) have a family of solutions? It is, we think, impossible to answer this question fully without specifying the functions $g_i(I)$. But some special (and relatively easy) cases, like the one of Theorem 2.9, can be traced. In particular, we make the following evident statement: a system of k equations with k unknowns can have a family of solutions if (at least) one equation is a *linear combination* of the others. This is neither a sufficient nor a necessary condition, but it helps to find a partial answer to the question above.

We come back for a minute to the linear circulant G. It is singular if

$$g \cdot \xi_{n,k} = 0 \tag{2.51}$$

(see (2.37)). We write the matrix G as

$$G = \begin{pmatrix} g \\ Sg \\ ... \\ S^{k-1}g \end{pmatrix}$$

and consider a linear combination of the rows

$$(\mathrm{Re}\,(g \cdot \xi_{n,k}) \quad \mathrm{Re}\,(Sg \cdot \xi_{n,k}) \quad ... \quad \mathrm{Re}\,(S^{k-1}g \cdot \xi_{n,k}))^T.$$

Because of (2.51) and $S^m g \cdot \xi_{n,k} = g \cdot S^{-m}\xi_{n,k} = e^{i\frac{2\pi n}{k}m} g \cdot \xi_{n,k}$, this vector is *zero*. A linear combination of the rows consisting of the imaginary parts of $S^m g \cdot \xi_{n,k}$ is also zero. The linear combination is trivial if k is even and $n = \frac{k}{2}$ since in this case $\operatorname{Im} \xi_{n,k} = 0$. Therefore the rank of G is (at most) $k-1$ in this last case, or (at most) $k-2$ otherwise.

Arguing in exactly the same way, we notice that if

$$\exists\, 0 < n \leq \tfrac{k}{2} : \forall I \geq 0 \quad g(I) \cdot \xi_{n,k} = 0 \tag{2.52}$$

the nonlinear circulant system (2.49) can have a family of solutions. Indeed, making the same linear combinations as in the case of linear circulants, we can get rid of two (or, in the case $n = \frac{k}{2}$, one) equations. Therefore, we obtain a system of $k-2$ (respectively, $k-1$) equations with k unknowns which possesses, generally speaking, a two- (one-) parameter family of solutions.

Just as in the case of a linear circulant, we can restrict ourselves to the interval $n \in [0, \frac{k}{2}]$ (see Remark after (2.37)) because other values of n give the same conditions on $g(I)$. We exclude $n = 0$ because in this case we have $\sum_{j=0}^{k-1} g_j(I) = 0$ for any I or, in other words,

$$\Pi(I) = \prod_{j=0}^{k-1} h_j(I) = 1 \qquad \forall I,$$

which contradicts the assumption (ii) on Π (after (2.13)).

For low values of k we can rewrite (2.52) in terms of the original functions as follows (cf. Corollary 2.28 and Theorem 2.29):

$$\begin{array}{ll} k=2 & h_0(I) = h_1(I) \\ k=3 & h_0(I) = h_1(I) = h_2(I) \\ k=4 & \begin{array}{l} h_0(I) = h_2(I) \\ h_1(I) = h_3(I) \end{array} \quad \text{or} \quad h_0(I)h_2(I) = h_1(I)h_3(I) \end{array} \tag{2.53}$$

After these motivating considerations, we now formulate some rigorous results and begin with the case: k is even, $n = \frac{k}{2}$ (cf. Proposition 2.19 and Theorem 2.22.i).

Proposition 2.31. *Let k be even and assume that for all $I \geq 0$*

$$\sum_{i=0}^{k/2-1} g_{2i}(I) = \sum_{i=0}^{k/2-1} g_{2i+1}(I)$$

(or, equivalently, $\prod_{i=0}^{k/2-1} h_{2i}(I) = \prod_{i=0}^{k/2-1} h_{2i+1}(I)$ *). The one-parameter set*

$$\begin{cases} I_{2i} & = \bar{I}_0 \\ I_{2i+1} & = \bar{I}_1, \end{cases} \qquad i = 0, ..., \tfrac{k}{2} - 1,$$

with $G_\Sigma(\bar{I}_0) + G_\Sigma(\bar{I}_1) = 0$ *and* $G_\Sigma := \sum_{i=0}^{k-1} g_i$ *, is both contained in* $\{\mathbf{I} : G(g, \mathbf{I}) = 0\}$ *and invariant under the shift* S *.*

Proof. Noticing that $\sum_{i=0}^{k/2-1} g_{2i} = \sum_{i=0}^{k/2-1} g_{2i+1} = \frac{1}{2} G_\Sigma$, the proof is straightforward. □

Thus we have found a family of nonuniform solutions of the nonlinear circulant system (2.49) under a condition on the nonlinearities (which translates into a condition on parameters in case of a parametrized family (2.17)). In the general case (2.52) it is unclear how to obtain a family of nonuniform solutions explicitly. However, in some cases we can simplify the form of the solution and, in particular, notice that the value of the environmental variable I can have periodicity lower than k (cf. Proposition 2.21).

Proposition 2.32. *Let* $m < k$ *be a divisor of* k *. If* $(\bar{I}_0, \bar{I}_1, ..., \bar{I}_{m-1})$ *is a solution of the nonlinear circulant of order* m

$$G(g_\Sigma, \mathbf{I}) = 0 \tag{2.54}$$

defined by the m *-dimensional vector*

$$g_\Sigma = \begin{pmatrix} g_0 + g_m + ... + g_{k-m} \\ g_1 + g_{m+1} + ... + g_{k-m+1} \\ ... \\ g_{m-1} + g_{2m-1} + ... + g_{k-1} \end{pmatrix}, \tag{2.55}$$

then

$$\begin{cases} I_{mi} & = \bar{I}_0 \\ I_{mi+1} & = \bar{I}_1 \\ ... & \\ I_{mi+m-1} & = \bar{I}_{m-1} \end{cases} \qquad i = 0, ..., \tfrac{k}{m} - 1, \tag{2.56}$$

is a solution of the nonlinear circulant of order k *(2.49).*

In addition, if the condition (2.52) is satisfied for g *and* $\frac{n}{k} = \frac{l}{m}$ *with* $l \in \mathbb{Z}$ *, the condition (2.52) on* g *translates into the condition*

$$\exists\, 0 < l \leq \tfrac{m}{2} : \forall I \geq 0 \quad g_\Sigma(I) \cdot \xi_{l,m} = 0.$$

for g_Σ *.*

Proof. If we substitute (2.56) into the nonlinear circulant (2.49) we obtain a $\frac{k}{m}$ –times repetition of the first m equations and the first m equations form the nonlinear circulant (2.54). This proves the first assertion of the proposition. The second assertion can be obtained similarly to Proposition 2.21. □

Now we want to formulate a more general analogue of Theorem 2.9.

Theorem 2.33. *Let (2.52) be satisfied.*

i) If k is even and $n = \frac{k}{2}$, the $(k-1)$-dimensional manifold

$$M_\theta = \{N : N_0 N_2 ... N_{k-2} = \theta N_1 N_3 ... N_{k-1}, \theta > 0\}$$

is mapped by (1.7) onto $M_{\theta^{-1}}$.

ii) In all other cases the $(k-2)$-dimensional manifold

$$M_a = \{N : \ln N \cdot \xi_{n,k} = a\},$$

where a is a complex number, is mapped by (1.7) onto $M_{ae^{-i\frac{2\pi n}{k}}}$. (Here $\ln N$ denotes the vector with components $\ln N_i$.)

Proof. We begin with the second assertion. Let N be contained in M_a for a certain a. Then for the image N' of N under (1.7) we have

$$\begin{aligned}
\ln N' \cdot \xi_{n,k} &= \sum_{i=0}^{k-1} \lambda_{n,k}^{-i} \ln N_{i-1} h_{i-1}(I) \\
&= \lambda_{n,k}^{-1} \left(\sum \lambda_{n,k}^{-(i-1)} \ln N_{i-1} + \sum \lambda_{n,k}^{-(i-1)} \ln h_{i-1}(I) \right) \\
&= \lambda_{n,k}^{-1} \left(\ln N \cdot \xi_{n,k} + g(I) \cdot \xi_{n,k} \right) \\
&= \lambda_{n,k}^{-1} a
\end{aligned}$$

The first assertion follows by restricting to real a (in order to guarantee $N_i > 0$) and by taking $\theta = e^a$. □

For a particular nonuniform solution $(I_0, ..., I_{k-1})$ we can find a corresponding fixed point of the Full-Life-Cycle map using the equation (2.25) which is linear with respect to N. Notice also that this fixed point is also a fixed point of an m-th iterate of the map (1.7) (where m is a divisor of k), if the value of I has periodicity $m < k$. The fixed point exists and is unique if the matrix in the left-hand side of (2.25)

$$\begin{pmatrix}
c_0 & c_1 & ... & c_{k-1} \\
c_1 h_0(I_0) & c_2 h_1(I_0) & ... & c_0 h_{k-1}(I_0) \\
c_2 h_0(I_0) h_1(I_1) & c_3 h_1(I_0) h_2(I_1) & ... & c_1 h_{k-1}(I_0) h_0(I_1) \\
... & & & \\
c_{k-1} h_0(I_0) ... h_{k-2}(I_{k-2}) & c_0 h_1(I_0) ... h_{k-1}(I_{k-2}) & ... & c_{k-2} h_{k-1}(I_0) ... h_{k-3}(I_{k-2})
\end{pmatrix} \tag{2.57}$$

is nonsingular. In the case of uniform sensitivity (see the end of Section 2.4) the determinant of this matrix is zero if and only if the determinant of the corresponding circulant matrix C is singular. We proved that there exists a family of periodic points (Proposition 2.10 and its corollary), i.e. a vertical bifurcation takes place, if C is not singular. We did not manage to construct a family of periodic points in the general case with $k > 3$ and neither we did prove that such a family exists, so below we provide only a conjecture. But first we give a corollary of Theorem 2.33.

Corollary 2.34. *Let (2.52) be satisfied.*

i) If k is even and $n = \frac{k}{2}$, M_θ is invariant under the second iterate of the map (1.7). The restriction of this twice-iterated map to M_θ is a $(k-1)$-dimensional map parametrized by θ. The value of $I = c \cdot N$ performs a two-cycle (see Proposition 2.31).

ii) In all other cases, let $\frac{n}{k} = \frac{l}{m}$, where $\frac{l}{m}$ is the irreducible fraction. The manifold M_a is invariant under the m-times iterated map (1.7). The restriction of this map to M_a is a $(k-2)$-dimensional map parametrized by a (i.e., by $\operatorname{Re} a$ and $\operatorname{Im} a$). The value of $I = c \cdot N$ performs an m-cycle (see Proposition 2.32).

Conjecture 2.35. *Under the corresponding conditions of the corollary above and for $k > 3$.*

i) Fixed points of the second iterate form a one-parameter family of 2-periodic points of (1.7), parametrized by θ.

ii) Fixed points of the m-th iterate form a two-parameter family of m-periodic points of (1.7), parametrized by a.

2.8 The characteristic equation for the internal steady state.

If we put $N(t) = \bar{N} + y(t)$ in (1.7), where $\bar{N} = \mathbf{1}\bar{I}$ is the internal steady state, cf. (2.21), and, for small $y(t)$, Taylor expand and ignore higher than first order terms, we obtain the linearized problem:

$$y(t+1) = S\,y(t) + c \cdot y(t)\; L(h'(\bar{I}))\,\bar{N}.$$

This problem has solutions of the form $y(t) = \mu^t x$ provided x is an eigenvector corresponding to eigenvalue μ, i.e.

$$Sx + c \cdot x\; L(h'(\bar{I}))\,\bar{N} = \mu x. \tag{2.58}$$

Note that the relevant matrix is a rank one perturbation of S. As already observed in Section 2.5, the eigenvalues of S are the k-th roots of unity

$$\lambda_{n,k} = e^{n\frac{2\pi i}{k}}, \qquad n = 0, 1, ..., k-1$$

and the corresponding eigenvectors are

$$\xi_{n,k} = \begin{pmatrix} 1 \\ \lambda_{n,k}^{-1} \\ ... \\ \lambda_{n,k}^{-k+1} \end{pmatrix}.$$

The matrix $S^T = S^{-1}$ has eigenvectors

$$\eta_{n,k} = \frac{1}{k} \begin{pmatrix} 1 \\ \lambda_{n,k} \\ ... \\ \lambda_{n,k}^{k-1} \end{pmatrix} = \frac{1}{k}\bar{\xi}_{n,k},$$

which are normalized such that

$$\eta_{n,k} \cdot \xi_{n',k} = \delta_{nn'}$$

(where the right hand side is the Kronecker δ).

Next we observe that

$$L(h'(\bar{I}))\,\mathbf{1} = Sh'(\bar{I})$$

and that, consequently,

$$\eta_{n,k} \cdot L(h'(\bar{I}))\,\bar{N} = \bar{I}\,\eta_{n,k} \cdot Sh'(\bar{I}) = \bar{I}\,\lambda_{n,k}\eta_{n,k} \cdot h'(\bar{I}).$$

Now let the (unknown) vector α represent x with respect to the basis $\{\xi_{n,k}\}$, i.e., put

$$x = \sum_{n=0}^{k-1} \alpha_n \xi_{n,k},$$

then (2.58) amounts to the system of linear equations

$$\lambda_{n,k}\alpha_n + a\,\bar{I}\,\lambda_{n,k}\eta_{n,k} \cdot h'(\bar{I}) = \mu\,\alpha_n \tag{2.59}$$

with

$$a = \sum_{m=0}^{k-1} \alpha_m\, c \cdot \xi_{m,k}.$$

Theorem 2.36. *The eigenvalues μ are the roots of the characteristic equation*

$$\mu^k - 1 - \bar{I} \sum_{m=0}^{k-1} \lambda_{m,k} \left(\eta_{m,k} \cdot h'(\bar{I})\right) (c \cdot \xi_{m,k}) \prod_{\substack{n=0 \\ n \neq m}}^{k-1} (\mu - \lambda_{n,k}) = 0, \tag{2.60}$$

which can also be written as

$$\mu^k - \bar{I} \sum_{l=0}^{k-1} \mu^l \, S^l c \cdot h'(\bar{I}) - 1 = 0. \tag{2.61}$$

Proof. Write (2.59) as

$$(\mu - \lambda_{n,k})\alpha_n = a \, \bar{I} \, \lambda_{n,k} \eta_{n,k} \cdot h'(\bar{I})$$

and multiply both sides with $c \cdot \xi_{n,k} \prod_{\substack{j=0 \\ j \neq n}}^{k-1} (\mu - \lambda_{j,k})$. Since $\prod_{j=0}^{k-1} (\mu - \lambda_{j,k}) = \mu^k - 1$ this yields the identity

$$(\mu^k - 1)\alpha_n \, c \cdot \xi_{n,k} = a \, \bar{I} \, \lambda_{n,k} (c \cdot \xi_{n,k})(\eta_{n,k} \cdot h'(\bar{I})) \prod_{\substack{j=0 \\ j \neq n}}^{k-1} (\mu - \lambda_{j,k}),$$

which we sum with respect to n to obtain

$$(\mu^k - 1) \, a = a \, \bar{I} \sum_{n=0}^{k-1} \lambda_{n,k} (c \cdot \xi_{n,k})(\eta_{n,k} \cdot h'(\bar{I})) \prod_{\substack{j=0 \\ j \neq n}}^{k-1} (\mu - \lambda_{j,k}).$$

If μ is such that (2.60) does *not* hold then necessarily $a = 0$ and hence, returning to the original form of the equation, we must have that

$$(\mu - \lambda_{n,k}) \, \alpha_n = 0 \quad \text{for } n = 0, 1, ..., k-1.$$

If for all n the inequality $\mu \neq \lambda_{n,k}$ holds then $\alpha_n = 0$ for all n and x is trivial, so not an eigenvector. If $\mu = \lambda_{j,k}$ for some j then $\alpha_n = 0$ for $n \neq j$ and, since we must have that $a = 0$, this requires that $c \cdot \xi_{j,k} = 0$. But then (2.60) is actually satisfied (since all terms in the sum are zero and $\mu^k - 1 = \lambda_{j,k}^k - 1 = 0$). We conclude that, in order for μ to be an eigenvalue, (2.60) must hold. As the left hand side of (2.60) is a polynomial of degree k, it must be the characteristic polynomial.

The rewriting of (2.60) into the form (2.61) involves a few observations. First we note that

$$\prod_{\substack{n=0\\ n\neq m}}^{k-1} (\mu - \lambda_{n,k}) = \frac{\mu^k - 1}{\mu - \lambda_{m,k}} = \sum_{j=0}^{k-1} \mu^{k-1-j} \lambda_{m,k}^{j} = \sum_{l=0}^{k-1} \mu^l \lambda_{m,k}^{-1-l}.$$

Next we note that

$$(\eta_{m,k} \cdot h'(\bar{I}))(c \cdot \xi_{m,k}) = \tfrac{1}{k} \sum_{i=0}^{k-1} \sum_{j=0}^{k-1} h_i'(\bar{I})\, c_j\, \lambda_{m,k}^{i-j}.$$

Finally we note that

$$\sum_{m=0}^{k-1} \lambda_{m,k}^{p} = \begin{cases} k & \text{if } p \text{ is a multiple of } k, \\ 0 & \text{otherwise.} \end{cases}$$

(This can be seen as follows. Since $\lambda_{m,k} = e^{m\frac{2\pi i}{k}}$ we have that $\lambda_{m,k}^{p} = \lambda_{p,k}^{m}$. So if $\lambda_{p,k} = 1$ we do have $\sum_{m=0}^{k-1} \lambda_{m,k}^{p} = k$ while, for $\lambda_{p,k} \neq 1$, we have $\sum_{m=0}^{k-1} \lambda_{m,k}^{p} = \sum_{m=0}^{k-1} \lambda_{p,k}^{m} = \frac{1-\lambda_{p,k}^{k}}{1-\lambda_{p,k}} = 0$.)

Using the first two observations we write the sum in (2.60) as

$$\tfrac{\bar{I}}{k} \sum_{m=0}^{k-1} \sum_{i=0}^{k-1} \sum_{j=0}^{k-1} h_i'(\bar{I}) c_j \sum_{l=0}^{k-1} \mu^l \lambda_{m,k}^{i-j-l}$$

and, after changing the order of summation, we can use the third observation to obtain

$$\bar{I} \sum_{l=0}^{k-1} \mu^l \sum_{i=0}^{k-1} h_i'(\bar{I}) c_{i-l} = \bar{I} \sum_{l=0}^{k-1} \mu^l\, S^l c \cdot h'(\bar{I}).$$

□

Corollary 2.37. *The linearized problem has eigenvalue* $\lambda_{n,k}$ *if and only if either* $c \cdot \xi_{n,k} = 0$ *or* $\eta_{n,k} \cdot h'(\bar{I}) = 0$.

In connection with this corollary, please observe that $c \cdot \xi_{0,k} = 1$ and $\eta_{0,k} \cdot h'(\bar{I}) < 0$ (recall the assumption (ii) concerning Π after 2.13). Since $\lambda_{n,k}$ is on the unit circle, the condition $c \cdot \xi_{n,k} = 0$ is a local bifurcation condition. In fact, however, a "vertical" bifurcation occurs as we already know: recall Theorem 2.22 and Lemma 2.16 with the equality (2.37)

Also note that $\eta_{n,k} \cdot h'(\bar{I}) = 0$ iff $h'(\bar{I}) \cdot \xi_{n,k} = 0$ and that, unless k is even and $n = \frac{k}{2}$, if $\lambda_{n,k}$ is an eigenvalue so is $\lambda_{k-n,k}$ (indeed,

$\bar{\lambda}_{n,k} = \lambda_{k-n,k}, \bar{\xi}_{n,k} = \xi_{k-n,k}, \bar{\eta}_{n,k} = \eta_{k-n,k}$). This is also a condition for a local bifurcation of the internal steady state, but it does not imply, generally speaking, a vertical bifurcation. For a counter example see Section 3.11. However, in some cases (Ricker and Beverton-Holt) it *does* correspond to a vertical bifurcation. Notice also that the identity $h'(\bar{I}) \cdot \xi_{n,k} = 0$ coincides exactly with the condition (2.47) for zero Jacobian of the nonlinear circulant (2.24).

If $\mu = 1$ the characteristic polynomial in the left-hand side of (2.61) becomes

$$\begin{aligned} -\bar{I} \sum_{l=0}^{k-1} S^l c \cdot h'(\bar{I}) &= -\bar{I} \sum_{j=0}^{k-1} c_j \sum_{l=0}^{k-1} h'_l(\bar{I}) \\ &= -\bar{I} \sum_{l=0}^{k-1} h'_l(\bar{I}) > 0. \end{aligned}$$

This expression is positive because all functions h are non-increasing and at least one h is strictly decreasing. So, we have the following

Corollary 2.38. *$\mu = 1$ is never a root of the characteristic equation (2.61) (as to be expected from the uniqueness of the internal steady state).*

Of course, the characteristic equation (2.60)/(2.61) may also have roots on the unit circle away from the k-th roots of unity. In Chapter 4 we shall analyse the details for the relatively simple case $k = 3$.

2.9 The other extreme: SYC and transversal stability.

Thus far we have more or less concentrated on (the stability of) steady states in which all year classes are present and on certain degenerate bifurcation phenomena associated with singular circulants. The other extreme is the case in which a single year class (SYC) dominates the world, as it happens in the cicada species mentioned in the introduction. The "Full-Life-Cycle map" is defined as the k-th iterate of the map featuring in (1.7). Our first result is a direct consequence of (2.22).

Lemma 2.39. *The set $\{N : N_j = 0$ for some $j\}$ is invariant under the full life cycle map.*

If we consider an orbit of the full life cycle map, we say that as many year classes are *missing* as there are indices j for which $N_j = 0$. The extreme case is when all but one year classes are missing. Note that indeed we have a

Corollary 2.40. *All coordinate axes are invariant under the full life cycle map.*

The dynamics generated by the restriction of the full life cycle map to an invariant axis is called SYC-dynamics. It is studied in Chapter 5, to which we refer for further information (note that the restriction to the various axes are "equivalent", but *not* necessarily by a homeomorphism). Here we focus on another aspect, the *transversal stability*: do perturbations away from the invariant axis damp out or grow? Or, in biological terms, is a missing year class, when introduced in small numbers, doomed to go extinct or will it persist?

Because of the invariance described in Lemma 2.39, there is indeed a well defined eigenvalue/multiplier associated with each of the missing year classes, so the biological terminology and the mathematical formulations are in precise correspondence.

Every fixed point of the full life cycle map corresponds to a k-periodic orbit of the original recursion (1.7). So, in particular, the environmental variable I is k-periodic.

Now consider a SYC fixed point. Let $I_0, I_1, ..., I_{k-1}$ denote the values I takes and let the numbering be chosen such that $N_0 > 0$ when I_0 prevails. According to (2.23) we then need to have that

$$\prod_{i=0}^{k-1} h_i(I_i) = 1. \tag{2.62}$$

Next, observe that (2.22) immediately yields an invasibility test: the year class which is j years older than the ruling year class can grow when

$$\prod_{i=0}^{k-1} h_{j+i}(I_i) > 1 \tag{2.63}$$

and is doomed to go extinct when the opposite inequality holds (this is the familiar phenomenon that in population models the stability with respect to missing species can be determined by way of a decoupled eigenvalue problem, whose definition doesn't involve any differentiation; mathematically, of course, the key point is invariance of coordinate hyperplanes).

Simple as the test may be, to say something systematic about the outcome is considerably more complicated. We have only one result to offer. It gives sufficient conditions for transversal stability, i.e., conditions which guarantee that none of the missing year classes can invade successfully.

The result substantiates a key point (which is relevant for the cicada phenomenon): it is not at all exceptional that a SYC fixed point is an attractor for the recursion (1.7). Or, more precisely, there are large classes of functions h and vectors c for which stable SYC fixed points exist. (A preliminary version of this result was obtained in 1999 by Jennifer Baker).

A key assumption will be that the function

$$I \mapsto \frac{h_i(I)}{h_{i+1}(I)} \quad \text{is strictly monotone increasing for } i = 0, 1, ..., k-2 \tag{2.64}$$

or, equivalently, that for $i = 0, 1, ..., k-2$

$$h_i(I^+)h_{i+1}(I^-) > h_i(I^-)h_{i+1}(I^+) \quad \text{for all } I^\pm \text{ with } I^+ > I^-.$$

Note that (2.64) implies that also

$$I \mapsto \frac{h_i(I)}{h_{i+j}(I)} \quad \text{is strictly monotone increasing}$$

for i, j–combinations with $i \geq 0$ and $i + j \leq k - 1$. Hence for such i, j–combinations we as well have that

$$h_i(I^+)h_{i+j}(I^-) > h_i(I^-)h_{i+j}(I^+) \quad \text{for all } I^\pm \text{ with } I^+ > I^-. \tag{2.65}$$

Theorem 2.41. *Let $I_0, I_1, ..., I_{k-1}$ be such that*

i) (2.62) holds,

ii)

$$i \mapsto I_i \quad \textit{is strictly decreasing on } \{0, 1, ..., k-1\}. \tag{2.66}$$

Assume that (2.64) holds. Then for $j = 1, 2, ..., k-1$

$$\prod_{i=0}^{k-1} h_{j+i}(I_i) < 1. \tag{2.67}$$

Proof. Define $m = k - j$ then the left hand side of (2.67) can also be written as

$$h_0(I_m)h_1(I_{m+1})...h_{k-1-m}(I_{k-1})h_{k-m}(I_0)h_{k-m+1}(I_1)...h_{k-1}(I_{m-1})$$

This expression can be viewed as a cyclic shift of indices of the arguments I_i of the expression

$$h_0(I_0)h_1(I_1)...h_{k-1}(I_{k-1})$$

which, by (2.62), equals one. Note that such a shift can be realised by repeatedly interchanging two neighbours which, in the starting position, are ordered according to the index. In detail: consider the transformation from $0\,1...(k-1)$ to $m\,(m+1)...(m-1)\,0\,1...(m-1)$; starting from

$0\,1...(m-1)\,m...(k-1)$ first bring $(m-1)$ to the end position by repeatedly interchanging it with its right neighbour; next bring $(m-2)$ to the one-but-last position by the same procedure; et cetera. In each step two neighbours interchange their position with, at the start of the step, the I with the highest index to the right. By (2.66) and (2.65) the value of the expression decreases in each step. It follows that (2.67) holds. □

Remark. The "strict" part in (2.64) and (2.66) is a bit stronger than really needed, as it suffices that there is a strict decrease in at least one of the steps.

The condition (2.66) is not directly in terms of the ingredients of the model. Our next objective is to give a sufficient condition, in terms of c, for (2.66) to hold. In order to facilitate the application, we do so in terms of the unscaled c. In this connection it is important to recall that h_i^u is, for $i = 0, 1, ..., k-2$, a survival probability, so that it takes values less than (or equal to) one.

Lemma 2.42. *Let $\bar{N}^{ss}$ be a SYC fixed point ("ss" denotes the doubly scaled variable N, see Section 2.3). Define*

$$I_i = c_i^s \bar{N}_i^{ss} = c_i^u \bar{N}_i^u.$$

Assume that

$$i \mapsto c_i^u \quad \textit{is strictly monotone decreasing on } \{0, 1, ..., k-1\}. \tag{2.68}$$

Then (2.66) is satisfied.

Proof.

$$I_{i+1} = c_{i+1}^u \bar{N}_{i+1}^u = c_{i+1}^u h_i^u(I_i) \bar{N}_i^u \leq c_{i+1}^u \bar{N}_i^u < c_i^u \bar{N}_i^u = I_i,$$

where the first inequality derives from the interpretation of h_i^u as a survival probability and the second from assumption (2.68). □

Remark. Note that the condition (2.64) on h is invariant under our scaling, as the scaled version of the quotient differs only by the constant $\frac{h_{i+1}^u(\bar{I})}{h_i^u(\bar{I})}$ from the unscaled version.

In the Ricker case (2.18) the assumption (2.64) amounts to the strict monotonicity of

$$i \mapsto g_i.$$

The interpretation of this condition is that the sensitivity is an increasing function of age, while (2.68) means that the impact is a decreasing function of age. So in case of (2.18) one can say that this combination of age dependence of sensitivity and impact guarantees that a SYC fixed point is transversally stable (this is the result originally proved by J. Baker).

One can also formulate a variant of Theorem 2.41 in which both assumptions (2.64) and (2.66) are reversed (meaning that "decreasing" is changed into "increasing" and vice versa). The corresponding variant of Lemma 2.42 is more problematic, as the bound on h_i^u works in the wrong direction. So one has to replace (2.68) by the condition that $i \mapsto c_i^u$ increases sufficiently strongly, where "sufficiently" incorporates quantitative details.

Finally, note that one can also formulate transversal *instability* results in the spirit of Theorem 2.41. We refrain from doing so.

2.10 Discussion

Of course, the analysis of the recursion (1.7) is far from complete. To see that the dynamics can be very complicated it is enough to look at it for $k = 1$ and $k = 2$. In the first case the description of the dynamics is typically given by a bifurcation diagram with period-doubling cascades. In the latter case the occurence of a strange attractor (either on the boundary or in the interior of the phase space) is a rather common situation. To amuse the reader we include a couple of pictures (Figure 2.3).

However, we believe that we have shed some light on those problems which are the most interesting from a biological point of view. In particular, the "coexistence versus exclusion" problem. We think that the most important phenomenon governing the dynamics of the system is the occurence of the vertical bifurcations. They serve as a switch between coexistence and exclusion. Let us give some comments on that.

We know that manifolds filled with cycles exist only for some particular parameter combinations corresponding to vertical bifurcations. Moreover, if k is even and the vertical bifurcation corresponds to the eigenvalue -1 (Corollary 2.37), it has a codimension 1, because we have only one condition on parameter values (see, e.g. Table 2.1). The vertical bifurcation is a degenerate case of period-doubling bifurcation. An example is the vertical bifurcations happening for $c_0 = c_1$ if $k = 2$. Codimension 1 means also that it happens for points in a m-dimensional parameter space lying on $m-1$-dimensional curves or (hyper)-surfaces. We ask ourselves how the dynamics change if the values of the parameters vary so that we intersect such a surface transversally. In other words, what happens in a neighbourhood of a vertical

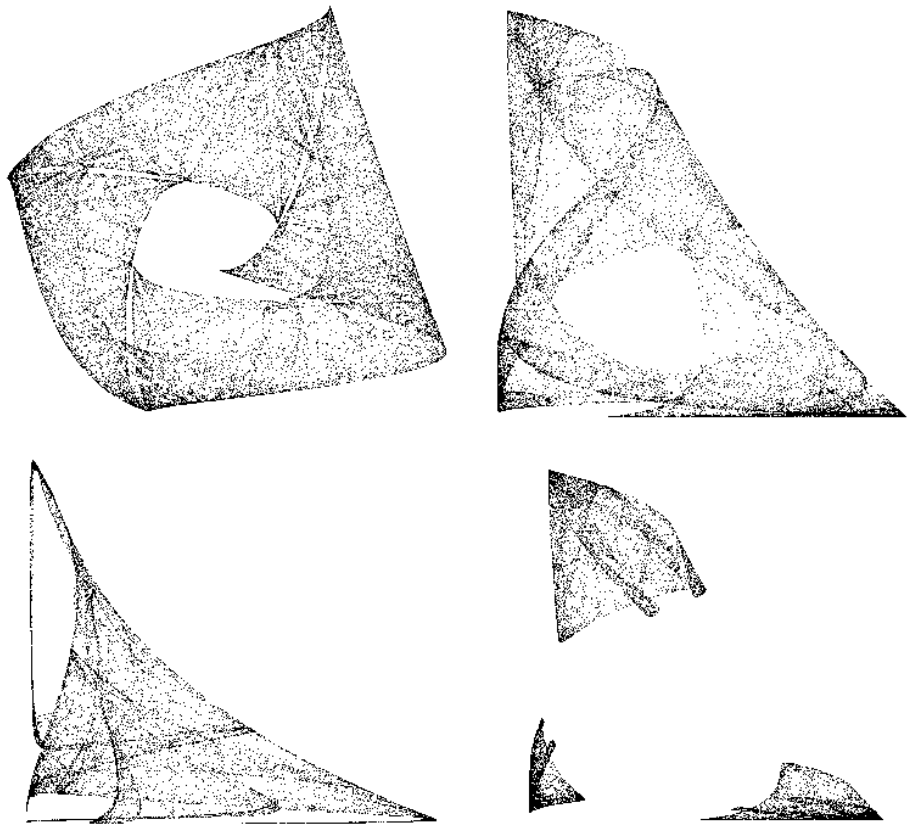

Figure 2.3: Four examples of strange attractors of the recursion (2.10) with the Ricker nonlinearities.

bifurcation. We restrict ourselves to a case of a singular circulant.

Let a condition for a singular circulant be satisfied and let the corresponding manifold $\mathcal{L}_k$ (see Theorem 2.22) be normally hyperbolic and attracting. Then, under small changes in the parameters, the manifold persists and we restrict our attention only to the dynamics on the manifold. Under the condition for the vertical bifurcation the internal steady state has an eigenvalue -1, corresponding to neutral stability within the invariant manifold. We change c slightly in such a way that the eigenvalue moves inside the unit circle. In this case the internal steady state becomes stable. Indeed, it belongs to a stable manifold and is stable within the manifold. All orbits starting near the steady state eventually approach it. We conjecture that *all orbits* in a neighbourhood of the invariant manifold converge to the internal steady

state. The intuition behind it, is that if some orbits diverge, there should be a boundary of the basin of attraction of the steady state. This boundary is an invariant set in the interior of the manifold and, most likely, this set is a 2-cycle. If we exclude situations like those described in Section 3.11, in which there is an isolated 2-cycle in the interior of the phase space, we come to a contradiction. However, to prove the result rigorously probably requires a detailed perturbation analysis of the vertical bifurcation. Now we change c so that the eigenvalue of the steady state moves outside the unit circle. If again there are no cycles in the interior, all orbits diverge from the steady state and go to the boundary of the phase space. So half of the year classes go extinct and become missing.

Summarizing what we have said above, the vertical bifurcation is a boundary between stability of the internal steady state and the stability of a boundary cycle, i.e. the boundary between coexistence and exclusion. This result is proven rigorously for $k = 2$ in Section 3.10.

What we described above concerns the case when the coexistence equilibrium has an eigenvalue -1. In Discussion of Chapter 4 we give a description of what we can expect if the coexistence equilibrium has a couple of non-real eigenvalues which are roots of unity.

The problem remains how many year classes go missing if we switch from coexistence to exclusion. In a neighbourhood of a vertical bifurcation the dynamics is restricted to an invariant manifold which is "almost" the line segment $\mathcal{L}_k$ or the polygon $\mathcal{P}_{n,k}$. The first situation is only possible if k is even. In this case, if the internal steady state loses stability via the vertical bifurcation, we switch to a boundary 2-cycle with exactly half of the year classes missing, more precisely all even or all odd year classes are missing. In the case of the polygon $\mathcal{P}_{n,k}$ the edges correspond to the situation of $\frac{k}{m}$ year classes missing and the vertices to $\frac{2k}{m}$ year classes missing, where m is the least common multiple of n and k (see the end of Section 2.6). Our conjecture, supported by numerical simulations, is that the attractor is exactly the m-cycle consisting of the vertices of the polygon.

In the present analysis we have not exploited the "competitiveness" of the Full-Life-Cycle map (see [Wang & Jiang] and the references in there). We are optimistic that, in fact, this property can be exploited to deduce that there exists an invariant $(k-1)$–dimensional manifold which contains all ω-limit sets. Moreover, the intersection of this manifold with invariant coordinate (hyper)planes yields further invariant subsets of lower dimension. Thus for $k = 3$ a proof of both the existence of the heteroclinic cycle and the (internal) instability of the MYC points in region I of Figure 4.7 should come within (easy) reach.

We think that the Full-Life-Cycle map is competitive when the func-

tions h_i are of Beverton-Holt type (by which we mean, in particular, that $N_i \mapsto N_i h_i(c \cdot N)$ is monotone increasing, for any given combination of $N_j, j = 0, ..., i-1, i+1, ..., k-1$, while h_i itself is monotone decreasing). When the functions $N_i \mapsto N_i h_i(c \cdot N)$ have a humped graph, as they do in the Ricker case, the situation is more complicated in general. Yet for some parameter region the attractor may be confined to a region of the phase space in which the nonlinearities are Beverton-Holt like. So we expect that the theory of competitive maps will also yield information about global aspects of the dynamics for the Ricker type maps under additional parameter constraints. We intend to investigate these matters in the near future.

Chapter 3

Year Class Coexistence or Competitive Exclusion for Strict Biennials?

3.1 Introduction

In this chapter we consider the case $k = 2$, i.e. we focus on strict biennials. The population consists of two age classes. The interaction between individuals is modelled as a feedback via the environment (see Chapter 1 for more details). We assume the environmental quantity I to be one-dimensional and equal to a weighted sum $c_0N_0 + c_1N_1$ of the population numbers of the age classes, where the weights c_0 and c_1 are called impacts of the corresponding age classes on the environment. Note that larger values of I correspond to "worse" environmental conditions because of stronger competition. The age classes differ also by their sensitivity to the environment. If sensitivity can be described by a scalar quantity, we denote sensitivities of the age classes by g_0 and g_1. The main question of this chapter is when, in terms of the impacts c_i and the sensitivities g_i, we get coexistence of the two year classes and when competitive exclusion.

The model of Bulmer [Bulmer] is specified in terms of the quantities β_{ij} which measure the influence of the presence of i year old individuals on the survival (or, in the case $j = k - 1$, also reproduction) of j year old individuals. Here we consider the special case $\beta_{ij} = g_jc_i$ (so the matrix β has one-dimensional range spanned by the vector g). The components of g then correspond to the age-specific sensitivity to environmental conditions and the components of c to the age-specific impact on the environmental conditions.

By numerical experimentation Bulmer [Bulmer] arrives at the following conclusion: competitive exclusion prevails if competition is more severe *be-*

This chapter is a modified and generalized version of [DDvG1]

tween than *within* age classes (i.e., the off-diagonal elements of the matrix β are bigger than the diagonal elements). Our analytical results for the special case allow a somewhat different conclusion: competitive exclusion prevails if the sensitivity increases with age while the impact decreases with age and, also, if the sensitivity decreases with age while the impact increases sufficiently strongly with age (see Theorem 3.19).

In [DMD] the authors have analysed the special case of nursery competition (only c_{k-1} and g_{k-1} are different from zero). In that special case the interaction is restricted to the own year class and, as a consequence, we simply deal with k copies of one and the same discrete time dynamical system. The classification of all (essentially different, i.e. unrelated by time translation) periodic patterns that arise is presented in [Diekmann & van Gils]. The papers [DMD, Mylius & Diekmann] deal with the competition between species with different values of k. Key words are "resonance mediated coexistence" and "invasible yet invincible strategy" (or "the resident strikes back").

In Section 3.2 we formulate the model. In Section 3.3 we consider a steady state of the system and look for its (local) stability. In particular, we show (in the case of Ricker nonlinearity) that the region of stability becomes smaller as the basic reproduction ratio R_0 grows and above a certain threshold the steady state is no more stable. This destabilization of the dynamics for larger values of the basic reproduction ratio is a rather general phenomenon in population models with delayed negative feedback (see e.g. the classic paper [May & Oster]).

In Section 3.4 we introduce a new approach in the analysis of matrix models, which is also biologically motivated. Namely, we first assume that the environmental conditions are periodical with a certain period and then look which solutions of the system are consistent with this assumption. In particular, we show that if the environment is constant then the population numbers are also constant, i.e. the system is in steady state. Another result is that if the environmental conditions have period two, i.e. repeat themselves after exactly two years, the only possible situation is that one of the two year classes is excluded.

There are special parameter combinations for which the conclusions of Section 3.4 fail to be true. We consider these special cases in Sections 3.6 and 3.5. Namely, we have two situations: "uniform impact" of both age classes on the environment and "uniform sensitivity" to the environment. These parameter combinations form in a sense "symmetry axes" of the system. One might say that upon passing these "axes" the year classes interchange their characteristics. Remarkably, these special parameter combinations coincide with a stability boundary of the steady state (Section 3.3) as

well as with the stability boundary of a single year class (SYC) fixed point (Section 3.8). A SYC fixed point corresponds to the situation of exclusion of a year class while the dynamics of the other year class is stationary. Sections 3.3, 3.6, 3.5 and 3.8 together lead to the conclusions of Section 3.10 (see below).

In Section 3.7 we deal with SYC-dynamics and show that even if a single year class is present, the dynamics of the system are far from simple. Fortunately, all the complications occur for quite large values of the basic reproduction ratio R_0.

In Section 3.9 we show that it is possible to have bistability in the system. In particular, depending on initial conditions we can observe either coexistence of year classes or competitive exclusion. But again, to have such bistability R_0 should be large enough.

The main, from a biological point of view, conclusions of this paper are presented in Section 3.10. They take the form of a clear-cut alternative: for not too high values of the basic reproduction ratio R_0, either the two year classes coexist in steady state or one is missing and the other is steady in every phase of its life, so performs a two-cycle. We characterize precisely the parameter combinations that lead to either of these alternatives and, in addition, interpret these parameter conditions biologically.

The last section contains a detailed summary of assumptions and results. Besides we give some examples of how to interpret the model and we discuss in detail how our assumptions and results relate to various published papers. After this section a number of technical appendices follow.

3.2 The model formulation.

The aim of this chapter is to analyse the qualitative dynamical behaviour of the nonlinear Leslie matrix iteration, which is a particular case (2.10) for $k = 2$,

$$N(t+1) = L(\, I(t)\,)\, N(t), \tag{3.1}$$

where

$$N(t) = \begin{pmatrix} N_0(t) \\ N_1(t) \end{pmatrix}, \tag{3.2}$$

so the components of $N(t)$ measure the size of the various age classes at time t, and

$$L(I) = \begin{pmatrix} 0 & h_1(I) \\ h_0(I) & 0 \end{pmatrix}, \tag{3.3}$$

$$I = c \cdot N = c_0\, N_0 + c_1\, N_1. \tag{3.4}$$

with normalization of parameters such that

$$\begin{aligned} c_0 + c_1 &= 1 \\ h_0(\bar{I}) &= 1 \\ h_1(\bar{I}) &= 1. \end{aligned} \tag{3.5}$$

The quantity I is the environmental variable; the parameters c_0 and c_1 are impacts of corresponding age classes on the environment; the functions $h_i(I)$ are sensitivity functions. See Section 2.3 for more details on the notation and properties of the functions $h_i(I)$. In particular, we demand that

$$h_0(0)h_1(0) = R_0 > 1. \tag{3.6}$$

The quantity $h_0(0)h_1(0)$ is, by definition (2.13), the basic reproduction ratio. If it is less than 1 the population goes extinct.

In this chapter we deal often with the Ricker density dependence. Then

$$\begin{aligned} h_0(I) &= e^{g_0(\ln R_0 - I)} \\ h_1(I) &= e^{g_1(\ln R_0 - I)} \end{aligned} \tag{3.7}$$

with normalization $g_0 + g_1 = 1$. Notice that

$$\bar{I} = \ln R_0.$$

The formulations above are obtained by a scaling described in detail in Section 2.3 (see Theorems 2.4 and 2.5). Here we rewrite the relations between scaled and unscaled quantities of impact and sensitivity that we need in the sequel

$$\begin{aligned} c_0^s &= c_0^u\,\theta_0 & c_1^s &= c_1^u\,\theta_0 h_0^u(\bar{I}) \\ g_0^s &= \frac{g_0^u}{g_0^u + g_1^u} & g_1^s &= \frac{g_1^u}{g_0^u + g_1^u}, \end{aligned} \tag{3.8}$$

where

$$\theta_0 = \left(c_0^u + c_1^u h_0^u(\bar{I})\right)^{-1}.$$

The model is symmetric with respect to interchanging of indices. If we choose $h_i(I)$ from the same family

$$h_i(I) = \frac{H(g_i I)}{H(g_i \bar{I})} \tag{3.9}$$

(cf. (2.17)) with normalization $g_0 + g_1 = 1$, we can formulate the following proposition (which is just a corollary of Proposition 2.3).

Proposition 3.1. *For a fixed $\bar{I}$, the dynamics do not change if we interchange both c_0 and c_1 as well as g_0 and g_1 (or, in other words, replace c_0 by $1-c_0$ and g_0 by $1-g_0$).*

Note that the shift of indices is just a reflection and that, for given $\bar{I}$, we need only to investigate half of the parameter square

$$\left\{ \begin{pmatrix} c_0 \\ g_0 \end{pmatrix} : 0 \le c_0 \le 1, 0 \le g_0 \le 1 \right\}.$$

3.3 Steady coexistence of the year classes.

Before providing precise formulations and detailed derivations we give a section-summary in one sentence: there is a unique steady state (3.10) and the region in parameter space corresponding to its stability is described completely in Proposition 3.3.

The steady state is given by

$$\bar{N} = \begin{pmatrix} \bar{N}_0 \\ \bar{N}_1 \end{pmatrix} = \bar{I} \begin{pmatrix} 1 \\ 1 \end{pmatrix}. \tag{3.10}$$

This is shown in Theorem 2.7.

Theorem 3.2. *The steady state (3.10) is locally asymptotically stable whenever both the inequalities*

$$\left(|h_1'(\bar{I})| - |h_0'(\bar{I})|\right)(c_1 - c_0) > 0 \tag{3.11}$$

$$\left(|h_1'(\bar{I})| - |h_0'(\bar{I})|\right)(c_1 - c_0) < \frac{4-\theta}{\bar{I}} \tag{3.12}$$

with

$$\theta = -\bar{I}(h_0'(\bar{I}) + h_1'(\bar{I})), \tag{3.13}$$

hold, and unstable if at least one of these inequalities is reversed.

Proof. The characteristic equation derived in Theorem 2.36 has the following form

$$\mu^2 + a_1\mu + a_0 - 1 = 0 \tag{3.14}$$

with

$$\begin{aligned} a_1 &= -\bar{I}(c_1 h_0'(\bar{I}) + c_0 h_1'(\bar{I})) \\ a_0 &= -\bar{I}(c_0 h_0'(\bar{I}) + c_1 h_1'(\bar{I})). \end{aligned}$$

It is simple to prove in the two-dimensional case that the eigenvalues μ are inside the unit circle if and only if

$$\begin{aligned} &|a_1| < a_0 \\ &|a_0 - 1| < 1 \end{aligned}$$

Since the functions h are decreasing, a_0, a_1 are nonnegative, so these inequality can be rewritten as

$$\begin{aligned} &a_1 - a_0 < 0 \\ &a_0 < 2 \end{aligned}$$

From the first inequality we immediately have (3.11). Since $a_1 + a_0 = \theta$, the second inequality can be rewritten as

$$a_0 - a_1 < 4 - \theta,$$

from which we obtain (3.12). □

Equality in the condition (3.11) corresponds to a period-doubling (PD) bifurcation, because the characteristic equation (3.14) has -1 as a root, while equality in (3.12) corresponds to a Neimark-Sacker (NS) bifurcation, i.e. a Hopf bifurcation for maps (see, for example, [Kuznetsov]), because there are two complex conjugated roots on the unit circle.

We notice that for the Ricker nonlinearity (3.7) $\theta = \bar{I} = \ln R_0$ and

$$g_i = \tfrac{\bar{I}}{\theta}|h_i'(\bar{I})|. \tag{3.15}$$

Let us *define* a parameter g_i for arbitrary functions h_i by the expression above. Then we obtain that $g_0 + g_1 = 1$. (Notice that the parameters g_i, used in the formula for the Beverton-Holt family (2.19), *do not coincide* with g_i calculated with the aid of the above definition. But we hope that this will not produce misunderstanding, because we do not deal with the Beverton-Holt family in this chapter.)

It is convenient to give a graphical representation of the two stability conditions (3.11) and (3.12) in the (g_0, c_0)-square for various values of θ. We notice also that $c_0 + c_1 = 1$ and rewrite the conditions in the following form

$$\begin{aligned} &(c_0 - \tfrac{1}{2})(g_0 - \tfrac{1}{2}) > 0 && (a) \\ &(c_0 - \tfrac{1}{2})(g_0 - \tfrac{1}{2}) < \tfrac{1}{\theta} - \tfrac{1}{4}. && (b) \end{aligned} \tag{3.16}$$

The condition (3.16a) holds in the North-East and in the South-West quadrant of the partitioning of the square by two lines $g_0 = \frac{1}{2}$ and $c_0 = \frac{1}{2}$ (Fig. 3.1).

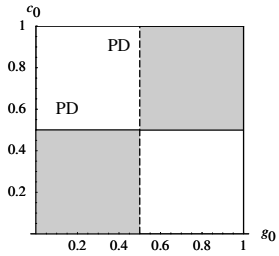

Figure 3.1: The regions in the (g_0, c_0)-square where the condition (3.16a) holds are shaded. The internal boundary is formed by two PD-curves. For $\theta < 2$ the condition (3.16b) is satisfied for all (g_0, c_0) and so these regions are also regions of local stability of the nontrivial steady state.

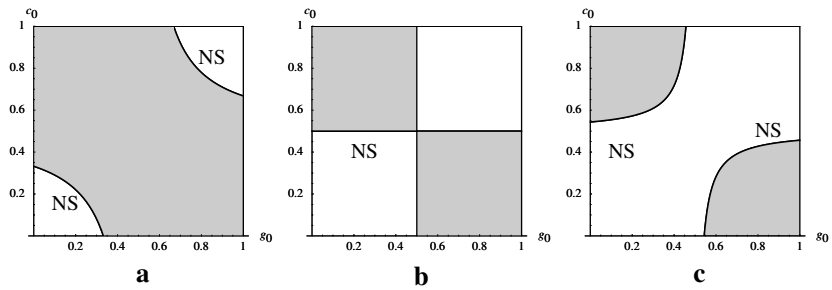

Figure 3.2: The regions in the (g_0, c_0)-square where the condition (3.16b) holds are shaded. **a**: $2 < \theta < 4$. **b**: $\theta = 4$. **c**: $\theta > 4$.

We can rewrite the inequality (3.16b) as follows

$$\begin{cases} c_0 > \psi(g_0, \theta), & g_0 < \frac{1}{2} \\ c_0 < \psi(g_0, \theta), & g_0 > \frac{1}{2} \end{cases}, \tag{3.17}$$

where by definition

$$\psi(g_0, \theta) = \frac{1}{2} + \left(\frac{1}{\theta} - \frac{1}{4}\right) \Big/ \left(g_0 - \frac{1}{2}\right). \tag{3.18}$$

The curve $c_0 = \psi(g_0, \theta)$ for a fixed θ corresponds to a Neimark-Sacker bifurcation. Accordingly, we will call this an NS-curve.

Note that for $\theta < 2$ the inequality (3.16b) is satisfied for all (g_0, c_0). For $\theta > 2$ the regions where (3.16b) holds are shown in Figure 3.2. For

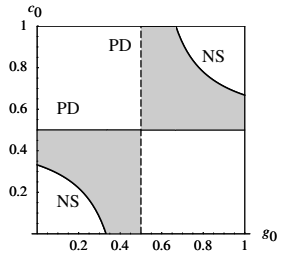

Figure 3.3: The regions of stability of the steady state are shaded. They are bounded by the two PD-curves and the two NS-curves. $2 < \theta < 4$.

$2 < \theta < 4$ the conditions (3.16) give regions of stability for the nontrivial steady state as they are depicted in Figure 3.3. As θ grows from 2 to 4 the regions become more narrow and for $\theta = 4$ the NS-curve coincides with the PD-curve. After that, for $\theta > 4$, the conditions (3.16a) and (3.16b) can not hold simultaneously and accordingly the steady state is unstable. To be precise we formulate the following proposition.

Proposition 3.3.

i) For $\theta > 4$ the steady state (3.10) is unstable.

ii) For $\theta = 4$ and either $g_0 = \frac{1}{2}$ or $c_0 = \frac{1}{2}$ there is a double eigenvalue -1 associated with the steady state (3.10). For $\theta = 4$ and other (g_0, c_0) -values the steady state is unstable.

iii) For $2 < \theta < 4$ the steady state is stable in the parameter region

$$\psi(g_0, \theta) < c_0 < \frac{1}{2}, \quad 0 \leq g_0 < \frac{1}{2}$$

and its mirror image with respect to the point $g_0 = \frac{1}{2}, c_0 = \frac{1}{2}$. For $g_0 = \frac{1}{2}$ and for $c_0 = \frac{1}{2}$ there is an eigenvalue -1 , while for $c_0 = \psi(g_0, \theta)$ there is a pair of complex eigenvalues on the unit circle. For all remaining (g_0, c_0) -values the steady state is unstable.

iv) For $\theta < 2$ the steady state is stable in the parameter regions

$$\begin{cases} c_0 < \frac{1}{2}, & g_0 < \frac{1}{2} \\ c_0 > \frac{1}{2}, & g_0 > \frac{1}{2} \end{cases} . \tag{3.19}$$

For $g_0 = \frac{1}{2}$ and for $c_0 = \frac{1}{2}$ there is an eigenvalue -1 . For all remaining (g_0, c_0) -values the steady state is unstable.

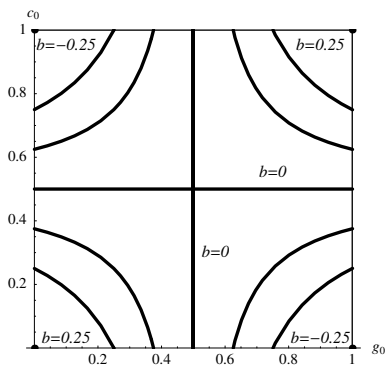

Figure 3.4: The level curves of $b(g_0, c_0)$, where eigenvalues of the steady state are constant, are hyperbolas, degenerate cases are the corners of the (g_0, c_0)-square, where $b = \pm\frac{1}{4}$ and the lines $c_0 = \frac{1}{2}$ and $g_0 = \frac{1}{2}$, where $b = 0$.

The form of the inequalities (3.16) suggests introducing a new parameter. Let

$$b = (c_0 - \tfrac{1}{2})(g_0 - \tfrac{1}{2}). \tag{3.20}$$

Therefore, instead of three parameters, we have only two which determine the linear stability of the steady state: θ and b.

In the (g_0, c_0)-plane the level curves of $b(g_0, c_0)$ are hyperbolas; degenerate cases are the corners of the (g_0, c_0)-square, where $b = \pm\frac{1}{4}$ and the lines $c_0 = \frac{1}{2}$ and $g_0 = \frac{1}{2}$, where $b = 0$ (Fig. 3.4). Along all these curves eigenvalues of the steady state are constant. Note that one of the level curves, on which the determinant of the Jacobian of the steady state is 1, corresponds to the Neimark-Sacker bifurcation. Hence along the whole NS-curve in the (g_0, c_0)-plane (for $2 < \theta < 4$) the eigenvalues do not change.

Since we have only two parameters, we can plot a linearized stability diagram of the steady state in a parameter plane, say, $(\frac{1}{\theta}, b)$, with $\frac{1}{\theta} \in (0, 1], b \in [-\frac{1}{4}, \frac{1}{4}]$. The stability condition (3.16a) then translates to

$$b > 0$$

and the stability condition (3.16b) translates to

$$b < \tfrac{1}{\theta} - \tfrac{1}{4}.$$

The linear stability diagram is shown in Figure 3.5. In the light-grey regions one of the stability conditions above is satisfied, while in the dark-grey region both are satisfied and the steady state is stable.

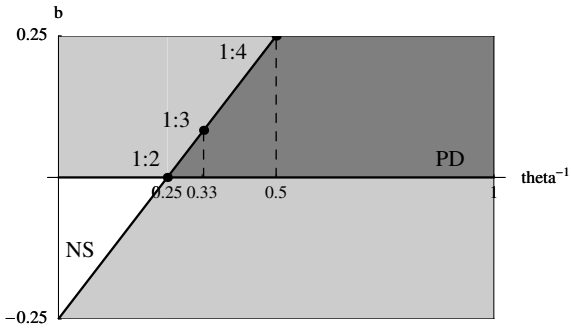

Figure 3.5: A linear stability diagram of the steady state. In the dark-grey region the steady state is stable, i.e. for $2 < \theta < 4$ it is stable if $0 < b < \frac{1}{\theta} - \frac{1}{4}$, for $\theta < 2$ it is stable if $b > 0$. For $\theta > 4$ the steady state is unstable. The points of strong resonances 1:2, 1:3 and 1:4 are also shown.

In Appendix A we consider also codimension 2 bifurcations, so-called strong resonances. These bifurcations can give a clue to an explanation of cycles of periods 3 and 4 which we observe numerically for the Ricker nonlinearity (3.7).

Let us now summarize in words the results that we need in the sequel.

- The map (3.1) has a unique nontrivial fixed point.
- If $\theta < 2$ the stability regions of this steady state are bounded by the PD-curves and shown as shaded in Figures 3.1 and 3.5.
- If $2 < \theta < 4$ the stability regions are bounded by the PD-curves and the NS-curves as presented in Figures 3.3 and 3.5.
- If $\theta > 4$ the steady state is unstable.

Remark. We notice that for the Ricker nonlinearity $\theta = \ln R_0$, i.e., the conditions on θ can be immediately translated into conditions on the biologically relevant parameter R_0. In general, a linear approximation of θ in the neighbourhood of $\bar{I} = 0$ is

$$\theta \approx -\bar{I}(h_0'(0) + h_1'(0)).$$

Therefore θ is small for small $\bar{I}$. Since small $\bar{I}$ corresponds to R_0 slightly bigger than 1 (see Remark after (2.19)), we can conclude that, for small values of the basic reproduction ratio, the steady state is stable in the parameter regions (3.19).

3.4 Environmental conditions of period one or two.

Results of this and several of the next sections are, in principle, a translation of more general results of Chapter 2 for the case $k = 2$ in more explicit and/or biologically relevant form.

The structure of (3.1) suggests the following method of analysis:

– first assume a certain periodicity of I and analyse the consequences for N;

– next verify whether the assumptions and consequences are compatible with the relation (3.4) between I and N.

In particular, we will show in this section that generically,

- constant environmental conditions require that the system is in steady state;
- solutions with minimal period two and both year classes present do not exist.

The exceptional parameter combinations are pointed out explicitly. The study of the dynamics in these special cases is the subject of the sections 3.5 and 3.6.

Theorem 3.4. *Provided $c_0 \neq \frac{1}{2}$, the environmental condition I is constant only if the system is in steady state.*

Proof. When $I(t) = \bar{I}$ for all t, the recurrence relation (3.1) is *linear* and

$$L(\bar{I}) = S = \begin{pmatrix} 0 & 1 \\ 1 & 0 \end{pmatrix},$$

i.e. the recursion is just a shift. Any initial condition $(N_0, N_1)^T$ leads to a 2-periodic orbit, the second point on the orbit being $(N_1, N_0)^T$. In order for such an orbit to be consistent with our assumption that $I(t) = \bar{I}$ for all t, we should have that

$$\begin{aligned} c_0 N_0 + c_1 N_1 &= \bar{I} \\ c_1 N_0 + c_0 N_1 &= \bar{I}. \end{aligned}$$

Provided the determinant $c_0^2 - c_1^2$ is non-zero we find a unique point $\bar{N}$ which is, in fact, given by (3.10). Since c_0 and c_1 are nonnegative, the condition on the determinant translates into $c_0 \neq c_1$, which, in turn, translates into $c_0 \neq \frac{1}{2}$ since $c_0 + c_1 = 1$. □

In this theorem we have revisited the linear circulant system (2.26) and excluded the case $c_0 = \frac{1}{2}$ for which it is singular (see Proposition 2.18).

Theorem 3.5. *Let $\frac{h_0}{h_1}(I)$ be strictly monotone for all $I > 0$ and $c_0 \neq \frac{1}{2}$. Assume that $I(t)$ is periodic with period two and that both year classes are present. Then, in fact, the system must be in the nontrivial steady state (and, correspondingly, $I(t)$ must be constant and therefore equal to $\bar{I}$).*

This theorem is just a translation of Corollary 2.28.

Proposition 3.6. *For the Ricker nonlinearity (3.7) the ratio $\frac{h_0}{h_1}(I)$ is strictly monotone for all $I > 0$ if and only if $g_0 \neq \frac{1}{2}$.*

3.5 The special case $c_0 = \frac{1}{2}$ of " uniform impact".

We now concentrate on the case $c_0 = \frac{1}{2}$ which was excluded in Theorems 3.4 and 3.5 and which corresponds to the second factor at the left hand side of the condition (3.11) being zero. We call this the "case of uniform impact".

Remark. One should distinguish the case of "uniform impact" from the case of "equal impact" $c_0^u = c_1^u$, often used in modelling ([Wikan] and references in there), where c_0^u and c_u^1 denote the unscaled impacts (see (3.5)). In the scaled parameters this equality implies that $c_0^s > c_1^s$. Note also that in the case of uniform impact $c_0^s \bar{N}_0^s = c_1 \bar{N}_1^s$ (because $\bar{N}_0^s = \bar{N}_1^s$) and consequently (see (2.16)) $c_0^u \bar{N}_0^u = c_1^u \bar{N}_1^u$, i.e. at the equilibrium the contributions of both age classes to the quantity $\bar{I}$ are equal.

Theorem 3.7. *Let $c_0 = \frac{1}{2}$ (or, equivalently, $c_0 = c_1$), then the line $\{(N_0, N_1) : I = \frac{1}{2}(N_0 + N_1) = \bar{I}\}$ is invariant. On this invariant line the dynamics are given by $N(t+1) = \begin{pmatrix} 0 & 1 \\ 1 & 0 \end{pmatrix} N(t)$ and consequently every point is periodic with period two (with the steady state as the only exception, this is also the minimal period).*

This theorem is a particular case of Theorem 2.8.

We can explain the bifurcation that happens when (3.16a) gets violated by c_0 moving through the value $\frac{1}{2}$. First, note that equality in (3.16a) corresponds to an eigenvalue -1 for the linearization, so, in principle, to period-doubling. We find a "vertical bifurcation" variant of period-doubling, in the sense that exactly for the bifurcation value $c_0 = \frac{1}{2}$ there is a one-parameter family of 2-cycles that forms a straight line in (N_0, N_1)-space (see Chapter 1 for more details).

In [Cushing & Li] Cushing and Li deduce a result that is similar to our Proposition 3.23 below and they say on p. 513: "... what the nature of the bifurcation phenomena at both the equilibria and the synchronous 2-cycles is, are interesting mathematical questions which we leave unexplored". No doubt the vertical bifurcations that we find here and in the next section also occur in their model and, accordingly, we think that the questions are now answered.

Theorem 3.8. *For the case of Ricker nonlinearity (3.7) the invariant line is an attractor at least for* $1 < R_0 < e^2$.

The proof of this theorem we give in Appendix B.

3.6 The special case $h_0(I) = h_1(I)$ of " uniform sensitivity".

For $h_0(I) = h_1(I)$, or for $g_0 = \frac{1}{2}$ in the Ricker case, the two-dimensional map decomposes into a one-parameter family of one-dimensional maps. This observation reveals a branch of 2-cycles and thus how the steady state (3.10) undergoes a vertical period-doubling bifurcation.

The following theorem and its corollary are particular cases of Theorem 2.9.

Theorem 3.9. *Let* $h_0(I) = h_1(I) = h(I)$. *In terms of polar coordinates, the map (3.1) is given by*

$$(r, \varphi) \mapsto \left(r\, h(\alpha(\varphi)\, r), \frac{\pi}{2} - \varphi \right), \tag{3.21}$$

where

$$\alpha(\varphi) = c_0 \cos\varphi + c_1 \sin\varphi. \tag{3.22}$$

Proof. The key point is that for $h_0(I) = h_1(I)$ the nonlinearity is a scalar factor in front of a fixed matrix:

$$N(t+1) = r\, h(I) \begin{pmatrix} 0 & 1 \\ 1 & 0 \end{pmatrix} N(t)$$

Now note that the matrix $\begin{pmatrix} 0 & 1 \\ 1 & 0 \end{pmatrix}$ maps the line through the origin with angle φ into the line with angle $\frac{\pi}{2} - \varphi$. If $\begin{pmatrix} N_0 \\ N_1 \end{pmatrix} = r \begin{pmatrix} \cos\varphi \\ \sin\varphi \end{pmatrix}$ then the image point has radius $r\, h(\alpha(\varphi)\, r)$ with $\alpha(\varphi)$ as above. □

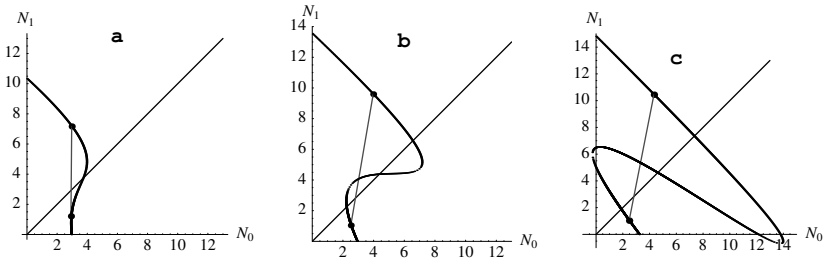

Figure 3.6: Three kinds of patterns of 2-cycles in the degenerate case $g_0 = \frac{1}{2}$ for the Ricker nonlinearity (3.7). The line segment represents a 2-cycle (symbolically) taking its values on the different sides of the curve with respect to the diagonal. There exists such a 2-cycle for each point on the curve. a: $R_0 = 40 < e^4, c_0 = 0.4$ there exists a unique 2-cycle for each φ, b: $R_0 = 80 > e^4, c_0 = 0.45$ if φ is close to the diagonal there are three 2-cycles, c: $R_0 = 100 > e^4, c_0 = 0.483$ the three 2-cycles exist for all values of φ, including the axes. See also the end of Section 3.7.

In the case of Ricker nonlinearity the map (3.21) can be rewritten as

$$(r, \varphi) \mapsto \left(\sqrt{R_0} r e^{-\frac{1}{2}\alpha(\varphi) r}, \frac{\pi}{2} - \varphi \right), \tag{3.23}$$

Corollary 3.10. *Let $h_0(I) = h_1(I)$. The line with angle $\frac{\pi}{4}$ is invariant. Every other straight line through the origin is mapped into itself by the second iterate. The position along the line with angle φ evolves under the second iterate according to the one-dimensional map*

$$r \mapsto r\, h(r\,\alpha(\varphi))\, h\left(r\, h(r\,\alpha(\varphi))\, \alpha(\frac{\pi}{2} - \varphi)\right). \tag{3.24}$$

Nontrivial fixed points of (3.24) correspond, for $\varphi \neq \frac{\pi}{4}$, to 2-cycles of (3.1). These lie on a curve in (N_0, N_1)-space which, in polar coordinates, is determined by the equation

$$h(r\,\alpha(\varphi))\, h\left(r\, h(r\,\alpha(\varphi))\, \alpha(\tfrac{\pi}{2} - \varphi)\right) = 1. \tag{3.25}$$

Notice that this equation has solutions for all φ because of the property (3.6) and because $h(I)$ decreases strictly to zero for $I \to \infty$. The point $\varphi = \frac{\pi}{4}$, $r = \sqrt{2}\,\bar{I}$ on this curve corresponds to the steady state (3.10).

In the Ricker case for the bifurcation value $g_0 = \frac{1}{2}$ there is a one-parameter family of 2-cycles determined, implicitly, by (3.25), which can be rewritten as

$$r(\alpha(\varphi) + \sqrt{R_0}\, \alpha(\tfrac{\pi}{2} - \varphi) e^{-\frac{1}{2}\alpha(\varphi) r}) = 2 \ln R_0. \tag{3.26}$$

If we fix φ there are in the Ricker case (see Section 3.7) either one or three solutions of equation (3.26) for r. This tells us how the curve defined by (3.26) can, and cannot, fold in (N_0, N_1)-space. The three possibilities for the global behaviour of the curve are illustrated in Figure 3.6. If $R_0 < e^4$ there exists only one 2-cycle corresponding to each value of $\varphi \in [0, \frac{\pi}{4})$ (Fig. 3.6a). (The values of $\varphi \in (\frac{\pi}{4}, \frac{\pi}{2}]$ correspond to the second point of the 2-cycle.) If $R_0 > e^4$ we see that a line $\varphi = const$ can have three intersections with the curve (3.26) if φ close to $\frac{\pi}{4}$ (Fig. 3.6b), hence there exist three 2-cycles for these values of φ (but the one corresponding to the middle intersection is unstable, see the end of the next section). For even larger R_0 the three 2-cycles exist for all values of φ, even for $\varphi = 0$ and $\frac{\pi}{2}$, i.e., on the axes (Fig. 3.6c).

In conclusion of this section, we look at the very special case when *both* conditions $h_0(I) = h_1(I)$ and $c_0 = \frac{1}{2}$ are satisfied. The easiest way to analyse the dynamics is to trace the additional features in the results of Section 3.5 that derive from putting $h_0(I) = h_1(I)$ and to fit these in with the results in this section so far.

For $c_0 = \frac{1}{2}$ we have (cf. 3.22)

$$\alpha(\varphi) = \frac{1}{2}(\cos\varphi + \sin\varphi) = \alpha\left(\frac{\pi}{2} - \varphi\right).$$

Consequently, the family of maps (3.24), parametrized by φ, has fixed points

$$r = \frac{1}{\alpha(\varphi)}\,\bar{I},$$

which form the straight line $N_0 + N_1 = 2\bar{I}$. In fact, the maps (3.24) differ from each other only by a scaling of r. Indeed, by scaling r with α we obtain the map

$$r \mapsto r\,h(r)\;h\,(r\,h(r))$$

which does not depend on φ.

3.7 Single year class dynamics.

The "Full-Life-Cycle" map F is, by definition, obtained by applying the "one year ahead" map $N \mapsto L(I)N$ (introduced in (3.1)) twice. To represent F explicitly, it is convenient to now call I by the name I_0, so

$$I_0 = c \cdot N = c_0 N_0 + c_1 N_1 \tag{3.27}$$

and to introduce the environmental condition in the next year as

$$I_1 = c_0 h_1(I_0) N_1 + c_1 h_0(I_0) N_0 \tag{3.28}$$

(note that I_1 depends nonlinearly on N). With these notations available we can write

$$F(N) = L(I_1)L(I_0)N = R_0 \begin{pmatrix} h_0(I_0)h_1(I_1) & 0 \\ 0 & h_0(I_1)h_1(I_0) \end{pmatrix} \begin{pmatrix} N_0 \\ N_1 \end{pmatrix}. \tag{3.29}$$

Since the matrix is diagonal, the coordinate axes are invariant under F. In this section we look at the dynamics of iterating the restriction of F to one such axis, which biologically corresponds to the situation that one of the two year classes is missing.

It is irrelevant to which axis we restrict F. This is biologically evident, but the mathematical underpinning is of some interest. Denote the N_0-axis by X_0 and the N_1-axis by X_1. The map $N \mapsto L(I)N$ maps X_0 into X_1 and, likewise, X_1 into X_0. Let $\hat{f} : X_0 \to X_1$ and $\tilde{f} : X_1 \to X_0$ denote the corresponding restrictions of $N \mapsto L(I)N$. Then $F|_{X_0} = \tilde{f} \circ \hat{f}$ and $F|_{X_1} = \hat{f} \circ \tilde{f}$. So, $F|_{X_0} \circ \tilde{f} = \tilde{f} \circ F|_{X_1}$ and $\hat{f} \circ F|_{X_0} = F|_{X_1} \circ \hat{f}$. By induction it follows that an orbit of $F|_{X_1}$ is mapped, by $\tilde{f}$, to an orbit of $F|_{X_0}$ while, conversely, an orbit of $F|_{X_0}$ is mapped by $\hat{f}$ to an orbit of $F|_{X_1}$. (And if we map an orbit of $F|_{X_1}$ first to X_0 by $\tilde{f}$ and then back to X_1 by $\hat{f}$, every point is mapped to the next point on the same orbit.) So the phase portraits (i.e. the qualitative orbit structures) of $F|_{X_0}$ and $F|_{X_1}$ are identical. Note that neither $\hat{f}$ nor $\tilde{f}$ is an homeomorphism (as the graphs are humped and, consequently, the functions cannot be inverted) so this "equivalence" of $F|_{X_0}$ and $F|_{X_1}$ is *not* the standard one from the theory of dynamical systems.

The map $F|_{X_0}$ is given by

$$N_0 \mapsto N_0\, h_0(c_0 N_0)\, h_1(c_1 N_0\, h_0(c_0 N_0)).$$

For $c_0 \neq 0$, introduce $y = c_0 N_0$, the map becomes then

$$y \mapsto y h_0(y)\, h_1\left(\gamma\, y h_0(y)\right) \tag{3.30}$$

with $\gamma = \frac{c_1}{c_0}$. The map (3.30) should be called the "single year class, full life cycle" map, but we shall write SYC-map for short.

Definition 3.11. *We call nontrivial periodic points of the SYC-map SYC periodic points and nontrivial fixed points SYC fixed points.*

A SYC fixed point corresponds to a 2-periodic point the original map (3.1). This point lies on the N_0-axis and its image lies, of course, on the N_1-axis, so we can consider a SYC fixed point as a 2-cycle of the original map which takes the values at the axes. We therefore also call it a boundary 2-cycle.

Similarly, a SYC m-periodic point corresponds to a boundary $2m$-cycle of the original map.

We consider SYC-maps in Chapter 5. In particular, we investigate a so-called parametric SYC-map (see Subsection 5.2.2). Namely, we choose h_0 and h_1 from the same parameter family (3.9). In addition, we demand a technical property $S\Big(xH(x)\Big) < 0$, where

$$SF = \frac{F'''}{F'} - \frac{3}{2}\left(\frac{F''}{F'}\right)^2 \tag{3.31}$$

is a so-called Schwarzian derivative (Appendix A, Chapter 5). Then one of the main results of Chapter 5 says: *a parametric SYC-map in the case $k = 2$ has a globally stable nontrivial fixed point if $R_0 \le \frac{1}{h^2(c)}$ where c is the (unique) point of maximum of the function $xH(x)$.*

In the Ricker case, the SYC-map is

$$N_0 \mapsto R_0 N_0 e^{-(g_0c_0 + g_1c_1R_0^{g_0}e^{-g_0c_0N_0})N_0}. \tag{3.32}$$

If either $g_0c_0 = 0$ or $g_1c_1 = 0$ this is the well-studied (and consequently well-understood) Ricker map. For $g_0c_0 \neq 0$, introduce the scaled variable $x = g_0c_0N_0$ to transform (3.32) into the two (rather than three) parameter family of one-dimensional maps:

$$x \mapsto R_0 x e^{-h(x,p)}, \tag{3.33}$$

where

$$h(x,p) = x(1 + pe^{-x}) \tag{3.34}$$

with

$$p = R_0^{g_0}\frac{g_1c_1}{g_0c_0}. \tag{3.35}$$

Note that for $p = 0$ (3.33) is the Ricker map. Results in this case are summarized in the form of the bifurcation diagram Fig. 5.7. (The same bifurcation diagram, but less detailed and in another parameter plane, is presented in [Nisbet & Onyiah].) The Ricker SYC-map inherits the symmetry of the original map (3.1) and $p = \sqrt{R_0}$ is the symmetry axis. The main conclusions are

- for $1 < R_0 \le e^2$ the Ricker SYC-map (3.33) has a unique nontrivial fixed point which is globally stable;
- for $e^2 < R_0 < e^4$ the fixed point is stable for an interval $[p_1, p_2]$ of values of p around the symmetry axis $p = \sqrt{R_0}$, for other values of p the map can have more complicated attractors, in particular, periodic attractors;

- for $R_0 > e^4$ there exists an interval of values of p around the symmetry axis such that the map has three nontrivial fixed points.

Let us now make a connection between the SYC-map (3.30) and the map (3.24) which describes the dynamics in the special case of uniform sensitivity. After the scaling $x = \alpha(\varphi)r$ (for $\alpha(\varphi) \neq 0$) the map (3.24) has a form similar to the SYC-map (3.30)

$$x \mapsto xh(x)\, h\left(\gamma_\varphi\, xh(x)\right) \tag{3.36}$$

with the parameter

$$\gamma_\varphi = \frac{\alpha(\frac{\pi}{2} - \varphi)}{\alpha(\varphi)} = \frac{c_0 \sin\varphi + c_1 \cos\varphi}{c_0 \cos\varphi + c_1 \sin\varphi}.$$

(Note that, as should indeed be the case, setting $\varphi = 0$ in this expression yields the same map as setting $h_0(I) = h_1(I)$ in (3.30).)

The parameter γ_φ changes in a monotone fashion from $\frac{c_1}{c_0}$ to $\frac{c_0}{c_1}$ as φ changes from 0 to $\frac{\pi}{2}$. Hence for different φ the map (3.24) shows behaviour corresponding to different values of the parameter γ of the SYC-map. If $c_0 = c_1 = \frac{1}{2}$ the parameter $\gamma_\varphi = 1$ for all values of φ. Thus the dynamics of the map (3.24) is the same on all the lines through the origin. This is the doubly-degenerate case: uniform impact and uniform sensitivity. The larger the difference $|c_0 - c_1|$ the larger the interval over which γ_φ changes. In particular, if either c_0 or c_1 is zero, γ_φ moves over the whole interval from 0 to $+\infty$.

Consider the Ricker case. The map (3.24) can be rewritten as

$$x \mapsto R_0 x e^{-h(x, p_\varphi)}$$

with $p_\varphi = \sqrt{R_0}\gamma_\varphi$. If $\varphi = \frac{\pi}{4}$, i.e. on the diagonal $N_0 = N_1$, $\gamma_\varphi = 1$ which corresponds to the symmetry axis of the SYC-map. We move through the bifurcation diagram (Fig. 5.7) along a line with fixed R_0 and with values of p from $\sqrt{R_0}\frac{c_1}{c_0}$ to $\sqrt{R_0}\frac{c_0}{c_1}$. We conclude that for $1 < R_0 \leq e^2$ the map (3.24) has a unique nontrivial fixed point for all φ. If $e^2 < R_0 \leq e^4$ the map (3.24) has a stable fixed point for values of φ close to $\frac{\pi}{4}$, while it has a periodic or a chaotic attractor in a neighbourhood of the axes N_0 and N_1, i.e. for values of φ close to either 0 or $\frac{\pi}{2}$ (Fig. 3.7).

For $R_0 > e^4$ the situation is more complicated, but we can say that the bistability in the map (3.24) (Fig. 3.6) occurs for values of φ close to the diagonal $\varphi = \frac{\pi}{4}$. It happens because the region of three nontrivial fixed

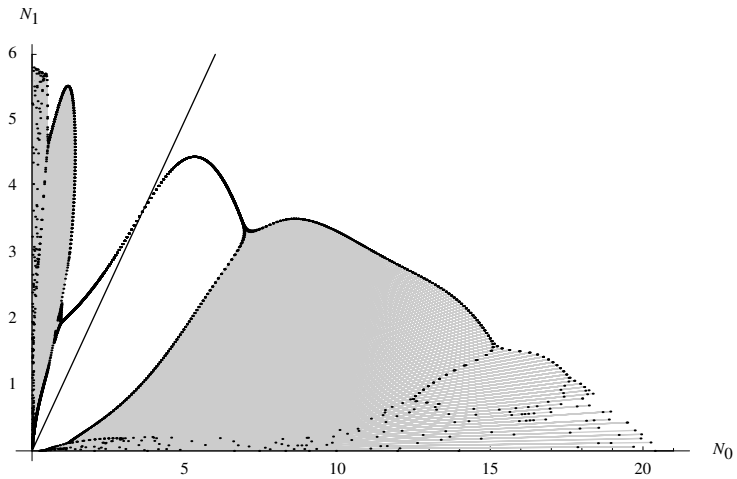

Figure 3.7: The dynamics of the map (3.24) for different φ in the case of Ricker nonlinearity. We see that for φ close to the diagonal the map has a stable fixed point while it shows periodic or chaotic behaviour in a neighbourhood of the axes. $R_0 = 40, c_0 = .8$. The "shaded area" consists of line segments connecting points lying on the same cycle (we draw them in order to distinguish between fixed points and cycles).

points of the SYC-map lies around the symmetry axis $p = \sqrt{R_0}$, which corresponds to the diagonal $\varphi = \frac{\pi}{4}$.

3.8 Transversal stability of SYC fixed points.

Recall from the beginning of Section 3.7 that the Full-Life-Cycle map F is given by (3.29), which we here rewrite as

$$F(N) = R_0 \begin{pmatrix} h_0(I_0)h_1(I_1) & 0 \\ 0 & h_0(I_1)h_1(I_0) \end{pmatrix} \begin{pmatrix} N_0 \\ N_1 \end{pmatrix}. \tag{3.37}$$

Consider a nontrivial fixed point on the N_0-axis, i.e. a SYC fixed point, then I_0 and I_1 are constant, say, respectively, $\bar{I}_0$ and $\bar{I}_1$, and these quantities are such that

$$h_0(I_0)h_1(I_1) = 1. \tag{3.38}$$

If we now introduce the missing year class, i.e. if we make N_1 slightly positive, then this year class will either grow (and then we say the SYC fixed point is transversally unstable) or decline (in which case we say the SYC fixed point is transversally stable). In fact we have transversal instability if

$$h_0(I_1)h_1(I_0) > 1 \tag{3.39}$$

and stability if the reverse inequality holds (see Section 2.9). Let

$$h_0(I_1)h_1(I_0) = \alpha \tag{3.40}$$

and, dividing (3.40) by (3.38), we obtain

$$\tfrac{h_0}{h_1}(I_1) - \tfrac{h_0}{h_1}(I_0) = (\alpha - 1)\tfrac{h_0}{h_1}(I_0).$$

Thus

$$\operatorname{sign}(\alpha - 1) = \operatorname{sign}\left(\tfrac{h_0}{h_1}(I_1) - \tfrac{h_0}{h_1}(I_0)\right). \tag{3.41}$$

Proposition 3.12. *Let g_0 and g_1 be parameters of the functions $h_0(I)$ and $h_1(I)$ respectively such that, for $g_0 > g_1$, the ratio $\frac{h_0}{h_1}(I)$ is strictly monotone decreasing for all I and, for $g_0 < g_1$, $\frac{h_0}{h_1}(I)$ is strictly increasing. Then*

$$\operatorname{sign}\left(\tfrac{h_0}{h_1}(I_1) - \tfrac{h_0}{h_1}(I_0)\right) = \operatorname{sign}(g_0 - g_1)(I_0 - I_1). \tag{3.42}$$

The proof is straightforward.

Theorem 3.13. *Let the condition of Proposition 3.12 hold. If there exists a unique nontrivial SYC-point on each of the axis N_0 and N_1, it is transversally unstable if*

$$(g_1 - g_0)(c_1 - c_0) > 0 \tag{3.43}$$

and transversally stable otherwise.

The proof of this theorem is given in Appendix C. Comparison of (3.43) and (3.11) reveals a striking resemblance which can even be strengthened by the following result.

Corollary 3.14. *Let g_i be given by (3.15) and let the condition of Proposition 3.12 hold. If there exists a unique non-trivial SYC point, the condition (3.43) holds if and only if the condition (3.11) holds.*

Now the only problem is to determine whether there exists a unique fixed point. For the Ricker nonlinearity this is the case for $1 < R_0 < e^4$, we mention this in Section 3.7. Also there we say that a general parametric SYC-map has a globally stable nontrivial fixed point for R_0 small enough.

In Section 3.10 we consider the consequences of this result, with due attention for the biological interpretation.

3.9 Transversal stability of SYC periodic points in the Ricker case.

We concentrate on the Ricker nonlinearity now and assume $e^2 < R_0 < e^4$. We combine the bifurcation diagram for the local behaviour near the internal

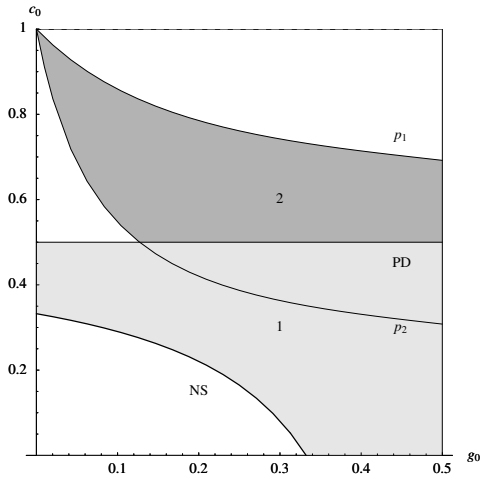

Figure 3.8: A combined bifurcation diagram depicting the regions of local stability of the internal fixed point and the SYC fixed point in the Ricker case. $e^2 < R_0 = 20 < e^4$.

fixed point (Fig. 3.3) and the bifurcation diagram of the SYC-map (3.33) (Fig. 5.7). The result is Figure 3.8. (We show only half of the diagram because of the reflection symmetry with respect to the point $g_0 = \frac{1}{2}, c_0 = \frac{1}{2}$.) The curves PD (period-doubling bifurcation (3.16a)) and NS (Neimark-Sacker bifurcation (3.16b)) bound the region of stability of the internal fixed point. The curves p_1 and p_2 correspond to a period-doubling bifurcation of a SYC fixed point. Recall that for $e^2 < R_0 < e^4$ the SYC-map has a unique nontrivial fixed point (see Chapter 5 for details).

In the preceding section we showed that the curve PD is also the transversal stability boundary for a SYC fixed point. Therefore, in region 1 of the bifurcation diagram Figure 3.8 an attractor of the system is the stable internal fixed point while in region 2 this fixed point is unstable and the boundary 2-cycle is an attractor.

We have proved only local attractivity of the internal fixed point. So we cannot exclude that the system has more than one attractor. Numerical simulations show that there exist at least two parametric regions for $e^2 < R_0 < e^4$ where the system admits bistability (Fig. 3.9): the stable internal fixed point coexists either with a boundary attractor (4) (which is not a boundary 2-cycle) or with a stable internal 3-cycle (3).

The aim of this section is to prove that bistability of the first type is possible, namely that the stable internal fixed point can coexist with a boundary attractor. In particular, we will show that a boundary $2m$-cycle ($m > 1$) is

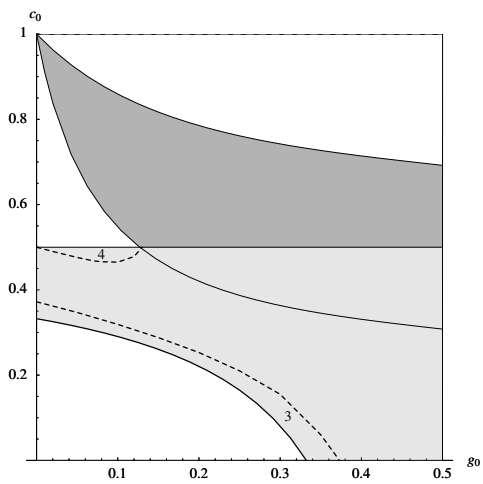

Figure 3.9: The same bifurcation diagram as in Figure 3.8 but with regions of bistability indicated: the stable internal fixed point coexists either with a boundary attractor (4) or with a stable internal 3-cycle (3). $e^2 < R_0 = 20 < e^4$.

still transversally stable when a boundary 2-cycle loses its transversal stability. Since the internal fixed point becomes stable when the boundary 2-cycle loses its transversal stability, there exists a parameter region of bistability.

Remark. For $1 < R_0 < e^2$ the combined bifurcation diagram looks like the bifurcation diagram for the local stability of the internal steady state (Fig. 3.1), because for these values of R_0 the curves p_1 and p_2 do not exist and the SYC-map has a unique stable nontrivial fixed point. The shaded regions of the bifurcation diagram Figure 3.1 correspond to the case when the map (3.1) has an interior fixed point as an attractor, and in the white regions an attractor is a boundary 2-cycle. Numerical simulations indicate that there are no other attractors (bistability does not occur).

We can write down the m th-iterate of the Full-Life-Cycle map in the Ricker case

$$F^m(N) = R_0^m \begin{pmatrix} e^{-g_0 J_0 - g_1 J_1} & 0 \\ 0 & e^{-g_0 J_1 - g_1 J_0} \end{pmatrix} \begin{pmatrix} N_0 \\ N_1 \end{pmatrix}, \tag{3.44}$$

where

$$\begin{aligned} J_0 &= \sum_{i=0}^{m-1} I_{2i} \\ J_1 &= \sum_{i=0}^{m-1} I_{2i+1} \end{aligned} \tag{3.45}$$

and the I's are the values of the environmental variable at the time point as indicated by the index. Fixed points of this map correspond to m-periodic points of the Full-Life-Cycle map F and when they lie on one of the two axes these are SYC m-periodic points.

In this section we adopt the convention that we focus our attention on the SYC m-periodic points that lie on the N_0-axis. Consider a nontrivial SYC m-periodic point and let $\bar{J}_0$, $\bar{J}_1$ denote the corresponding values of J, then we should have that

$$g_0\bar{J}_0 + g_1\bar{J}_1 = m \ln R_0. \tag{3.46}$$

The m-periodic point is transversally unstable if

$$g_0\bar{J}_1 + g_1\bar{J}_0 \ < \ m \ln R_0. \tag{3.47}$$

Using (3.46) we rewrite (3.47) as

$$(g_0 - g_1)(\bar{J}_1 - \bar{J}_0) < 0. \tag{3.48}$$

We immediately see that the uniform sensitivity condition $g_0 = g_1 = \frac{1}{2}$ is again a stability boundary for all SYC periodic points.

Theorem 3.15. *Suppose for $g_0 = 0$ and $c_0 = \frac{1}{2}$ there exists a SYC m-periodic orbit (with $m > 1$) with "internal" multiplier different from one. Then this SYC m-periodic orbit can be continued for small positive g_0 in the neighbourhood of the line $c_0 = \frac{1}{2}$ and it is transversally stable for such g_0.*

The proof is given in Appendix D.

Corollary 3.16. *Let $e^2 < R_0 < e^4$. Whenever R_0 and $m > 1$ are such that the Ricker map $x \mapsto R_0 x e^{-x}$ has a linearly stable m-cycle, there exists a (g_0, c_0)-parameter region, with $(g_0, c_0) = (0, \frac{1}{2})$ as a boundary point, in which the map (3.1) shows bistability.*

Proof. By the symmetry the SYC-map for $g_0 = 0$ is equivalent to the Ricker map. So, applying Theorem 3.15 we obtain that for small g_0 and for c_0 slightly less than $\frac{1}{2}$ the SYC-map has a stable m-cycle which is also transversally stable. For $e^2 < R_0 < e^4$ the internal fixed point of (3.1) is also stable for (at least some of) these parameter values and the corollary is proved. □

Remark. The set of parameter values for which the Ricker map has a stable periodic point, which is the unique attractor, is dense and has a positive Lebesgue measure [Thunberg].

The next section is devoted to the consequences of the results and their interpretation.

3.10 Coexistence or competitive exclusion?

We put together results from Sections 3.3 and 3.8:

- for $\theta < 2$ (where θ is given by (3.13)) the internal steady state is stable if
$$(g_1 - g_0)(c_1 - c_0) > 0;$$
- for $R_0 < \frac{1}{h^2(c)}$ (where c is the point of maximum of the function $xH(x)$) the SYC-map has a unique nontrivial fixed point which is internally stable and whcih is transversally stable if
$$(g_1 - g_0)(c_1 - c_0) < 0.$$

Noticing that θ is small for R_0 small enough (Remark on p. 67), we can reformulate Corollary 3.14 as a strict dichotomy.

Theorem 3.17. *Under the following conditions*

- R_0 *is small enough (see above), but* $R_0 > 1$ *(for the Ricker case* $1 < R_0 < e^2$ *);*
- h_0 *and* h_1 *are from the same parameter family (3.9) with* g_i *given by (3.15) and* $S\Big(xH(x)\Big) < 0$ *(see (3.31));*
- *the ratio* $\frac{h_0}{h_1}(I)$ *is strictly monotone for* $g_0 \neq g_1$ *;*
- $g_0 \neq \frac{1}{2}, c_0 \neq \frac{1}{2}$.

either *the internal steady state (3.10) is asymptotically stable and the SYC fixed point is transversally unstable,*

or *the internal steady state (3.10) is unstable and the SYC-fixed point is transversally stable.*

The first alternative applies when inequality (3.16a) holds, the second when (3.16a) is violated.

In fact we conjecture that these local stability results govern the global behaviour and that

either the interior of the positive quadrant belongs to the domain of attraction of the internal steady state (3.10),

or the internal steady state is a saddle point with a one-dimensional stable manifold and the positive quadrant is the union of this stable manifold and the domains of attraction of the SYC fixed point at the N_0-axis and its image at the N_1-axis.

In biological terms this amounts to

either the two year classes coexist in steady state,

or one outcompetes the other.

The inequality (3.16a) determines, in terms of the parameters, which of the two alternatives applies. (See Figure 3.1. The model predicts coexistence of the two year classes in steady state for parameter combinations belonging to the shaded domain, and competitive exclusion for the complement.) In order to interpret the condition we do some rewriting and, in particular, undo the scaling (3.8). First, note that

$$\operatorname{sign}\left(g_0 - \frac{1}{2}\right) = \operatorname{sign}\left(g_0^u - g_1^u\right).$$

Secondly, note that

$$\begin{aligned}\operatorname{sign}\left(c_0 - \tfrac{1}{2}\right) &= \operatorname{sign}\left(c_0 - c_1\right)\\ &= \operatorname{sign}\left(c_0^u - c_1^u\, h_0^u(\bar{I})\right).\end{aligned}$$

Note that the quantity $c_1^u\, h_0^u(\bar{I})$ is the *expected impact* in a year $t+1$ of an individual born in year t under the constant environmental conditions corresponding to the equilibrium. The expected impact is, of course, less than c_1^u because h_0^u has the meaning of survival probability in the first year. Therefore, in order to decide whether we have coexistence or competitive exclusion we should compare the impact of a newborn with its *expected* impact one year later. Reiterating our scaling arguments in section 3.2, we emphasize that the rescaling we propose makes these two impacts equal.

Combining the two observations above we arrive at the following conditions for competitive exclusion.

Theorem 3.18. *Competitive exclusion occurs if $g_0^u < g_1^u$, i.e. sensitivity increases with age, while $c_0^u > c_1^u s_0\, h_0^u(\bar{I})$, i.e. expected impact decreases with age. It also occurs if sensitivity decreases with age ($g_0^u > g_1^u$), while expected impact increases with age ($c_0^u < c_1^u s_0\, h_0^u(\bar{I})$).*

The notion of expected impact still makes these conditions implicit, as it involves the steady environmental conditions. So we provide (in the form of a corollary) an incomplete collection of sufficient conditions for competitive exclusion.

Corollary 3.19. *Competitive exclusion occurs if* $g_0^u < g_1^u$ *, i.e. sensitivity increases with age, while* $c_0^u \geq c_1^u$ *, i.e. impact decreases with age. It also occurs if sensitivity decreases with age (* $g_0^u > g_1^u$ *), while impact increases sufficiently strongly with age (* $c_0^u / h_0^u(\bar{I}) < c_1^u 1$ *).*

The following corollaries reveal two "paradoxical" (at first sight) situations.

Corollary 3.20. *In the case of "equal" impact* $c_0^u = c_1^u$ *, sensitivity should increase with age (* $g_0^u < g_1^u$ *) to have exclusion.*

Corollary 3.21. *Competitive exclusion is possible if both sensitivity and impact increases with age. (More precisely, it occurs if* $g_0^u < g_1^u$ *and* $c_1^u h_0^u(\bar{I}) < c_0^u < c_1^u$ *.)*

We emphasize one particular aspect of the results: it is not at all unusual, in terms of the parameters, that the attractor is characterized by one of the two year classes being missing.

So far we restricted our attention to $\theta < 2$ ($1 < R_0 < e^2$ in the Ricker case) but, in fact, the above picture extends to much of the subset of the parameter space where $2 < \theta < 4$ ($e^2 \leq R_0 < e^4$ in the Ricker case). In particular, the internal steady state (3.10) and the SYC fixed point cannot simultaneously be stable: if one is stable, the other is not. (In [Cushing & Li, Nisbet & Onyiah] this conclusion was derived for similar models.) The difference with the region where $\theta < 2$ is, first, that for $2 < \theta < 4$ it becomes possible that both are unstable. Indeed, the extra conditions that matter for $e^2 \leq R_0 < e^4$ are (3.16b) for the interior steady state and, for the Ricker case, $p_1 < p < p_2$, where p_1 and p_2 are values of p ,for which the SYC fixed point undergoes a period-doubling (within dynamics on the axis). In particular, in the parameter region which lies under the NS-curve (Fig. 3.8) the system has an internal attractor which can be either a limit cycle or even a strange attractor. In the white regions above the PD-curve (Fig. 3.8) the system has a boundary attractor, which is either a boundary $2m$-cycle with $m > 1$ or a boundary chaotic attractor.

But, secondly, as we have shown in Section 3.9, for the Ricker case and $e^2 < R_0 < e^4$, at least two types of bistability are possible in the system (see Fig. 3.9 for details). Figure 3.10 presents an example of coexistence of the stable internal fixed point and a stable boundary 4-cycle. So, in other words,

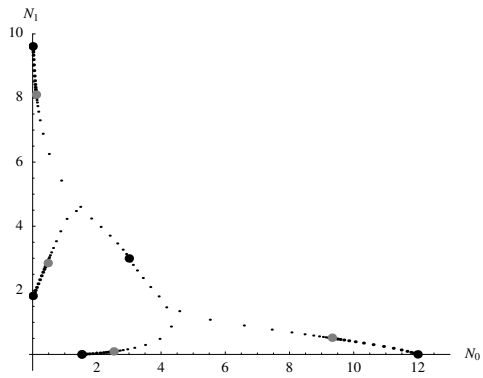

Figure 3.10: Coexistence of two attractors: the interior steady state and a boundary 4-cycle. An internal saddle 4-cycle is also shown (in grey). The attractors belong to the closure of the unstable manifold of the saddle cycle. $R_0 = 20, g_0 = 0.08, c_0 = 0.48$.

the strict dichotomy of Theorem 3.17 does not extend to all of parameter space and it is possible that it depends on the initial conditions whether or not the two year classes will coexist indefinitely.

Finally, we want to remark that the dynamics of the system is very rich. In the Ricker case, for $R_0 > e^2$ in a region where (non-steady) coexistence is possible, one can find all sorts of different attractors with both year classes are present. Among them we have found numerically (by way of the software package CONTENT [Kuznetsov & Levitin]):

- invariant circles;
- three-, four- (see Appendix A), five- and higher-cycles;
- their second (and probably higher) harmonics (i.e. six-, eight-, ten-cycles);
- invariant circles for some iterate of the map (e.g. an attractor that consists of three circles that are visited successively);
- strange attractors (Figure 2.3).

3.11 Nonmonotone $\frac{h_0}{h_1}$.

This section is not contained in [DDvG1], it is a section in [DDvG2].

The condition $c_0 = c_1 = \frac{1}{2}$ in Theorem 3.7 defines a co-dimension one surface in parameter space (recall that $c_0 + c_1 = 1$) and hence it can serve as a full-fledged stability boundary. In the case (3.9) the same can be said about $g_0 = g_1 = \frac{1}{2}$ in connection with Theorem 3.9. The main conclusion of the previous section is that there is, for R_0 not too large, a strict dichotomy: either the coexistence steady state is stable or the period two SYC state is stable. The transition between these two generic situations is by way of vertical period-doubling bifurcations as they occur when either $c_0 = c_1 = \frac{1}{2}$ or $g_0 = g_1 = \frac{1}{2}$. We now understand better the underlying reason for this. The fact that I is a one-dimensional quantity is crucial for the phenomenon of Section 3.5. And, finally, the phenomenon of Section 3.6 occurs because we deal with functions h_i given by (3.9) such that the quotient $\frac{h_0}{h_1}$ switches from decreasing for $g_0 > g_1$ to increasing for $g_0 < g_1$ by way of being constant for $g_0 = g_1$.

To illustrate the last point, we shall briefly look at the corresponding period-doubling bifurcation when $\frac{h_0}{h_1}$ is *not* monotone. First recall from Theorem 3.2 that the internal steady state has eigenvalue -1 when $h_0'(\bar{I}) = h_1'(\bar{I})$. Secondly, recall Theorem 3.9.

We shall now focus on a particular example, but analyse it in a way that exposes the general pattern for non-monotone $\frac{h_0}{h_1}$. Consider h_i defined by (recall the normalization (3.5))

$$\begin{aligned} h_0(I, \bar{I}) &= e^{\bar{I} - I} \\ h_1(I, \bar{I}) &= \tfrac{1+2\bar{I}}{1+2I}, \end{aligned}$$

where we write $\bar{I}$ as another argument of h_i. Then

$$\frac{h_0}{h_1}(I, \bar{I}) = \frac{f(I)}{f(\bar{I})},$$

where by definition

$$f(I) = (1 + 2I)e^{-I}.$$

From $f'(I) = (1 - 2I)e^{-I}$ we deduce that f is strictly increasing on $[0, \frac{1}{2})$ and strictly decreasing on $(\frac{1}{2}, \infty)$. For $1 \le y < 2e^{-\frac{1}{2}} \approx 1.213$ the function f assumes the value y twice, once in $I_0(y) \in [0, \frac{1}{2})$ and once in $I_1(y) \in (\frac{1}{2}, \tilde{I})$, where $\tilde{I}$ is the positive solution of $f(I) = 1$. Thus we find a family, parametrized by y, of solutions to the equation

$$\frac{h_0}{h_1}(I_0, \bar{I}) = \frac{h_0}{h_1}(I_1, \bar{I}). \tag{3.49}$$

We look for a two-cycle with both age classes present. Such a cycle is a fixed point of the Full-Life-Cycle map (3.29). Hence

$$\begin{aligned} h_0(I_0)h_1(I_1) &= 1 \\ h_0(I_1)h_1(I_0) &= 1 \end{aligned} \tag{3.50}$$

(cf. the nonlinear circulant system (2.45)). Thus, having (3.49), we should in addition also satisfy

$$h_0(I_0, \bar{I})\; h_1(I_1, \bar{I}) = 1. \tag{3.51}$$

The idea now is to consider (3.51) as an equation for $\bar{I}$. For our particular example (3.51) can be rewritten as

$$(1 + 2\bar{I})e^{\bar{I}} = (1 + 2I_1(y))e^{I_0(y)} \quad (= (1 + 2I_0(y))e^{I_1(y)}),$$

which has a unique solution $\bar{I}(y)$. So by considering (3.50) as two equations in three unknowns $(I_0, I_1, \bar{I})$, we were able to find a one-parameter family of non-trivial solutions. (By inserting $\bar{I}(y)$ into the defining equation $h_i(\bar{I}) = 1$, one can find one of the parameters in the original unscaled h_i^u in terms of y and, provided the relationship is invertible, parametrize the branch of non-trivial (I_0, I_1) solutions of (3.50) by this parameter.)

For $y = 2e^{-\frac{1}{2}}$ we have $I_0 = I_1 = \frac{1}{2}$ and, also, $\bar{I}(y) = \frac{1}{2}$. So the non-trivial branch "originates" as a symmetry breaking bifurcation from the trivial branch $(I_0, I_1) = (\bar{I}, \bar{I})$ (note that $h_0'(\bar{I}) = -1$ and $h_1'(\bar{I}) = \frac{-2}{1+2\bar{I}}$, which is indeed equal to -1, hence to $h_0'(\bar{I})$, for $\bar{I} = \frac{1}{2}$). To see that the branch also connects to the SYC boundary states, we need to investigate the equations

$$\begin{array}{lcll} c_0N_0 & + & c_1N_1 & = I_0 \\ c_0N_1h_1(I_0) & + & c_1N_0h_0(I_0) & = I_1, \end{array} \tag{3.52}$$

which have the solution

$$\begin{pmatrix} N_0 \\ N_1 \end{pmatrix} = \frac{1}{c_0^2h_1(I_0) - c_1^2h_0(I_0)} \begin{pmatrix} c_0h_1(I_0)I_0 - c_1I_1 \\ c_0I_1 - c_1h_0(I_0)I_0 \end{pmatrix}. \tag{3.53}$$

First note that for $I_0 = I_1 = \bar{I} = \frac{1}{2}$ we do indeed recover the steady state (3.10): $N_0 = N_1 = \bar{I}$. Secondly, note that the branch ceases to be biologically relevant when we "hit the wall", i.e., when one of the two components becomes zero. The limiting point then is a SYC fixed point, so a period two point at the boundary.

In (3.53) any of the two components can become zero, but this reflects the choice of the phase rather than an intrinsic phenomenon. Indeed, the

point defined by (3.53) forms, together with its image

$$\begin{pmatrix} h_1(I_0)N_1 \\ h_0(I_0)N_0 \end{pmatrix}$$

a period two orbit. If instead of (3.52) we solve the equations

$$\begin{array}{lcll} c_0\tilde{N}_0 & + & c_1\tilde{N}_1 & = I_1 \\ c_0\tilde{N}_1 h_1(I_1) & + & c_1\tilde{N}_0 h_0(I_1) & = I_0 \end{array}$$

we find, as one can easily verify using (3.50), the solution

$$\begin{pmatrix} \tilde{N}_0 \\ \tilde{N}_1 \end{pmatrix} = \begin{pmatrix} h_1(I_0)N_1 \\ h_0(I_0)N_0 \end{pmatrix}.$$

So if we choose to represent the branch of period two orbits by the solution of (3.50), rather than by that of (3.52), it is the other axis that is hit.

If a SYC fixed point is characterized by

$$h_0(I_0)h_1(I_1) = 1$$

the transversal (in)stability is determined by (cf. (3.39))

$$\operatorname{sign}\left(h_0(I_1)h_1(I_0) - 1\right).$$

Along the branch of interior period two points (2.45) holds, so when the branch hits the wall, there is a stability switch for the SYC fixed point. So, just as for the vertical bifurcation, there is a branch of period two orbits "originating" in the uniform steady state and "dying" in the (boundary) SYC fixed points and related to stability changes of, respectively, the uniform steady state and the SYC fixed points. But whereas for the Ricker case the branch is vertical, i.e., exists for a particular parameter combination, here it is of a standard type, involving changes in a parameter as well (most easily expressed in terms of changes in $\bar{I}$ but these, in turn, can be regarded as being caused by changes in some other, suitable, parameter).

3.12 Discussion

Let us repeat, without formulating theorems and not using formulas, the main points of this paper.

In the following two lists we give the assumptions on which our model is based and the conclusions we have arrived at.

Assumptions

i) strictly biennial semelparous species:

   (a) life cycle is two years;
   (b) only the oldest age class reproduces;
   (c) the reproduction is simultaneous during a short reproduction season;

ii) all interactions are via the environment:

   (a) the environmental condition is described by a one-dimensional quantity which is a linear function of age class numbers;
   (b) the survival probability (and/or the fertility) is a decreasing function of the environmental quantity;
   (c) this function takes the same functional form for both age classes;

iii) so the two age classes are characterized by their

   - sensitivity to the environment;
   - impact on the environment;

Conclusions

i) Types of dynamics.

   (a) We distinguish two types of *steady* dynamics:
      - steady coexistence of the year classes;
      - two-year cycle with a single year class present.
   (b) Other possible (observed in simulations for the Ricker case) *non-steady* dynamical regimes with both year classes present are:
      - three- (very often);
      - four- (rare: non-sensitivity of the oldest, nursery competition and symmetric situation - see Appendix A);
      - five-, six- and more-year cycles;
      - invariant circles;
      - strange attractors.
   (c) Other possible *non-steady* dynamical regimes with a single year class present are:

- four-, eight-, six- and other even-cycles;
- aperiodic attractors.

ii) The two types of *steady* dynamics can not occur for the same parameter values: if one is stable, the other is not.

iii) A two-year cycle with both year classes present is not possible if the ratio $\frac{h_0}{h_1}(I)$ is monotone for all I.

iv) How the dynamics change with the value of the basic reproduction ratio R_0 for the Ricker case:

(a) If the basic reproduction ratio is less than one, the population goes extinct.

(b) For not so very large basic reproduction ratio ($1 < R_0 < e^2$ for the Ricker case) the dynamics is *steady* and we have a strict dichotomy between the two *steady* types of dynamics: competitive exclusion in the form of the two-year cycle occurs if

- sensitivity increases with age, while impact decreases with age,
- sensitivity decreases with age, while impact increases sufficiently strongly with age,

otherwise we have steady coexistence of the year classes.

(c) For larger values of R_0 ($e^2 < R_0 < e^4$ in the Ricker case) other dynamical regimes are also possible for both the situation of exclusion and the situation of coexistence. Moreover, bistability is possible in the sense that it depends on the initial conditions whether we have coexistence or exclusion (but either one or both these situations are non-steady).

(d) For very large values of R_0 ($R_0 > e^4$ in the Ricker case)

- steady coexistence is not possible;
- steady dynamics are possible only in the situation of exclusion;
- multiple attractors are possible (at least) in the situation of exclusion.

In our opinion, the main result is the dichotomy between the steady regimes (ii, iii and ivb) and the vertical period-doubling which separates the two cases. Non-steady dynamical regimes and all complications we observe for large values of R_0 result from bifurcations in a "transverse" direction (either a Neimark-Sacker bifurcation or a period-doubling for the SYC-map). In

fact, it is possible to choose a form of response to the environment so that the only possible dynamical regimes are the steady ones. Namely, we choose the survival probability to be of Beverton-Holt type $\frac{1}{1+aI}$. The essential result concerning the conditions to have either coexistence or exclusion remains the same, but no bistability is possible and no non-steady regimes exist.

We have found an essential difference in the underlying reason for the two vertical bifurcations ("uniform impact" and "uniform sensitivity"). The first one is connected to the fact that the environment is described by a one-dimensional quantity (which is also a linear function of age class numbers). The second is because the responses of both year classes to the environment have the same functional form and, in fact, at the moment of bifurcation ($g_0 = g_1$) the responses are identical. So, the age-specific sensitivities are really switched while passing the bifurcation.

If the functional responses are of different form (different families), say, one is exponential (i.e., of Ricker type) and the other is of Beverton-Holt type, the period-doubling bifurcations is generic, i.e. we do not have a vertical bifurcation and a sensitivity switch as described above (see also Section 3.11). Simulations show that it is possible to have a two-year cycle with both year classes present (cf. iii) and, also, bistability of the steady regimes (cf. ii).

By varying impact and sensitivity coefficients we can focus on different mechanisms of interaction. For example, cannibalism corresponds to the combination of large impact of the older age class with large sensitivity of the younger age class. This gives us immediately competitive exclusion of the year classes and so *no* cannibalism observable anymore, yet it is the reason for exclusion!

Another example is competition for accommodation of larvae on roots of trees (see the model of Hoppensteadt and Keller in [Murray, Hoppensteadt & Keller] and Chapter 6). In a limiting case, all but the youngest larvae have impact on the environment (by taking places on the roots) while only the youngest larvae suffer from it (they do not yet have a place). In our terms this translates again in large impact of the oldest and large sensitivity of the youngest that again leads to competitive exclusion.

One is inclined to think that the opposite situation, in which competitive pressure from the youngest leads to exclusion, is impossible. But examples can be found [de Roos et al.]. Old and large daphnia's need more resource to maintain their large body-size. Thus they are more sensitive to shortage of food compared to the young and small. The per capita consumption of food by small daphnia's is rather small. Competitive exclusion is indeed observed in the model in [de Roos et al.]. Our Corollary 3.21 is inspired by such situations , but, of course, comparisons between continuous time- and discrete time models are difficult to make and the analogy is certainly not

complete.

Nisbet and Oniyah in [Nisbet & Onyiah] consider a model which has a lot in common with ours. It is also a model with two larval stages, but the survival probability of small larvae depends only on the number of large larvae while the survival probability of the latter can depend on both the number of small and the number of large larvae. In our terminology, the environmental condition in this case is described by a two-dimensional quantity (the number of small larvae and the number of large larvae). The functional responses of the age classes are essentially different. The result that they get is the dichotomy of the steady regimes for small values of the basic reproduction ratio; which of the two regimes prevails depends on the ratio between the strengths of intra- and inter-cohort interactions. For larger values of the basic reproduction ratio the model possesses multiple equilibria with all year classes present. This is not possible in our model and the reason for this is that we have a one-dimensional environment. (But even in our model multiple "equilibria" with a single year class present are possible.) The authors distinguish two-types of two-year cycles: single-cohort and two-cohort (both year classes are present). The latter is possible because the functional responses are of different form. The authors have found numerically three- and four-year cycles as most robust. Our numerical observations support this result, the only difference is that four-year cycles are almost always single year class in our model (ib and ic). We have found that cycles with longer periods are possible as well.

In [WM95, Wikan] Wikan and Mjølhus show that the most common periodicity is four (with both year classes present) while in our model four-year cycles are rare (ib). What is the reason for that? The authors consider the two-, three-, four- and even the general k-dimensional case, but in our description here and further on we restrict to the two-dimensional case. In their model density dependence is introduced only in the survival probability of the youngest age class, not in that of the oldest age class (the survival probability of the oldest year class is incorporated in the fertility/fecundity factor and not considered separately). In our setting this translates into having the oldest age class completely non-sensitive ($g_1 = 0$). Moreover, in [Wikan] Wikan emphasizes that in order to have four-periodicity the impact of the oldest age class should be less than or equal to the impact of the youngest, otherwise three-periodicity prevails. Numerical simulations show that in the first case (which corresponds to nursery competition) we indeed have a "quandrangular" attractor, moreover, in the case of low reproduction ratio it is exactly a four-cycle.

Comparison of [WM95] and [Solberg] leads to interesting conclusions. In the first paper density dependence is introduced only in the survival prob-

ability of the youngest ($g_1 = 0$) while in the second it is introduced only in the survival probability and offspring production of the oldest ($g_0 = 0$). In both models impacts are taken to be equal. The outcome of the models is completely different. In the first model no competitive exclusion is possible while in the second only competitive exclusion is possible. As we have already remarked (Corollary 3.20), the case of "equal impact" requires increasing sensitivity with age to get competitive exclusion. This condition is satisfied only in [Solberg]. An interesting interpretation follows: *if impacts of both age classes are equal, density dependent adult survival/fertility results in competitive exclusion, while density dependent juvenile survival results in coexistence of year classes.*

In [WM96] the authors consider a model with also density dependence in the fertility term, but one-year-old individuals can reproduce as well. The outcome of this model is completely different. You do not see exclusion any more but coexistence (steady or not). A two-year cycle with both year classes present is possible. (In mathematical terms, the model exhibits both Neimark-Sacker and period-doubling bifurcation, moreover both are generic). The reason for not having competitive exclusion is quite clear. If individuals are able to reproduce every year, there is no way to separate the population into year classes. One can say that *it is the reproductive delay which causes competitive exclusion* but this is the case only if the delay is exactly the length of the life cycle, i.e. we deal with strict biennials, triennials etc. The authors supported this conjecture numerically for two-, three- and four-dimensional cases.

Ebenman [Ebenman 87, Ebenmann 88] has considered a model which is quite similar to ours. The main conclusion of his work is: *if juvenile survival is density dependent, competition between age classes has a stabilizing effect; if adult survival/reproduction is density dependent, competition destabilizes.* Ebenman assumed that competition between age classes was always weaker than competition within age classes. So strong competition in his sense means again the case of "equal impact". No wonder, that he came to the conclusion similar to one (two paragraphs) above with the difference that in his model there is no competitive exclusion. Indeed, if competition between year classes is weak, exclusion is unlikely. Destabilization in his model leads to an internal attractor with both year classes present. The analog of our environmental quantity in Ebenman's model is two-dimensional.

Returning to the cicada case, we note that predator satiation has been put forward as an explanation for the long life cycle [Heliövaara et al.] (and even for the remarkable fact that the length is a prime number). In such explanations one usually starts from the observed fact that cicadas are periodical, that is, the population consists of just one year

class. We agree with Heliövaara e.a. [Heliövaara et al.] that this fact needs explanation too. One of our motivations for the present work was to provide analytically such an explanation in the context of a caricatural model, thus extending earlier more numerical studies by Bulmer, Hoppensteadt [Bulmer, Hoppensteadt & Keller, Murray].

Appendices

A Strong resonances.

Our aim is to have a closer look at the eigenvalues of the internal steady state which are roots of the characteristic equation (3.14) and, especially, at their arguments along the NS-curve in the $(\frac{1}{\theta}, b)$-plane (Fig. 3.5). We are looking for strong resonances (see, for example, [Kuznetsov]).

Along the NS-curve the absolute value of the eigenvalues is 1 and the argument ϕ is given implicitly by

$$\cos\phi = \theta(b - \tfrac{1}{4}).$$

Note that $-1 \leq \cos\phi \leq 0$ and $\frac{\pi}{2} \leq \phi \leq \pi$. Taking into account that on the NS-curve $b = \frac{1}{\theta} - \frac{1}{4}$, we get

$$\cos\phi = 1 - \tfrac{1}{2}\theta.$$

- *1:2 resonance.* In this case $\phi = \pi$, hence $\theta = 4$ and $b = 0$ (i.e. either $c_0 = \frac{1}{2}$ or $g_0 = \frac{1}{2}$). This is the point of intersection of the PD and NS-curves. In this point we have double eigenvalue -1. Numerical observations show that this resonance does not have a standard unfolding. The reason for this is that no non-trivival 2-cycle can exist in the interior of the phase-plane.

- *1:3 resonance.* It corresponds to $\phi = \frac{2\pi}{3}$, $\theta = 3$ and $b = \frac{1}{12}$. We have investigated numerically the behaviour of the system in the neighbourhood of the resonant point. It coincides with the standard blow-up [Kuznetsov]. In particular, there exists a saddle 3-cycle around the steady state. We observe a stable 3-cycle as well, but its existence is not directly connected with this resonance.

- *1:4 resonance.* In this case $\phi = \frac{\pi}{2}$, $\theta = 2$ and $b = \frac{1}{4}$ (hence $g_0 = c_0 = 0$ or 1). The eigenvalues are $\pm i$. Numerical blow up of this point reveals the following bifurcation sequence: stable equilibrium, then stable invariant circle as a result of Neimark-Sacker bifurcation and finally "phase-locking" into 4-cycle, i.e. appearance of four 4-periodic points on the circle itself due to a saddle-node bifurcation.

B The proof of Theorem 3.8.

Proof of Theorem 3.8. Every point of the line is a fixed point for the second iterate of the map (3.1). So the Jacobi matrix of this second iterate has an eigenvalue one in every point of the line. Our task is to compute the second eigenvalue (let's call it λ) and to check that it is less than one in absolute value for $1 < R_0 < e^2$.

The second eigenvalue λ equals the determinant of the Jacobi matrix. The Jacobi matrix is the product of two Jacobi matrices of the map (3.1), one in a point $(N_0, N_1)^T$ on the invariant line and the other in the image (under (3.1)) point $(N_1, N_0)^T$ which, by invariance, is on the same line. So the second eigenvalue λ equals the product of two determinants of the Jacobi matrix of (3.1) corresponding to two such points.

One derives that the Jacobi matrix of (3.1) in a point $(N_0, N_1)^T$ on the invariant line is given by

$$\begin{pmatrix} -g_1c_0N_1 & 1-g_1c_1N_1 \\ 1-g_0c_0N_0 & -g_0c_1N_0 \end{pmatrix}.$$

Since $c_0 = c_1 = \frac{1}{2}$ its determinant equals

$$\tfrac{1}{2}(g_0N_0 + g_1N_1) - 1$$

and accordingly the determinant in the image point equals

$$\tfrac{1}{2}(g_1N_0 + g_0N_1) - 1$$

So the second eigenvalue, being the product of these two determinants, is given by the formula

$$\lambda = 1 - \ln R_0 + \frac{1}{4}\left(g_0g_1\,(N_0^2 + N_1^2) + (g_0^2 + g_1^2)\,N_0N_1\right).$$

Hence $\lambda \geq 1 - \ln R_0$ and consequently $\lambda > -1$ for $R_0 < e^2$. Since $1 = (g_0 + g_1)^2 = g_0^2 + g_1^2 + 2g_0g_1$ we may rewrite the expression for λ as follows

$$\lambda = 1 - \ln R_0 + \frac{1}{4}\left(N_0N_1 + g_0g_1\,(N_0 - N_1)^2\right).$$

Since $g_0g_1 = g_0(1-g_0) \leq \frac{1}{4}$ and, on the invariant line

$$\frac{1}{4}(N_0 - N_1)^2 + N_0N_1 \leq \frac{1}{4}(N_0 + N_1)^2 = (\ln R_0)^2$$

we have $\lambda < 1$ whenever $\frac{1}{4}(\ln R_0)^2 - \ln R_0 < 0$ or, equivalently (for $R_0 > 1$), whenever $R_0 < e^4$.

Note that the condition on R_0 is sharp if we want uniformity in g_0. (Indeed, take $g_0 = 0$ and $N_0 = \ln R_0$.) □

C The proof of Theorem 3.13.

For a SYC 2-cycle we have

$$\begin{aligned} I_0 &= c_0 N_0 \\ I_1 &= c_1 N_0\, h_0(I_0). \end{aligned} \tag{3.54}$$

In order to prove the theorem we formulate

Proposition 3.22. *Let the system of equations (3.38),(3.54) have a unique solution for all* c_0, c_1 *. Then*

$$\operatorname{sign}\left(I_0 - \bar{I}\right) = \operatorname{sign}\left(c_0 - c_1\right). \tag{3.55}$$

Proof. If $c_0 = 0$ the proof is immediate. For $c_0 \neq 0$ we write an equation for I_0 excluding N_0 and I_1

$$h_0(I_0)\, h_1(\tfrac{c_1}{c_0} I_0 h_0(I_0)) = 1. \tag{3.56}$$

Consider the function

$$\chi(x) := h_0(x)\, h_1(\tfrac{c_1}{c_0} x h_0(x)).$$

Notice that

$$\chi(0) = h_0(0) h_1(0) > 1$$

by the property (3.6). Since I_0 is a unique solution,

$$\operatorname{sign}\left(\chi(x) - 1\right) = \operatorname{sign}\left(I_0 - x\right)$$

and, in particular,

$$\operatorname{sign}\left(\chi(\bar{I}) - 1\right) = \operatorname{sign}\left(I_0 - \bar{I}\right).$$

Noticing that $\chi(\bar{I}) = h_1(\frac{c_1}{c_0}\bar{I})$ and that h_1 is a decreasing function normalized so that $h_1(\bar{I}) = 1$, we have that

$$\operatorname{sign}\left(\chi(\bar{I}) - 1\right) = \operatorname{sign}\left(c_0 - c_1\right)$$

and the proposition is prooved. □

Now we can prove the theorem.

Proof. If we take (3.38) and the normalization $h_i(\bar{I}) = 1$ into account, we obtain, for not equal I_0 and I_1 , that $I_i < \bar{I} < I_j, i, j = 0, 1$. Therefore, the relations (3.41) and (3.42) can be rewritten as

$$\operatorname{sign}\left(\alpha - 1\right) = \operatorname{sign}\left(g_0 - g_1\right)(I_0 - \bar{I}). \tag{3.57}$$

Combining (3.57) and (3.55) we obtain that

$$\operatorname{sign}\left(\alpha - 1\right) = \operatorname{sign}\left(g_0 - g_1\right)(c_0 - c_1). \tag{3.58}$$

□

D The proof of Theorem 3.15

First we formulate a proposition which helps proving the theorem.

Proposition 3.23. *Let $g_0 = 0$. Any SYC periodic point is transversally stable if and only if the SYC fixed point is transversally stable.*

Proof. Consider a SYC periodic point on the N_0-axis, then $I_0 = c_0 N_0$ and, for $g_0 = 0$, $I_1 = c_1 N_0 = \frac{c_1}{c_0} I_0$, so $I_1 < I_0$ if and only if $\frac{c_1}{c_0} < 1$. The latter condition is according to Lemma 3.13 and condition (3.43) exactly the condition for transversal stability of the SYC fixed point. Exactly the same argument shows that $I_{2i+1} < I_{2i}$ for arbitrary i if and only if $c_0 > \frac{1}{2}$. Combining this information with (3.48) we find, via (3.45), the desired conclusion. □

Proof of Theorem 3.15. The possibility to continue derives from the assumption that the multiplier associated with the one-dimensional map does not equal one (a manifestation of the general result that hyperbolic fixed points can be continued as a function of a parameter).

Now we prove that SYC m-periodic orbit is transversally stable for small g_0 along the line $c_0 = c_1 = \frac{1}{2}$. Then, by continuity, it is also stable in a neighbourhood of the line.

It is convenient to forget about the $N_i(t)$ and to work with the quantities I_j instead. In general we have

$$I_{2i+1} = \frac{c_1}{c_0} I_{2i}\, e^{g_0(\ln R_0 - I_{2i})},$$

and along the line $c_0 = c_1$ this becomes

$$I_{2i+1} = R_0^{g_0} I_{2i}\, e^{-g_0 I_{2i}}. \tag{3.59}$$

Since $g_0 - g_1 < 0$ we have, according to (3.48), transversal stability whenever

$$\sum_{i=0}^{m-1} (I_{2i} - I_{2i+1}) > 0.$$

According to Proposition 3.23, condition (3.43) and Lemma 3.13, the quantity at the left hand side equals zero for $g_0 = 0$. We therefore intend to prove that the derivative with respect to g_0 is strictly positive for $g_0 = 0$. Differentiating the identity (3.59) with respect to g_0 we obtain

$$\frac{\partial I_{2i+1}}{\partial g_0} = (\ln R_0)\, R_0^{g_0} I_{2i} e^{-g_0 I_{2i}} - R_0^{g_0} (I_{2i})^2 e^{-g_0 I_{2i}} + R_0^{g_0} (1 - g_0) \frac{\partial I_{2i}}{\partial g_0} e^{-g_0 I_{2i}}$$

which, putting $g_0 = 0$, simplifies to

$$\frac{\partial I_{2i+1}}{\partial g_0} = (\ln R_0)\ I_{2i} - (I_{2i})^2 + \frac{\partial I_{2i}}{\partial g_0}.$$

Hence we have, for $g_0 = 0$,

$$\frac{\partial}{\partial g_0} \sum_{i=0}^{m-1} (I_{2i} - I_{2i+1}) = \sum_{i=0}^{m-1} (I_{2i}^2 - (\ln R_0)\ I_{2i}).$$

From (3.59) and (3.46), with g_0 put equal to zero in both, we infer that

$$\sum_{i=0}^{m-1} I_{2i} = \sum_{i=0}^{m-1} I_{2i+1} = m \ln R_0$$

or, in words, the average of the I_{2i} equals $\ln R_0$. Hence

$$\sum_{i=0}^{m-1} (I_{2i}^2 - (\ln R_0)\ I_{2i}) = \sum_{i=0}^{m-1} I_{2i}^2 - m(\ln R_0)^2 = \sum_{i=0}^{m-1} (I_{2i} - \ln R_0)^2$$

is strictly positive, unless $I_{2i} = \ln R_0$ for all i, which implies $m = 1$. $\square$

Chapter 4

Dynamics of Triennials.

4.1 Introduction

In this chapter we consider the case $k = 3$ which correspond to the dynamics of triennial species. We do not perform as detailed an analysis as in the case of biennials (Chapter 3), we mostly focus on specific features of triennial dynamics which differ from biennial dynamics.

The map (2.10) is given for $k = 3$ explicitly by

$$N(t+1) = L\Big(h(I(t))\Big)\ N(t) \tag{4.1}$$

with

$$L(h) = \begin{pmatrix} 0 & 0 & h_2 \\ h_0 & 0 & 0 \\ 0 & h_1 & 0 \end{pmatrix}$$

and $I = c_0N_0 + c_1N_1 + c_2N_2$, where N_i are age class numbers for three age classes, c_i are their impacts on the environment I and $h_i(I)$ are sensitivity functions to the environment (see Section 2.3 for more details). We have the following normalization

$$\begin{aligned} &c_0 + c_1 + c_2 = 1 \\ &h_0(\bar{I}) = h_1(\bar{I}) = h_2(\bar{I}) = 1, \end{aligned}$$

where $\bar{I}$ is a parameter of the model which has the meaning of a steady environmental quantity. In this chapter we deal often with the Beverton-Holt density dependence

$$h_i(I) = \frac{1 + g_i\bar{I}}{1 + g_iI}, \quad i = 0, 1, 2 \tag{4.2}$$

with the normalization $g_0 + g_1 + g_2 = 1$ (Theorem 2.5).

In Theorem 2.7 we have shown that the recursion (4.1) possesses a unique steady state given by $\bar{N} = \bar{I}(1, 1, 1)^T$ and the characteristic equation for this steady state is given by (2.61) with $k = 3$.

In the case of general k we were forced to stop the analysis of the characteristic equation, it did not give a full classification of possible bifurcations. However in the case $k = 2$ this classification was done (Theorem 3.2) as well as in the case $k = 3$. In Section 4.2 below we derive stability conditions of a steady state for a three-dimensional discrete time dynamical system and in Section 4.3 we apply these conditions to our particular system and construct a bifurcation diagram (Figure 4.2) for the local stability of the internal steady state. Just as in the case $k = 2$ we find a period–doubling and a Neimark-Sacker bifurcation. However, for $k = 2$ the period–doubling can be vertical, while for $k = 3$ it is the Neimark-Sacker bifurcation which can have this property (see also [Roeger]). But the codimension of the vertical bifurcation is 2 in the latter case, so it is of less importance.

There is a more generic route from coexistence to competitive exclusion. One can trace it on the bifurcation diagram (Fig. 4.7). This diagram is made for the Beverton-Holt nonlinearity and for a special case, when only the youngest age class is sensitive to competition (actually, due to the symmetry it does not matter which particular age class we choose). There are two possible routes, say, catastrophic and noncatastrophic. The latter is via soft destabilization of the coexistence equilibrium and coexistence of year classes in a fluctuating regime, then the so-called heteroclinic behaviour occurs and finally the Single Year Class (SYC) dynamics (when the population consists of only one year class and other year classes are missing, for details see Chapter 1). The catastrophic route from coexistence to exclusion is via a sudden switch to the heteroclinic behaviour and then again to the SYC-dynamics. By the "heteroclinic behaviour" we mean dynamics corresponding to a heteroclinic cycle in the phase space for the Full-Life-Cycle map. In biological terms we observe first one year class which dominates the population and the other two year classes are much less abundant, then an exchange of dominance occurs between year classes, etc. (see also [Roeger]).

We want to mention also the so-called Multiple Year Class (MYC) dynamics, when several but not all year classes are present. Analysis of corresponding equilibria is unpleasant because of technical difficulties. However we have some numerical results for $k = 3$ and $k = 4$. It seems that one year class missing is impossible (for larger k either). On the bifurcation diagram in Figure 4.7 one can see that either the MYC points are internally stable and transversally unstable, or vice versa. For $k = 4$ we can observe attractors with two year classes present, moreover, there are two types of them: either a 2 periodic MYC-cycle (0-th and 2-nd age classes present, then 1 and 3, and again 0 and 2), or a 4-periodic MYC-cycle ($0\,1 — 1\,2 — 2\,3 — 3\,0 — 0\,1$).

This chapter is provided with a discussion (Section 4.5) where we interpret the obtained results in biological terms.

4.2 Stability conditions for $k = 3$.

Let us start it up by presenting some preliminary results concerning stability conditions of a steady state for a three-dimensional discrete time dynamical system. For completeness we derive these in detail.

Lemma 4.1. *Consider, for given real numbers* a_i *, the equation*

$$\mu^3 + a_0\mu^2 + a_1\mu + a_2 = 0. \tag{4.3}$$

Then

i) $\mu = 1$ *is a root iff* $1 + a_0 + a_1 + a_2 = 0$ *;*

ii) $\mu = -1$ *is a root iff* $1 - a_0 + a_1 - a_2 = 0$ *;*

iii) $\mu = e^{\pm i\phi}$ *, with* $0 < \phi < \pi$ *, are complex-conjugate roots iff*

$$\begin{array}{c} -2 < a_2 - a_0 < 2 \\ 1 - a_2^2 = a_1 - a_0 a_2 \end{array}$$

and then $\cos\phi = \frac{1}{2}(a_2 - a_0)$ *.*

Lemma 4.2. *The relations*

$$1 - a_0 + a_1 - a_2 = 0$$

and

$$1 - a_2^2 = a_1 - a_0 a_2$$

are both satisfied iff either

$$a_2 = 1, \quad a_0 = a_1$$

or

$$a_0 = 2 + a_2, \quad a_1 = 1 + 2a_2$$

(or both). In the first case (4.3) has both a simple root at -1 *and a pair of complex roots* $e^{\pm i\phi}$ *iff* $-1 < a_0 < 3$ *and then* $\cos\phi = \frac{1}{2}(1 - a_0)$ *(hence there is a triple root at* -1 *for* $a_0 = 3$ *and a double root at* $+1$ *for* $a_0 = -1$ *). In the second case (4.3) has a double root at* -1 *(which is actually a triple root if both conditions are satisfied, i.e. for* $a_2 = 1$, $a_0 = a_1 = 3$ *).*

Proof. Writing $1 - a_2^2 = (1 - a_2)(1 + a_2)$ and $a_1 - a_0 a_2 = a_0 - (1 - a_2) - a_0 a_2 = (a_0 - 1)(1 - a_2)$ we see that for $a_2 \neq 1$, we can divide out a factor $1 - a_2$ to obtain $1 + a_2 = a_0 - 1$. Elementary considerations then yield the desired conclusions. □

Lemma 4.3. *All roots of (4.3) lie strictly inside the unit circle iff*

$$\begin{array}{ll} 1 + a_0 + a_1 + a_2 > 0 & (a) \\ 1 - a_0 + a_1 - a_2 > 0 & (b) \\ |a_2| < 1 & (c) \\ 1 - a_2^2 > a_1 - a_0 a_2 & (d) \end{array} \tag{4.4}$$

Proofs of the first and the third lemma are given in Appendix. We remark that the stability conditions (4.4) can be found in many books such as [Edelstein-Keshet, Jury, Lewis, May, Murray]. Usually condition (d) is written as

$$|1 - a_2^2| > |a_1 - a_0 a_2|.$$

Given (a)–(c), this is equivalent to the more informative version presented in [Jury] and here, which also fits much better to Lemma 4.1.iii.

4.3 Local stability of the coexistence equilibrium.

For $k = 3$ the characteristic equation (2.61) is of the form (4.3) with

$$\begin{array}{l} a_0 = -\bar{I}\, S^2 c \cdot h'(\bar{I}) \\ a_1 = -\bar{I}\, S\ \ c \cdot h'(\bar{I}) \\ a_2 = -\bar{I}\ \ \ \ c \cdot h'(\bar{I})\ - 1 \end{array}$$

so that (since $c + Sc + S^2 c = (c_0 + c_1 + c_2)\mathbf{1} = \mathbf{1}$)

$$a_0 + a_1 + a_2 = -\bar{I}(h_0'(\bar{I}) + h_1'(\bar{I}) + h_2'(\bar{I}))\ - 1.$$

This motivates us to consider

$$\begin{pmatrix} a_0 \\ a_1 \\ a_2 \end{pmatrix} = \theta \begin{pmatrix} \alpha_0 \\ \alpha_1 \\ \alpha_2 \end{pmatrix} - \begin{pmatrix} 0 \\ 0 \\ 1 \end{pmatrix}$$

with

$$\theta = -\bar{I}(h_0'(\bar{I}) + h_1'(\bar{I}) + h_2'(\bar{I})), \tag{4.5}$$

$\alpha_i \geq 0$ and $\alpha_0 + \alpha_1 + \alpha_2 = 1$ (so, in a sense, θ gives the magnitude of the vector a and α the direction, as far as these depend on the original model parameters). We shall make pictures of stability regions in the (α_2, α_0)–plane for various values of θ. Due to the above conditions on α we consider only a triangle in this plane defined by $\alpha_0 \geq 0, \alpha_2 \geq 0, \alpha_0 + \alpha_2 \leq 1$.

The first stability condition (4.4a) is always satisfied (easy to check, but see also Corollary 2.38).

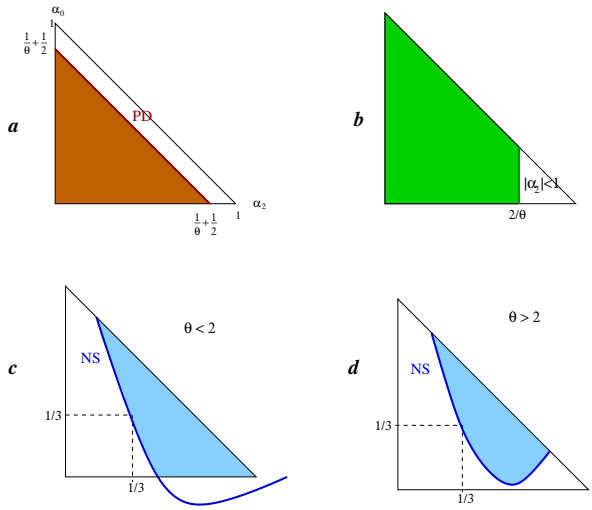

Figure 4.1: In this figure one can see parameter regions (as shaded) where the stability conditions (4.4) are satisfied: **a** condition (b) or (4.6); **b** condition (c); **c** condition (d) or (4.7) for $\theta < 2$; **d** condition (d) or (4.7) for $\theta > 2$.

The second condition (4.4b) can be written as

$$\alpha_0 < \frac{1}{\theta} + \frac{1}{2} - \alpha_2. \tag{4.6}$$

For $\theta < 2$ this inequality is always satisfied, but for $\theta > 2$ it is only satisfied in a θ–dependent part of the (α_2, α_0) parameter–triangle (corresponding to the shaded area in Figure 4.1a). At the boundary, where (4.6) turns into an equality, a period–doubling bifurcation can take place.

The third condition (4.4c) amounts to $\alpha_2 < \frac{2}{\theta}$ which is a constraint only if $\theta > 2$ (Fig. 4.1b).

The fourth condition (4.4d) can be written as

$$\alpha_0 > \alpha_2 + \frac{1}{\theta}\left(\frac{1}{\alpha_2} - 3\right). \tag{4.7}$$

Define, for $\alpha_2 > 0$,

$$\varphi(\alpha_2) := \alpha_2 + \frac{1}{\theta}\left(\frac{1}{\alpha_2} - 3\right).$$

From $\varphi'(\alpha_2) = 1 - \frac{1}{\theta}\frac{1}{\alpha_2^2}$ we deduce that φ has a unique minimum for $\alpha_2 = \frac{1}{\sqrt{\theta}}$, given by

$$\varphi\left(\tfrac{1}{\sqrt{\theta}}\right) = \tfrac{1}{\sqrt{\theta}}\left(2 - \tfrac{3}{\sqrt{\theta}}\right).$$

The graph of φ intersects the line $\alpha_2 \mapsto 1-\alpha_2$ at

$$\alpha_2^{\pm} = \tfrac{1}{4}\left(\tfrac{3}{\theta}+1\right) \pm \sqrt{\left(\tfrac{3}{4\theta}+\tfrac{1}{4}\right)^2 - \tfrac{1}{2\theta}}.$$

Note that there are, for all θ, two intersections (this follows most easily by checking that the minimum of φ computed above is less than $1-\frac{1}{\sqrt{\theta}}$ for all $\theta > 0$). For $\theta = 2$ these occur at $\alpha_2^+ = 1$ and $\alpha_2^- = \frac{1}{4}$.

In view of the second (and the third) condition we are also interested in intersections of the graph of φ with the line $\alpha_2 \mapsto \frac{1}{\theta}+\frac{1}{2}-\alpha_2$. Since

$$\varphi(\alpha_2) - \tfrac{1}{\theta} - \tfrac{1}{2} + \alpha_2 = (\alpha_2 - \tfrac{2}{\theta})(2 - \tfrac{1}{2\alpha_2})$$

these occur for $\alpha_2 = \frac{1}{4}$ and for $\alpha_2 = \frac{2}{\theta}$. According to Lemma 4.3, there is a double root at -1 for $\alpha_2 = \frac{1}{4}$, while for $\alpha_2 = \frac{2}{\theta}$ and $0 < \theta < 8$ there is a simple root at -1 and a pair of roots $e^{\pm i\phi}$ with $\cos\phi = 1 - \frac{\theta}{4}$.

Based on this information we now draw stability diagrams in the (α_2, α_0)–triangle for various values of θ (Figure 4.2). The PD-curve corresponds to $\mu = -1$ being a root of the characteristic equation where a period doubling bifurcation may occur. The NS-curve corresponds to a pair of complex–conjugate roots lying on the unit circle, on this curve a so-called Neimark-Sacker bifurcation may occur when an invariant circle emerges from the internal equilibrium (a Hopf bifurcation for maps).

The complex 3 rd–roots of unity are characterized by $\cos\phi = -\frac{1}{2}$. With $\cos\phi = \frac{1}{2}(a_2 - a_0) = \frac{1}{2}\theta(\alpha_2 - \alpha_0) - \frac{1}{2}$ this amounts to $\alpha_2 = \alpha_0$. So a vertical bifurcation occurs where the 45°–line intersects the NS-curve. This happens for $\alpha_0 = \alpha_2 = \frac{1}{3}$ (but in order for this point to lie on the stability boundary, it should be below the PD-curve; this amounts to $\theta < 6$).

Presumably the direction of bifurcation of the invariant circle changes along the NS-curve in the point $\left(\frac{1}{3}, \frac{1}{3}\right)$. This means that on one part of the curve the internal equilibrium loses stability and a stable invariant circle appears around it, while on the other part the equilibrium becomes unstable because an unstable invariant circle, surrounding it, lands on the equilibrium (Figure 4.3). (Of course, there should exist (at least) a bifurcation curve intersecting the NS-curve in the point $\left(\frac{1}{3}, \frac{1}{3}\right)$ and corresponding to a non-local bifurcation in which the (stable and unstable) invariant circles (dis)appear. But we come to that later in this chapter).

The main conclusion of our analysis is that for $k = 3$ the stability boundary of the internal steady state (in some parameter space) consists of a PD part and a NS part, and that the set of vertical bifurcation points forms a lower dimensional subset of the NS part.

We realize that a "translation" of the stability conditions in terms of α and θ into conditions in terms of parameters like c and g may still involve

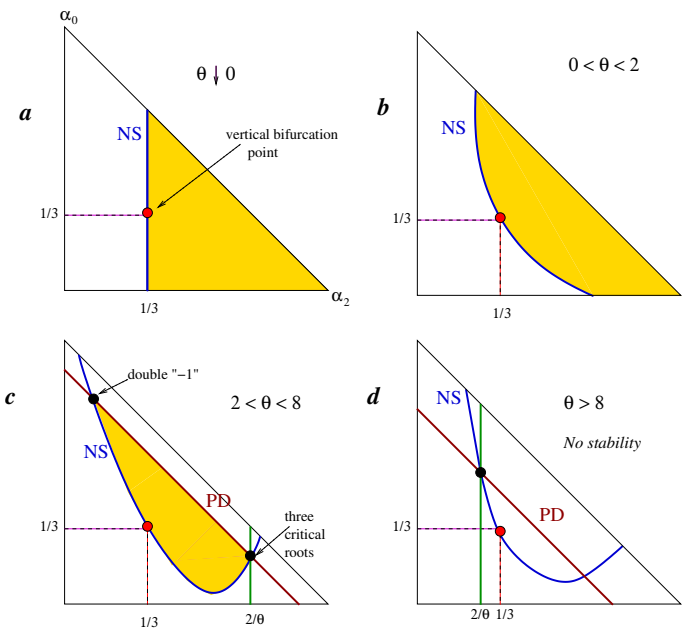

Figure 4.2: Stability diagrams of the internal steady state in the case $k = 3$ for different values of θ. The relevant parameter region is the triangle defined by $\alpha_0 \geq 0, \alpha_2 \geq 0, \alpha_0 + \alpha_2 \leq 1$. For $0 < \theta \leq 2$ the gray area corresponding to the stability of the steady state is bounded by the NS-curve on which a pair of complex–conjugate roots lies on the unit circle. For $2 < \theta < 8$ the stability region is bounded also by the PD-curve where -1 is a root of the characteristic equation. For $\theta \geq 8$ the stability domain is empty because the area between the PD and NS curve lie to the right of the line $\alpha_2 = \frac{2}{\theta}$.

a considerable investment of energy (if possible at all). Yet we notice that, with the results as presented here available, one can always check whether the steady state is stable for particular values of the original parameters just by calculating the corresponding values of α and θ.

Let us now consider the particular case of Beverton-Holt dependence (4.2) which demonstrates that the bifurcations shown in Figure 4.2 do not always take place. Using (2.19) we have

$$-\bar{I}\, h_i'(\bar{I}) = \frac{g_i \bar{I}}{1 + g_i \bar{I}} < 1$$

and hence

$$\begin{aligned} 0 \leq a_i < 1 \qquad & i = 0, 1 \\ -1 \leq a_2 < 0 \qquad & \end{aligned}$$

In particular, we have the following consequence of it.

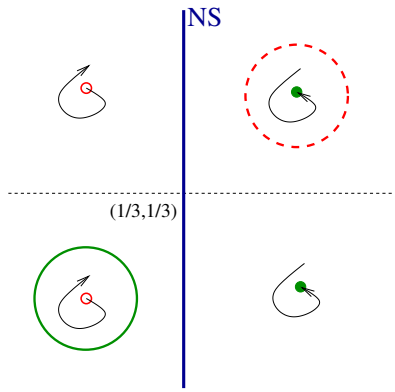

Figure 4.3: Two directions of the Neimark-Sacker bifurcation. On one part of the curve the internal equilibrium loses stability and a stable invariant circle appears around it, while on the other part the equilibrium becomes unstable because an unstable invariant circle, surrounding it, lands on the equilibrium.

Proposition 4.4. *For $k = 3$ and the Beverton-Holt nonlinearity (2.19), $\mu = -1$ is never a root of the characteristic equation (2.61).*

Proof. We substitute $\mu = -1$ in the left-hand side of (2.61) and obtain $-1 + a_0 - a_1 + a_2 < 0$ because $a_0 - 1 < 0$, $-a_1 \leq 0$ and $a_2 < 0$. □

Corollary 4.5. *In the case $k = 3$ and the Beverton-Holt nonlinearity a period–doubling bifurcation of the internal steady state is impossible.*

(If we calculate θ we notice that $\theta < 3$, i.e. it can be larger than 2 and we can in principle expect the period–doubling (Figure 4.2). But

$$\alpha_0 + \alpha_2 = \frac{a_0}{\theta} + \frac{a_2 + 1}{\theta} < \frac{1}{\theta} + \frac{1}{\theta} < \frac{1}{\theta} + \frac{1}{2}$$

and hence the condition (4.6) is always satisfied.)

4.4 Bifurcation diagram.

We perform further analysis of the case $k = 3$ for a very specific situation: $h_1(I) = h_2(I) = h_1(\bar{I}) = h_2(\bar{I}) = 1$, i.e., we assume that only the survival probability of the youngest year class is density dependent. This is not an unusual assumption in age-structured population modelling (see e.g. [Mjølhus et al.] and references therein).

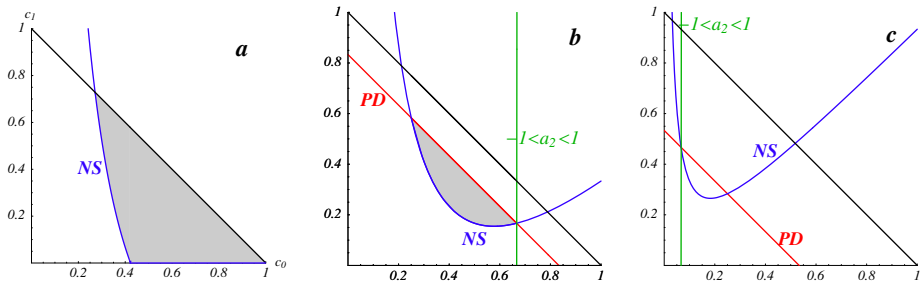

Figure 4.4: Stability regions of the internal steady state in the original parameter plane (c_0, c_1) for the case $h_1(I) = h_2(I) = 1$: **a** $\theta < 2$, **b** $2 < \theta < 8$, **c** $\theta > 8$.

The recursion (4.1) is now given by

$$\begin{aligned} N_0(t+1) &= N_2(t) \\ N_1(t+1) &= N_0(t)h_0(I(t)) \\ N_2(t+1) &= N_1(t) \end{aligned}$$

with

$$I = c_0N_0 + c_1N_1 + c_2N_2.$$

The quantity $\theta = -\bar{I}h_0'(\bar{I})$ and

$$\begin{aligned} a_0 &= \theta c_1 \\ a_1 &= \theta c_2 \\ a_2 &= \theta c_0 - 1. \end{aligned}$$

The stability conditions (4.4 b-d) can be rewritten (noticing that $c_0+c_1+c_2 = 1$) in the original parameters as, respectively,

$$\begin{aligned} c_1 &< \tfrac{1}{2} + \tfrac{1}{\theta} - c_0 \\ c_0 &< \tfrac{2}{\theta} \\ c_1 &> c_0 + \tfrac{1}{c_0\,\theta} - \tfrac{3}{\theta}. \end{aligned} \tag{4.8}$$

Regions of stability in the parameter plane (c_0, c_1) are shown in Figure 4.4 for different values of θ . We notice that only a triangle $c_0 \geq 0, c_1 \geq 0, c_0 + c_1 \leq 1$ is relevant. Of course, we see precise correspondence with Figure 4.2: for $\theta < 2$ only the NS-curve bounds the region of stability, while for $2 < \theta < 8$ a PD curve appears and finally for $\theta > 8$ the internal steady state is always unstable. For the Beverton-Holt nonlinearity we have in this case $\theta = -\bar{I}h_0'(\bar{I}) = \frac{g_0\bar{I}}{1+g_0\bar{I}} < 1$.

Now we look at Single Year Class (SYC) equilibria (see Chapter 1 and 2 for definitions) and consider their transversal stability. For $k = 3$ a SYC fixed point is determined by the system

$$h_0(I_0)\, h_1(I_1)\, h_2(I_2) = 1$$

$$\begin{aligned} I_0 &= c_0\, N_0 \\ I_1 &= c_1\, N_0\, h_0(I_0) \\ I_2 &= c_2\, N_0\, h_0(I_0)\, h_1(I_1). \end{aligned}$$

Since in our case $h_1(I) = h_2(I) = 1$ for any I, the first identity becomes $h_0(I_0) = 1$ and consequently

$$\begin{aligned} I_0 &= \bar{I} \\ I_1 &= \tfrac{c_1}{c_0}\bar{I} \\ I_2 &= \tfrac{c_2}{c_0}\bar{I}. \end{aligned}$$

According to (2.63) a one year older year class can invade if

$$h_1(I_0)h_2(I_1)h_0(I_2) = h_0(\tfrac{c_2}{c_0}\bar{I}) > 1$$

and a two years older year class invades if

$$h_2(I_0)h_0(I_1)h_1(I_2) = h_0(\tfrac{c_1}{c_0}\bar{I}) > 1.$$

Since $h_0(I) > 1$ for $I < \bar{I}$, these inequalities simplify to

$$\begin{aligned} c_2 &< c_0 \\ c_1 &< c_0. \end{aligned}$$

In Figure 4.5 we show schematically whether a missing year can or can not invade in different regions of the (c_0, c_1)-triangle.

Now we turn our attention to MYC-equilibria in which one year class of the three is missing. Let at time t two age classes N_0 and N_1 be present. Then after three years we shall have again these age classes. According to (2.22) their densities are at equilibrium if

$$\begin{aligned} h_0(I_0)h_1(I_1)h_2(I_2) &= h_0(I_0) = 1 \\ h_0(I_2)h_1(I_0)h_2(I_1) &= h_0(I_2) = 1 \end{aligned}$$

and hence $I_0 = I_2 = \bar{I}$. On the other hand (see (2.25))

$$\begin{aligned} I_0 &= c_0N_0 + c_1N_1 \\ I_1 &= c_1N_0h_0(I_0) + c_2N_1h_1(I_0) \\ I_2 &= c_2N_0h_0(I_0)h_1(I_1) + c_0N_1h_1(I_0)h_2(I_1), \end{aligned}$$

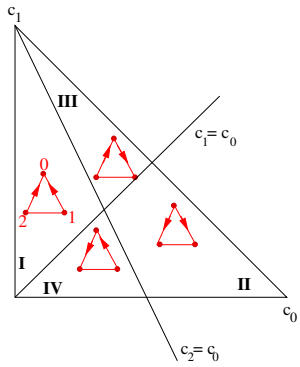

Figure 4.5: Bifurcation diagram for a SYC point. The vertices 0, 1 and 2 of the small triangles represent points on the axes N_0, N_1 and N_2 corresponding to the SYC 3-cycle. An arrow pointing from 0 to 1 shows that the one year older year class can invade, an opposite arrow means that it can not invade. Similarly, for arrows between 0 and 2.

which simplifies to

$$\begin{aligned} c_0N_0 + c_1N_1 &= \bar{I} \\ c_2N_0 + c_0N_1 &= \bar{I} \end{aligned} \tag{4.9}$$

$$I_1 = c_1N_0 + c_2N_1.$$

From the first two identities we have

$$\begin{aligned} N_0 &= \bar{I}\tfrac{c_1-c_0}{c_2c_1-c_0^2} \\ N_1 &= \bar{I}\tfrac{c_2-c_0}{c_2c_1-c_0^2}. \end{aligned} \tag{4.10}$$

Biologically relevant values of N_i are positive. There are two parameter regions where this is indeed the case: either

$$\begin{aligned} c_1 &> c_0 \\ c_2 &> c_0 \end{aligned} \tag{4.11}$$

or

$$\begin{aligned} c_1 &< c_0 \\ c_2 &< c_0. \end{aligned} \tag{4.12}$$

If we compare these sets with the parameter sets in Figure 4.5 we see an interesting correspondence: in the first region (4.11) the SYC-cycle is stable: neither of the missing year classes can invade, while in the second region (4.12) both can invade. Therefore *MYC equilibria with two year classes present exist (in the positive cone) only if the SYC equilibria are either stable or unstable in both directions* (see Figure 4.6).

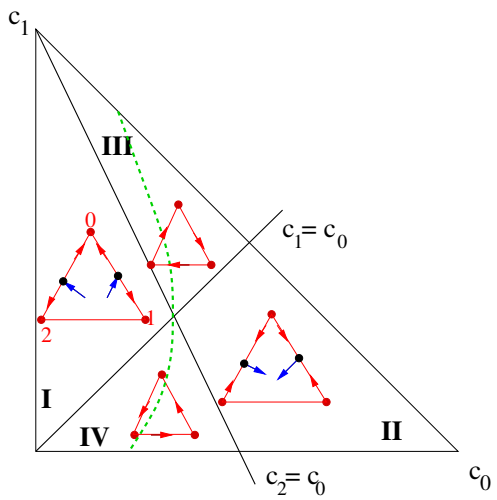

Figure 4.6: Combined bifurcation diagram for SYC-points and MYC-points. The MYC-points exist only in the regions I and II. In the region I the MYC-points are transversally stable (arrows inside the triangles), and in the region II they are transversally unstable. We conjecture that a heteroclinic cycle may exist in regions III and IV. The dashed curve is its stability boundary: to the left of it the heteroclinic cycle is stable, to the right it is unstable.

We conjecture even more: in regions III and IV there exists a *heteroclinic cycle for the third iterate of the map (1.7)*. The existence of the heteroclinic cycle means that the unstable manifold of a SYC fixed point has another SYC fixed point as its ω–limit set so that, by cyclic symmetry a cycle of connecting manifolds is formed.

We reformulate this in biological terms (see Figure 4.8). Notice that if we look three years ahead, "age class" coincides with "year class". Let us have a population consisting of a single year class 0. If we introduce a one year older year class 1, it invades and takes over. Eventually we have a population consisting of the single year class 1. If however a one year older year class 2 can invade, it takes over again and the population will consist of the single year class 2. Here the year class 0 can invade. If the latter does invade, we approach the original situation with the year class 0 dominating the population.

Although it may not be easy to prove the existence of the heteroclinic cycle, numerous simulations confirm the conjecture. (In a special case, about which we learned by reading [Cushing], the proof is actually very easy. If $c_2 = 0$ the Full-Life-Cycle map restricted to a boundary plane is partly decoupled: one of the recursions is independent of the other. So one can

analyse the global asymptotic behaviour rather easily.)

The heteroclinic cycle can be stable or unstable. The condition for its stability is that the product of the eigenvalues λ_1 and λ_2 corresponding to the stable and the unstable manifolds is less than one [Hofbauer & Sigmund]. These eigenvalues are $\lambda_1 = h_0(I_2)h_1(I_0)h_2(I_1)$ and $\lambda_2 = h_0(I_1)h_1(I_2)h_2(I_0)$. In our case

$$\lambda_1\lambda_2 = h_0(\tfrac{c_2}{c_0}\bar{I})\, h_0(\tfrac{c_1}{c_0}\bar{I}).$$

This product is less than one in the region I, because there both eigenvalues are less than one; and it is larger than one in the region II, because there both eigenvalues are larger than one. Since the eigenvalues are continuous functions of c's, the product is equal to 1 in the point $(c_0, c_1) = (\frac{1}{3}, \frac{1}{3})$. Moreover, the condition

$$h_0(\tfrac{c_2}{c_0}\bar{I})\, h_0(\tfrac{c_1}{c_0}\bar{I}) = 1 \tag{4.13}$$

can hold only in the regions III and IV because if, for example, $c_1 > c_0$ we need $c_2 < c_0$ to satisfy this identity (since $h_0(I) > 1$ for $I < \bar{I}$ and $h_0(I) < 1$ for $I > \bar{I}$). The equation (4.13) can be rewritten as

$$\tfrac{c_2}{c_0} = \tfrac{1}{\bar{I}} h_0^{-1}\left(\frac{1}{h_0(\frac{c_1}{c_0}\bar{I})}\right).$$

The right-hand side is a function (on an appropriate domain) because $h_0(I)$ is strictly decreasing and can be inverted. Since there is one-to-one correspondence between the interior of the (c_0, c_1) triangle and the interior of the positive cone of the plane $(\frac{c_1}{c_0}, \frac{c_2}{c_0})$, (4.13) is a curve in (c_0, c_1) lying in the regions III and IV and intersecting the point $(\frac{1}{3}, \frac{1}{3})$ (the dashed line in Figure 4.6).

We notice also a useful property of this curve, viz. that it is vertical in the point $(\frac{1}{3}, \frac{1}{3})$. If we differentiate the identity (4.13) with respect to c_1 considering c_0 as a function of c_1 (in a neighbourhood of $(\frac{1}{3}, \frac{1}{3})$) and taking into account that $c_0 + c_1 + c_2 = 1$ we find that $\frac{dc_0}{dc_1}(\frac{1}{3}) = 0$.

Let us now consider the transversal stability of the MYC-point (4.10). It is transversally stable (i.e., the missing year class can not invade) if

$$h_0(I_1)\, h_1(I_2)\, h_2(I_0) < 1$$

or in our case, if

$$h_0(I_1) < 1 = h_0(\bar{I}).$$

Since h_0 is strictly decreasing, this is the case if

$$I_1 > \bar{I}.$$

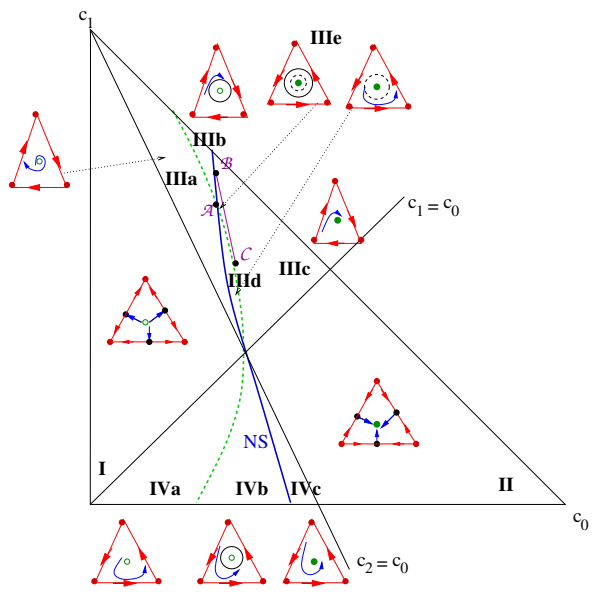

Figure 4.7: A combination of the bifurcation diagrams presented earlier in Figures 4.4a and 4.6.

From (4.9) $I_1 = c_1 N_0 + c_2 N_1$ and, if we substitute N_0 and N_1 from (4.10), we obtain

$$I_1 = \frac{c_1^2 - c_1 c_0 + c_2^2 - c_2 c_0}{c_2 c_1 - c_0^2} \bar{I}$$

and $I_1 > \bar{I}$ if

$$\frac{c_1^2 - c_1 c_0 + c_2^2 - c_2 c_0}{c_2 c_1 - c_0^2} > 1$$

In the region I $c_2 c_1 - c_0^2 > 0$, hence the above identity is equivalent to

$$c_1^2 + c_2^2 + c_0^2 - c_1 c_0 - c_2 c_0 - c_1 c_2 > 0$$

This we can rewrite as

$$(c_0 + c_1 + c_2)^2 - 3(c_1 c_0 + c_2 c_0 + c_1 c_2) > 0$$

which, since $c_0 + c_1 + c_2 = 1$, is equivalent to

$$c_1 c_0 + c_2 c_0 + c_1 c_2 < \tfrac{1}{3}$$

The left-hand side attains its maximum $\frac{1}{3}$ in the point $c_0 = c_1 = c_2 = \frac{1}{3}$. So, in all other points in the region I this inequality is satisfied, i.e., the MYC-point is transversally stable in the region I.

In the region II $c_2c_1 - c_0^2 < 0$ and the above inequality must be reverted. Therefore, it can never be satisfied. Hence the MYC-point is transversally unstable in the region II. We indicate this in Figure 4.6 by arrows inside the small triangles.

Now we combine the bifurcation diagram for the internal steady state in Figure 4.4 with the bifurcation diagram in Figure 4.6. For simplicity we restrict ourselves to $\theta < 2$ (as indeed the case for the Beverton-Holt nonlinearity). The combined bifurcation diagram is represented in Figure 4.7. A lot of things which are shown on the diagram we do not prove (as, for example, existence of the heteroclinic cycle), but numerical simulations corroborate it.

Notice that for $\theta < 9$ the Neimark-Sacker curve $c_1 = c_0 + \frac{1}{c_0\theta} - \frac{3}{\theta}$ (cf. the second inequality in (4.8)) is decreasing in the point $(\frac{1}{3}, \frac{1}{3})$. Recalling that the curve corresponding to stability change of the heteroclinic cycle is vertical in this point, the mutual position of these curves near this point is such as shown in Figure 4.7.

Do these two curves intersect at other points? For the Beverton-Holt case they indeed intersect (the point $\mathcal{A}$ in Figure 4.7). Generically, in a neighbourhood of such a point there should be a region with two invariant circles. "Generically" means that the Neimark-Sacker bifurcation is not degenerate in this point, more precisely that the first Lyapunov value is not zero. Using the package CONTENT [Kuznetsov & Levitin] we can look for points on the NS-curve where the Lyapunov value is zero. We find a point $\mathcal{B}$ and this point does not coincide with $\mathcal{A}$. The parameter region with two invariant circles (the region IIIe in Figure 4.7) is extremely small, but we have managed to find it (one can check it: choose, for example, $\bar{I} = 1.5, c_0 = 0.32486, c_1 = 0.45539$). This region is bounded by the NS-curve, by the curve corresponding to stability of the heteroclinic cycle and by a small curve segment $\mathcal{BC}$, corresponding to fold bifurcation or collision of stable and unstable invariant circles. The point $\mathcal{C}$ on this curve is an analogue of the point $\mathcal{B}$ on the NS-curve. Namely, in this point a coefficient of a cubic term in the normal form of the heteroclinic stability bifurcation is zero.

Let us explain the behaviour of the system corresponding to different regions in the diagram in Figure 4.7. We will make a tour around the point $(\frac{1}{3}, \frac{1}{3})$ moving successively from region to region.

- In region I the attractor of the system is the SYC 3-cycle. The MYC-points exist and are transversally stable, but seem to be unstable with respect to the dynamics within the coordinate planes (this we have not proven).

- In region IIIa the MYC-points leave the positive cone and we observe

a stable heteroclinic cycle. We can leave this region either intersecting the dashed line or the NS-curve.

- The dashed line corresponds to change of stability of this cycle, i.e., in region IIIb the heteroclinic cycle is unstable and numerical observations show that there appears a stable invariant circle in the interior of the positive cone.

- If we leave IIIa by intersecting the NS-curve and entering the region IIId, the heteroclinic cycle remains stable but the internal equilibrium becomes also stable and an unstable invariant circle appears around it. Thus we have bistability in this region.

- From both the regions IIIb and IIId we can immediately enter IIIc. There are no more invariant circles in it. The internal equilibrium is stable and the heteroclinic cycle is unstable.

- From IIIb and IIId we can also enter the region IIIe of two invariant circles: the larger one is stable and the smaller one is unstable. Intersecting a curve where these circles come together, we enter IIIc again.

- In region II the MYC-points enter the positive cone again, but they are unstable and the only attractor is again the internal steady state.

- In region IVc the MYC-points disappear again. The difference with the region IIIc is that the unstable heteroclinic cycle rotates in the opposite direction.

- By intersecting the NS-curve we enter the region IVb where the internal equilibrium becomes unstable and a stable invariant circle appears around it. This region is an analogue of the region IIIb but with the opposite rotation direction.

- The invariant circle grows if we move to the left in the region IVb and finally disappears on the dashed line. In the region IVa the heteroclinic cycle inherits the stability.

- But on the diagonal the cycle breaks down by the MYC-points entering the positive cone and we are back in region I.

In this bifurcation diagram we clearly see two directions of the Neimark-Sacker bifurcations around the point $(\frac{1}{3}, \frac{1}{3})$ shown schematically in Figure 4.3. But also in the neighbourhood of the point $\mathcal{B}$ one observes the two directions of the Neimark-Sacker.

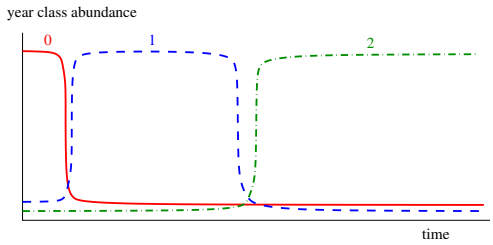

Figure 4.8: Heteroclinic dynamics with switches of year class dominance. This visualizes the attracting heteroclinic cycle of the third iterate of the map (4.1).

4.5 Discussion

One can notice that the phase diagrams which we draw (the small triangles in Figure 4.7) are flat and, moreover, the dynamics of the third iterate of the map (4.1) look like those of a planar vector field in the case of the Beverton-Holt nonlinearity (if we consider a time-shift map along the flow). There is a good reason to have a planar dynamics. While it is not easy to prove, we conjecture that in the Beverton-Holt case or in a general case with $\theta < 2$ there exists an attracting invariant manifold in the phase space. The system loses this property for larger θ. We know already that a period-doubling bifurcation of the internal steady state is possible. The instability occurs in the direction transversal to the invariant manifold and the latter does not exist any longer. The SYC-points and the MYC-points can also become *internally unstable* (as opposed to transversal (in)stability) by means of a period–doubling or a saddle–node bifurcation.

We have concluded from numerical observations in the case of Beverton-Holt nonlinearity that the dynamics of our recursion is similar to dynamics of a vector field. In particular, we have not observed phase-locking in cycles of whole periods in a neighbourhood of the NS-curve, or so-called Arnold tongues. Of course, this does not prove that the tongues do not exist, just they can be extremely narrow.

The heteroclinic cycle corresponds to a very interesting type of behaviour (let us call it heteroclinic dynamics/behaviour). During some period of time (several years) one observes a year class which is much more abundant than the other two (but they are not extinct). Then, at some year, the number of one of the less-abundant year classes grows fast and, in the next year, it dominates the population, while the former dominant declines. In other words, a switch between year classes occurs (see Figure 4.8).

We notice that the bifurcation diagram in Figure 4.7 is constructed for the special case $h_1(I) = h_2(I) \equiv 1$. Amazingly enough, the bifurcation

diagram remains qualitatively the same if we have density dependence of the Beverton-Holt type for all age classes. We have found this numerically. More precisely, we mean that no extra parameter regions occur. But the regions of two cycles can disappear for some parameter combinations. We think that this is also true for other types of nonlinearity for $\theta < 2$ (probably, we need that the ratios of the functions h_i are monotone). Positions of the parameter regions inside the (c_0, c_1)-triangle do change depending on sensitivity of age classes to competition. In particular, due to the cyclic symmetry of Lemma 2.3, we will have exactly the same bifurcation diagram in (c_1, c_2)– or (c_2, c_0)–triangles, if, respectively, only the age class N_1 is sensitive to competition or the age class N_2 [Mjølhus et al.].

On the basis of the bifurcation diagram in Figure 4.7, and taking into account the cyclic symmetry, we can make the following biological conclusions:

- If the sensitive age class (the only age class which suffers from competition) has the largest (expected) impact on the environment, all age classes coexist in a steady equilibrium (region II in the diagram).
- If the sensitive age class has the smallest impact, single year class behaviour occurs (region I).
- If the sensitive age class has an intermediate impact (less than one of the other age classes, but larger than the second), all age classes can coexist either in a steady equilibrium or while oscillating (quasiperiodic behaviour) (regions IIIb, IIIc, IVb and IVc).
- If the sensitive age class has a small, but not the smallest, impact, heteroclinic dynamics is possible with switches of year class dominance (Figure 4.8) (regions IIIa and IVa).
- Bistability is possible for some impacts combinations (the region IIId). Depending on initial conditions the population either stabilizes in a coexistence steady state or tends to a heteroclinic cycle.

We do not describe the tiny region IIIe in the biological conclusions, because any kind of stochasticity (say, environmental or demographic) will drive the system out of this region. However, we emphasize the importance of its existence. It is crucial for understanding of the continuous change in the phase portraits and non-existence of a (second) degenerate Neimark-Sacker point (like one corresponding to the vertical bifurcation). In other words it demonstrates a structural stability aspect of the system. More precisely, we mean that slight modifications of the functions h can not lead to appearance of parametric regions with new behaviour. Another useful aspects of the existence of this region is described below.

Let us now continue the discussion starting in the end of Chapter 2. There we considered the case when the coexistence equilibrium has an eigenvalue -1. We came to the conclusion that the vertical bifurcation serves as a switch between coexistence and competitive exclusion. Here we want to discuss the role of the vertical bifurcation if the coexistence equilibrium has a couple of non-real roots on the unit circle as indeed the case for $k = 3$.

In this case there are two conditions (corresponding to the real and the imaginary parts of the eigenvalues) on parameter values guaranteeing the vertical bifurcation and, therefore, the vertical bifurcation is of codimension 2. It is a degenerate case of a Neimark-Sacker bifurcation. In the neighbourhood of the vertical bifurcation there is a change of direction of the Neimark-Sacker bifurcation as shown in Figure 4.3. Therefore we have two ways from coexistence to exclusion: catastrophic or sharp loss of stability (above the dashed line in Figure 4.3) and non-catastrophic or mild loss of stability (under the dashed line). Concluding, we do not necessarily have a *switch* from coexistence to exclusion, a soft transition via growing fluctuations is possible, but whenever we have a vertical bifurcation of codimension 2 there is always a branch of Neimark-Sacker bifurcation (which is of codimension 1) corresponding to sharp loss of stability of the coexistence equilibrium. Do we necessarily end up with a situation of exclusion if this happens? Our experience says *No*: if we move from region IIIe in the diagram 4.7 to region IIIb, we have a sharp loss of stability, but the new attractor is the outer invariant circle with all year classes present. (This is indeed the usefulness of noting that the tiny region IIIe exists: the sharp loss of stability does not necessarily imply competitive exclusion, even though in most cases it does.)

Appendix. Proofs of lemmas from Section 4.2.

First we formulate an extra lemma which is useful for the proofs.

Lemma 4.6. *Let μ_1, μ_2 and μ_3 be the three roots of the equation (4.3). Then the products $\mu_1\mu_2$, $\mu_1\mu_3$ and $\mu_2\mu_3$ are roots of the equation.*

$$p^3 - a_1p^2 + a_0a_2p - a_2^2 = 0 \tag{4.14}$$

Proof. We have the identity

$$(\mu_2\mu_3)^3 - (\mu_2\mu_3 + \mu_1\mu_2 + \mu_1\mu_3)(\mu_2\mu_3)^2 + \mu_1\mu_2\mu_3(\mu_1 + \mu_2 + \mu_3)(\mu_2\mu_3) - (\mu_1\mu_2\mu_3)^2 = 0.$$

It can, using $a_0 = -(\mu_1 + \mu_2 + \mu_3)$, $a_1 = \mu_2\mu_3 + \mu_1\mu_2 + \mu_1\mu_3$ and $a_2 = -\mu_1\mu_2\mu_3$, be rewritten as (4.14) for $p = \mu_2\mu_3$. □

Proof of Lemma 4.1.

Proof. The assertions (i) and (ii) can be verified by substitution. For the case (iii) let the equation (4.3) have a pair of complex-conjugate roots $\mu = e^{\pm i\phi}, 0 < \phi < \pi$ .Then we have two identities

$$\begin{array}{llll} e^{3i\phi} & +a_0 e^{2i\phi} & +a_1 e^{i\phi} & +a_2 = 0 \\ e^{-3i\phi} & +a_0 e^{-2i\phi} & +a_1 e^{-i\phi} & +a_2 = 0 \end{array} \tag{4.15}$$

Multiplying the second identity by $e^{2i\phi}$ and subtracting the first identity, we obtain

$$(a_0 - a_2)(e^{2i\phi} - 1) = e^{-i\phi}(1 - e^{4i\phi}).$$

Dividing out $(e^{2i\phi} - 1)$ (which is not zero because the roots are not real) we achieve

$$a_0 - a_2 = -2\cos\phi. \tag{4.16}$$

Hence $|a_0 - a_2| < 2$. By Lemma 4.6 the product of the roots satisfies (4.14) and, since the product is 1 ,

$$1 - a_1 + a_0 a_2 - a_2^2 = 0.$$

Conversely, suppose this relation holds. Then, by substitution, $\mu = -a_2$ is a root of the equation (4.3) and the equation can be rewritten as

$$(\mu + a_2)(\mu^2 + (a_0 - a_2)\mu + 1) = 0$$

If, in addition, $-2 < a_2 - a_0 < 2$, then the second polynomial factor at the left-hand side has complex roots $\mu = e^{\pm i\phi}$ with $\phi \in (0, \pi)$ defined by $\cos\phi = \frac{1}{2}(a_2 - a_0)$. □

Proof of Lemma 4.3.

Proof. Necessity. First assume that all roots lie strictly inside the unit circle. Define

$$f(\mu) = \mu^3 + a_0\mu^2 + a_1\mu + a_2.$$

For real μ one finds $f(+\infty) = +\infty$ and $f(-\infty) = -\infty$ so, since f can not change sign outside the interval $(-1, 1)$, we must have $f(1) > 0$ and $f(-1) < 0$, which are exactly the conditions (a) and (b) of (4.4). If we denote the three roots of (4.3) by μ_1 , μ_2 and μ_3 , then $a_2 = \mu_1\mu_2\mu_3$ and accordingly (c) holds.

For products of pairs of roots we have the equation (4.14). Applying the same arguments to this equation as we applied above to f , we find two conditions

$$1 - a_1 + a_0 a_2 - a_2^2 > 0$$

and

$$1 + a_1 + a_0 a_2 + a_2^2 > 0.$$

The latter is satisfied whenever (a)–(c) are, and the former is (d).

Sufficiency. Assume that (a)–(d) hold. By (a) and (b) the function f has a real root in $(-1, 1)$. We consider first the case that the other two roots are complex (with non-zero imaginary part). Then, of the three possible products of two roots, two are complex and only one is real, which is the square of the modulus of the complex-conjugate roots. Hence (4.14) has a unique real root which lies in $(0, 1)$ if (d) is satisfied. Namely, define for $m = r^2 \geq 0$

$$g(m) = m^3 - a_1 m^2 + a_0 a_2 m - a_2^2$$

Since $g(0) = -a_2^2 < 0$, this function has a root $0 < m < 1$ if $g(1) > 0$, i.e. exactly if (d) is satisfied. Hence the complex-conjugate roots are inside the unit circle.

We now consider the case that all three roots of (4.3) are real. By (a)-(b) the number of roots in $(-1, 1)$ is odd. If all three are in $(-1, 1)$ we are done. So assume that $|\mu_1| < 1$ but $|\mu_2| > 1$ and $|\mu_3| > 1$. Applying exactly the same arguments to the function g we find that $|\mu_1 \mu_2| < 1$, $|\mu_2 \mu_3| > 1$ and $|\mu_1 \mu_3| > 1$ (when the numbering corresponds to the absolute value). But if $|\mu_2| > 1$ and $|\mu_1 \mu_3| > 1$ then also $|\mu_1 \mu_2 \mu_3| > 1$ which is in contradiction with (c). We conclude that also in the case of three real roots they all must lie in the unit circle. $\square$

Chapter 5

Dynamics and Bifurcations of Single Year Class Maps.

5.1 Introduction.

In this chapter we will concentrate on the single year class dynamics, i.e., at a given year we have individuals of the same age. We write a model for a semelparous population consisting of one year class in the following form:

$$\begin{array}{lll} N_0(t+k) & = N_{k-1}(t+k-1) & h_{k-1}(N_{k-1}(t+k-1)) \\ N_{k-1}(t+k-1) & = N_{k-2}(t+k-2) & h_{k-2}(N_{k-2}(t+k-2)) \\ \ldots & & \\ N_1(t+1) & = N_0(t)h_0(N_0(t)). & \end{array}$$

The number of newborns $N_0(t+k)$ in a year $t+k$ is proportional to the number of $(k-1)$-years old individuals in the previous year and the proportionality factor h_{k-1} is the expected number of offspring of a $(k-1)$-years old individuals after one year. Similarly, $N_i(t+i)$, $i = 1, ..., k-1$ is the number of individuals of age i at a year $t+i$ and it is proportional to the number N_{i-1} of the previous age class in the previous year with the factor $h_{i-1}(N_{i-1})$ which is a survival probability. It is a decreasing function of the age class number N_{i-1} that reflects the fact that the larger the population is, the stronger is the competition. We make the same assumption about the function $h_{k-1}(N_{k-1})$ arguing that the *expected* number of offspring is proportional to the survival probability in the last year of life. (See Chapter 1 for a more detailed description of the modelling procedure).

This model can be rewritten in the form of a one-dimensional composite map

$$N_0(t+k) = f_{k-1} \circ ... \circ f_0(N_0(t)),$$

where $f_i(x) = xh_i(x)$, or

$$x \mapsto f_{k-1} \circ ... \circ f_0(x).$$

This chapter is a version of [Davydova]

This *composition-map* or, a *SYC- (for Single Year Class), map* is the object of our study. A formal definition is given in Section 5.2 as is a (partial) classification of SYC-maps.

In Section 5.2 we introduce a parametrization of SYC-maps. Let a SYC-map be a composition of unimodal functions of the same form. Each of these functions is characterized by one parameter, the relative (w.r.t. the x–scale) height of its peak. Then the resulting composite map has k parameters. In terms of these parameters we can discuss bifurcations. If $k = 1$, we observe well-known cascades of period-doublings. We do not consider this case and refer to the excellent review of [Thunberg]. In Section 5.3 we recover the cyclic symmetry of Lemma 2.3 applied to SYC-maps.

In Section 5.4 we look for fixed points of SYC-maps. We find that for small values of the parameters, a SYC-map has a unique fixed point, while the maximal number of nontrivial fixed points depends on the order of the map and equals $2^k - 1$. Also in this section we consider a SYC-map which is composed of increasing functions, and show that it has a unique globally stable nontrivial fixed point. This simple result leads however to an important conclusion in modelling context. In order to avoid complex behaviour in the model, one should choose monotone nonlinearities whenever possible (e.g. Beverton-Holt like, see (1.6)).

Of our particular interest is the case $k = 2$. Analysis of local and global bifurcations of 2-SYC-maps constitutes the body of this chapter (Sections 5.5-5.8). In Section 5.5 we show that a large class of the 2-SYC-maps possesses a cusp bifurcation of spring type. We believe that this bifurcation is an organizing center of the bifurcation diagram of a 2-SYC-map.

Section 5.6 is devoted to the detailed analysis of local bifurcations of fixed points in 2-Ricker-maps. The results are summarized in the bifurcation diagram of Figure 5.2.

In Section 5.7 we consider global aspects of the dynamics of the 2-SYC-maps such as the maximal number of attractors, global stability of a unique nontrivial fixed point and homoclinic bifurcations. Application of these results to the 2-Ricker-maps yields a much better understanding of the dynamics and helps to produce a more complete bifurcation diagram (Figure 5.7). A detailed description of this diagram, combining analytical results and numerical insights, is presented in Section 5.8. Moreover we discuss four numerical bifurcation diagrams of a 2-Ricker-map in this section: Figure 5.8 and the three figures on the back cover of this book produced with the aid of the packages CONTENT [Kuznetsov & Levitin] and DYNAMICS [Nusse & Yorke: Dynamics], on which one observes such interesting phenomena as windows of successive periods and cascades of cusp bifurcations. The challenge is to describe the sequence of these cusps (see also [Branner]).

The bifurcation diagram has an intrinsic symmetry which, perhaps, gives a clue to the solution of this problem.

We conclude with a couple of remarks concerning general k-SYC-maps. The symmetry gives some intuition concerning the dynamics for higher values of k (Section 5.9). But a detailed description of bifurcations is quite problematic just because the dimension of a parameter space is more than 2.

Most sections begin with a short description of the results followed by subsections containing precise statements.

5.2 What is a single year class map?

The aim of this section is to introduce some notation and to give a formal definition of a single year class map. We also give alternative formulations and parametrizations of the map.

Definition 5.1. *A single year class map of order k, $k \geq 2$, also called a k-SYC-map, is a one-dimensional map:*

$$x \mapsto f_{k-1} \circ ... \circ f_0(x), \tag{5.1}$$

defined on $[0, \infty)$, where for $i = 0, 1, ..., k-1$

$$f_i(x) = xh_i(x), \tag{5.2}$$

with h_i defined on $[0, \infty)$, positive and bounded. We call $x \mapsto f_i(x)$ a building block of (5.1).

Remark. As both the functions h and f, with $f(x) = xh(x)$, are useful in various formulations below, we shall switch freely between them. So, whenever we use the symbols h and f (with or without a specific index), they are related by (5.2).

Note that from the interpretation in the introduction it follows that the functions h_i for $i = 0, ..., k-2$ are bounded by 1 from above because they are survival probabilities. We do not put this restriction into the Definition 5.1, to keep it more general and, in particular, to allow for various forms of rescaling.

Sometimes it is convenient to write the map (5.1) as

$$x \mapsto C(\mathbf{f})(x), \tag{5.3}$$

using a *composition operator*

$$C(\mathbf{f}) = f_{k-1} \circ ... \circ f_0,$$

with

$$\mathbf{f} = (f_0, ..., f_{k-1}).$$

5.2.1 Classes of SYC-maps

In this subsection we introduce several classes of building block functions f defining a SYC-map. The way we do it is somewhat formal and if the reader is not very interested in the technical details, (s)he can skip this. All the notation from this subsection which we use later on, is summarized in the Definitions 5.2 and 5.3.

First of all, we always require continuity for the functions f. The class H_1 consists of functions f such that the corresponding h is a function decreasing to zero. The interpretation of it is that the survival probability decreases due to competition and there is no Allee effect (roughly speaking, this effect is that at very low densities survival and reproduction *increase* with population density, for instance because it becomes easier to find mates).

The class H_2 is a subset of H_1 and consists of functions f, which first increase to a maximum and then decrease to zero. So, these functions are unimodal but the domain is unbounded. The interpretation of the class H_2 is that there is a population number for which the number of individuals in the next age-class is maximal. Clearly, if f belongs to H_1 it need not belong to H_2. In principle, it is possible to construct a function h such that $x \mapsto f(x)$ has several or no extrema. For example, if a function h is of the form $\frac{1}{1+x}$ (Beverton-Holt nonlinearity), it is decreasing, but the corresponding f is strictly increasing. We define the class H_3 so that f belongs to H_3 if and only if f is increasing but h is decreasing; we deal with such maps in Section 5.4.2.

Note that the functions f of class H_2, as well as their compositions, are bounded. Hence, despite the fact that the domain of f is $[0, \infty)$, after one iteration step we are confined to a bounded interval.

Next we introduce an important class H_S, characterized by smoothness and negative Schwarzian derivative (see Appendix A). We define

$$H_S = \{f : f \in H_2 \cap C^3, Sf < 0 \text{ for all } x; \text{such that } f'(x) \neq 0\}.$$

(The symbol S denotes the Schwarzian derivative in this chapter unlike the other chapters where it denotes the cyclic shift, see also a remark in Section 5.3.)

Note that the Ricker map

$$x \mapsto \lambda x e^{-x}$$

as well as the Hassell map

$$x \mapsto \frac{\lambda x}{(1+x)^{\beta}},$$

(which are both widely used in modelling), have negative Schwarzian [Thunberg].

To conclude the description of the various classes we give formal definitions.

Definition 5.2. *A continuous function* f *defined on* $[0,\infty)$ *such that* $f(0)=0$ *and* $f(x)>0$ *for* $x>0$ *, is of class*

- H_1 *if the function* h *, such that* $f(x)=xh(x)$ *, is strictly decreasing and* $\lim_{x\to\infty} h(x)=0$ *;*
- H_2 *if it is* H_1 *and there exists a point* $c\in(0,\infty)$ *such that it is strictly increasing on* $(0,c)$ *and strictly decreasing on* (c,∞) *;*
- H_3 *if it is* H_1 *and strictly increasing on* $[0,\infty)$ *;*
- H_S *if it is* H_2 *,* C^3 *and* $Sf(x)<0$ *for all* $x\neq c$ *.*

Frequently one considers a SYC-map with all the functions f_i from the same class. So the following definition is reasonable.

Definition 5.3. *We say that a SYC-map (5.1) is* H_j *,* $j\in\{1,2,3,S\}$ *, if all the functions* f_i *,* $i=0,...,k-1$ *, defining the map are of class* H_j *.*

Remark. A result that we will often use is that a function which is a composition of functions with negative Schwarzian has itself negative Schwarzian. However a composition of H_j functions with $j\in\{1,2,3,S\}$, is not necessarily an H_j function!

5.2.2 Parametrization of a SYC-map.

We shall parametrize a SYC-map in order to describe bifurcations. The idea is very simple. In examples like the well-known quadratic family $x\mapsto\lambda x(1-x)$ and the Ricker family $x\mapsto\lambda xe^{-x}$, the bifurcation parameter λ is a multiplicative factor. A SYC-map is a composition of such functions. For each building block we choose a multiplicative factor as a parameter (if the functions are unimodal, this factor gives the relative height of their peaks with respect to the x-scale). Thus a SYC-map of order k will have k parameters.

Let us write a function h_i in the following form

$$\begin{aligned} h_i(x) &= s_i\,\hat{h}_i(x)\\ s_i &= h_i(0). \end{aligned}$$

Note that since h_i is bounded (see Definition 5.1), $h_i(0) < \infty$. If h_i is also decreasing, then the function $\hat{h}_i$ reaches its maximum 1 at zero.

The biological meaning of s_i for $i = 0, ..., k-2$ is a survival probability from age i to age $i+1$ if there is no density dependence, for example, there is no competition in the population. The value s_{k-1} is the expected number of offspring of a $(k-1)$-year old individual in the next year, again in the case with no density dependence.

This form of the functions h_i suggests the following definition. We call a positive function h *normalized if* $h(0) = 1$.

Using the normalized functions $\hat{h}_i(x)$ and omitting hats we can rewrite the SYC-map (5.1) as follows

$$x \mapsto R_0\, x\Pi(x), \tag{5.4}$$

with

$$R_0 = s_0 ... s_{k-1}$$

$$\Pi(x) = h_0\left(x\right)\ h_1\left(f_0(x)\right)\ h_2\left(f_1 \circ f_0(x)\right) ... h_{k-1}\left(f_{k-2} \circ ... \circ f_0(x)\right),$$

where $f_i(x) = s_i\, x h_i(x), i = 0, ..., k-1$.

Note that the function Π is a product of normalized functions h_i. If all these functions are decreasing, then the product Π (as well as all h_i), has maximum 1 at zero.

The parameter

$$R_0 = h_0(0) ... h_{k-1}(0),$$

which is known in population dynamics as *the basic reproduction ratio*, is the expected number of offspring per newborn individual if this individual experiences no competition.

Of special importance is the case when the functions h_i are of the following two-parameter class

$$h_i(x) = s_i\, h(g_i x) \tag{5.5}$$

where h is a normalized function which has the additional property that $|h'(0)| = 1$ (note that this second normalization amounts to a proper choice of the parameters g_i, see also (2.9)). We call a positive function h defined on $[0, \infty)$ *doubly normalized if it is normalized and* $|h'(0)| = 1$. For example, the functions e^{-x} and $\frac{1}{1+x}$ are doubly normalized.

The interpretation of the parameters g_i is *sensitivity* of individuals of age i to competition (or, in general, to density dependence). The larger the value of g_i is, the less individuals survive the competition.

We make the following rescaling and reparametrization

$$\begin{aligned} &g_0 x \mapsto x \\ &p_i = s_i \, \tfrac{g_{i+1}}{g_i}, \quad i = 0, ..., k-1, \end{aligned} \tag{5.6}$$

where the indices are taken modulo k. Then we can rewrite the map (5.1) as

$$x \mapsto (p_{k-1} f) \circ (p_{k-2} f) \circ ... \circ (p_0 f)(x), \tag{5.7}$$

i.e. the functions f_i are given by

$$f_i(x) = p_i \, f(x).$$

We call (5.7) the *parametric SYC-map*. It is H_j if the function f is of class H_j. The factor R_0 is in this case the product of the p's:

$$R_0 = p_0 ... p_{k-1}.$$

In principle, one can choose either $\{p_0, ..., p_{k-1}\}$ or $\{R_0, p_0, ..., p_{k-2}\}$ as parameters of a SYC-map. There is a slight difference. If you choose the first set, then a symmetry property of the map is easy to formulate (see the next section). The alternative set helps to find explicit expressions for bifurcation curves (Section 5.6). Moreover it allows to decrease the order of a SYC-map by a restriction to one of the coordinate hyper-planes $p_i = 0$ of the parameter space. This is impossible in the first case because the map reduces to $x \mapsto 0$ on the coordinate planes. So, throughout the chapter, we assume

$$(p_0, ..., p_{k-1}) \in \{(p_0, ..., p_{k-1}) : p_i > 0, i = 0, ..., k-1\}$$

$$(R_0, p_0, ..., p_{k-2}) \in \{(R_0, p_0, ..., p_{k-2}) : R_0 > 0, \; p_i \geq 0, i = 0, ..., k-2\}$$

In the sequel we consider often the case $k = 2$, i.e., we deal with a family of parametric 2-SYC-maps which we write here as

$$x \mapsto p_1 f \circ p_0 f. \tag{5.8}$$

We choose often the function h in the form $h(x) = e^{-x}$. The building blocks are then the well-known Ricker maps:

$$x \mapsto p_i \, x e^{-x}$$

and the 2-SYC-map (which we call 2-Ricker-map) is

$$\begin{aligned} &x \mapsto R_0 \, x e^{-\nu(x, p_0)}, \\ &\nu(x, p_0) = x(1 + p_0 \, e^{-x}). \end{aligned} \tag{5.9}$$

5.3 Symmetry

An ingredient we need to formulate the symmetry property is a cyclic shift of indices. We define it as follows

$$\mathbb{S}\begin{pmatrix} f_0 \\ f_1 \\ \dots \\ f_{k-1} \end{pmatrix} = \begin{pmatrix} f_{k-1} \\ f_0 \\ \dots \\ f_{k-2} \end{pmatrix}$$

(In other chapter of this thesis we denote the cyclic shift by the regular symbol S, but in this section we use $\mathbb{S}$ in order to distinguish from the Schwarzian derivative, see p. 122.)

Proposition 5.4. *The dynamics generated by a SYC-map (5.1) does not change under the cyclic shift of indices.*

Proof. We will use the form (5.3) of the map.

Write

$$\begin{aligned} \psi_1 &= f_0 \\ \psi_2 &= f_{k-2} \circ \dots \circ f_0, \end{aligned}$$

then

$$\begin{aligned} \psi_1 \circ C(\mathbf{f}) &= f_0 \circ f_{k-1} \circ \dots \circ f_0 = C(\mathbb{S}^{-1}\mathbf{f}) \circ \psi_1 \\ \psi_2 \circ C(\mathbf{f}) &= f_{k-2} \circ \dots \circ f_0 \circ f_{k-1} \circ f_{k-2} \dots \circ f_0 = C(\mathbb{S}\mathbf{f}) \circ \psi_2 \end{aligned}$$

Let, for given x_0, the sequence $\{x_n\}$ be defined recursively by

$$x_{n+1} = C(\mathbf{f})(x_n).$$

Similarly, for given y_0, let $\{y_n\}$ be defined by

$$y_{n+1} = C(\mathbb{S}\mathbf{f})(y_n).$$

If $y_0 = \psi_2(x_0)$ then, by induction, $y_n = \psi_2(x_n)$. And, similarly, if $x_0 = \psi_1(y_0)$ then $x_n = \psi_1(y_n)$. So ψ_1 and ψ_2 map orbits to orbits. □

Note that neither ψ_1 nor ψ_2 is necessarily an homeomorphism (the functions need not be monotone) so the equivalence of the map (5.1) and its shifted versions is *not* the standard one from the theory of dynamical systems.

Corollary 5.5. *The dynamics generated by a parametric SYC-map (5.7) does not change under the cyclic shift of indices*

$$(p_0, p_1, \dots, p_{k-1}) \mapsto (p_{k-1}, p_0, \dots, p_{k-2}) \tag{5.10}$$

Corollary 5.6. *A bifurcation diagram of a parametric SYC-map (5.7) in the parameter space* $(p_0, p_1, ..., p_{k-1})$ *is symmetric, i.e., invariant under the cyclic shift (5.10). In particular, a bifurcation diagram of a parametric 2-SYC-map is invariant under the reflection* $(p_0, p_1) \mapsto (p_1, p_0)$.

If we choose $\{p_0, ..., p_{k-2}, R_0\}$ as a parameter set, we can formulate the symmetry property as well. We will do it for the case $k = 2$, but it is easy to generalize.

Corollary 5.7. *A bifurcation diagram of a parametric 2-SYC-map in the parameter space* (R_0, p_0) *is invariant under the reflection* $(R_0, p_0) \mapsto (R_0, \frac{R_0}{p_0})$.

5.4 Fixed points.

A SYC-map has always a trivial fixed point. In this section we are looking for nontrivial fixed points. The question of stability we leave for later sections.

Using the alternative form (5.4) of a SYC-map, we can say that all nontrivial fixed points have to satisfy the equation

$$\Pi(x) = \frac{1}{R_0}. \tag{5.11}$$

In various propositions below we estimate maximal and minimal number of nontrivial fixed points. In particular, we show that if the factor R_0 is less than one, an H_1 SYC-map has no nontrivial fixed points. The biological interpretation of this fact is very simple: if the expected number of offspring per individual is less than one even under ideal conditions, a population goes extinct.

For $R_0 = 1$ we have a transcritical bifurcation. For R_0 slightly bigger than one, a SYC-map has one nontrivial fixed point.

H_3 SYC-maps have a unique nontrivial fixed point for all $R_0 > 1$ while for other SYC-maps the number of fixed points can vary. They appear and disappear in fold bifurcations. The maximal number of fixed points depends on the order of a SYC-map and for H_S k-SYC-maps it is $2^k - 1$.

However in the following subsection we will show that, firstly, for $R_0 - 1 > 0$ small enough and, secondly, for all but one p's small enough, any H_S k-SYC-map has a unique nontrivial fixed point. Therefore in the neighbourhood of the axes of the parameter space $(R_0 - 1, p_0, ..., p_{k-2})$ or, alternatively, $(p_0, ..., p_{k-1})$ the SYC-map has a unique fixed point. In some cases this point is also globally stable (we show it for $k = 2$, Section 5.7).

The biological interpretation of this fact is rather important: for R_0 slightly bigger than 1 the population is stable. It is also stable (even for R_0 large) if all but one parameters p_i are small, for example, if the survival

probabilities are very low, but the number of offspring per reproducing individual is large. Or, if sensitivity to competition g_i in one of the age classes is much higher than in all the others.

We use the following terminology: if F is a one-dimensional map with fixed point $\bar{x}$, we call the derivative $F'(\bar{x})$ the *multiplier* of $\bar{x}$.

5.4.1 Small R_0 and small p's.

Proposition 5.8. *If $R_0 \leq 1$ an H_1 SYC-map $x \mapsto F(x)$ has no nontrivial fixed points and the trivial fixed point is a global attractor.*

Proof. For all $x > 0$ $|F(x)| < |x|$. Hence $x = 0$ is the unique global attractor. □

Proposition 5.9. *Given an H_1 SYC-map, there exists $\bar{R}_0$ such that for any $R_0 \in (1, \bar{R}_0)$ this map has a unique nontrivial fixed point.*

Proof. The function $\Pi(x)$ decreases from $\Pi(0) = 1$ to a local minimum m. Hence for $1 < R_0 < \frac{1}{m}$ the map has a fixed point. In the rest of its domain the function $\Pi(x)$ can have several local maxima. Notice that all these maxima are strictly less than 1. Denote by M the largest of these maxima. Take $\bar{R}_0 = \frac{1}{M}$. □

Theorem 5.10. *Let $R_0 > 1$. A parametric H_S SYC-map given by (5.7) has at most one nontrivial fixed point if for $i = 0, ..., k-2$ $p_i \leq \frac{c}{f(c)}$ where c is a critical point of f. And the multiplier of this fixed point is less than 1.*

In order to prove this theorem we first formulate a lemma and a corollary of it, which will also be useful later on.

Lemma 5.11. *Let a C^3 function F be increasing and assume that $SF < 0$ for all x such that $F'(x) \neq 0$. Then the map $x \mapsto F(x)$ has at most one fixed point with multiplier larger or equal to 1.*

Proof. In this and some other proofs we exploit the following simple fact. If a fixed point of the map, defined by a C^1 function, has a multiplier larger (less) than 1, then its neighbouring fixed points (if they exist, of course) have multipliers less (larger) or equal to 1.

Let there exist two fixed points $x_1 < x_2$ with multipliers strictly larger than 1. Then there should be a fixed point x_3 between them with $F'(x_3) \leq 1$. Let $G(x) = F(x) - x$, then $G(x_1) = G(x_3) = G(x_2) = 0$ and $G(x) > 0$ on (x_1, x_3) and $G(x) < 0$ on (x_3, x_2). Hence there exist $y_1 \in (x_1, x_3)$ and $y_2 \in (x_3, x_1)$ such that $G'(y_1) = G'(y_2) = 0$ and $G'(x) < 0$ on (y_1, y_2). Hence there exists z such that $G''(z) = F''(z) = 0$

and, in addition, $G'''(z) = F'''(z) \geq 0$. Since $SF < 0$, $\frac{F'''(z)}{F'(z)} < 0$. Hence $F'''(z) \neq 0$ and $F'(z) < 0$; but F is, by the condition of the lemma, an increasing function. So, we get a contradiction.

Let now x_1 have multiplier 1. Then there are two possible cases: there is still a point x_3 between x_1 and x_2 with multiplier $F'(x_3) \leq 1$ and we are back to the previous proof, or there is no point between x_1 and x_2. In this last case $G(x) < 0$ on (x_1, x_2) and there is a y_2 with $G'(y_2) = 0$. Noticing that $G'(x_1) = 0$, we are back to the previous proof again. □

Corollary 5.12 (of Lemma 5.11). *Let a C^3 function F with $SF < 0$ (for all x such that $F'(x) \neq 0$) be increasing on intervals $I_0, I_2, I_4, \ldots$ and decreasing on $I_1, I_3, I_5, \ldots$. Then it has at most one fixed point with multiplier larger or equal to 1 on each interval I_{2m}, $m = 0, 1, \ldots$. And between any two successive of these points there is a fixed point with multiplier strictly less than 1.*

Now let us prove Proposition 5.10.

Proof of Proposition 5.10. Recall that c is a unique critical point of maximum because f belongs to H_2.

The range of the function $f_0 = p_0 f$ is $[0, p_0 f(c)]$. This interval is at the same time the domain of the function f_1 if we consider the composition $f_1 \circ f_0$. By the condition of the proposition $p_0 f(c) \leq c$, hence f_1 is increasing on its domain.

Reasoning in exactly the same way we can say that the composition $f_{k-1} \circ \ldots \circ f_1$ is an increasing function. Hence the composition $f_{k-1} \circ \ldots \circ f_0$ is increasing on $[0, c)$ and decreasing on (c, ∞).

Since $R_0 > 1$, 0 is a fixed point with multiplier larger than 1 and by Corollary 5.12 the proposition is proved. □

Corollary 5.13 (of Theorem 5.10). *A parametric H_S 2-SYC-map (5.8) has at most one nontrivial fixed point if $1 < R_0 \leq \left(\frac{c}{f(c)}\right)^2$. And the multiplier of this point is less than 1.*

Proof. If R_0 is in the given interval, then one of the parameters p_0 or p_1 or both are less or equal to $\frac{c}{f(c)}$. □

5.4.2 Monotone maps.

The dynamics of an H_3 map are very simple. We have the following theorem.

Theorem 5.14. *Let $R_0 > 1$. The H_3 SYC-map has a unique nontrivial fixed point which is globally stable.*

Proof. Any composition $f_j \circ ... \circ f_0$ of strictly increasing functions f_i is again a strictly increasing function. Hence for any j $h_{j+1}(f_j \circ ... \circ f_0)$ is a strictly decreasing function with $\lim_{x\to\infty} h_{j+1}(x) = 0$ and therefore their product Π is also a decreasing function and $\lim_{x\to\infty} \Pi(x) = 0$. Since $\Pi(0) = 1$ and $\frac{1}{R_0} < 1$ the equation (5.11) has a unique positive solution x_0.

Since $x < x\Pi(x) < x_0$ for $x \in (0, x_0)$ and the opposite holds for $x \in (x_0, \infty)$ the fixed point x_0 is globally stable.

□

Remark. What we needed for this theorem is only strictly decreasing (to zero) Π and strictly increasing $x \mapsto x\Pi(x)$.

5.4.3 The maximal number of fixed points.

Theorem 5.15. *Let $R_0 > 1$. An H_S SYC-map of order k has at most $2^k - 1$ nontrivial fixed points. In particular, for $k = 2$ the map has at most three nontrivial fixed points.*

In order to prove this theorem we first formulate the following lemma.

Lemma 5.16. *The function $f_{k-1} \circ ... \circ f_0$, where all f_i are of class H_2, has at most $2^k - 1$ critical points: $2^{k-1} - 1$ points of minimum and 2^{k-1} points of maximum. Moreover, if the function has the maximal number of critical points, all the maxima are equal to the maximum of f_{k-1} and it has a minimum in the critical point c_0 of f_0.*

Proof. Let c_i be the critical points of the functions f_i.

Let $k = 2$. The function f_0 maps both $(0, c_0)$ and (c_0, ∞) to $(0, f_0(c_0))$ and it is one-to-one on each of the intervals. If f_1 has its maximum on $(0, f_0(c_0))$, the composition $f_1 \circ f_0$ has two points of maximum on $(0, \infty)$, moreover, both maxima are equal to the maximum of f_1, and as a consequence there is a minimum in between (in the point c_0).

Let $k = 3$. Clearly, $f_2 \circ f_1$ has the same property, i.e., at most two maxima and a minimum in between. If all the critical points lie in the interval $(0, f_0(c_0))$, then the composition of the three functions has $2 + 2$ maxima (two on the interval $[0, c_0)$ and two on (c_0, ∞)) and $1 + 1 + 1$ minima (the first minimum is on $(0, c_0)$, the second on (c_0, ∞) and the third is in the point c_0).

By induction, if $f_j \circ ... \circ f_1$ has $2^{(j-1)}$ points of maxima and $2^{(j-1)} - 1$ points of minima and all of them lie in $(0, f_0(c_0))$, then $f_j \circ ... \circ f_0$ has $2 \cdot 2^{j-1}$ points of maxima and $2 \cdot (2^{j-1} - 1) + 1$ points of minima.

□

Now the proof of the Theorem 5.15 is very simple.

Proof of Theorem 5.15. From Corollary 5.12 we see that the larger the number of critical points is, the larger the number of fixed points of a map can be. Let $c_1, ..., c_{2^{k-1}-1}$ be points of minimum of $f_{k-1} \circ ... \circ f_0(x)$ and $C_1, ..., C_{2^{k-1}}$ be points of maximum.

On $[0, C_1]$ 0 is the fixed point with multiplier larger than one, on all other intervals $[c_m, C_{m+1}]$ there can be at most one such a point. In addition, there are points with multipliers less than one between them and to the right of the largest of them. So, in total there are $2(2^{k-1} - 1) + 1 = 2^k - 1$ nontrivial fixed points. □

5.5 Cusp bifurcation and fold curves. $k = 2$.

We have already said that the fixed points appear and disappear in pairs in a *fold* bifurcation. Namely two neighbouring fixed points (one with a multiplier > 1 and another with multiplier < 1) move to each other as a parameter varies. At the moment of the fold bifurcation they collide creating a fixed point with multiplier equal to one. And after that they disappear.

A fixed point can collide with its right or its left neighbour. If these two bifurcations happen simultaneously (i.e., for some fixed parameter values) we have a *cusp* bifurcation: three fixed points collide. This bifurcation is of codimension 2 while the fold bifurcation is of codimension 1. This means that two parameters should be tuned to find the cusp bifurcation. (For more details see, e.g., [Kuznetsov].)

In this section we consider parametric 2-SYC-maps. They have a lot in common with maps with two extrema and, in particular, with cubic maps [Branner, Skjolding et al.]. In [Branner] the author considers odd functions with two extrema. He describes various bifurcations of codimension 1 and 2 of n-periodic points and gives ordering of periods.

We find in this section that a family of parametric 2-SYC-maps has a cusp point on its symmetry axis $p_0 = p_1$ (see Section 5.3) and two symmetric fold curves originate from this point. This is a local result in a neighbourhood of the cusp point. But for an arbitrary fold curve in the parameter plane (p_0, p_1) we can say that it is either invariant under the parameter reflection $(p_0, p_1) \to (p_1, p_0)$, or there should exist another symmetric fold curve which is obtained by this reflection.

For an H_S family of 2-SYC-maps the cusp is *of spring type* [Broer et al., Section 4.1.2]. The normal form for this bifurcation is

$$x \mapsto b + (1 + a)x - x^3.$$

And a bifurcation diagram of such a family in the neighbourhood of the cusp point can be found in [Kuznetsov, Section 9.2]. In our case of 2-SYC-maps this structure is presented in the Figure 5.1. Namely, we have a wedge in a parameter plane consisting of two fold curves originating from the cusp point. Inside the wedge the map has three nontrivial fixed points, outside it has only one. (A detailed description of Figure 5.1 is given in Theorem 5.25.)

The cusp point $(\bar{x}, \bar{p}, \bar{p})$ lies on the symmetry axis $p_0 = p_1$. It "coincides" with a *flip* point $(\bar{x}, \bar{p})$ of a building-block map $x \mapsto p\, f(x)$. (In the flip point the multiplier of a fixed point is -1. As a result of this bifurcation the fixed point loses its stability and, generically, a two–cycle appears around it.)

5.5.1 Fold curves. General case.

First we give a definition of a fold curve which is convenient in our case.

Definition 5.17. *A two–parameter family of C^2 maps $x \mapsto F(x, p_0, p_1)$ (or, alternatively, $x \mapsto F(x, R_0, p_0)$) has a* fold point *at (x, p_0, p_1) if the conditions*

$$\begin{aligned} F(x, p_0, p_1) &= x \\ F_x(x, p_0, p_1) &= 1 \end{aligned} \tag{5.12}$$

are satisfied. We call a continuous branch of solutions to (5.12) a fold curve *in the space (x, p_0, p_1) if*

$$F_{xx}(x, p_0, p_1) > 0 \text{ or } F_{xx}(x, p_0, p_1) < 0$$

on this branch. Also we call the corresponding curve in the parameter space (p_0, p_1) parametrized by x a fold curve *in (p_0, p_1).*

We adopt the convention that if the second derivative changes the sign, we move to another fold curve.

In a smooth enough family of 2-SYC-maps (5.8) a fold point should satisfy

$$\begin{aligned} &p_0 p_1\, h(x)\, h(p_0 f(x)) = 1 \\ &p_0 p_1\, f'(x)\, f'(p_0 f(x)) = 1. \end{aligned} \tag{5.13}$$

We can rewrite (5.13) as follows

$$\begin{aligned} &y = p_0 f(x) \\ &x = p_1 f(y) \\ &p_0 f'(x)\, p_1 f'(y) = 1. \end{aligned} \tag{5.14}$$

The second derivative at a fold point is

$$F_{xx}(x, p_0, p_1) = p_0 p_1\, G(x, p_0 f(x), p_0)$$

with

$$G : (x, y, p) \mapsto f''(x)f'(y) + p(f'(x))^2 f''(y)$$

We observe immediately the symmetry of Section 5.3.

Proposition 5.18. *If there exists a fold curve of a parametric 2-SYC-map (5.8) in* (p_0, p_1)*, there exists also a symmetric fold curve given by the transformation* $(p_0, p_1) \to (p_1, p_0)$*. Moreover, if* $(\bar{x}, \bar{p}_0, \bar{p}_1)$ *is a fold point,* $(\bar{p}_0 f(\bar{x}), \bar{p}_1, \bar{p}_0)$ *also is a fold point.*

Proof. The system (5.14) is invariant under $(x, y, p_0, p_1) \to (y, x, p_1, p_0)$. Therefore if $(x, p_0, p_1) = (\bar{x}, \bar{p}_0, \bar{p}_1)$ is a fold point, $(y, p_1, p_0) = (\bar{p}_0 f(\bar{x}), \bar{p}_1, \bar{p}_0)$ also is a fold point. Hence a fold curve (if it exists) must have a symmetric one with respect to $(p_0, p_1) \to (p_1, p_0)$. □

Proposition 5.19. *Consider two symmetric fold curves in* (x, p_0, p_1)*. Let* (x, p_0, p_1) *and* (y, p_1, p_0) *be symmetric fold points on these curves, i.e.,* $y = p_0 f(x)$*. Then the derivatives* $f'(x)$ *and* $f'(y)$ *both are non zero and have the same sign along the curves. Moreover, if the sign is plus, the second derivative* F_{xx} *has the same sign on both the fold curves; otherwise,* F_{xx} *has a different sign on each curve.*

Proof. The first property follows from the last equation of (5.14) and from continuity of fold curves.

We notice that for the symmetric fold points

$$G(y, x, p_1) = p_1 f'(y)\, G(x, y, p_0).$$

Hence

$$F_{xx}(y, p_1, p_0) = p_1 f'(y)\, F_{xx}(x, p_0, p_1) \tag{5.15}$$

and the second assertion is proved. □

A trivial case of a fold curve is when $x = y = 0$.

Proposition 5.20. *A curve* $p_0 p_1 = 1$ *(or* $R_0 = 1$ *) is a fold curve for an* H_1 *parametric 2-SYC-map (5.8). It corresponds to the fold points* $(0, p_0, \frac{1}{p_0})$.

Proof. We notice that $f'(x) = h(x) + xh'(x)$ and $f''(x) = 2h'(x) + xh''(x)$. The function $h(x)$ is doubly normalized, i.e., $h(0) = 1$ and $h'(0) = -1$ ($h(x)$ is decreasing). Having this we get that $(x, p_0, p_1) = (0, p_0, \frac{1}{p_0})$ satisfies (5.14) for all $p_0 > 0$, and $F_{xx}(0, p_0, \frac{1}{p_0}) = -2(p_0 + 1) < 0$. □

Clearly, the curve $p_0 p_1 = 1$ is symmetric to itself. The derivative $f'(0) = 1$ is positive. And, indeed, the second derivative in a fold point does not change the sign along this curve. This curve corresponds to the situation when a nontrivial fixed point "emerges" from a trivial one. This is not a very interesting case, we have already considered the behaviour of an (even general k-) SYC-map in the neighbourhood of this bifurcation (Section 5.4).

Now we turn our attention to the case of nontrivial fold points. Let a fold curve in (x, p_0, p_1) intersect the symmetry plane $p_0 = p_1$ at a point $(\bar{x}, \bar{p}, \bar{p})$. Then a symmetric fold curve should intersect it at a point $(\bar{p} f(\bar{x}), \bar{p}, \bar{p})$. If the derivative $f'(x)$ is negative at some fold point, it should be negative along both the symmetric fold curves and the second derivative F_{xx} has a different sign on each curve (Proposition 5.19). If, in addition, $\bar{x} = \bar{p} f(\bar{x})$, i.e. the fold curves intersect $p_0 = p_1$ at the same point, the second derivative $F_{xx}(\bar{x}, \bar{p}, \bar{p})$ should be zero by continuity. This is exactly the case of a *cusp point*. Motivated by this, we will prove that there exists a cusp point on the symmetry axis.

5.5.2 Cusp point.

Definition 5.21. *A smooth enough two–parameter family $x \mapsto F(x, p_0, p_1)$ (or, alternatively, $x \mapsto F(x, R_0, p_0)$) has a cusp point at (x, p_0, p_1) if (with all the derivatives evaluated at the point (x, p_0, p_1))*

$$\begin{aligned} &F(x, p_0, p_1) = x \\ &F_x = 1 \\ &F_{xx} = 0 \end{aligned} \tag{5.16}$$

and the bifurcation is generic if

$$\begin{aligned} &F_{xxx} \neq 0 && (a) \\ &F_{p_0} F_{xp_1} - F_{p_1} F_{xp_0} \neq 0 && (b) \end{aligned} \tag{5.17}$$

(see [Kuznetsov, p. 398]). The cusp is of spring type [Broer et al., Section 4.1.2] if

$$F_{xxx} < 0.$$

Theorem 5.22. *A smooth enough family of parametric 2-SYC-maps (5.8) possesses a cusp bifurcation at a point $(\bar{x}, \bar{p}, \bar{p})$ with $\bar{x} \neq 0$ and*

$$\bar{p} = \frac{1}{h(\bar{x})} \tag{5.18}$$

if and only if there exists $\bar{x}$ such that

$$\frac{\bar{x}\, h'(\bar{x})}{h(\bar{x})} = -2. \tag{5.19}$$

The bifurcation is generic and of spring type if the map is H_S *and*

$$\frac{d}{dx}\left(\frac{xh'(x)}{h(x)}\right)\bigg|_{x=\bar{x}} \neq 0 \tag{5.20}$$

Proof. A cusp point is a fold point with the additional property of zero second derivative. Using $f(x) = xh(x)$, we rewrite the equations (5.14) for a fold point (x, p_0, p_1) in the following form

$$\begin{aligned} &y = p_0 f(x) \\ &x = p_1 f(y) \\ &\phi(x) + \phi(y) + \phi(x)\phi(y) = 0 \end{aligned} \tag{5.21}$$

with $\phi(x) = \frac{xh'(x)}{h(x)}$ (recall that $h(x)$ is positive for all x). If $x = y$, then $p_0 = p_1 = \bar{p}$. This is the case of intersection of fold curves with the symmetry plane $p_0 = p_1$ at the same point $(\bar{x}, \bar{p}, \bar{p})$. (We have discussed this situation in the end of the previous subsection.) In this case either $\phi(\bar{x}) = 0$ or $\phi(\bar{x}) = -2$. The first case corresponds to the fold curve $p_0 p_1 = 1$ which we have already considered in Proposition 5.20. So, we concentrate on the case

$$\phi(\bar{x}) = -2.$$

Since $\phi(x) + 1 = \frac{f'(x)}{h(x)}$, the derivative $f'(\bar{x})$ is negative. Using (5.15), we have

$$F_{xx}(\bar{x}, \bar{p}, \bar{p})(1 - \bar{p} f'(\bar{x})) = 0$$

and thus the second derivative is zero.

Finally, if $x = y$, $\bar{x} = \bar{p} f(\bar{x})$, hence $\bar{p} = \frac{1}{h(\bar{x})}$. So, under the conditions (5.18) and (5.19) we have a cusp point at $(\bar{x}, \bar{p}, \bar{p})$.

Let now the map be H_S. The Schwarzian of F in the cusp point is just F_{xxx} because $F_{xx} = 0$ and $F_x = 1$. It is negative, hence the first genericity condition (5.17a) is satisfied and the cusp bifurcation is of spring type.

Now we should check the second genericity condition (5.17b). It demands some calculations. We omit the argument $\bar{x}$ of the functions below.

$$\begin{aligned} F_{p_0} &= p_1 f'(p_0 f) f \\ F_{p_1} &= f(p_0 f) \\ F_{xp_0} &= p_1 p_0 f''(p_0 f) f f' + p_1 f'(p_0 f) f' \\ F_{xp_1} &= p_0 f'(p_0 f) f'. \end{aligned}$$

In the cusp point we have $\bar{p} f(\bar{x}) = \bar{x}$. The condition (5.17b) is satisfied if

$$\bar{p}^2 \Big((f')^3 f - f(f'' f' f + h(f')^2) \Big) \neq 0.$$

Noticing that $\bar{p}^2 \neq 0$, $f'(\bar{x}) \neq 0$ and $f(\bar{x}) \neq 0$, we divide by all these expressions to get

$$(f')^2 - f''f - hf' \neq 0$$

Finally, substituting $(f'(\bar{x}))^2 = f'(\bar{x})(h(\bar{x})+\bar{x}h'(\bar{x}))$ and dividing by $h^2(\bar{x}) \neq 0$, we have

$$\frac{d}{dx}\left(\frac{f'(x)}{h(x)}\right)\bigg|_{x=\bar{x}} \neq 0,$$

which is indeed equivalent to (5.20). □

Remark. Note that the conditions (5.19)–(5.20) are satisfied for the 2-Ricker family $h(x) = e^{-x}$ and the 2-Hassell family $h(x) = \frac{1}{(1+x)^\beta}$ with $\beta > 2$. It is interesting that the function $\frac{xh'(x)}{h(x)} = \frac{d\ln h(x)}{d\ln x}$ has a biological meaning, it is the so-called *elasticity* of survival [Caswell] (see also p. 40).

The condition (5.20) can be viewed as $\phi'(\bar{x}) \neq 0$. From the last equation of (5.21) we see that we can use the Implicit Function Theorem to find a branch of solutions $y = g(x)$ passing through $(x, y) = (\bar{x}, \bar{x})$. Moreover, from the symmetry with respect to $(x, y) \to (y, x)$ the function g is equal to its inverse, i.e. $g = g^{-1}$ in a neighbourhood of $\bar{x}$. This solution corresponds to symmetric fold curves originating from the cusp point.

The same result we have from the normal form theorem [Kuznetsov, Theorem 9.1]. Moreover, by proving Theorem 5.22 we have made a step towards discussion of stability properties. Namely, from the normal form it follows that in a neighbourhood of a generic cusp point, a map has either one stable fixed point (outside the wedge in Figure 5.1) or two stable fixed points with an unstable one in between (inside the wedge) or two points: one is stable and the other with multiplier 1 (on the fold curves).

5.5.3 Cusp point is a flip point in the building block map.

Definition 5.23. *A C^1 map $x \mapsto F(x, p)$ has a* flip point *at (x, p) if*

$$\begin{aligned} F(x,p) &= x \\ F_x(x,p) &= -1. \end{aligned}$$

Proposition 5.24. *If a building block map $x \mapsto p\,f(x)$ has a flip point at $(\bar{x}, \bar{p})$, the corresponding 2-SYC-map (5.8) has a cusp point at $(\bar{x}, \bar{p}, \bar{p})$.*

Proof. The conditions for a building block map to have a flip point are

$$\begin{aligned} \bar{p}f(\bar{x}) &= \bar{x} \\ \bar{p}f'(\bar{x}) &= -1 \end{aligned}$$

They can be rewritten as

$$\begin{aligned} \bar{p} &= \frac{1}{h(\bar{x})} \\ f'(\bar{x}) + h(\bar{x}) &= 0. \end{aligned}$$

And the last equation is equivalent to $\phi(\bar{x}) = -2$. From the proof of Theorem 5.22 these expressions are precisely the conditions (5.18) and (5.19) for the cusp point. □

5.6 Local dynamics of the 2-Ricker map.

We now consider the 2-Ricker-map (5.9) which we rewrite here, omitting the index 0 of p_0 (so $p \equiv p_0$), as

$$\begin{aligned} x &\mapsto R_0 x e^{-\nu(x,p)}, \\ \nu(x,p) &= x(1 + pe^{-x}). \end{aligned} \tag{5.22}$$

First we find explicit expressions for the fold curves and the cusp point in the parameter space (R_0, p). Then we consider local stability of the fixed points.

The linear stability is determined by the multiplier. If the absolute value of the multiplier is strictly less than 1, the fixed point is locally asymptotically stable. A fold bifurcation takes place when the multiplier equals $+1$. If the multiplier passes the value -1, we have a flip (or period-doubling) bifurcation: the (dis)appearance of a two–cycle around the fixed point.

We conjecture that the bifurcation diagram we obtained (Figure 5.2) for the 2-Ricker-map (5.22) is representative (in the qualitative sense) for general H_S SYC-maps of order 2. In particular, in [Broer et al, Section 4.1.2] there is a whole collection and even classification of areas around a cusp point and in most of the cases the organization of fold and flip curves around a cusp of spring type is like we find in the special case of the Ricker family.

5.6.1 Fold curves. Ricker case.

Theorem 5.25. *Let* $R_0 > 1$.

i) For $R_0 > e^4$ *and* $p \in (p_-, p_+)$, *where*

$$p_\pm = e^{x_\pm} \left(\frac{\ln R_0}{x_\pm} - 1 \right), \tag{5.23}$$

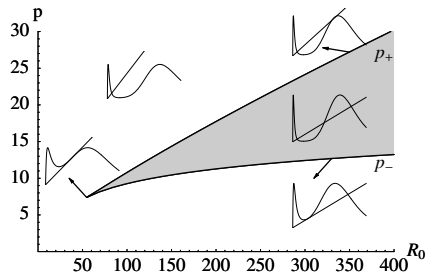

Figure 5.1: Fold curves and a cusp point for the 2-Ricker-map (5.22). We have a wedge consisting of the two fold curves originating from the cusp point. Inside the wedge the map has three nontrivial fixed points, outside it has only one. On the fold curves two of the three fixed points collide. In the cusp point the all three points collide.

$$x_\pm = \frac{\ln R_0 \pm \sqrt{(\ln R_0)^2 - 4\ln R_0}}{2}, \tag{5.24}$$

the map (5.22) has three nontrivial fixed points, the middle of which is always unstable.

ii) For $R_0 > e^4$ and $p = p_\pm$ there are two nontrivial fixed points. Moreover, if $p = p_+$ the upper fixed point is x_+ and its multiplier equals 1. If $p = p_-$ the lower fixed point is x_- and its multiplier is 1.

iii) In all other cases there is a unique nontrivial fixed point. Moreover, if $R_0 = e^4$ and $p = e^2$ this fixed point is $x = 2$. It is a generic cusp point of spring type (Definition 5.21).

The proof of the theorem is given in Appendix B. The fold–bifurcation curves $p_\pm(R_0)$, given by (5.23)–(5.24) are strictly monotone increasing for $R_0 \geq e^4$.

Remark. For a fixed value of R_0, the transformation $p_+ f(x_+)$ sends a fixed point x_+ corresponding to a fold point (R_0, p_+) with $F''(x_+) < 0$, to the other fixed point x_- corresponding to another fold point (R_0, p_-) with, correspondingly, $F''(x_-) > 0$ and vice versa. From the symmetry of Corollary 5.7 it follows that $p_+ = \frac{R_0}{p_-}$ and that the cusp point lies on the symmetry axis $p = \sqrt{R_0}$.

5.6.2 Local stability of the fixed points.

Let us now consider the stability properties of the fixed points. Similarly to fold curves (Definition 5.17), we give a definition for flip curves on which the

multiplier of a fixed point equals -1.

Definition 5.26. *A two–parameter family of C^1 maps $x \mapsto F(x, R_0, p)$ has a* flip point *at (x, R_0, p) if the conditions*

$$\begin{aligned} &F(x, R_0, p) = x && \text{(a)} \\ &F_x(x, R_0, p) = -1 && \text{(b)} \end{aligned} \tag{5.25}$$

are satisfied. We call a continuous branch of solutions to (5.25) parametrized by x a flip curve *in the space (R_0, p).*

We do not add extra conditions on the second derivative of F as in the fold case. However, we formulate the following lemma.

Lemma 5.27. *Let $(\bar{x}, \bar{p})$ be a flip point of a smooth enough one–parameter family of maps $x \mapsto F(x, p)$. Let, in addition,*

$$\begin{aligned} &SF(\bar{x}, \bar{p}) < 0 && \text{(a)} \\ &F_{xp}(\bar{x}, \bar{p}) < 0. && \text{(b)} \end{aligned} \tag{5.26}$$

Then

- *for p slightly less than $\bar{p}$ the map has a stable fixed point in a neighbourhood of $\bar{x}$;*
- *for p slightly larger than $\bar{p}$ the map has a stable two–cycle.*

This lemma is a particular case of the normal form theorem for the flip bifurcation [Kuznetsov, Theorem 4.4].

It is possible in the Ricker case to find explicit expressions for flip curves.

Theorem 5.28. *Let $R_0 > e^2$. Then the fixed point of the map (5.22), given explicitly by*

$$x_{1,2} = \frac{\ln R_0 \pm \sqrt{(\ln R_0)^2 - 4 \ln R_0 + 8}}{2}, \tag{5.27}$$

where x_1 corresponds to "+" and x_2 corresponds to "-", undergoes a flip bifurcation if $p = p_{1,2}$, respectively, where

$$p_{1,2} = e^{x_{1,2}} \left(\frac{\ln R_0}{x_{1,2}} - 1 \right). \tag{5.28}$$

As a result of this bifurcation a stable two–cycle appears around the corresponding fixed point, for parameter values in regions of (R_0, p) slightly below the curve $p_1(R_0)$ and slightly above $p_2(R_0)$.

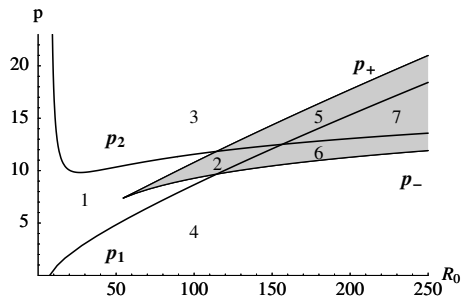

Figure 5.2: The bifurcation diagram of the map (5.22) where the local bifurcations are represented. See explanations in the text.

The proof of the theorem is given in Appendix B. The curves $p_1(R_0)$ and $p_2(R_0)$ corresponding to the flip bifurcation are shown in Figure 5.2.

Now a stability result is as follows.

Theorem 5.29. *Let* $R_0 > 1$.

i) If the map (5.22) has a unique nontrivial fixed point, it is stable in two cases: if $R_0 \le e^2$ *or* $R_0 > e^2$ *and* $p \in [p_1, p_2]$.

ii) If the map (5.22) has three nontrivial fixed points, the smallest of them is locally stable if $p \in (p_-, p_2]$.

iii) Similarly, if the map (5.22) has three nontrivial fixed points, the largest of them is locally stable if $p \in [p_1, p_+)$.

Remark. For $R_0 > e^4$ the map (5.22) has a unique fixed point if $p \notin [p_-, p_+]$. It is stable if $p \in [p_1, p_2]$. Thus in this case a unique fixed point can be stable only if $p_1 < p_-$ or $p_2 > p_+$, i.e., the flip bifurcation curves lie outside the region of three fixed points. Remark that intersections of the flip curves $p_{1,2}(R_0)$ with the fold curves $p_{\mp}(R_0)$ respectively, take place for the same value of R_0 due to the symmetry of the curves.

The proof of the theorem is given in Appendix B. Now we are able to describe all the local bifurcations of the fixed points which take place in the map (5.22) for positive values of R_0 and p. The bifurcation diagram is represented in Figure 5.2. There are four bifurcation curves for $R_0 > 1$, fold bifurcation curves $p = p_{\pm}(R_0)$ and flip bifurcation curves $p = p_{1,2}(R_0)$, where $p_{\pm}$ and $p_{1,2}$ are given by (5.23) and (5.28) respectively. The parameter space is divided into seven regions.

- In the region 1 the map has a unique nontrivial fixed point and it is locally stable. This region consists of three subregions. The first one

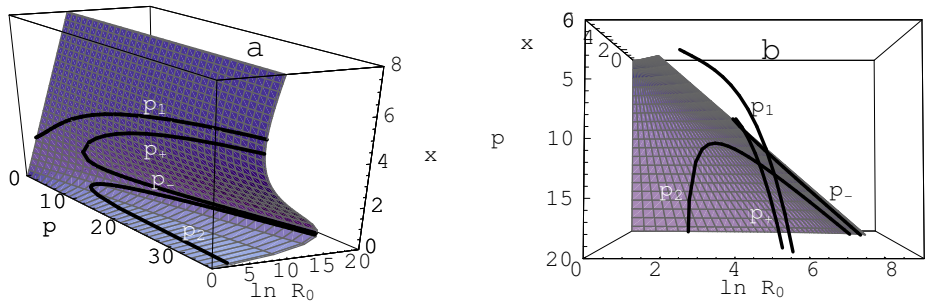

Figure 5.3: The surface of fixed points of the 2-Ricker-map in the space (R_0, p, x) with the fold curves $p_\pm$ and flip curves $p_{1,2}$ shown. **a:** The two flip curves correspond to distinct fixed points, so the curves do not intersect. **b:** A view from above, the upper part of the surface is removed and one sees the same diagram as in Figure 5.2.

is the domain $\{R_0 \in (1, e^2]$ and $p \in (0, \infty)\}$, the second one is $\{R_0 \in (e^2, e^4]$ and $p \in [p_1, p_2]\}$ and the third one is $\{R_0 \in (e^4, R_0']$ and $p \in [p_1, p_-) \cup (p_+, p_2]\}$, where R_0' is the value of R_0 which corresponds to the intersection of the flip curves $p_{1,2}(R_0)$ with the fold curves $p_\pm(R_0)$.

- In the region 2 the map has three nontrivial fixed points: the middle one is unstable while the upper and the lower ones are locally stable.
- The regions 3 and 4 are symmetric with respect to the transformation $p \mapsto \frac{R_0}{p}$. In these regions the map has a unique nontrivial fixed point which is locally unstable. Moreover, in a neighbourhood of the curves $p_{1,2}(R_0)$ in these regions there exists a stable two–cycle around the unstable fixed point.
- The regions 5 and 6 are also symmetric. The map has three nontrivial fixed points, two of which are unstable and one is stable: the upper (in the region 5) or the lower one (in the region 6). Moreover, in the region 5 in a neighbourhood of the curve $p_2(R_0)$ there exists a stable two–cycle around the lower fixed point. Similarly for the region 6.
- In the region 7 the SYC-map has three locally unstable fixed points. In a neighbourhood of $p_{1,2}(R_0)$ there exist two–cycles around the upper and the lower fixed points, respectively.

We emphasize that for arbitrary large values of the multiplicative factor R_0, there is still a window for p, where the map has a stable equilibrium.

One can get a wrong impression looking at Figure 5.2 that flip curves may intersect. It happens only because the curves p_1 and p_2 are projections

of flip curves in the space (R_0, p, x). In other words, the two flip curves correspond to distinct fixed points x_1 and x_2 (given by (5.27)) of the 2-Ricker-map. In Figure 5.3 we show a surface of fixed points of the 2-Ricker-map (5.22) for different values of R_0 and p which is given by

$$\nu(x, p) = \ln R_0.$$

We see that this surface "folds" in the space so that there can be one, two or three fixed points for different sets of (R_0, p). Curves, where the normal vector to the surface is parallel with the coordinate plane (R_0, p), are the fold curves p_+ and p_-. The flip curves p_1 and p_2 are also shown so one can see that they do not intersect indeed (Fig. 5.3a). If we look at the surface from above (along the x-axis) and remove the upper part of the surface (Fig. 5.3b), we see the diagram of Figure 5.2.

The structure similar to this diagram with a cusp point, two fold curves and two flip curves is well-known and rather universal (see, e.g. [Broer et al.] and references in there, [El-Hamouly et.al., Carcassès, Mira]), it is also called *crossroad area*. What is especially nice for the 2-Ricker-map is that the fold and flip curves are given by explicit formulas. As we will see later in this chapter (see the numerical bifurcation diagram in Figure 5.8), the same structure appear also for higher iterates of the map, i.e. we observe cusps of periodic points accompanied by fold and flip curves. Moreover, the cusp points accumulate, so there occur so-called *cascades of cusps*. We conclude it from the fact that flip curves which accompany cusp points accumulate indeed. (For example, if we fix $p < e^2$, the 2-Ricker-map is unimodal. So, if we let R_0 grow, we observe well-known Feigenbaum cascades of period-doublings.)

5.7 Some results on global dynamics. $k = 2$.

We have described local bifurcations of fixed points in the family of 2-Ricker-maps (5.22). Now we are going to consider some global aspects of the dynamics. The main goal of this section is to prove, at least partly, that the bifurcation diagram in Figure 5.7 of the 2-Ricker family is correct. However all the results in this section are formulated for a general 2-SYC-map.

To formulate the results we need various notions from one-dimensional dynamics. To help a non-expert reader we collect some basic notions and results in Appendix A.

First we show that a 2-SYC-map with one critical point can be viewed as an S-unimodal map and hence it has one metric attractor.

In the second subsection we show that a 2-SYC-map can have at most two metric attractors. We prove also that local stability of a unique fixed point

means automatically global stability. These results are valid for a general (even non-parametric) H_S 2-SYC-map.

Finally, we describe nonlocal homoclinic bifurcations which influence the number of attractors.

In this and the following sections we denote by c a unique turning point of the building block map f of an H_2 parametric 2-SYC-map (5.8). If $p_0 \leq \frac{c}{f(c)}$ the SYC-map F has a unique turning point which is again c (see Proof of Proposition 5.10 and Lemma 5.16), then $F(c)$ is the value of maximum. Otherwise, the SYC-map has three turning points: two maxima and a local minimum in between. The values of maxima are the same, we denote them by M. The local minimum is at the point c (Lemma 5.16) and the value of minimum is m.

5.7.1 One critical point. The map is S-unimodal.

Proposition 5.30. *Let an H_S 2-SYC-map $x \mapsto F(x)$ have one critical point c. Then the map is topologically conjugated to a unimodal map on an interval $[0, a]$ with $F(c) < a < \infty$.*

Proof. While the SYC-map is defined on $[0, \infty)$, after the first iteration we land in the interval $[0, F(c)]$. We choose a unimodal map $\tilde{F}$ on an interval $[0, a]$ with $F(c) < a < \infty$ such that $\tilde{F}(x) = F(x)$ for $x \in [0, F(c)]$ and $\tilde{F} : (F(c), a] \to (0, F^2(c))$ is decreasing. □

From Blokh and Lyubich's theorem (see Appendix A) the corollary below follows.

Corollary 5.31. *Let an H_S 2-SYC-map (5.1) have one nonflat critical point. Then it has a unique metric attractor.*

For a parametric 2-SYC-map (5.8) we can formulate the following corollary.

Corollary 5.32. *Consider a parametric H_S 2-SYC-map (5.8). Let $R_0 > 1$, c is a nonflat critical point of the building-block map f and $p_0 < \frac{c}{f(c)}$ or, alternatively, $R_0 < \left(\frac{c}{f(c)}\right)^2$. Then the map has a unique metric attractor.*

Proof. Note that if c is nonflat and $p_0 < \frac{c}{f(c)}$, the SYC-map has a unique nonflat critical point c. □

If $p_0 = \frac{c}{f(c)}$, the critical point of the 2-SYC-map can be flat, so the Blokh and Lyubich's theorem is not applicable, but we can apply another theorem, namely Singer's theorem 5.46 to prove the proposition below.

To apply Singer's theorem to a SYC-map we should consider it on a bounded interval. We can easily do it because the range of the SYC-map is bounded by its maximum $F(c)$. So after the first iteration all the values of x lie in the interval $[0, F(c)]$.

Proposition 5.33. *Let an H_S 2-SYC-map (5.1) have one critical point (flat or nonflat). Then it has at most one periodic attractor. In particular, if for a parametric H_S 2-SYC-map (5.8) $R_0 > 1$ and $p_0 \leq \frac{c}{f(c)}$ or, alternatively, $R_0 < \left(\frac{c}{f(c)}\right)^2$, the map has at most one periodic attractor.*

5.7.2 Three critical points. Number of attractors. Global stability of a unique fixed point.

Proposition 5.34. *If an H_S 2-SYC-map (5.1) has three critical points, it has at most two periodic attractors.*

Proof. We use the Singer's theorem again.

A 2-SYC-map has three critical points: two maxima and a minimum in between. The values of the maxima are the same. Hence the corresponding critical points belong to the immediate basin of the same periodic attractor.

We consider the SYC-map on a bounded interval $[0, M]$, where M is the value of maximum of F. Since the right bound of the interval M coincides with the maximum, this boundary point belongs to the same basin of attraction as the points of maximum.

Further, observe that the left boundary point 0 does not belong to any basin of attraction because it is itself a fixed point.

In conclusion, the map can have two periodic attractors, one that attracts the maximum of the map and one that attracts the minimum. □

Corollary 5.35. *Let an H_S 2-SYC-map have two stable fixed points. Then they are the only metric attractors in the system, moreover, their immediate basins are divided by the unstable fixed point between them.*

Proposition 5.36. *If an H_S 2-SYC-map $x \mapsto F(x)$ has a unique nontrivial fixed point, local stability implies global stability.*

Proof. For any H_1 SYC-map we have that $\lim_{x\to\infty} F(x) = 0$. We choose an a so that $a > M$, where M is the maximum value of $F(x)$, and, in addition, $F(a) < F(M)$ and $F(a) < m$, where m is a unique local minimum. We note that the interval $[0, a]$, is invariant and absorbs all initial conditions. Therefore we can restrict our consideration to this interval.

By Singer's theorem the immediate basin I of the nontrivial fixed point should contain either a boundary point or a critical point.

Let the basin contain the boundary point a (the boundary point 0 does not belong to any basin). Then it contains the interval $[F(a), a]$. This interval also absorbs all initial conditions, because $F(a) < \min(m, F(M))$. Hence the fixed point is globally stable.

If the basin I does not contain a, we have that I contains a critical point and that $F(\partial I) \subset \partial I$, because I is invariant. Since we have a unique nontrivial fixed point, the boundary ∂I can not contain a fixed point, hence points of the boundary are fixed points of the twice iterated map, i.e., $F^2(x) = x$ for $x \in \partial I$. The function $F(x)$ is decreasing in these points, otherwise I is not invariant. We assumed that I contains a critical point. It is a turning point, i.e. the derivative $F'(x)$ changes the sign in this point. Hence there should be two turning points in I. Therefore, the interval $[\min(m, F(M)), M] \subset I$. This interval absorbs all initial conditions, hence the fixed point is globally stable.

□

Corollary 5.37. *Let $R_0 < 1$. A parametric H_S 2-SYC-map (5.8) has a unique globally stable nontrivial fixed point if $p_0 \leq \frac{c}{f(c)}$ ($p \leq e$ for the Ricker case) or, alternatively, $R_0 \leq \left(\frac{c}{f(c)}\right)^2$ ($R_0 \leq e^2$).*

5.7.3 Three critical points. Homoclinic bifurcation.

It is a more subtle question whether attractors, which are not fixed points, can coexist. We are going to give sufficient conditions for existence of two attractors in the system. It has to do with the behaviour of critical points under the action of the map. We consider two cases for the maximum M:

$$\begin{array}{ll} F(M) > x_{mid} & \text{(a)} \\ F_l^{-1}(x_{mid}) < F(M) < x_{mid} & \text{(b)} \end{array} \tag{5.29}$$

where x_{mid} is the middle fixed point and $F_l^{-1}(x_{mid})$ is its closest preimage to the left (see Figure 5.4). Similarly, for the minimum m we also consider two cases:

$$\begin{array}{ll} m > F_l^{-1}(x_{mid}) & \text{(a)} \\ F_{ll}^{-1}(x_{mid}) < m < F_l^{-1}(x_{mid}) & \text{(b)} \end{array} \tag{5.30}$$

where $F_{ll}^{-1}(x_{mid})$ is the left side preimage of x_{mid} (Fig. 5.4). In Figure 5.5 we show four possible combinations: **A** corresponds to (5.29a) and (5.30a), **B** to (5.29a) and (5.30b), **C** to (5.29b) and (5.30a), **D** to other possibilities.

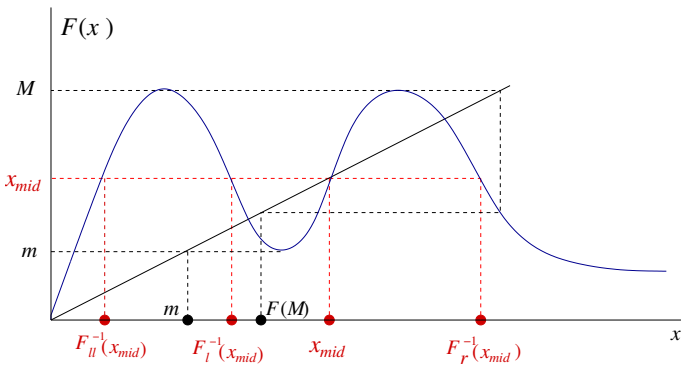

Figure 5.4: A graph of the SYC-map. The fixed point x_{mid} has four preimages. In the figure the cases (5.29b) and (5.30b) are illustrated.

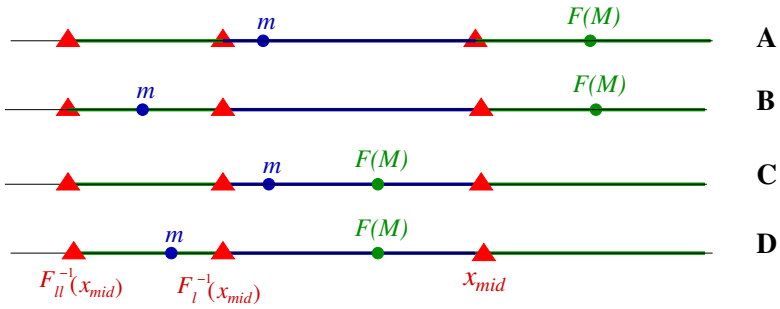

Figure 5.5: We show four possible combinations of mutual positions of $F(M)$ and m: **A** corresponds to (5.29a) and (5.30a), **B** to (5.29a) and (5.30b), **C** to (5.29b) and (5.30a), **D** to other possibilities.

Proposition 5.38. *Let an H_S 2-SYC-map F have three fixed points. If the condition (5.29a) is satisfied, the map is S-unimodal on $I_r = [x_{mid}, F_r^{-1}(x_{mid})]$, where $F_r^{-1}(x_{mid})$ is the right preimage of x_{mid}.*

Similarly, if (5.30a) is satisfied, the map is topologically conjugated to an S-unimodal map on $I_l = [F_l^{-1}(x_{mid}), x_{mid}]$.

Proof. Under the condition (5.29a) $F(I_r) \subseteq I_r$, the map has a unique critical point on this interval and the Schwarzian is negative. So, we get the desired conclusion.

For the case of minimum the proof is similar. □

Now, using Blokh & Lyubich's theorem 5.44, we obtain the following results.

Corollary 5.39. *Let an H_S 2-SYC-map 5.8 have three nonflat critical points and three nontrivial fixed points.*

i) Let (5.29a) and (5.30a) both be satisfied (Fig. 5.5 **A***). Then the map has two metric attractors: one belongs to I_l and one to I_r.*

ii) Let (5.29a) and (5.30b) both be satisfied (Fig. 5.5 **B***). Then the map has a unique metric attractor, which belongs to I_r.*

iii) Similarly, if (5.30a) and (5.29b) are both satisfied (Fig. 5.5 **C***), the map has a unique metric attractor which belongs to I_l.*

Proof. To show ii) we note that, under (5.30b), the image of the minimum m lies in the interval I_r, which is absorbing.

For the left interval the proof is similar. □

If we have both (5.29b) and (5.30b), or if either (5.29) or (5.30) does not hold (Fig. 5.5 **D**), it is not so easy to determine how many attractors there are. On the parameter plane (R_0, p) boundaries between regions corresponding to the a and b conditions are given by the following implicitly defined functions

$$F(M) = x_{mid} \tag{5.31}$$

and

$$F(M) = F_l^{-1}(x_{mid}) \tag{5.32}$$

for (5.29) (where $F(M)$ and x_{mid} are functions of R_0 and p) or

$$m = F_l^{-1}(x_{mid}) \tag{5.33}$$

and

$$m = F_{ll}^{-1}(x_{mid}) \tag{5.34}$$

for (5.30), respectively. These curves correspond to homoclinic bifurcations. More precisely, we mean the following. Consider, for example, the case (5.31). Take a right neighbourhood N^+ of x_{mid} (Figure 5.6). Since $F(x) > x$ on $(x_{mid}, \bar{x}_2)$ and $c_2 < \bar{x}_2$, where c_2 is the right point of maximum and $\bar{x}_2$ is the upper fixed point, there exists a number k such that $F^k(N^+) \supset M$. The image of M is x_{mid}. Therefore we can find an orbit which starts just to the right of x_{mid} (and converging to x_{mid} backwards in time) and which arrives in exactly x_{mid} in finitely many steps. This is a homoclinic orbit. It contains the critical point and we call this orbit degenerate. So, we say that a one–parametric family $x \mapsto F(x, a)$, with a as a parameter, possesses *a homoclinic bifurcation* if there exists a_0 such that the map $x \mapsto F(x, a_0)$ has a degenerate homoclinic orbit.

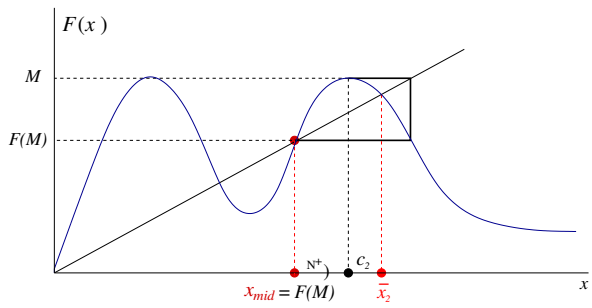

Figure 5.6: Homoclinic bifurcation in the 2-SYC-map (5.8). $F(M) = x_{mid}$.

To prove rigorously that these homoclinic orbits do exist for a parametric 2-SYC-map (5.8), we need to provide values of the parameters p and R_0 such that one of the conditions (5.31)–(5.34) is satisfied. It is not possible to give explicit expressions, but numerically (for the Ricker case) we can construct the corresponding curves in the bifurcation diagram in the plane (R_0, p) (Fig. 5.7). The curve M_1 corresponds to the homoclinic bifurcation (5.31), M_2 corresponds to (5.32), m_1 to (5.33) and the curve m_2 to (5.34). The homoclinic bifurcation is a complicated phenomenon, namely, in every parameter neighbourhood of this bifurcation the map has bifurcation of either fold or flip type [Devaney, p. 126]. Thus, this bifurcation is an accumulation point of simple bifurcations.

Again we find the symmetry of the section 5.3.

Proposition 5.40. *Let an H_2 parametric SYC-map (5.8) have three fixed points. In the parameter plane (R_0, p) the curves given by (5.31) and (5.33) are symmetric under the reflection $(R_0, p) \mapsto (R_0, \frac{R_0}{p})$. Similarly, (5.32) and (5.34) are also symmetric.*

Proof. Let a parametric SYC-map given by $F_1 = f_1 \circ f_0$ have parameters R_0 and p. Then a symmetric map $F_0 = f_0 \circ f_1$ has parameters R_0 and $\frac{R_0}{p}$. We denote the maxima of F_1 and F_0 as M_1 and M_0 respectively and the minima m_1 and m_0. We divide the domain of f_0 and f_1 into two parts and define invertible functions $i = \{0, 1\}$:

$$f_{il} = f_i : [0, c] \to [0, M_i] \quad f_{ir} = f_i : [c, \infty) \to [0, M_i],$$

where c is a unique turning point of the building block map f (recall that $f_i = p_i f$). We notice that $f_j(f_i(c)) = m_j, i \neq j$, $f_i(c) = M_i$ and hence

$$\begin{array}{ll} \text{a) } f_{0l}(m_1) = F_0(M_0) & \text{c) } f_{0r}(M_1) = m_0 \\ \text{b) } f_{1l}(m_0) = F_1(M_1) & \text{d) } f_{1r}(M_0) = m_1. \end{array} \tag{5.35}$$

We consider, for example, (5.31) and rewrite it as

$$F_1(M_1) = x^1_{mid}, \tag{5.36}$$

where x^1_{mid} is the middle fixed point of F_1. For the middle fixed points x^0_{mid} of F_0 and x^1_{mid} we have

$$f_{0r}(x^1_{mid}) = x^0_{mid}.$$

Having (5.35b) we apply f_{1l}^{-1} to both sides of the equation (5.36):

$$m_0 = f_{1l}^{-1}(x^1_{mid}) = f_{1l}^{-1}(f_{0r}^{-1}(x^0_{mid})) = F_{1l}^{-1}(x^0_{mid}),$$

i.e., we get (5.33). In a similar way we check the equivalence in the opposite direction and also show that (5.32) and (5.34) are symmetric too. □

5.8 Bifurcation diagrams of the 2-Ricker-map.

In this section we present detailed bifurcation diagrams of the 2-Ricker-map (5.22), i.e., we describe the behaviour of the system in different regions of the parameter plane (R_0, p). We summarize the analytical results we have got in the previous sections and add some numerical observations. In particular, we find cascades of cusps.

First we give a short description of the bifurcation diagram in Figure 5.7 and then explain it in detail.

- There exists a region $R_0 \leq 1$ (not shown in the picture) where the map has only the trivial fixed point which is globally stable.
- In the region 1 the map has a unique nontrivial fixed point which is globally stable (Proposition 5.36).
- In the regions 3 and 4 the unique fixed point is unstable and we observe cascades of cusps.
- In the region 2 the SYC-map has two stable fixed points and an unstable one in between. (Corollary 5.35 gives more info.)
- In the regions 5 and 6 one of these fixed points loses its stability and a cascade of period-doublings (-halfings) takes place.
- In the region 7 both fixed points are unstable and there exist two attractors, one "around" each of the fixed points.

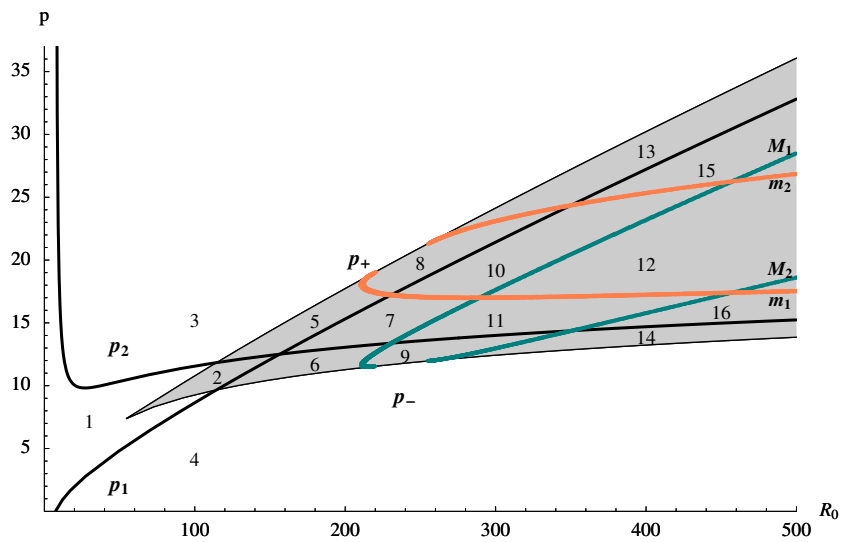

Figure 5.7: The bifurcation diagram of the 2-Ricker-map (5.22) on which the curves corresponding to homoclinic bifurcations are represented. For further explanations see the text.

- In the regions 8 and 9 the map has a unique metric attractor which is a fixed point.
- In the regions 10 and 11 the map has again a unique attractor: the stable fixed point from the regions 8 and 9 is now unstable and there is an attractor around it.
- In the regions 13 and 14 the map has a stable fixed point, but another attractor might exist as well.
- In the regions 12, 15 and 16 the map can have two metric attractors which are not fixed points. Cascades of cusps are observed in these regions.

We notice that the regions 4, 6, 9, 11, 14, 16 are symmetric to 3, 5, 8, 10, 13, 15, respectively. Let us consider the region of three fixed points, which is the interior of the wedge between p_- and p_+ (p_- and p_+ are fold curves, see section 5.6). We note first that the points of intersection of the curves p_- and p_+ with the flip-curves p_1 and p_2 respectively do not correspond to

a local bifurcation of higher codimension because these bifurcations happen with different fixed points of the SYC-map.

In the region 2 of the bifurcation diagram the SYC-map has two stable fixed points and one unstable between them. The stable fixed points are the only attractors in the system because, as we have shown in section 5.7 (Corollary 5.39 (i)), the SYC-map has two metric attractors. Changing the parameters (but staying within the wedge), we intersect generically either the p_1 or the p_2 flip-curve. Hence one of the stable fixed points loses its stability and a two-cycle appears. As long as we move to larger values of R_0, but do not leave regions 5 or 6, a sequence of period-doubling or, possibly, -halfing (see, for example, [Nusse & Yorke]) bifurcations of the two-cycle takes place. If we intersect the second flip-bifurcation curve and enter the region 7, the second fixed point becomes unstable and again a period-doubling cascade occurs. According to Corollary 5.39 in the regions 5–7 the map has two metric attractors.

If we intersect one of the homoclinic bifurcation curves, say, m_1, entering the regions 8 or 10, we have only one metric attractor left, which is in fact a fixed point in the region 8. Hence in the region 8 (and also in 9) the map has a stable fixed point (which attracts almost all initial values), a rather unexpected phenomenon. In the regions 12, 13 and 15, after the intersection of a second homoclinic curve either m_2 or M_1, this is no longer the case, i.e., we can have two attractors.

Numerical experiments, which we have made for the 2-Ricker-map, show however that the map can have two attractors also outside the wedge. More precisely, we have a cascade of cusp bifurcations ([Broer et al., Sections 4.2, 5.1.3] and references in there, see also [Skjolding et al.]). In Figure 5.8 we illustrate this cascade. The bifurcation diagram is produced by using the package CONTENT [Kuznetsov & Levitin]. Black curves correspond to the local bifurcations of the fixed points (cf. Figure 5.7), blue curves correspond to those of period 2 points, green curves — 4–points, red curves — 3–points.

Look at, say, the upper part of the diagram, at the region outside the black wedge. On the black flip curve the unique fixed point becomes unstable and a period-2 point occurs. The second iterate of the map has also a cusp bifurcation (blue one) associated with this point. Therefore we can have two period-2 points which can also become unstable, periodic and other attractors can arise around these points, the attractors can merge by a homoclinic bifurcation, i.e. 2–points repeat the fate of the fixed points of the map.

Above and below the blue wedge we have a period-4 point and similarly a cusp bifurcation (green one) in the fourth iterate of the map, et cetera.

A period-3 point (and other odd-period points) can not occur as a result of period-doubling. Hence we have a fold bifurcation resulting in the appearance

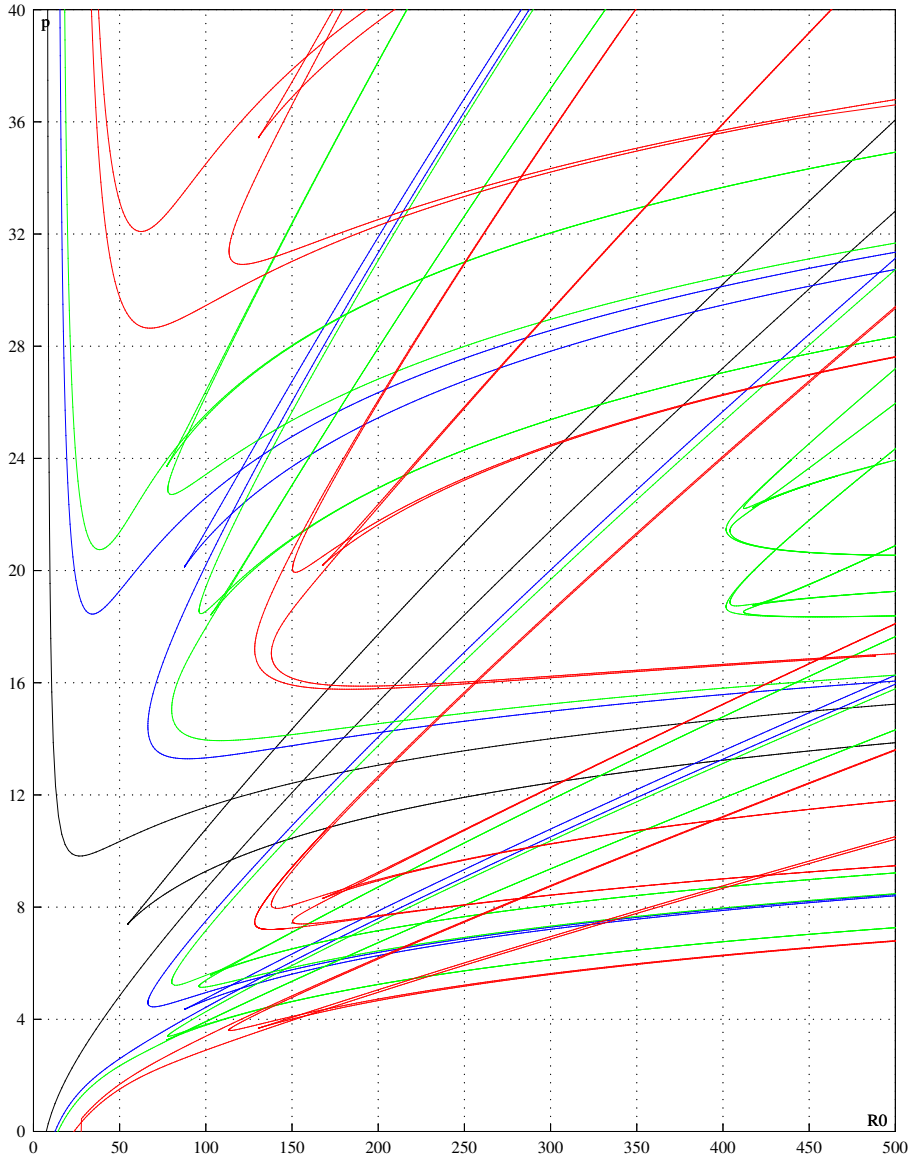

Figure 5.8: A numerical bifurcation diagram of the 2-Ricker-map (5.22). Black curves correspond to the local bifurcations of the fixed points (cf. Figure 5.7), blue curves correspond to that of period 2 points, green curves — 4–points, red curves — 3–points. A cascade of cusps is clearly presented. The bifurcation diagram is produced by using the package CONTENT [Kuznetsov & Levitin].

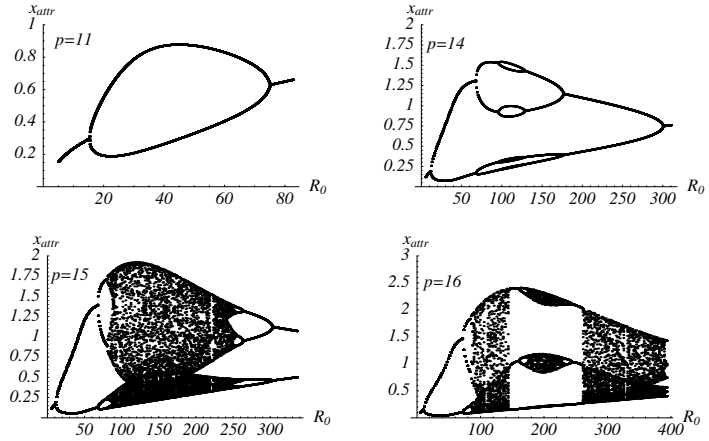

Figure 5.9: "Bubbles" in the bifurcation diagram of the 2-Ricker-map (5.22).

of such points. But the interesting thing is that even-period points can also appear in such fold bifurcations. Inside the black wedge, on the right of the bifurcation diagram we see that this happens for 4–points.

The precise pattern of cusps in the parameter plane is not clear, but we believe that in some intervals along a line $R_0 = const$ we have Sharkovski order of the cusps. This can be observed in Figure 3 on the back cover.

This figure is made using the package DYNAMICS [Nusse & Yorke: Dynamics]. We show the period of an attractor of the 2-Ricker-map (it is a so-called period plot). We can have bistability but we show only one of the attractors, namely, those which attracts the critical point of minimum $c = 1$ of the 2-Ricker-map. Fortunately, this critical point does not change its position as we change R_0 and p. The horizontal interval is $R_0 \in [0, 500]$, the vertical interval is $p \in [0, 40]$. Different colours correspond to different periods of attractors: cyan — fixed point (period 1), blue — period 2, red — 3, green — 4, yellow — 5, rose — 6, orange — 7, dark green — 8. Black regions are regions with other behaviour, e.g. higher periods, chaos.

Also in this figure we can see cusps inside the wedge (more precisely, in the regions 12, 15 and 16 of Figure 5.7).

If we follow an appropriate path in the bifurcation diagram, we can observe the Feigenbaum cascades of period-doublings. More interesting behaviour can be observed if we choose a path across flip curves (for example along a line with fixed p). If we intersect the same flip curve two times: at the first time we have the period-doubling bifurcation and, for example, a

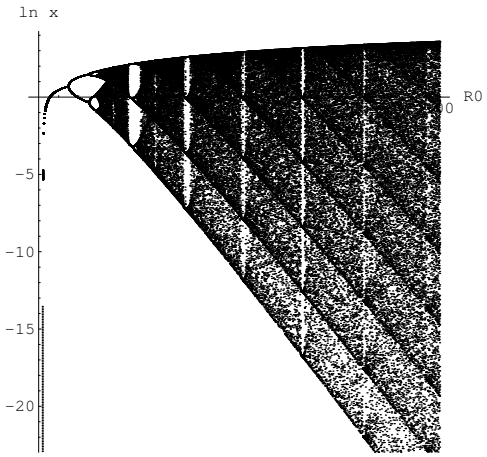

Figure 5.10: A bifurcation diagram of the Ricker map $x \mapsto R_0 x e^{-x}$ in which parametric windows are shown in which the map has a stable orbit of successive periods $2, 3, 4, 5, \ldots$. Notice the logarithmic scale of x .

two–cycle appears from the fixed point, at the second time a period-halfing bifurcation takes place and the two–cycle lands onto the fixed point which becomes stable (Figure 5.9). In between, for not so large values of p (say, $p = 11$), the two-cycle grows at first and then its amplitude decreases again. It forms a loop in a bifurcation diagram with coordinates (R_0, x_{attr}), where x_{attr} denotes points of an attractor. For larger values of p , the period-doubling cascade does take place if we move along $p = const$, but the cascade stops and evolves back (via period-halfing bifurcation) forming so-called "bubbles" in a bifurcation diagram [Nusse & Yorke].

We have not used the word "chaos" yet. However, chaotic dynamics is indeed observed in the 2-Ricker-map. In Figure 1 on the back cover we present a chaos plot of the 2-Ricker map produced with the aid of DYNAMICS [Nusse & Yorke: Dynamics]. To make it nicely symmetric we choose $(p_1, p_0) = (\frac{R_0}{p}, p)$ as axes. If an attractor is chaotic, any two initially close points yield trajectories that diverge and the rate of the divergence is given by the so-called Lyapunov exponent. A necessary condition for an attractor to be chaotic is that a corresponding Lyapunov exponent is positive. In the figure black regions correspond to negative values of the Lyapunov exponent, while blue to yellow regions correspond to positive values of the Lyapunov exponent, moreover, the larger the Lyapunov exponent, the lighter the color of a point.

Remark. There is one more interesting feature of the bifurcation diagram for the Ricker map $x \mapsto R_0 x e^{-x}$. In Figure 5.10 we see parametric windows in which the map has a stable orbit of successive periods $3, 4, 5, \ldots$. Similar windows we observe in the bifurcation diagram in Figure 2 on the back cover for the 2-Ricker-map (5.22). Figure 2 is a numerical bifurcation diagram, namely, a period plot, on which windows are shown in which the map has a stable orbit of successive periods $2, 3, 4, 5, \ldots$. The horizontal interval is $p_0 \in [0, 12]$, the vertical interval is $p_1 \in [10, 150]$. Different colours correspond to different periods of attractors: cyan — fixed point (period 1), blue — period 2, red — 3, green — 4, yellow — 5, rose — 6, orange — 7, dark green — 8. Black regions are regions with other behaviour, e.g. higher periods, chaos.

Remark. To produce the figures on the back cover, we used not the 2-Ricker-map (5.22) itself, but a topologically conjugated map

$$y \mapsto y + \ln R_0 - e^y \left(1 + p \exp(-e^y)\right),$$

which is obtained from the 2-Ricker-map by the transformation $y = \ln x,\ x > 0$. This choice was dictated by numerical needs. Namely, for large values of R_0 and p periodic points of the 2-Ricker-map, which lie near zero, are so close to each other that the programme is not able to distinguish between them. The logarithmic scale allows to overcome this problem.

Besides, if we consider a "logarithmic" version of the 1-Ricker-map

$$x \mapsto R_0\, x\, e^{-x},$$

which is given by

$$y \mapsto y + \ln R_0 - e^y,$$

we will find that this expression has a structure similar to the well-know *circle map*

$$y \mapsto y + \rho + c_1 \sin y \bmod 2\pi.$$

5.9 Discussion. General k.

In Section 5.2 we have defined a general SYC-map of order k, but most attention was paid to maps of order 2. The dynamics of a general SYC-map is beyond the scope of this work, but here we would like to mention some interesting properties of such maps.

Along the symmetry axis all parameters p_i of the parametric SYC-map (5.7) are equal (and equal to a value p) and the map is just the k-th iterate of the building block map $x \mapsto pf(x)$. We assume that the dynamics of this building block map are known. What are the corresponding dynamics of the SYC-map? For example, let the building block map have a period-n orbit. If n is a multiple of k, namely $n = km$, the SYC-map has k period-m orbit. If k is a multiple of n, the map has n fixed points. Otherwise, it has again a period-n orbit.

If an attractor in the SYC-map on the symmetry axis is structurally stable, small perturbations do not change its qualitative structure. Therefore we know the behaviour of the system in the neighbourhood of the axis. Besides it can serve as a starting point of a continuation analysis.

But what can we say about bifurcation points? We conjecture that a bifurcation point in the building block map (i.e., on the symmetry axis) is an intersection of corresponding bifurcation surfaces in the parameter space. For example, the first period-doubling of a 1-SYC-map is the cusp point in the corresponding 2-SYC-map (Proposition 5.24). A general question, that we leave out the scope of this article, is: given a bifurcation in the building block map, what does it "generate" as bifurcation on the symmetry axis for the k-SYC-map?

We have already mentioned that the multiplicative factor of the SYC-map R_0 has a clear biological meaning (it is the expected number of offspring per individual). Therefore, it makes sense to consider bifurcations which happen in the SYC-map when we change R_0. In particular, we choose all other parameters so that we are on the symmetry axis.

Let the building block map $x \mapsto pf(x)$ have the first period-doubling for some $p = p_*$ and let it have for $1 < p < p_*$ a (globally) stable (nontrivial) fixed point. Hence any iteration of this map has the same stable fixed point. And thus the k-SYC-map has a stable fixed point for all $1 < R_0 < p_*^k$. Therefore the interval of R_0 values for which the SYC-map is stable grows very rapidly with k. This has a very interesting (and counter-paradigmal) biological interpretation: *the introduction of age-structure in the population model allows for a much wider range of basic reproduction ratio values for which the system is stable.* We must say that a stable SYC fixed point corresponds to a k-years cycle with a single year class present, i.e. the population exhibits cyclic and not steady behaviour. However we consider this behaviour as "stable" comparing with (almost) irregular behaviour which corresponds to high-periods and chaotic attractors which one observes in the building block map for large values of R_0.

Another possibility to start continuation analysis is coordinate planes $\{(R_0, p_i) : p_j = 0, j \neq i\}$ of the parameter space $\{R_0, p_0, ..., p_{k-2}\}$. On these

planes a SYC-map of order k reduces to a 2-SYC-map whose dynamics are known.

The aim of this work was to introduce SYC-maps, a particular case of composition maps. They seem to be an interesting and a logical extension of unimodal maps. An extension in the sense that the dimension of the parameter space increases and also the number of fixed points increases. This allows to observe in these systems such interesting phenomena as homoclinic bifurcations and cascades of cusps.

Acknowledgments.

I would like to thank Odo Diekmann for proposing this problem to me and for help. I also would like to thank Helena Nusse for her valuable suggestions and remarks and for introducing me to the package DYNAMICS which allowed me to produce the beautiful pictures for this paper.

Appendices

A Basic notions of one-dimensional dynamics.

Here we present some basic notions of one-dimensional dynamics to make it easier for non-experts to understand the results. Definitions and results presented here are mostly taken from [Thunberg, De Melo & van Strien].

Definition 5.41. *The Schwarzian derivative SF of a function F is defined by*

$$SF = \frac{F'''}{F'} - \frac{3}{2}\left(\frac{F''}{F'}\right)^2$$

for all x such that $F'(x) \neq 0$.

Definition 5.42. *A continuous interval map $F : I = [a, b] \to I$ is* unimodal *if $F(\partial I) = \partial I$ and there is a unique point of maximum c in the interior of I such that F is strictly increasing on $[a, c)$ and strictly decreasing on $(c, b]$. The map F is* S-unimodal *if it is unimodal, C^3 and $SF(x) < 0$ for all $x \neq c$.*

Definition 5.43.
- *If a continuous map is increasing in a left neighbourhood of a point c and decreasing in its right neighbourhood, or vice versa, the point c is called a* turning point.

- *If for a* C^1 *map* $F'(c) = 0$ *, the point* c *is called a* critical point.
- *If for a* C^m *map* c *is a critical point such that* $F^{(n)}(c) = 0, 1 < n \leq m$ *, it is called a* flat critical point. *Otherwise, it is nonflat.*

If in a critical point the second derivative of the map is non-zero, this critical point is a turning point.

For S-unimodal maps we have the following significant property (which we copy from [Thunberg]).

Theorem 5.44. [Blokh & Lyubich] *Let* $F : I \to I$ *be an S-unimodal map with nonflat critical point. Then* F *has a unique metric attractor* Ω *, such that the* ω *-limit set* $\omega(x)$ *is equal to* Ω *for Lebesgue almost all* $x \in I$ *. The attractor* Ω *is of one of the following types:*

i) an attracting periodic orbit;

ii) a Cantor set of measure zero;

iii) a finite union of intervals with a dense orbit.

In the first two cases, $\Omega = \omega(c)$ *.*

The definition of *metric attractor* can be found in [Milnor]. We repeat it here. A set Γ is called *forward invariant* with respect to F if $F(\Gamma) = \Gamma$. The set $B(\Gamma) = \{x|\omega(x) \subset \Gamma\}$ is *the basin of attraction* of Γ .

Definition 5.45. [Milnor] *A forward invariant set* Ω *is called a* metric attractor *if*

i) $B(\Omega)$ *has positive Lebesgue measure;*

ii) Ω *is maximal in the sense that if* Ω' *is another forward invariant set, strictly contained in* Ω *, then* $B(\Omega)\backslash B(\Omega')$ *has positive measure.*

In Blokh & Lyubich theorem we read that the first two types of metric attractors attract the critical point c . To have this property it is not necessary to deal with a unimodal map. The following theorem says that the most important condition is negativity of the Schwarzian.

Theorem 5.46. [Singer] *Let* $F : I \to I$ *be a* C^3 *interval map with negative Schwarzian derivative. Then the immediate basin of any stable periodic orbit contains either a critical point of* F *or a boundary point of the interval* I *.*

The *immediate basin* of an attracting periodic orbit is the union of the connected components of its basin which contain a point of the periodic orbit. In the case of a stable fixed point the immediate basin is an interval around the point.

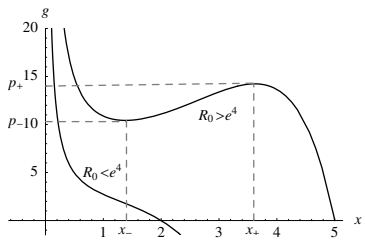

Figure 5.11: The function $g(x)$ given by (5.39) for two values of R_0 .

B Proofs of theorems from Section 5.6.

Proof of Theorem 5.25.

Proof. A nontrivial fixed point of the map (5.22) should satisfy the equation

$$\nu(x,p) = \ln R_0, \tag{5.37}$$

We can rewrite this equation in the form

$$g(x) = p, \tag{5.38}$$

with

$$g(x) = e^x \left(\frac{\ln R_0}{x} - 1 \right). \tag{5.39}$$

(i) If $R_0 > e^4$ the function g has two local extrema: a minimum at a point x_- and a maximum at a point x_+ , where x_- and x_+ satisfy

$$x^2 - \ln R_0 x + \ln R_0 = 0 \tag{5.40}$$

and hence they are given by (5.24) (Fig. 5.11).

If $p_- = g(x_-) < p < g(x_+) = p_+$ then the equation (5.38) has three simple roots, and, consequently, the map (5.22) has three nontrivial fixed points.

The multiplier of a fixed point $\bar{x}$ is equal to

$$1 - \bar{x}\nu_x(\bar{x}, p) \tag{5.41}$$

with

$$\nu_x(\bar{x}, p) = -\bar{x}g'(\bar{x})e^{-\bar{x}}. \tag{5.42}$$

Since the derivative $g'(\bar{x})$ at the middle point is positive, the multiplier of this point is always bigger than $+1$. Thus the first assertion of the theorem is proved.

(ii) For $p = p_\pm$ and $R_0 > e^4$ the equation (5.38) has exactly two roots (not counting multiplicity). If $p = p_+$ then the upper root coincides with the local maximum x_+ of the function g, and if $p = p_-$ the lower root is x_-. From (5.41) and (5.42) we see that the multipliers of these points are 1, because the derivative $g'(x)$ is zero.
(iii) If $R_0 \le e^4$ or $R_0 > e^4$, but p lays outside the interval $[p_-, p_+]$, then the equation (5.38) has just one root.

The point (e^4, e^2) is the cusp point in the plane (R_0, p), where the curves $p = p_+$ and $p = p_-$ intersect. It corresponds to the unique fixed point $x = 2$. Indeed, the functions $g(x)$ is monotone in this case and its derivative is given by

$$g'(x) = \frac{e^x}{x^2}\,(x-2)^2.$$

According to Theorem 5.22, this is a cusp point, since $h(x) = e^{-x}$,

$$\frac{xh'(x)}{h(x)} = -x.$$

and the conditions (5.19) and (5.18) are satisfied ($p \equiv p_0$ and $R_0 = p_0 p_1$). The cusp is generic and of spring type. Indeed, a Ricker map is H_S and the condition (5.20) is also satisfied. □

Proof of Theorem 5.28.

Proof. We can rewrite the condition (5.25a) in the following form:

$$\nu_x(\bar{x}, p)\bar{x} = 2,$$

where a fixed point $\bar{x}$ should satisfy the equation (5.38)–(5.39). From this we find that it satisfies

$$x^2 - \ln R_0 x + \ln R_0 - 2 = 0. \tag{5.43}$$

Hence $\bar{x} = x_{1,2}$, where $x_{1,2}$ are given by (5.27). To have nonnegative and bounded x and p we need $R_0 > e^2$. Thus we have proved that the flip bifurcation takes place under the conditions (5.27)–(5.28).

We are going to check the genericity conditions (5.26). Since the 2-Ricker-map has negative Schwarzian, (5.26a) is satisfied.

Now consider the transversality condition (5.26b). Let us fix R_0 and consider the derivative with respect to p. At a flip point $(\bar{x}, \bar{p}, \bar{R}_0)$

$$F_{xp}(\bar{x}, \bar{p}, \bar{R}_0) = \bar{x}e^{\bar{x}}(\bar{x} - 2).$$

We notice that for $R_0 > e^2$ $x_1 > 2$ and $x_2 < 2$. Therefore, slightly under $p_1(R_0)$ and slightly above $p_2(R_0)$ the map has a stable two–cycle according to Lemma 5.27. □

Proof of Theorem 5.29.

Proof. The multiplier of a fixed point is given by (5.41). For the fixed point to be locally stable the absolute value of the multiplier should be less than 1. If the multiplier is 1, the fixed point is stable if it is our cusp point (with $F_{xxx} < 0$) but not if it is a generic fold point. If the multiplier is -1 it is stable if $SF < 0$ that is, indeed, the case. Using (5.39), (5.41) and (5.42) we find that this is equivalent to

$$0 < x^2 - \ln R_0 x + \ln R_0 \leq 2 \tag{5.44}$$

(compare with (5.40) and (5.43)) or $x = x_{cusp}$. For $R_0 < e^4$ the left inequality is satisfied, while the right inequality holds if $x_2 \leq x \leq x_1$, where $x_{1,2}$ are given by (5.27). For $R_0 = e^4$ a fixed point x is also stable in this interval because we allow for the cusp. For $R_0 > e^4$ (5.44) is equivalent to $x \in [x_2, x_-) \cup (x_+, x_1]$.

Fixed points of the map are given by (5.38). We consider the function g for different values of R_0.

For $R_0 \leq e^4$ the function g is monotone decreasing. Hence we have a unique nontrivial fixed point which is stable in two cases: $R_0 \leq e^2$ or $e^2 < R_0 \leq e^4 \cup p \in [p_1, p_2]$.

For $R_0 > e^4$ the function $g(x)$ is not monotone. If $p \notin [p_-, p_+]$ the SYC-map has still a unique fixed point which is stable if $p \in [p_1, p_2]$.

If the map has three fixed points, the lower x_l and the upper x_u of them can be stable if $x_l \in [x_2, x_-)$ and $x_u \in (x_+, x_1]$, respectively. Since the function $g(x)$ is decreasing on these intervals the conditions are equivalent to the conditions of stability given in assertions (ii) and (iii) of the theorem. $\square$

Chapter 6

Magical cicada. A result of competitive exclusion?

6.1 Introduction.

Magicicada are known for their rare, sudden and perfectly synchronized emergences in huge numbers, during which they produce a lot of noise and a lot of eggs. But what is especially unusual, that these emergences occur once in thirteen or seventeen years. These relatively large prime numbers attracted much attention but still there is no really satisfactory explanation for this fact.

There was only one mechanism proposed to produce this behaviour. Cicada "do not want" to be in resonance with a 2–3-years periodic parasite or a predator. The only problem (but very incurable one) was that there was no such periodic parasite or predator found. Some people argued that this parasite could exist at the moment when species of Magicicada had been forming, but disappeared between then and the present. A similar point of view is that there could be even many of such predators appearing and dying out in the course of evolution [Webb]. This is possible, but unfortunately this hypothesis can hardly be checked.

We hope that we have found a candidate for a periodic parasite. *The "periodic parasite" for long–living cicadas is short–living cicadas.* So, we think that not predator–prey or host–parasitoid interactions, but competition between similar species can result in exclusion of non-prime numbers from cicada periods.

In this work we construct toy-models to check this hypothesis and perform simulations rather than performing an analysis of them. However we are sure that both the development of a detailed biological model with relevant parameters can be done on this basis as well as an application of analytical tools is possible to achieve deeper understanding of the underlying mecha-

This chapter is a work in progress.

nisms. We emphasize that the present work is very preliminary work and that the analysis can (and should) be done more thoroughly.

We begin with a short introduction to the cicada life cycle, describe modelling attempts and provide references. Cicadas belong to semelparous species whose individuals reproduce only once in their lives and die afterwards. All species of cicada have a fixed length of the life cycle: 3, 4, 7, 13 and 17 years (see e.g. [Murray]). (Magicicada are those with 13 and 17 years cycle.) Adults emerge simultaneously (within 24 hours) in the spring. They are present above the ground during two weeks up to two months for mating and lying eggs. After that they die. Eggs fall on the ground and hatch soon. Newborn cicada larvae get into the ground, attach themselves to grass roots for a couple of years and then go even deeper to attach to tree roots (they feed by sucking them) for the rest of the life cycle.

Short–living cicadas usually emerge each year, i.e. several cohorts or year classes are abundant in the population, while in a population of the Magicicada there is only one year class present; one calls this year class a *brood*. It means that at a given location there are only individuals of the same age in the population.

In 1976 F.C. Hoppensteadt and J.B. Keller [Hoppensteadt & Keller, Murray] developed a model which showed this property, namely that only one year class survives in the population. We call this situation *Single Year Class dynamics* or SYC-dynamics for short. This term was introduced in [Solberg] and independently by us in [DDvG1]. The Hoppensteadt-Keller model incorporated two important features of cicada dynamics: *competition for accommodation and a predator defense strategy.* When larvae get into the underground they need to attach themselves to roots. If all possible places are taken by other larvae, an entering individual must die. This is the competition for accommodation. This mechanism bounds population density. On the other hand, if the population during emergence is low in abundance, it can be completely destroyed by predators. The thing is that an individual cicada just emerged from its nymph skin is absolutely defenseless against various predators such as birds, rats, even dogs. A life-boat mechanism in this case is the presence of cicadas in such huge numbers that all predators are satiated. It is an Allee effect of increasing of per capita survival probability if population density increases. The Hoppensteadt-Keller model showed the possibility of Single Year Class dynamics and, in addition, for the same parameter set the model demonstrated coexistence of age classes for short–living cicadas and SYC behaviour for long–living ones.

In 2000 H. Behncke revisited the Hoppensteadt-Keller model, simulated it for a large variation of parameter sets and put extra details of cicada life into it such as two levels of underground: grass roots and tree roots and also

parasite fungus Massospora of cicada.

As we have already mentioned, the only mechanism producing prime numbers was assuming that emergence of cicada should not be in resonance with a periodic parasite or a predator. M. Markus and E. Goles proposed a model of coevolution of a cicada and its parasite in [Markus & Goles] which possesses the desired property. The main features were that the cicada had a lower survival probability in the presence of the parasite, and the parasite had a higher survival probability in the presence of cicada. A coevolution of such a parasite and such a cicada led to prime numbers of cicada periods. But the model was phenomenological, it did not incorporate real biological mechanisms.

In 2002 G. Webb [Webb] constructed a more biologically motivated model. He assumed presence of $2-3$ years periodic predator (arguing that there could be many of such predators around cicadas in the course of evolution) and got prime numbers. He even considered for a predator an age-structured model with 2 and 3 year classes allowing for SYC-dynamics. But this model was considered apart from cicada dynamics. In this work we put together the dynamics of long–living cicadas and its "periodic parasite" which is short–living cicadas.

We want to pay attention to biological papers too. R.C. Cox and C.E. Carlton propose *hybridization* as a mechanism for prime numbers periods ([Cox & Carlton] and references in there). Consider two broods of cicada with different life cycle length (e.g. 3 and 4) and assume that cross–reproduction is possible. Then hybrid cicada has genes awaking it to emerge after 3 and after 4 years. Assuming naturally that 3-years gene dominates, hybrid cicadas emerge together with 3-years brood. If the number of hybrids is large enough, mating between them is possible. As a result 4-years offspring can occur which emerge after 4 years alone (neither with 3 nor with 4-years brood) in small numbers and therefore should be completely destroyed by predators. Hence the less the number of coemergences of different broods the less the losses due to hybridization. And statistically prime numbers have less coemergences with other broods. However if a cicada period is a multiple of a lower period (say, 12 and 4), there will be no loss due to hybridization.

If we assume, on the contrary, that cross-mating is either unsuccessful or successful but hybrids are sterile or their biological clocks are broken, then losses on hybridization are unavoidable. We think that a mathematical model taking into account such a hybridization effect can be constructed similarly to one based on competition.

We want also to mention the *Ice Age hypothesis* [Yoshimura]. It attempts to explain Single Year Class behaviour and long cicada periods. If a summer

is rather cold, many nymphs are unable to emerge and adult cicadas are less active, so the number of offspring in such a year can be very low. It can even result in extinction of the corresponding year class. Larvae hiding under the ground suffer much less of cold weather. If a mutant had a longer period than a resident, it appeared rarely above the ground and therefore had a larger probability to survive through the Ice Ages.

To conclude this overview we want to mention an excellent website

`http://insects.ummz.lsa.umich.edu/fauna/Michigan_Cicadas/Periodical/`

of the The University of Michigan Museum of Zoology containing many photos and songs of cicada and providing other links and references to cicada resources.

6.2 A minimal model.

We begin with a minimal model which produces the desired behaviour: survival of a prime period cicada. Our aim is to illustrate the mechanism of extinction of non-prime periods. More precisely we assume that residents are two coexisting broods: biennials and triennials. We will show that only a mutant with a period which is *not* multiple of 2 and 3 can invade. Notice that numbers up to 24 are prime if they are not multiples of 2 and 3.

A competition model consists of three parts: dynamics of biennials, dynamics of triennials and dynamics of a k-years living mutant. We assume that all the three are different species, i.e., they are unable to cross, and the interaction between them is only due to competition. The species are subdivided into respectively 2, 3 and k age classes.

We explore the concept of *environmental variable* in order to construct the model. The idea is the following. We define environment so that individuals are independent if the environment is prescribed. If we model competition for food, for example, environment is amount of food available at a given moment. Since individuals are independent, their impacts on the environment are also independent. Thus the environmental variable is just a sum of impacts from all individuals. For more detailed description of this modelling approach, see Chapter 1.

First we assume the environmental variable to be one-dimensional, the simplest possible case. And it is a linear combination of age class numbers of the three species. Also we assume that there is only competition between newborns, i.e. between newly hatched larvae which are looking for accommodation on grass roots (so-called nursery competition). Thus we have the following expressions for the environmental variable:

$$I = B_0 + T_0 + N_0 \tag{6.1}$$

where B_0 is the number of newborns of the biennials, T_0 is newborns of the triennials and N_0 is newborns of k-ennials.

The dynamics of the biennials is given by the following recursion:

$$\begin{aligned} B_0(t+1) &= R_0\, B_1(t) \\ B_1(t+1) &= \frac{B_0(t)}{1+I(t)}, \end{aligned} \tag{6.2}$$

where B_0 and B_1 are age class numbers. Similarly, for the triennials we have

$$\begin{aligned} T_0(t+1) &= R_0\, T_2(t) \\ T_1(t+1) &= \frac{T_0(t)}{1+I(t)} \\ T_2(t+1) &= T_1(t). \end{aligned} \tag{6.3}$$

Finally, for the k-ennials

$$\begin{aligned} N_0(t+1) &= R_0\, N_{k-1}(t) \\ N_1(t+1) &= \frac{N_0(t)}{1+I(t)} \\ N_{i+1}(t+1) &= N_i(t) \qquad i = 2, ..., k-1, \end{aligned} \tag{6.4}$$

where N_i are age class numbers of the mutant.

The parameter R_0 is the *expected number of offspring*, it is equal to the product of the number of eggs per female and survival probability during the life cycle. We let this parameter be equal for all the three species. This is to keep the model more simple, but simulations show that slight differences in R_0 of the three species do not influence the results.

One can see that the survival probability of the older age classes is 1. It is not a restriction, it is just a simple rescaling. More precisely we collect all the survival probabilities in the quantity R_0.

Competition is modelled by the Beverton-Holt functional relation. We choose it because such a function produces simpler dynamics than, for example, the Ricker function. In this way we avoid complex attractors which are not of importance for the problem we consider.

In this model we take into account inter-specific competition between newborns of three species. But an attentive reader notices that we ignore competition *between age classes*. I.e. there is no mechanism for year class exclusion. However if we choose initial values properly we can create SYC-dynamics artificially.

$$\begin{aligned} &B_0(0) = T_0(0) = N_0(0) = 1 \\ &B_1(0) = T_1(0) = T_2(0) = N_1(0) = ... = N_{k-1}(0) = 0. \end{aligned} \tag{6.5}$$

Let us be happy with that for a moment. Later we try to make SYC behaviour an intrinsic feature of the dynamics.

A very nice thing about the model (6.1)–(6.5) is that it contains only one parameter R_0. And simulations show that the qualitative dynamics does not depend on it. Neither does it depend on the initial values of newborns.

The dynamics of the model is represented in Figures 6.1 and 6.2 for $k = 7, 12, 13, 14, 15, 17$ respectively. Thick line corresponds to the k-ennials, thin line to the biennials, dashed line to the triennials. We measure the number of newborns each k-th year starting from introduction of the mutant (i.e., a number on the horizontal axis refers to the number of life cycle of k-ennials counting from their first appearance). One can see that only 7–, 13– and 17–ennials species survive. Moreover, the population numbers oscillate with a period of $6 = 2 \times 3$ life cycles or $6\,k$ years.

From our point of view the main mechanism responsible for extinction of non-primes is the following. As one may notice an individuals suffers of competition only in the year of its birth. Moreover there are two types of the competition: intra-specific (which can not lead to extinction of a species, at least in the case of Beverton-Holt density dependence) and inter-specific competition, but the latter takes place only if newborns of other species are present. Since the biennials and the triennials have relatively prime periods, there are always years without inter-specific competition for both the species that gives possibility for each to survive. Introduction k-ennial species with $k \geq 6$ does not change this conclusion if we choose in-phase initial condition (6.5), since reproduction of the k-ennials is rare and happens at most once during the common biennial–triennial cycle of period 6. On the other hand if reproduction of k-ennials coincides *always* with reproduction of biennials and/or triennials the population declines because of the inter-specific competition. It happens exactly if k is a multiple of 2 and/or 3 (and for in-phase initial conditions). The population of the biennials/triennials declines as well at such years, but recovers itself at years with no inter-specific competition. Let us refer to this mechanism of extinction of non-primes as to *resonance mechanism.*

If neither biennials nor triennials reproduce in the same year with k-ennials the population of the latter grows. Therefore species with prime periods are able to survive.

There is a very weak point in this model. If, for example, the cycle of the 14-ennials is out of phase with the cycle of the biennials, the 14-ennials will not die (see Figure 6.3). Indeed, in this case some reproduction of 14-ennials happen to be without the other species and the population grows. We can argue that it is rather improbable that the perfect "out–of–phase–synchronization" would persist in the course of evolution. If the biennial

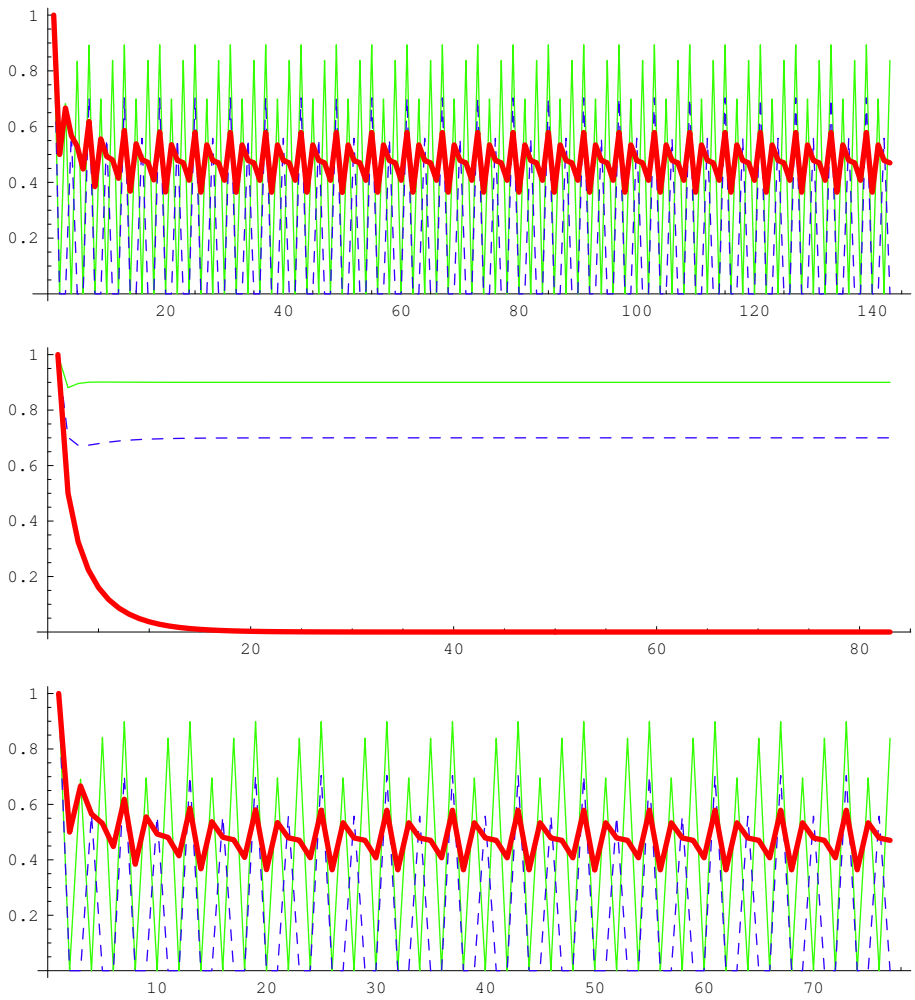

Figure 6.1: Dynamics of the recursion (6.1)–(6.5) for $k = 7, 12, 13$ respectively. The thick line corresponds to the k-ennials, the thin line to the biennials, the dashed line to the triennials. We measure the number of newborns each k-th year starting from introduction of the mutant (i.e., a number on the horizontal axis refers to the number of life cycle of k-ennials counting from their first appearance). One can see that only 7–, 13–ennials species survive.

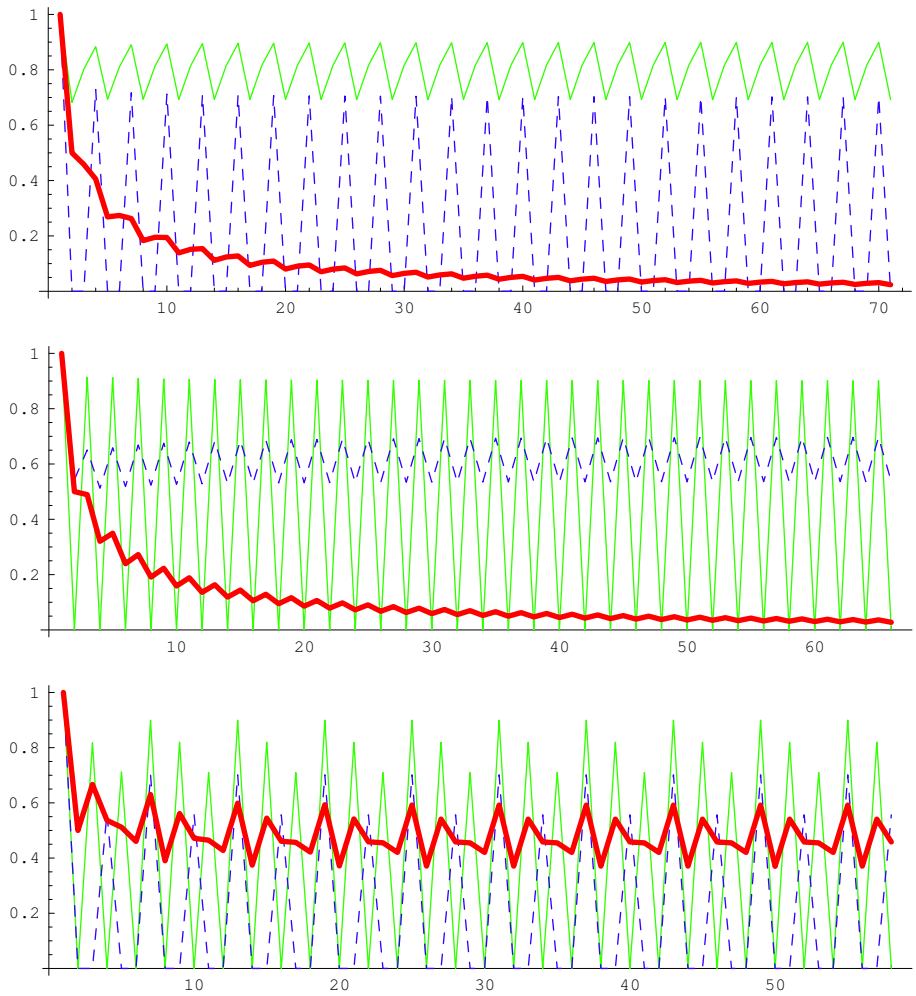

Figure 6.2: Dynamics of the recursion (6.1)–(6.5) for $k = 14, 15, 17$ respectively. The thick line corresponds to the k-ennials, the thin line to the biennials, the dashed line to the triennials. We measure the number of newborns each k-th year starting from introduction of the mutant (i.e., a number on the horizontal axis refers to the number of life cycle of k-ennials counting from their first appearance). One can see that only 17–ennials species survive.

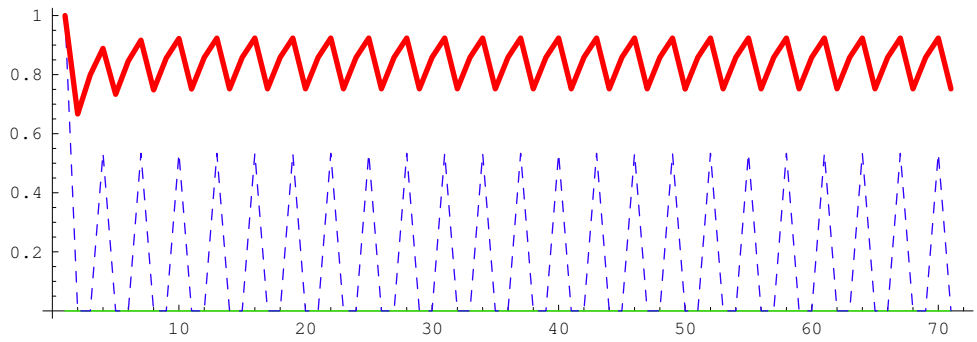

Figure 6.3: The 14-ennials survive if they are out of phase with the emergences of the biennials.

cycle shifts due to some reasons (e.g. environmental stochasticity) or if 14-ennials encounter "in–phase" biennials when migrating, they die unavoidably. However, we show in Section 6.5 how out–of–phase–synchronization can lead to the exclusion of non-prime periods and survival of prime periodic species.

6.3 Single species dynamics.

In the previous section we have considered a nursery competition model. However a nursery competition can not produce Single Year Class behaviour in the population because there is no competition between age classes. Therefore we should generalize the model (6.2)–(6.4) to allow for more general interaction. We begin with a single species dynamics. We construct a model which has a nice property also featured by the Hoppensteadt-Keller model [Hoppensteadt & Keller]. For the same set of parameters it produces coexistence of year classes for short–living species and SYC-dynamics for long–living ones. The difference with the Hoppensteadt-Keller model is that we do not include predator satiation mechanism and consider competition only, in particular competition for accommodation.

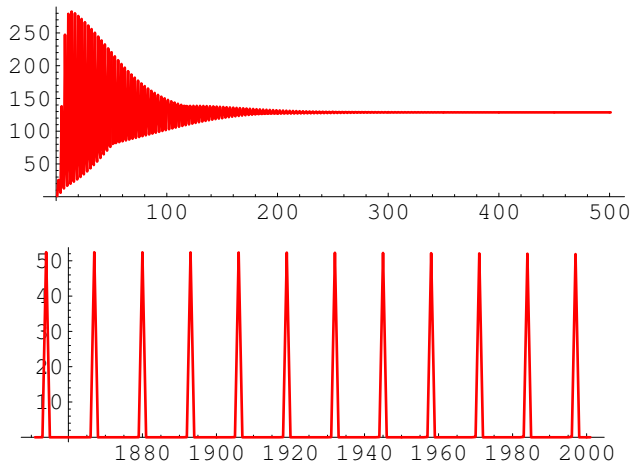

Figure 6.4: Dynamics of triennials and 13-ennials respectively generated by the single species model (6.6). For the same parameter set: $F = 30$, $c = .05$ and $p_0 = ... = p_{k-1} = .85$, all age classes coexist in the triennial population, while one observes SYC-dynamics for 13-ennials.

The model has the following form

$$\begin{aligned} N_0(t+1) &= F\, N_k(t) = F\, p_{k-1}\, N_{k-1}(t) \\ N_1(t+1) &= \frac{p_0\, N_0(t)}{1 + I(t)} \\ N_{i+1}(t+1) &= p_i\, N_i(t), \qquad i = 1, ..., k-2 \\ I &= c\, N_0 + \sum_{j=1}^{k-1} N_j, \end{aligned} \tag{6.6}$$

The quantity F is a fecundity. We assume that a year ends by a reproduction event and the number of newborns N_0 *in the beginning of year* $t+1$ is proportional to the number of adults N_k *in the end of year* t. The quantities p_i are survival probabilities of the i-th age class. Let us assume, for simplicity, that $p_0 = ... = p_{k-1} = p$. The parameter $c < 1$ is an *impact* of the newborns on the environment. Let us explain. If we model competition for accommodation all older age classes have equal impact on the environmental variable which is, in this case, the lack of free places on tree roots, while the impact of newborns is less $c < 1$ because they have not found a place yet.

In Figure 6.4 one can see dynamics of a single species population with respectively 3 and 13 year classes for the same $F = 30$, $c = .05$ and

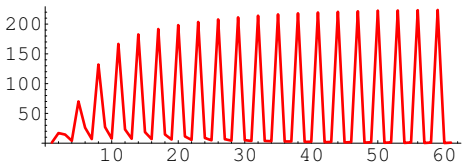

Figure 6.5: Dynamics of triennials for "Ice Ages parameter set": $F = 20$, $c = .05$, $p = .85$. One can see SYC-dynamics in the population.

$p = .85$. We start simulations with an equal abundance of each age class. As a result of simulation we see coexistence of all age classes for $k = 3$ and SYC-behaviour for $k = 13$.

We have noticed also an interesting feature of the SYC-behaviour. It exhibits sudden switches between year class dominance. This happens if the corresponding attractor in the phase space $\{N_0, ..., N_{k-1}\}$ is a heteroclinic cycle (see Chapter 4 of this thesis).

There is another very important property of this model. In a cold summer the fecundity F of cicada becomes less due to suppressed activity of mates and lower probability of eggs to hatch. As a result of it even short–living cicada exhibit SYC-behaviour (Fig. 6.5 for $k = 3$, $F = 20$, $c = .05$, $p = .85$). In other words, during Ice Ages even short–living cicada could have synchronized emergences.

The basic reproduction ratio R_0 is given in the case of the model (6.6) by

$$R_0 = F\, p_0 ... p_{k-1},$$

i.e., for long–living species this quantity is less than for short–living ones. However one often says that the severe weather of Ice Ages was the reason for prolongation of cicada periods, because it was easier for individuals hiding under the ground, to survive. We reduce the slope of decrease of R_0 for large k by considering two levels of underground: grass roots with low survival probability and tree roots with high survival. We choose namely $p_0 = p_1 = p = .85$ and $p_2 = ... = p_{k-1} = p' = .99$. Under this assumption R_0 does not differ so much for, say 7-ennials and 17-ennials. We use this "two levels parameter set" in Section 6.5.

(One of our referees has noticed that if older individuals go deeper underground, to tree roots, they can hardly influence settling newborns as it is assumed in the form of the environmental quantity. We are fully agree with this remark and apologize for the inconsistency. A detailed mechanistical modelling of two levels of underground is a probable matter of future work. In this case one would deal with (at least) two-dimensional environ-

ment which is nice because allows for coexistence of several species. Also competition should be considered not only on the nursery level, but at least on two levels: settling on grass roots and settling on tree roots. However this inconsistency is not crucial for the results of Section 6.5, because we choose initial conditions (6.11) so that the SYC-dynamics is assumed for k-ennials and the term $\sum_{j=1}^{k-1} N_j$ does not enter the value of the environmental quantity at years of reproduction, see (6.13)–(6.15).)

6.4 Coexistence of biennials and triennials.

As one may notice, the model (6.1)–(6.5) allows for coexistence of even three species on one shared resource (this is reflected in one–dimensionality of the environmental quantity I). But a well-known ecological paradigm says that one resource can support only one species. More detailed investigations of dynamics of the two species shows that if we introduce missing year classes, for example, in the triennial population (using the model (6.1)–(6.3)), the biennials go extinct, and vice versa (Fig. 6.6). This has a simple explanation. Let us have a species with all year classes present and a species with only one year class present. Then the latter, the species with SYC-dynamics, experiences inter-specific competition in each year of emergence, while it is not the case for the other species.

If we introduce missing year classes of both of the species, they still can coexist, because they have the same basic reproduction ratio and sensitivity to competition. However if we change one of this parameters to make one of the species a worse competitor, this species goes extinct.

Let us introduce a generalized version of the competition model for biennials and triennials with two-dimensional environmental feedback. There might be many possible mechanisms creating the two-dimensional environment. We did not yet get a chance to consult with a cicada zoologist on this matter, so we propose one possible (but probably debatable) mechanism. The idea is the following. Eggs of biennials and triennials do not hatch simultaneously, there can be a delay for one of the species. Earlier emerged larvae have an advantage: they do not compete with newborns of the other species, while later larvae do compete with the quicker ones. We have the following expressions for the environmental quantities (let us assume that biennial larvae are quicker):

$$\begin{aligned} I_B &= c\,B_0 + B_1 + T_1 + T_2 \\ I_T &= c\,T_0 + B_1 + T_1 + T_2 + c'\,B_0. \end{aligned} \tag{6.7}$$

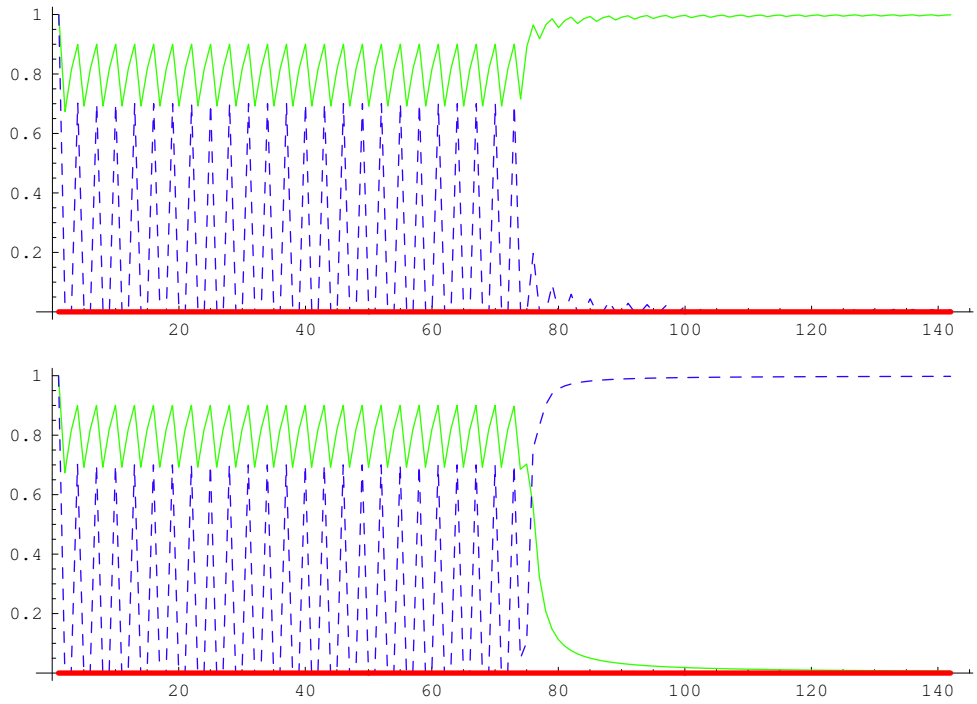

Figure 6.6: Dynamics of biennials and triennials generated by the model(6.1)–(6.3). In the first diagram we introduce a missing year class in the biennial population and see that the triennials are outcompeted. In the second diagram we introduce both missing year classes in the triennials population and see that the biennials are outcompeted.

Then a two-species model has the following form

$$\begin{aligned} B_0(t+1) &= Fp\,B_1(t) \\ B_1(t+1) &= \frac{p\,B_0(t)}{1+I_B(t)} \\ T_0(t+1) &= Fp\,T_2(t) \\ T_1(t+1) &= \frac{p\,T_0(t)}{1+I_T(t)} \\ T_2(t+1) &= p\,T_1(t). \end{aligned} \tag{6.8}$$

As a building block of this model we use the single species model (6.6), using for each of the species environment as defined in (6.7). (Notice that if we construct a two–species model on the basis of (6.6), but let the environment

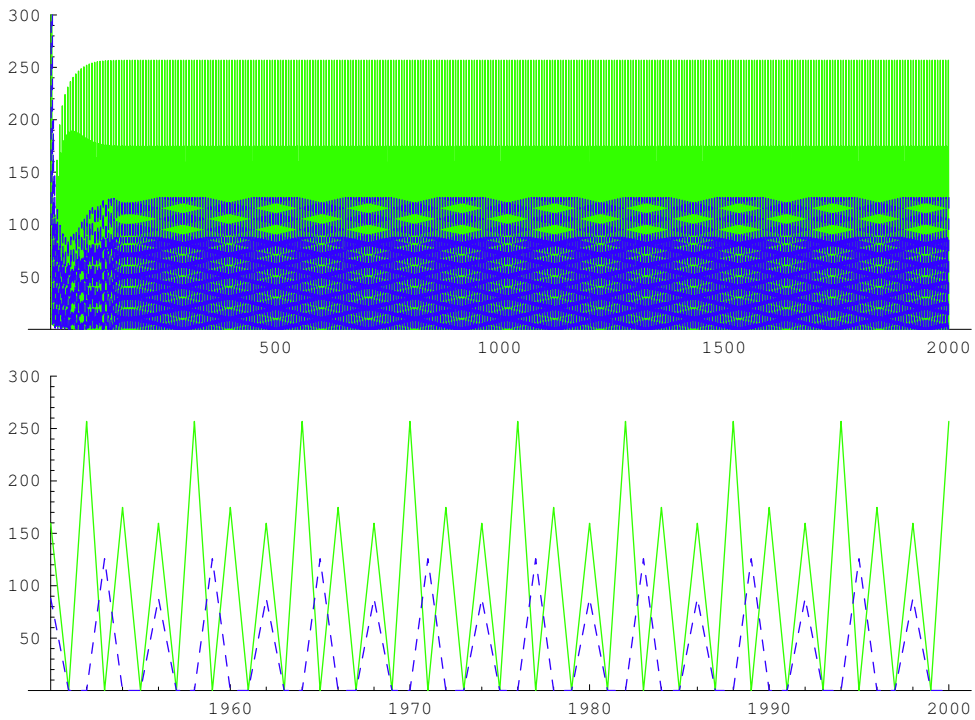

Figure 6.7: Coexistence of biennials and triennials in the model (6.8) with two-dimensional environmental feedback. The dynamics of biennials are shown by the light solid line and the dynamics of triennials by the dark dashed line. In the second panel the last 50 steps of the simulation are shown, one can clearly see SYC-dynamics in each population, both populations oscillate with period 6. We use "Ice Ages set": $F = 20$, $p = .85$, $c = .05$. The impact of newborns of biennials on the environmental variable of triennials is small $c' = .02$ comparing with c.

be one–dimensional, we can not obtain a coexistence of the two species, even if each of them consists of a single year class.)

If we use "Ice Ages set": $F = 20$, $p = .85$, which we have found in the previous section, each population exhibits the SYC-behaviour and for $c' \in [0, .02]$ approximately, the populations coexist (Fig 6.7). We start simulation from an equal abundance of age classes in each population.

The introduction of the parameter c' is a bit *ad hoc*. It is not clear why it should be less than c. However, we can take into account that only young larvae of biennials, who have found a place on roots, have impact on the environment. The number of them is $\frac{B0}{1+I_B}$. So, we can rewrite I_T in the

following form:

$$I_T = c\,T_0 + B_1 + T_1 + T_2 + c''\frac{B_0}{1 + I_B}.$$

To obtain coexistence of the two species using this environmental quantity and the "Ice Ages parameter set" we need that $c'' \in [0, .4]$ approximately. This is already a rather natural assumption. We can interpret it as follows: young larvae occupy less space because they are smaller, and hence they have smaller impact (comparing with the impact of older individuals which is 1).

If we assume that newborns of triennials go quicker to underground, we obtain similar results, i.e. possible coexistence of the two species. Interestingly enough, this type of competition can change the behaviour of the populations: if a population exhibits SYC-behaviour in isolation, it can have coexistence of year classes when it coexists with the other species. For example, if triennials are quicker, biennials can have coexistence of year classes for the "Ice Ages set", if the parameter c'' (characterizing inter-specific competition) is large enough. It is an analogue of "predator mediated coexistence" for two competing species.

We think that the difference in emergence time allowing for coexisting of two species is not the only possibility. One can propose other mechanisms: slightly different ecological niches, for example, triennials can escape deeper under ground. The main idea is that we need (at least) two-dimensionality of the environmental variable (i.e. two-dimensional feedback) and that intra-specific competition is more severe than inter-specific.

6.5 Competition of the three species.

We can construct a model of three species dynamics for biennials, triennials and k-ennials, in the same way as in the previous section. We want to achieve that k-ennials can invade the population of the two species. There are different possibilities of coupling k-ennials with the two other species. In our approach the difference is in the moment when newborn larvae go underground. We can assume therefore that k-ennials go down either earlier or later or simultaneously than/with biennials/triennials. We have tried different possibilities and conclude that the difference between them are only quantitative.

If we assume that k-ennials have their own moment in time to go underground, we should introduce a third component of the environmental variable in the way similar to the previous section. But actually two-dimensional environmental variable is enough to achieve our purpose (for k-ennials to be able

to invade). So, for simplicity, we assume that k-ennials go down together with one of the other species. To make coemergences with the others less pleasant for k-ennials, we assume that they go down with the late species. Let it be triennials. Then the environmental quantities have the following form:

$$\begin{aligned} I_B &= c\,B_0 + B_1 + T_1 + T_2 + \sum_{j=1}^{k-1} N_j \\ I_T &= c\,(T_0 + N_0) + B_1 + T_1 + T_2 + \sum_{j=1}^{k-1} N_j + c''\frac{B_0}{1+I_B}. \end{aligned} \tag{6.9}$$

And the three species competition model consists of the model for biennials and triennials (6.8) with I_B and I_T given by (6.9) and the following model for k-enials:

$$\begin{aligned} N_0(t+1) &= F\,p'\,N_{k-1}(t) \\ N_1(t+1) &= \frac{p\,N_0(t)}{1+I_T(t)} \\ N_2(t+1) &= p\,N_1(t) \\ N_j(t+1) &= p'\,N_{j-1}(t) \qquad j = 3, ..., k-1. \end{aligned} \tag{6.10}$$

For simplicity we incorporate two levels of underground only for k-ennials, but not for triennials, i.e., we assume that triennials do not go deeper into underground for the last year of their life cycle. It seems for us to be a rather natural assumption, anyway it is not crucial. Actually, the whole idea of two (or more) levels of underground can be incorporated in the model more thoroughly. It is the matter of future work.

We have simulated the model for the "Ice Ages two levels parameter set": $F = 20$, $p = .85$, $p' = .99$, $c = .05$, $c'' = .1$ and for the in–phase initial conditions (6.5). The results are very amazing. We have obtained a counter-effect: species with large primes: 11, 13, 17, go extinct! While all other periods invade (we consider $k = 4, ..., 17$).

We explain it as follows. We recall that the biennials and the triennials have SYC-dynamics for the "Ice Ages parameter set". The SYC-dynamics is a consequence of the fact that expected impacts of the older age classes are larger in comparison with the impact of newborns (and only newborns are sensitive to competition), this is a one of the main conclusions of Chapters 2 and 3. Therefore the environment is formed mostly by older age classes and thus newborns of k-ennials compete *not* with newborns of the short–living species, but rather with older individuals. So, the interspecific competition of k-ennials with the other two species is stronger at those years (of birth) when older age classes of biennials and triennials are present, and otherwise

the competition is the least severe during the coemergences of all the three species. The consequence is that the resonance mechanism, as it described in the end of Section 6.2, does not work.

More precisely, newborns of species with non-prime periods which are *in phase* with biennials and/or triennials experience mild environment *always* during the settling and this is the reason for their survival. However, if we assume that they are *out of phase*, the situation is opposite: the newborns of k-ennials experience severe environment *always* which can lead to their extinction. Therefore the counter-effect gives us a key to a slightly different resonance mechanism which can be favourable to survival of prime periodic species. So, we choose "out–phase" initial conditions as follows

$$\begin{aligned} &B_1(0) = T_1(0) = T_2(0) = 10 \quad N_0(0) = N0 \\ &B_0(0) = T_0(0) = N_1(0) = ... = N_{k-1}(0) = 0. \end{aligned} \tag{6.11}$$

If we simulate the model for these initial values (for $N0 = 10$) and for the "Ice Ages two levels parameter set", only 5- and 9-ennials survive (we consider $k = 4, ..., 17$). At a first sight it is a strange result and we did not reach our purpose: extinction of non-primes. Fortunately, we can explain this result and propose modifications of the model to produce survival of only primes.

We rescale the model in the way of Section 2.3. We need it because we should deal with *expected impacts* in order to explain survival or extinction. First we rescale the one species model (6.6) and it has then the following form

$$\begin{aligned} &N_0(t+1) = N_{k-1}(t) \\ &N_1(t+1) = \frac{R_0\, N_0(t)}{1 + I(t)} \\ &N_{i+1}(t+1) = N_i(t), \qquad i = 1, ..., k-2 \\ &I = cN_0 + \sum_{j=1}^{k-1} c_j\, N_j, \end{aligned}$$

where $R_0 = Fp_0...p_{k-1}$ is the basic reproduction ratio, $c_j = \frac{p_0}{R_0} p_1...p_{j-1}$ is the expected impact of a j-years old individual (we notice that the survival probability as a result of competition in the steady environment $\bar{I} = R_0 - 1$ is $\frac{1}{R_0}$, see also the rescaling in Section 2.3). The expected impact of newborns is, of course, its direct (unscaled) impact c.

As an example of how to use the expected impacts in order to decide whether we should expect coexistence or exclusion, we show that k-ennials have SYC-dynamics for the "Ice Ages two levels parameter set". A sufficient

(but, probably, not necessary) condition for SYC-dynamics is that the expected impact of newborns c is less than the other impacts c_j (Section 2.9 of this thesis). The smallest of these latter impacts is c_{k-1}. So, if

$$c < \frac{p_0}{R_0} p_1 ... p_{k-2}$$

or

$$c < \frac{1}{F p_{k-1}}$$

the SYC-dynamics is guaranteed. For our "Ice Ages two levels parameter set": $F = 20$, $c = .05$, $p_{k-1} = p' = .99$ this condition is satisfied.

Let us now rescale the three-species model (6.10) in the same way. The environmental variables are given then by following expressions containing expected impacts:

$$\begin{aligned} I_B &= \frac{R_0^B}{R_0}(cB_0 + c_1^B B_1) + \frac{R_0^T}{R_0}(c_1^T T_1 + c_2^T T_2) + \sum_{j=1}^{k-1} c_j N_j \\ I_T &= \frac{R_0^B}{R_0}(c'' \frac{B_0}{1+I_B} + c_1^B B_1) + \frac{R_0^T}{R_0}(cT_0 + c_1^T T_1 + c_2^T T_2) + cN_0 + \sum_{j=1}^{k-1} c_j N_j, \end{aligned} \tag{6.12}$$

where $R_0^B = F p_0 p_1$ and $R_0^T = F p_0 p_1 p_2$ are the basic reproduction ratios for biennials and triennials respectively, $c_1^B = \frac{p_0}{R_0^B}$ is the expected impact of the one year old biennials and similarly for triennials: $c_1^T = \frac{p_0}{R_0^T}$ and $c_2^T = \frac{p_0 p_1}{R_0^T}$.

The quantities $\frac{R_0^B}{R_0}$ and $\frac{R_0^T}{R_0}$ appear before the expected impacts of bienials and triennials because we should take into account differences in scales of population numbers for the three species, a unit on this scale is determined by the basic reproduction number.

We notice also that

$$\begin{aligned} c_1^B \frac{R_0^B}{R_0} &= c_1^T \frac{R_0^T}{R_0} = c_1 \\ c_2^T \frac{R_0^T}{R_0} &= c_2 \end{aligned}$$

To understand why only 5- and 9-ennials survive we should consider values of the environmental quantity I_T which k-ennials encounter during their emergences (we recall that I_T is not only the environmental variable for triennials but also for k-ennials, see (6.10)). Since we use the initial values (6.11), some of the terms in the expression for I_T above will be missing. In particular, $\sum_{j=1}^{k-1} c_j N_j$. Also we notice that initially we have, for triennials, two year classes present (6.11), but eventually one of them declines (it is indeed the case for the "Ice Ages parameter set"). Hence only one of the terms:

either with T_0 or with T_1 or with T_2, will appear in the quantity I_T. Similarly, either the term with B_0 or with B_1 will appear. Therefore there are six different combinations of terms with B_i and T_j. All these six combinations appear one after another in the environmental variable in the dynamics of a prime periodic species. While there are three such combinations for species with even periods, namely

$$\begin{aligned} I_T^1 &= c\,N_0 + c_1 B_1 + \tfrac{R_0^T}{R_0} c T_0 \\ I_T^2 &= c\,N_0 + c_1 B_1 + c_1 T_1 \\ I_T^3 &= c\,N_0 + c_1 B_1 + c_2 T_2, \end{aligned} \tag{6.13}$$

because even periodic species are out–of–phase with biennials. And for the species whose period is a multiple of three there are two possibilities: either their emergences are one year after the emergences of triennials, then

$$\begin{aligned} I_T^1 &= c\,N_0 + c_1 T_1 + c_1 B_1 \\ I_T^2 &= c\,N_0 + c_1 T_1 + \tfrac{R_0^B}{R_0} c'' \frac{B_0}{1 + I_B}, \end{aligned} \tag{6.14}$$

or they are one year before the emergences of triennials, then

$$\begin{aligned} I_T^1 &= c\,N_0 + c_2 T_2 + c_1 B_1 && (a) \\ I_T^2 &= c\,N_0 + c_2 T_2 + \tfrac{R_0^B}{R_0} c'' \frac{B_0}{1 + I_B}. && (b) \end{aligned} \tag{6.15}$$

Very roughly, we can say that if the expected impact of the newborn k-ennials N_0 is small "in comparison with" the impacts of the two other species, k-ennials go extinct. (We do not mean that the impact of k-ennials is precisely smaller than the other two. Probably we would need that it is an order of magnitude smaller. A detailed analysis is needed for a precise statement.)

It is clear that

i) species with k large enough, go extinct.

This is because R_0 is small for large k. Assume for a moment that

$$c_2 < c < c_1, \tag{6.16}$$

(but remember that for the "Ice Ages two levels parameter set" this is not true), then

ii) species with even periods go extinct;

because the expected impact of B_1, which is c_1, is larger than c and the term B_1 appears in each of the expressions of (6.13). Other conclusions are that

iii) species with periods which are a multiple of three go extinct in the case (6.14);

because of the term $c_1 T_1$ with the impact c_1 appearing in each expression, and

iv) species with "multiple of three" periods can survive in the case (6.15);

because c is larger than the impact c_2 of T_2 and it can be also larger than the impact $\frac{c''}{1+I_B}$ of B_0 in (6.15b). For the same reason

v) species with prime periods can survive;

Indeed, one of the possible combinations of the environmental quantity is again (6.15b), but this (favourable) structure appears only once in six emergences, while for species with "multiple of three" periods it happens more often, once in three emergences. In other words,

vi) species with "multiple of three" periods survive for a larger interval of parameter values than prime periodic species.

Notice that c is smaller than c_j for the "Ice Ages two levels parameter set". Hence we should conclude that neither primes nor non-primes can survive, because c is smaller than both c_1 and c_2 appearing in (6.13)-(6.15). However 5- and 9-ennials survive. This is because "smallness" of c is a necessary but not sufficient condition to guarantee extinction. In other words, we conclude that c is "not enough small" comparing with c_2 (but "enough small" comparing with c_1). Thus we have an analogue of the condition (6.16).

We understand, of course, how inaccurate these speculations are, but still they give us a right intuition which allows to modify the model so that it produces the desired behaviour: exclusion of non-primes.

Using the knowledge above we can see why 9-periodic species survives in the simulations described above (the conclusion (iv)). Indeed, other multiples of three are $6, 12$ and 15. The first two are even, that is why they are excluded (the conclusion (ii)). And 15 is already too large (i). 5-periodic species survives because 5 is prime (v) and small enough (i).

Now the question is how to modify the model (6.8), (6.9)–(6.11) or how to choose parameters to let primes survive and the other periods be excluded.

We see that the model has to be modified because the conclusion (vi) contradicts the property that only primes survive. To change this, we assume that *"old" triennials T_2 have a larger impact on the environment.* It is a very natural assumption, because older individuals are larger and occupy more space and/or consume more resource. Therefore we write $c_T c_2 T_2$ instead of $c_2 T_2$ in the quantities I_B and I_T (6.12), where $c_T c_2 \geq c_1$ or $c_T p \geq 1$.

We have seen that prime periodic species with $k \geq 7$ decline, because their impact is small. We can make k-ennials better competitors if we assume that *fecundity of long–living species is larger*, i.e. we introduce $F_N > F$. This assumption is also biologically motivated: it is well known that Magicicada have a high fecundity.

With these two changes we obtain a model which produces the desired behaviour. Let us rewrite the model here in the complete form:

$$B_0(t+1) = Fp\,B_1(t) \qquad T_0(t+1) = Fp\,T_2(t)$$

$$B_1(t+1) = \frac{p\,B_0(t)}{1+I_B(t)} \qquad T_1(t+1) = \frac{p\,T_0(t)}{1+I_T(t)}$$

$$T_2(t+1) = p\,T_1(t)$$

$$\begin{aligned} N_0(t+1) &= F_N\,p'\,N_{k-1}(t) \\ N_1(t+1) &= \frac{p\,N_0(t)}{1+I_T(t)} \\ N_2(t+1) &= p\,N_1(t) \\ N_j(t+1) &= p'\,N_{j-1}(t) \qquad j = 3, ..., k-1 \end{aligned} \tag{6.17}$$

$$I_B = c\,B_0 + B_1 + T_1 + c_T\,T_2 + \sum_{j=1}^{k-1} N_j$$

$$I_T = c\,(T_0 + N_0) + B_1 + T_1 + c_T\,T_2 + \sum_{j=1}^{k-1} N_j + c''\frac{B_0}{1+I_B}.$$

We choose the following parameters: "Ice Ages two levels parameter set" $F_N = 20$, $p = .85$, $p' = .99$, $c = .05$; the fecundity of short–living species is smaller $F = .8\,F_N$; the impact of newborn biennials $c'' = .1$ and the impact of old triennials is $c_T = 1.5$. And we choose the initial conditions (6.11).

The dynamics of the recursion (6.17),(6.11) are shown in Figures 6.8 and 6.9. We see that only prime periodic cicadas survive and, moreover outcompete the other two species. We choose initial conditions in the form (6.11) for $N0$ not very large, because for $N0 >> 10$, we will have that k-ennials

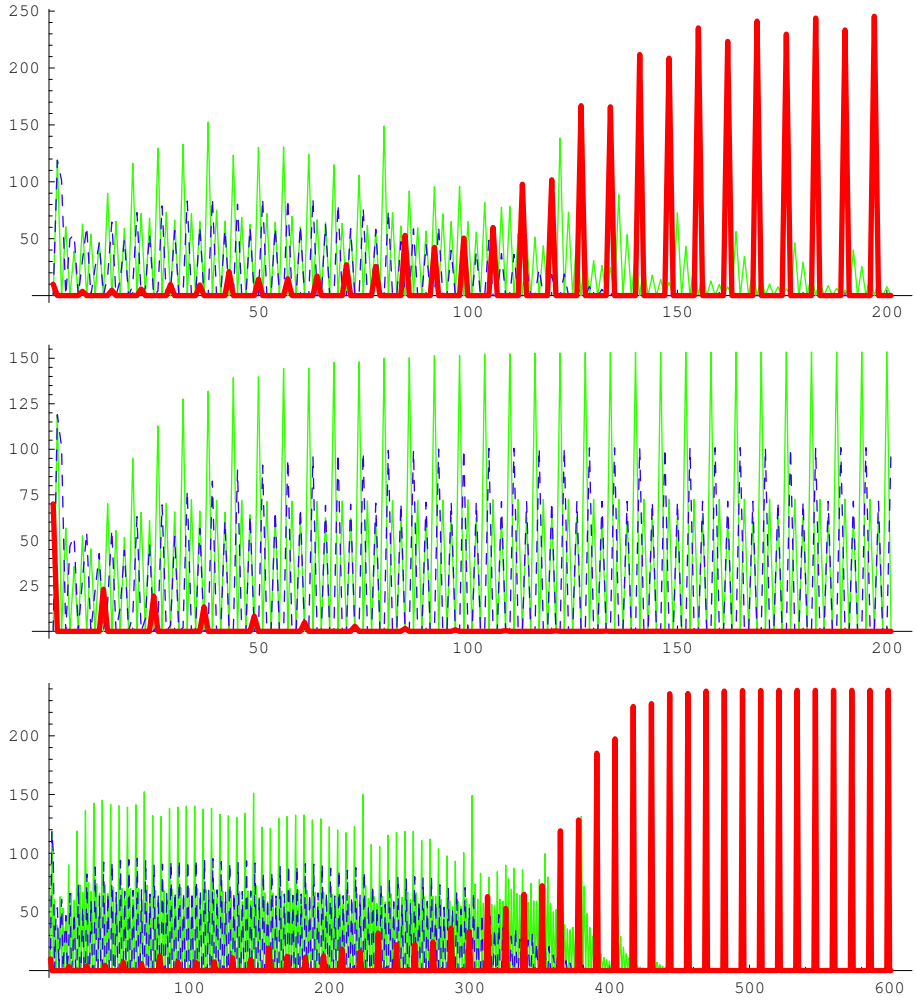

Figure 6.8: Dynamics of the recursion (6.17),(6.11) for $k = 7, 12, 13$ respectively. The thick line corresponds to the k-ennials, the thin line to the biennials, the dashed line to the triennials One can see that only 7- and 13-ennials species survive.

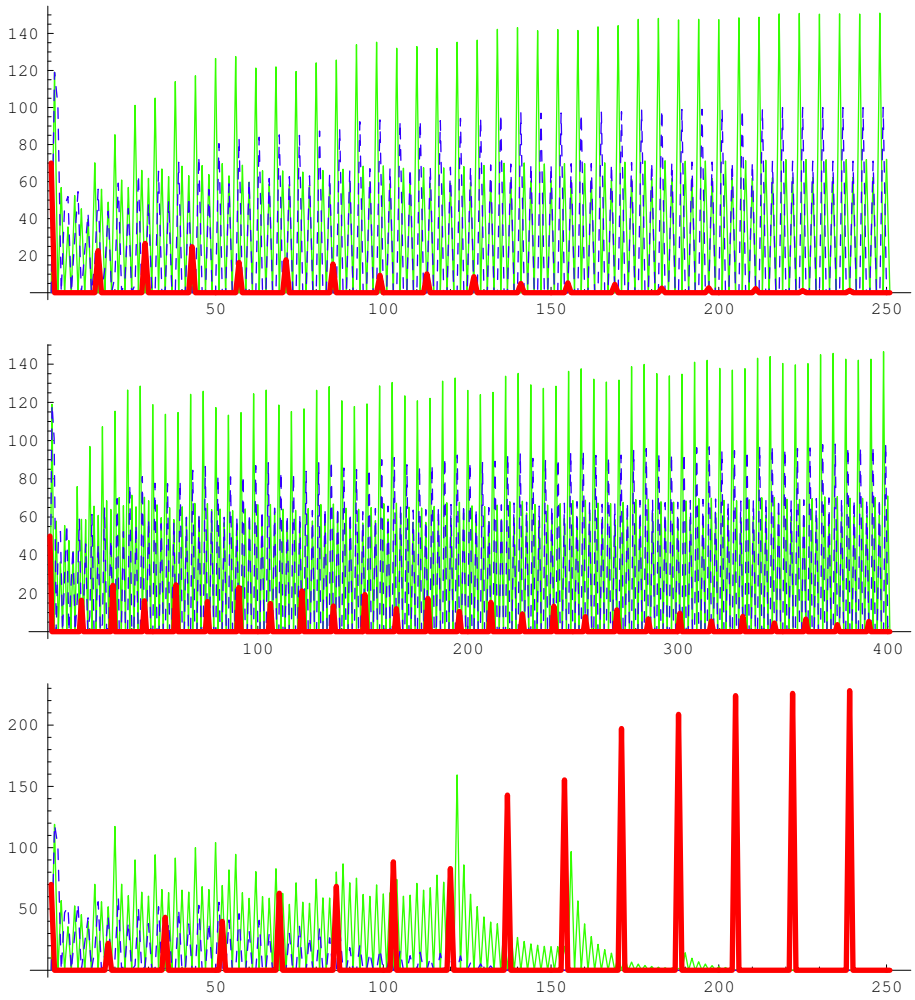

Figure 6.9: Dynamics of the recursion (6.17),(6.11) for $k = 14, 15, 17$ respectively. The thick line corresponds to the k-ennials, the thin line to the biennials, the dashed line to the triennials. One can see that only 17-ennials species survive.

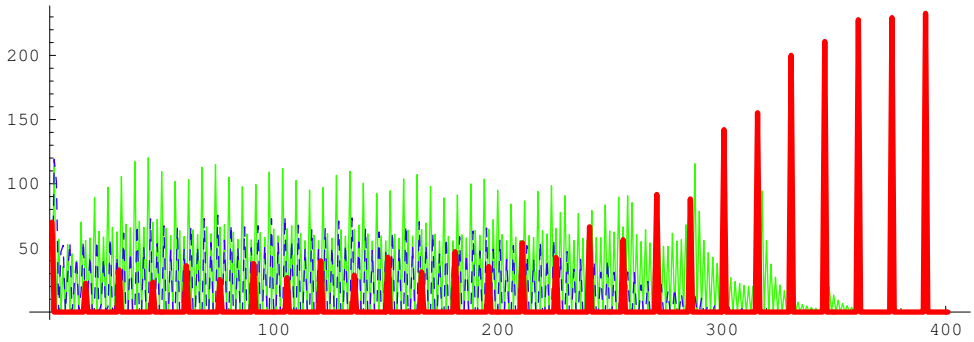

Figure 6.10: Dynamics of the recursion (6.17) for $k = 15$. Initial conditions are in the form (6.11) with $N0 >> 10$. We see that k-ennials outcompete the other two species.

with any k survive (Fig. 6.10). In other words, the dynamics exhibits bistability. It can be interpreted as follows. Non-prime periodic species can not invade a population consisting of biennials and triennials. And, vice versa, biennials and triennials can not invade a population of k-ennials. Notice that we have these conclusions only in the case of out–of–phase synchronization. If k-ennials are in phase with bi- or triennials, they outcompete the short–living species.

6.6 Discussion.

We conclude this chapter by summarizing the result: *competition of long–living species with biennials and triennials can result in exclusion of non-prime periods.* We have shown actually two possible mechanisms. In Section 6.2 we have illustrated, by means of a very simple model, how nursery competition can lead to exclusion of non-primes. We needed in–phase–synchronization for that. In Section 6.5 we obtained a similar result but as a consequence of competition of the youngest age class of k-ennials with older age classes of biennials and triennials. In this case we need out–of–phase–synchronization to obtain the desired behaviour.

It is not necessary to have biennials and triennials as residents to obtain two- and three-periodic environment. It is even improbable that a 13- or 17-years mutant can appear from biennials and triennials. However cicadas with longer life cycle can exhibit two-/three-periodic dynamics also. In particular, simulations of the model (6.6) show that cicadas with even periods can have two-periodic dynamics with no reproduction each second year. This is a kind of dynamics which is in between of coexistence of all age classes and Single

Year Class dynamics. This remark is important because biennial cicadas do not exist, but there are cicadas with period 4 which could exhibit two-periodic dynamics (with a half of year classes missing) during the Ice Ages. There is also a biological reason why two-/three-periodic dynamics could be rather common between cicadas. We have mentioned already that cicadas live on two levels of underground: grass and tree roots. They spend $2-3$ years on grass roots where the competition is much more severe than on tree roots. We have simulated these situation, we do not discuss it in detail here, however we conclude that this type of competition stimulates two-/three-periodic dynamics of long–living species whose periods are multiples of two and three respectively.

We did not perform an analysis of the recursion (6.17). However, we saw in many simulations that the dynamics of this model is very rich. Depending on parameters and initial conditions we can have different types of resonance: either only prime periodic species survive or even periodic ones or species with multiple of three periods. It depends on impacts of age classes on the environmental variable.

It was not our task here, but one needs to estimate the parameters of the model from biological data to (dis)prove that the competition for accommodation is a possible mechanism of prime numbers occurence. There can be, of course, other mechanisms. We think that hybridization [Cox & Carlton] is a good reason for the prime numbers effect. We have already tried to implement this mechanism, and simulations showed that it can lead to the desired behaviour.

It can be very interesting to implement two (or more) levels of underground into the model and also larval competition at the level of grass roots (i.e., assume that not only the youngest age class is sensitive to competition). Since cicada spend $2-3$ years on grass roots, this can lead to some extra resonances with biennials and triennials and, probably, the parameter region, for which prime periodic species survive, would enlarge.

Environmental and demographic stochasticity can be also included in the model. We think that it is important because this stimulates Single Year Class dynamics. Also the robustness of results can be checked in this way. Environmental stochasticity played, probably, a major role during Ice Ages, that can result in extinction of short–living species and prolongation of cicada periods.

And it is unreasonable to forget predator–prey interactions completely, the effect of predators on cicada dynamics should be also investigated.

We conclude by saying that modelling of competition between age-structured semelparous species promises to be a rich and exciting research field.

Bibliography

[Behncke] Behncke, H.: Periodical cicadas. J. Math. Biol., **40**, 413–431 (2000)

[Bergh] Bergh, M. O., Getz, W. M.: Stability of discrete age-structured and aggregated delay-difference population models.: J. Math. Biol., **26,** 551-581 (1988)

[Blokh & Lyubich] Blokh, A. M., Lyubich, M. Yu.: Measurable dynamics of S-unimodal maps of the interval. Ann. Scuola Norm. Sup. Pisa Cl. Sci. 4, **24**, 545–573 (1991)

[Branner] Branner, B.: Iterations by Odd Functions with Two Extrema. J. Math. Anal. Appl., **105**, 276–295 (1985)

[Broer et al.] Broer, H., Simó C., Tatjer J. C.: Towards global models near homoclinic tangencies of dissipative diffeomorphisms. Nonlinearity, **11**, 667-770 (1998)

[Bulmer] Bulmer, M. G.:Periodical Insects. The American Naturalist, **111**, 1099–1117 (1977)

[Carcassès] Carcassès, J.-P.: Determination of different configurations of fold and flip bifurcation curves of a one- or two-dimensional map. Internat. J. Bifur. Chaos Appl. Sci. Engrg. **3**, no. 4, 869–902 (1993)

[Caswell] Caswell, H.: Matrix Population Models. Second Edition. Sinauer Associates, Inc. Publishers, Sunderland, Massachusetts 2001

[Chossat & Golubitsky] Chossat, P., Golubitsky, M.: Symmetry-increasing bifurcation of chaotic attractors. Phys. D **32**, no. 3, 423–436 (1988)

[Cox & Carlton] Cox, R.T., Carlton, C.E.: A commentary on prime numbers and life cycles of periodical cicadas. American Naturalist, **152**, N 1, 162–164

[Cushing] Cushing, J. M.: Cycle chains and the LPA model. J.Difference Equations and Applications, **9(7),** 655–670 (2003)

[Cushing & Li] Cushing, J. M., Li, J.: Intra-specific competition and density dependent juvenile growth. Bulletin of Mathematical Biology, **54,** 503–519 (1992)

[Davis] Davis, P. J.: Circulant matrices. New York: Wiley. 1979

[Davydova] Davydova N. V.: Dynamics and bifurcations in families of single year class maps. Under revision for SIAM J. Appl. Dyn. Sys.

[DDvG1] Davydova, N. V., Diekmann, O., Gils, S. A. van: Year Class Coexistence or Competitive Exclusion for Strict Biennials? J. Math. Biol., **46**, 95–131 (2003)

[DDvG2] Davydova, N. V., Diekmann, O., Gils, S. A. van: On circulant populations. I. The algebra of semelparity. Submitted to J. Lin. Alg. Appl.

[Devaney] Devaney, R. L.: An Introduction to Chaotic Dynamical Systems. Second Edition. Addison-Wesley Publishing Company 1989

[Diekmann & van Gils] Diekmann, O., Gils, S. A. van: Difference Equations with Delay. Japan J. Indust. Appl. Math., **17**, 73–84 (2000)

[DGHKMT] Diekmann, O., Gyllenberg, M., Huang, H., Kirkilionis, M., Metz, J. A. J., Thieme, H. R.: On the Formulation and Analysis of General Deterministic Structured Population Models. II. Nonlinear Theory. J. Math. Biol, **43,** 157–189, (2001)

[DGM] Diekmann, O., Gyllenberg, M., Metz, J.A.J.: Steady state analysis of structured population models. Theor.Pop.Biol., **63,** 309–338 (2003)

[DMD] Diekmann, O., Mylius, S. D., Donkelaar, J. R. ten: Saumon á la Kaitala et Getz, sauce hollandaise. Evol. Ecol. Res., **1,** 261–275 (1999)

[Ebenman 87] Ebenman, B. Niche Differences Between Age Classes and Intraspecific Competition in Age–structured Population. J. theor. Biol., **124,** 25–33 (1987)

[Ebenmann 88] Ebenman, B. Competition Between Age Classes and Population Dynamics. J. theor. Biol., **131,** 389-400 (1988)

[Edelstein-Keshet] Edelstein-Keshet, L.: Mathematical Models in Biology. Random House, New York, 1988.

[El-Hamouly et.al.] El-Hamouly, H.M., El-Khouly, E.M., Allam, R.M.: On some bifurcation structures of a two-dimensional diffeomorphism. J.Math.An.Appl., **195**, 1–15 (1995)

[Heliövaara et al.] Heliövaara, K., Väisänen, R., Simon, C.: Evolutionary ecology of periodical insects. Tree, **9**, 475–480 (1994)

[Hofbauer & Sigmund] Hofbauer, J., Sigmund, K.: *Evolutionary Games and Population Dynamics.* Cambridge University Press (1998)

[Hoppensteadt & Keller] Hoppensteadt, F. C., Keller, J. B.: Synchronization of periodical cicada emergences. Science, **194,** 335–337 (1976)

[Jacobson] Jacobson, M.: Absolutely continuous invariant measure for one-parameter families of one-dimensional maps. Comm. Math. Phys., **81,** 39–88 (1981)

[Jury] Jury, E.I.: Theory and application of the z–transform method. Wiley, 1964

[Kuznetsov & Levitin] Kuznetsov, Yu.A., Levitin, V.V.: CONTENT: A multiplatform environment for analyzing dynamical systems. Dynamical Systems Laboratory, CWI, Amsterdam. `ftp://ftp.cwi.nl/pub/CONTENT` 1997

[Kuznetsov] Kuznetsov, Yu. A.: Elements of Applied Bifurcation Theory. Second Edition. Springer-Verlag 1998

[Lewis] Lewis, E.R. Network Models in Population Biology. Springer-Verlag, Berlin, Heidelberg, New York, 1977.

[Markus & Goles] Markus, M., Goles, E.: Cicadas showing up after a prime number of years. The Mathematical Intelligencer, **24,** N 2, 30–32 (2002)

[May] May, R.M.: Stability and Complexity in Model Ecosystems. Princeton Univ. Press, Princeton and Oxford, 2001.

[May & Oster] May, R. M., Oster, G.F.: Bifurcations and dynamical complexity in simple ecological models. Am. Nat., **110,** 573–599 (1976)

[De Melo & van Strien] Melo, W. de and Strien, S. van.: One-Dimensional Dynamics. Springer-Verlag 1993.

[Milnor] Milnor, J.: On the concept of attractor. Comm. Math. Phys., **99,** 177–195 (1985)

[Mira] Mira, C.; Carcassès, J.-P.: On the "crossroad area–saddle area" and "crossroad area–spring area" transitions. Internat. J. Bifur. Chaos Appl. Sci. Engrg. **1,** no. 3, 641–655 (1991)

[Mjølhus et al.] Mjølhus, E., Wikan, A., Solberg, T. On synchronization in semelparous populations. To appear in to J. Math. Biol.

[Murray] Murray, J. D.: *Mathematical Biology.* Springer-Verlag (1989)

[Mylius & Diekmann] Mylius, S. D., Diekmann, O.: The resident strikes back: invader-induced switching of resident attractor. J. Theor. Biol., **211**, 297–311 (2001)

[Nisbet & Onyiah] Nisbet, R. M., Onyiah, L. C.: Population dynamics consequences of competition within and between age classes. J. Math. Biol., **32,** 329–344 (1994)

[Nusse & Yorke: Dynamics] Nusse, H. E., Yorke, J. A.: Dynamics: Numerical Exploration. Second Edition. Springer-Verlag 1994.

[Nusse & Yorke] Nusse, H. E., Yorke, J. A.: Period halving for $x[n+1] = MF(x[n])$, where F has negative Schwarzian derivative. Physics Lett., **127A,** 328–334 (1988)

[Roeger] Roeger, L.-I.W.: Discrete May-Leonard competition models III. Submitted to J. Difference Eqs. Appl.

[de Roos et al.] Roos, A. M. de, Metz, J. A. J., Evers, E., Leipoldt, A.: A size dependent predator-prey interaction: who pursues whom? J. Math. Biol., **28,** 609–643 (1990)

[Seneta] Seneta, E.: Non-negative matrices : an introduction to theory and applications. Allen and Unwin, London, 1973.

[Silva & Hallam] Silva, J.A.L., Hallam, T. G.: Effects of delay, truncations and density dependence in reproduction schedule on stability of nonlinear Leslie matrix models. J. Math. Biol., **31,** 367–395 (1993)

[Singer] Singer, D.: Stable orbits and bifurcations of maps on the interval. SIAM J. Appl. Math., **35,** 260–267 (1978)

[Skjolding et al.] Skjolding, H., Branner-Jørgensen, B., Christiansen, P. L. and Jensen, H. E.: Bifurcations in discrete dynamical systems with cubic maps. SIAM J. Appl. Math., **43**, No. 3, 520–534 (1983)

[Solberg] Solberg, T. S.: Rare Phenomena in an Age-Structured Population Model. Master Thesis, University of Tromsø, (1998)

[Thunberg] Thunberg, H.: Periodicity versus Chaos in One-Dimensional Dynamics. SIAM Review, **43,** 3–30 (2001)

[Wang & Jiang] Wang, Y., Jiang, J.: The general properties of discrete-time competitive dynamical systems. J. Diff. Eqs., **176,** 470–493 (2001)

[Webb] Webb, G.F.: The prime number periodical cicada problem. Discrete Cont. Dyn. Sys – Ser. B, **1,** N 3, 387-399 (2001)

[Wikan] Wikan, A.: Dynamic Consequences of Reproductive Delay in Leslie Matrix Models with Nonlinear Survival Probabilities. Math. Biosciences, **146,** 37–62 (1997)

[WM96] Wikan, A., Mjølhus, E.: Overcompensatory recruitment and generation delay in discrete age-structured population models. J. Math. Biol, **35,** 195–239 (1996)

[WM95] Wikan, A., Mjølhus, E.: Periodicity of 4 in Age-structured Population Models with Density Dependence. J. theor. Biol, **173,** 109–119 (1995)

[Yoshimura] Yoshimura, J. The evolutionary origins of periodical cicadas during ice ages. American Naturalist, **149**, 112–124 (1997)

Samenvatting

Dit proefschrift gaat over soorten waarvan de individuen zich slechts eenmaal in hun leven voortplanten en daarna sterven. Voorbeelden van zulke soorten zijn éénjarige en tweejarige planten, vissen (zalm) en veel soorten insekten.

Als voortplanting slechts plaatsvindt gedurende een korte periode per jaar en de levensduur voor elk individu gelijk is, zeg k jaar, dan kan de populatie worden onderverdeeld in jaarklassen, i.e., groepen individuen met hetzelfde geboortejaar (modulo k), of equivalent, in groepen van individuen die in hetzelfde jaar geslachtsrijp zullen zijn (ook modulo k gerekend). Let op de terminologie: een individu behoort tot dezelfde jaarklasse gedurende zijn gehele leven, terwijl de leeftijdsklasse waartoe een individu behoort, bepaald wordt door de leeftijd van het individu en daarom elk jaar met 1 zal toenemen. Aangezien een jaarklasse wat betreft voortplanting geïsoleerd is van de andere jaarklassen, kan iedere jaarklasse zelf ook als zelfstandige populatie gezien worden.

Echter, jaarklassen zullen elkaar beïnvloeden, bijvoorbeeld via competitie om voedsel. Het kan voorkomen dat een bepaalde jaarklasse daardoor uit zal sterven. Bulmer noemt een insekt periodiek als slechts 1 van de jaarklassen voorkomt (en de andere $k-1$ jaarklassen ontbreken). Beroemd voorbeelden hiervan zijn de dertien- en zeventienjaarscicaden. Het fenomeen van periodieke insekten leidt tot de volgende vraag: Kan een jaarklasse de omgeving zo beïnvloeden dat andere kleine jaarklassen zullen uitsterven? Of kan een ontbrekende jaarklasse succesvol invaderen? Ontstaat er coëxistentie of juist non-coëxistentie als gevolg van de competitie?

We zullen de dichtheidsafhankelijke interactie beschrijven door terugkoppeling via de omgeving. We nemen aan dat als de omgeving gegeven is, alle individuen onafhankelijk van elkaar zijn. Deze onafhakelijkheid geldt ook voor de invloed van individuen op de omgeving. We nemen aan dat de omgeving 1-dimensionaal is, (competitie voor slechts 1 hulpbron) en we geven de omgeving weer met I. I is dan de som van de invloed van alle individuen. Als alle individuen binnen een leeftijdsgroep identiek zijn, en een invloed c_i hebben, dan kunnen we I schrijven als:

$$I = \sum_{i=0}^{k-1} c_i N_i = c \cdot N, \tag{1}$$

waarin N_i het aantal individuen in de i^{de} leeftijdsklasse aangeeft, $N = (N_0, \ldots, N_{k-1})^T$ de corresponderende vector is en $c = (c_0, \ldots, c_{k-1})$ de invloedvector is.

Als de leeftijdsklasse i in jaar t uit $N_i(t)$ individuen bestaat, geldt dat:

$$N_{i+1}(t+1) = N_i(t)h_i\left(I(t)\right), \quad i = 0, \ldots, k-2, \tag{2}$$

waarin h_i de overlevingskans is van leeftijd i naar $i+1$. Voor het aantal nieuwgeboren individuen geldt:

$$N_0(t+1) = N_{k-1}(t)h_{k-1}\left(I(t)\right), \tag{3}$$

met h_{k-1} het verwachte aantal nakomelingen voor een individu dat $k-1$ jaar oud is. Aangezien zowel de overlevingskansen als het verwachte aantal nakomelingen af kunnen hangen van de omgeving I, noemen we $h_i(I)$ de sensitiviteit voor de omgeving.

We kunnen de vergelijkingen (2) en (3) compacter herschrijven als

$$N(t+1) = L\left(h\left(I(t)\right)\right)N(t) \tag{4}$$

met behulp van de vectoren $N = (N_0, \ldots, N_{k-1})^T$ en $h = (h_0, \ldots, h_{k-1})^T$. Met $L(h)$ noteren we de Lesliematrix die correspondeert met h:

$$L(h) = \begin{pmatrix} 0 & 0 & \ldots & 0 & h_{k-1} \\ h_0 & 0 & \ldots & 0 & 0 \\ 0 & h_1 & \ldots & 0 & 0 \\ \ldots & & & & \\ 0 & 0 & \ldots & h_{k-2} & 0 \end{pmatrix} \tag{5}$$

Het belangrijkste doel van deze studie is de recursierelatie (4) beter te begrijpen. Het model voor algemene k wordt in hoofdstuk 2 bestudeerd, terwijl in hoofdstuk 3 en 4 de speciale gevallen voor tweejarige ($k = 2$) en driejarige soorten ($k = 3$) beschouwd worden.

De recursierelatie (4) heeft een cyclische symmetrie, i.e., de relatie is invariant onder een cyclische permutatie van de indices van de drie vectoren N, c en h. Een populatie die deze eigenschap heeft noemen we een circulerende populatie. Door de symmetrie komt er een speciaal soort bifurcaties voor, de zogenaamde verticale bifurcatie, waarbij een variëteit ontstaat, gevuld met periodieke banen van een bepaalde periode, voor specifieke parameterwaardes. Verticale bifurcaties spelen een essentiële rol in de dynamica van (4): wij beweren dat verticale bifurcaties als overgang fungeren tussen coëxistentie en non-coëxistentie. Voor $k = 2$ wordt dit formeel bewezen in Paragraaf 3.10.

Er bestaan twee soorten verticale bifurcaties. Het eerste type correspondeert met een singulariteit van een cyclische matrix gevormd uit de invloeden c_i. Alle mogelijke combinaties van invloeden die tot een verticale bifurcatie leiden zijn in kaart gebracht. Bij deze bifurcatie ontstaat een affiene

deelverzameling (of zelfs een lijn of vlak) gevuld met periodieke banen. Bij het tweede type verticale bifurcatie is een niet-lineair cyclisch systeem van de sensitiviteitsfuncties $h_i(I)$ gedegenereerd.

Het model (4) heeft een uniek evenwicht waarin alle jaarklassen voorkomen. In Paragraaf 2.8 leiden we een karakteristieke vergelijking af die behoort bij dit coëxistentie-evenwicht. Hoewel de karakteristieke vergelijking een mooie vorm heeft, kan men er geen stabiliteitscriteria uit destilleren voor algemene k. Voor tweejarige soorten, $k = 2$, en driejarige soorten, $k = 3$, is dit wel mogelijk en dit wordt in respectievelijk Paragraaf 3.3 en Paragraaf 4.3 gedaan.

De dynamica die correspondeert met de situatie dat er slechts één jaarklasse aanwezig is, zoals bij de eerder genoemde cicaden, en alle individuen dus even oud zijn, noteren we met de Engelse term "Single Year Class"-dynamica (SYC-dynamica). SYC-punten zijn evenwichten van de levenscyclusafbeelding, de k^{de} iteratie van de oorspronkelijke afbeelding, die op een van de assen in de faseruimte liggen. In Paragraaf 2.9 onderzoeken we of de SYC-punten stabiel zijn met betrekking tot invasie van ontbrekende jaarklassen. Deze stabiliteit noemen we transversale stabiliteit. We vinden het volgende resultaat: Als de sensitiviteit toeneemt met de leeftijd, terwijl de invloed op de omgeving juist afneemt met de leeftijd, dan zijn de SYC-punten transversaal stabiel.

In hoofdstuk 5 onderzoeken we de interne (in)stabiliteit van de SYC-punten. Een SYC-punt is een vast punt van de SYC-afbeelding, die een samenstelling is van de functies $x \mapsto xh_i(x)$. Hoofdstuk 5 is voor een groot deel gewijd aan het geval $k = 2$ en een dichtheidsafhankelijkheid van het Ricker-type, i.e., $h_i(I) = e^{-g_i I}$. We hebben een uitgebreide bifurcatie analyse uitgevoerd en verscheidene bifurcatiediagrammen geconstrueerd. We hebben het basis reproductiegetal R_0 als een van de bifurcatieparameters gekozen. Voor grote R_0 wordt de dynamica instabiel. Ook valt op dat door een leeftijdsstructuur in te voeren in het populatiemodel, de dynamica stabieler kan worden vergeleken met het corresponderende niet-gestructureerde model. Merk op dat een stabiel SYC-punt correspondeert met een periodieke baan van periode k waarin maar één jaarklasse aanwezig is; de populatie is dus niet constant maar vertoont cyclisch gedrag. We beschouwen dit gedrag echter als "stabiel" vergeleken met het onregelmatige gedrag van periodieke banen met een grote periode en chaotische attractoren die in het niet-gestructureerde model voorkomen voor grote R_0.

Hoofdstuk 3 is gewijd aan tweejarige soorten, i.e., $k = 2$. Uit de lokale bifurcatie-analyse van het evenwicht met coëxistentie blijken er twee soorten bifurcaties op te treden: een periode-verdubbellende en een Neimark-Sacker bifurcatie (een Hopf-bifurcatie voor afbeeldingen). De Neimark-Sacker bifur-

catie treedt alleen op voor vrij grote waardes voor R_0. Voor nog grotere waarden kan het evenwicht met coëxistentie niet meer stabiel zijn. De periode-verdubbelende bifurcatie kan voor alle waarden van R_0 optreden. Deze bifurcatie is gedegenereerd, het is namelijk de hierboven genoemde verticale bifurcatie. Deze bifurcatie kan in twee gevallen optreden: ofwel de invloed of de gevoeligheid van beide jaarklassen is gelijk. Als aan een van deze twee gevallen voldaan is, zien we een kromme (of zelfs een lijn) in de faseruimte die gevuld is met periodieke banen (van periode 2). Voor andere waarden van de parameters, als de verhouding $\frac{h_0}{h_1}(I)$ monotoon is, is er geen baan met periode 2 in het inwendige van de faseruimte. Elke baan van periode 2 ligt dus op een van de assen en correspondeert met de situatie dat slechts een jaarklasse aanwezig is.

We bewijzen deze strikte tweedeling (Stelling 3.17) voor vrij kleine waarden van R_0: Of het evenwicht met coëxistentie is stabiel en de SYC-baan is transversaal instabiel of precies andersom. Biologisch geldt dus (Stelling 3.18 en de bijbehorende corollaria) dat door competitie tussen de twee jaarklassen, er slechts één blijft bestaan als de sensitiviteit voor de omgeving toeneemt met de leeftijd terwijl de invloed op de omgeving juist afneemt met de leeftijd, of omgekeerd als de sensitiviteit afneemt en de invloed juist toeneemt met de leeftijd.

Aan de hand van een voorbeeld laten we zien dat als de verhouding $\frac{h_0}{h_1}(I)$ niet monotoon is, er een algemene periode-verdubbelende bifurcatie op kan treden en dat er een cyclisch gedrag met periode 2 op kan treden waarbij beide jaarklassen voorkomen. De overgang van coëxistentie naar non-coëxistentie is dus niet plotseling, maar via steeds groeëinde fluctuaties.

In Hoofdstuk 4 kijken we naar het geval $k = 3$. Een lokale stabiliteitsanalyse van het coëxistentie-evenwicht laat zien dat er weer een periode-verdubbeldende bifurcatie en een Neimark-Sacker bifurcatie optreden. De rollen zijn echter omgedraaid. De Neimark-Sacker bifurcatie treedt op voor alle waarden van R_0 terwijl de periode-verdubbeldende bifurcatie op kan treden voor grotere waarden van R_0. Beide bifurcaties zijn generiek, maar er is een speciaal geval van de Neimark-Sacker bifurcatie als de bifurcatie verticaal wordt. Deze verticale bifurcatie correspondeert weer met de situaties dat de invloed of de sensitiviteit gelijk is voor elke jaarklasse. De verticale bifurcatie is voor het geval $k = 3$ echter minder belangrijk dan voor het geval $k = 2$ omdat de bifurcatie codimensie 2 heeft. Er is een andere, algemenere, route van coëxistentie naar non-coëxistentie die gevonden kan worden in het bifurcatiediagram (Fig 4.7). Ook beschrijven we een gedrag voor $k = 3$, dat niet kan optreden voor $k = 2$. Dit gedrag wordt gekenmerkt door een heterocliene baan die als attractor optreedt voor een groot interval van parameterwaarden. Dit gedrag kan gezien worden als dynamica waarin het feit

welke jaarklasse dominant is, plotseling kan veranderen.

Het laatste hoofdstuk, Hoofdstuk 6, gaat over magicicaden. Deze insekten zijn vooral bekend om hun zeldzame, plotselinge verschijning in grote aantallen. Wat helemaal bijzonder is, is dat deze verschijningen slechts eens per dertien of zeventien jaar optreden. Hoewel deze grote priemgetallen zeer opvallend zijn, is er nog geen goede verklaring voor dit gedrag. In Hoofdstuk 6 proberen we het optreden van priemgetallen als periode te modelleren. De enige verklaring die tot nu toe gegeven is voor deze priemgetallen is dat de cicaden niet in resonantie "willen" zijn met een periodieke parasiet of predator met een twee- of driejarige cyclus. Echter, er is geen geschikte kandidaat voor zo'n parasiet of predator. Daarom opperen wij de mogelijkheid dat cicaden met een veel kortere levensduur optreden als "periodieke parasiet". Met andere woorden, door de competitie met periodieke cicaden met een korte periode, kunnen alleen die mutanten invaderen, die een priemgetal als periode hebben.

Acknowledgments

Without any doubts the first person I want to thank is my supervisor Odo Diekmann. Dear Odo, thank you for your friendly and frank manner and for your open mind. I want to repeat what your other PhD students say: we were lucky to have had you as a supervisor. It was a pleasure to meet such an original mind. In particular, I would like to mention your style of thinking and writing: the exactness of formulation and the responsibility for each word said.

I want to thank our third coauthor Stephan van Gils for the fresh look at our work, discovery of unexpected aspects of problems which Odo and I missed and also for the kindly and refined atmosphere he creates around him.

I thank the reading committee for valuable suggestions and comments: André de Roos (André, thank you for the last chapter!), Yuri Kuznetsov, Frits Beukers, Jim Cushing and Faina Berezovskaya.

I want to thank Faina Berezovskaya also as my former supervisor, for her enthusiasm and energy in discussions, for her sincere interest in me and my work, and for her very personal and even a little romantical approach to scientific problems, which stimulated my interest.

I thank Martin Bootsma for an accurate translation of the summary in Dutch. I thank Philip Getto and Yunxin Huang for being my roommates. I thank other AiO fellows and postdocs from Utrecht University for creating a nice atmosphere there: Hil, Taoufik, Barbara, Theo, Bob, Martijn, Michiel, Liesbeth, Arno, Jasper, Yaroslav, Timothy, Steven, Erik, Fieke, Igor, Behrooz, Jordan; all professors and docents in Utrecht with whom I was lucky to work and communicate: Roelof Bruggeman, Yuri Kuznetsov, Frits Beukers, Ferdinand Verhulst, Hans Duistermaat, Jan Stienstra, Andreas Kyprianou, Eduard Belitser, Alexander Gnedin, Thijs Ruijgrok; computer, library and administration staff: Frank van de Wiel, André de Meijer, Toos Raats, Olga Lozovskaia, Ria Bekkering, Martijn Dekker, Els de Vries, Jean Arthur, Patty Grondman, Marian Brands and many-many others (excuse me if I haven't mentioned you personally).

I thank all my colleagues from Leiden, Amsterdam and abroad for stimulating discussions and a lively scientific atmosphere: Hans Metz, André de Roos, Stephan Geritz, Geza Meszena, Mats Gyllenberg, Jozef Hofbauer, Dmitry Logofet, Sergei Petrovski, Bob Kooi, Arild Wikan, Einar Mjølhus, Horst Behncke, Frank Hoppensteadt, Ulf Dieckmann, Paulien Hogeweg, Alexander Panfilov, Silvia Cuadrado, Kalle Parvinen, Claus Rueffler, Tom van Dooren, Helena Nusse, Bob Planqué, Geertje Hek, Guido Terra, Fabio Dercole, Natalia Sapoukhina and others.

I am happy to have a chance to thank my husband Dmitri both for the direct help with preparation of the thesis and drawing funny fishes on the cover and for his love and support.

I thank my daughter Nadja for providing a nice and refreshing contrast to my research.

I thank my mother Nina, my father Victor and my grandmothers Katja and Lida for making me the person I am at the moment and am happy to remain. I thank my other relatives and friends from Russia for their inspiration and support: Vladimir Andreevich, Nikolaj Dmitrievich and Galina Nasyrovna, Sasha Znamenski, Kostya and Luda Shundyak, Ada and Boris Fine, Irina Philipova, Irina and Petr Sobesski, Olga and Valentin Drach.

I thank my school teacher in maths, Vera Nikolaevna Fateeva, for giving me a solid basis for further study and for stimulation of my interest in mathematics. I thank my Alma Mater: Moscow Institute of Physics and Technology, her professors and docents which gave me a deep and diverse knowledge of mathematics, physics and biology, and created, together with my fellow students, a sincere, romantic and devoted atmosphere of a scientific institution.

Curriculum Vitae

I was born in Russia on September, 30, 1975 in a small town Dolgoprudny near Moscow which is known for Moscow Institute of Physics and Technology being situated there. Two interesting memoires from my school years are a couple of books "Funny Mathematics" which I had at home and a mathematical "club" organized by our school teacher of mathematics.

In 1992 I successfully graduated school and entered the Faculty of Physical-Chemical Biology of the above mentioned Moscow Institute of Physics and Technology. That was the moment when I chose to specialize in Applied Mathematics or, more precisely, in Mathematical Biology. In 1995 I chose to specialize further in Mathematical Ecology, probably because it was the most theoretical and least experimental option. With a small group of just a three students we had a nice variety of courses, during one of which I met my first supervisor Faina Semenovna Berezovskaya. I still remember her lecture "Introduction to Bifurcation Theory" when she managed to give an overview of the subject starting from a simple one-dimensional differential equation and finishing by codimension 2 Bogdanov-Takens bifurcation in just two academic hours! At that time Faina Semenovna was busy with the modelling of population dynamics of forest insects. I remember my first phone call to her, she asked: "Where are you more interested in: in insects or in mathematics?" and I answered: "In mathematics."

In 1997-98 I participated in the Master Class "Spatio-Temporal Patterns" organized by Mathematical Research Institute in the Netherlands. One of the organizers was Odo Diekmann who became my supervisor during the Master Class research program and later during my PhD study in Utrecht. Here I want to take a chance to thank organizers of the Master Class: Odo Diekmann and Ronald Meester for giving us a nice opportunity to meet and listen to the lectures of leading researchers of the Netherlands in the field of Applied Mathematics. It is only much later that I understood true value of it. Not an unimportant fact: it was during the Master Class that I chanced to meet my husband-to-be!

In 1998 I returned to Russia for a defense of my Master Thesis and to give birth to my daughter. But in 2000 I came back to the Netherlands for PhD study and now you can see the end product of it in the form of this thesis.

Publications

[1] On circulant populations. I. The algebra of semalparity. (with O. Diekmann and S.A. van Gils) Submitted to J.Lin.Alg.Appl.

[2] Dynamics and bifurcations in families of Single Year Class maps. Under revision for SIAM J.Appl.Dyn.Sys.

[3] Semelparous Species: switching between coexistence and exclusion. In proceedings of 5th ESMTB Conference "Mathematical Modelling and Computing in Biology and Medicine", 2002, Milan, Italy.

[4] Year Class Coexistence or Competitive Exclusion for Strict Biennials? (with O. Diekmann and S.A. van Gils) J.Math.Biol., **46**, 95–131 (2003)

[5] Reconstruction of Sea Surface Temperature from the Oxygen Isotope Composition of Fossil Planktic Foraminifera. (with J.B. van den Berg, B. van der Fliert, F. Peeters, B. Planque, H. van der Ploeg, G. Terra). In proceedings of Study Group "Mathematics with Industry", 2002, Amsterdam, the Netherlands, 91–120

[6] Migration waves and spacial dynamics of insects-phytofagae (with F.S. Berezovskaya, A.S. Isaev, G.P. Karev, R.G. Khlebopros) Siberian ecological journal, **4**, 1999. In Russian.

[7] Effects of migration in spatial dynamics of forest insects. (with F.S. Berezovskaya, G.P. Karev, R.G. Khlebopros.) In proceedings of the 3-d International conference: "Mathematics, computer, education". Dubna, Russia, 1996.

Figures on the back cover

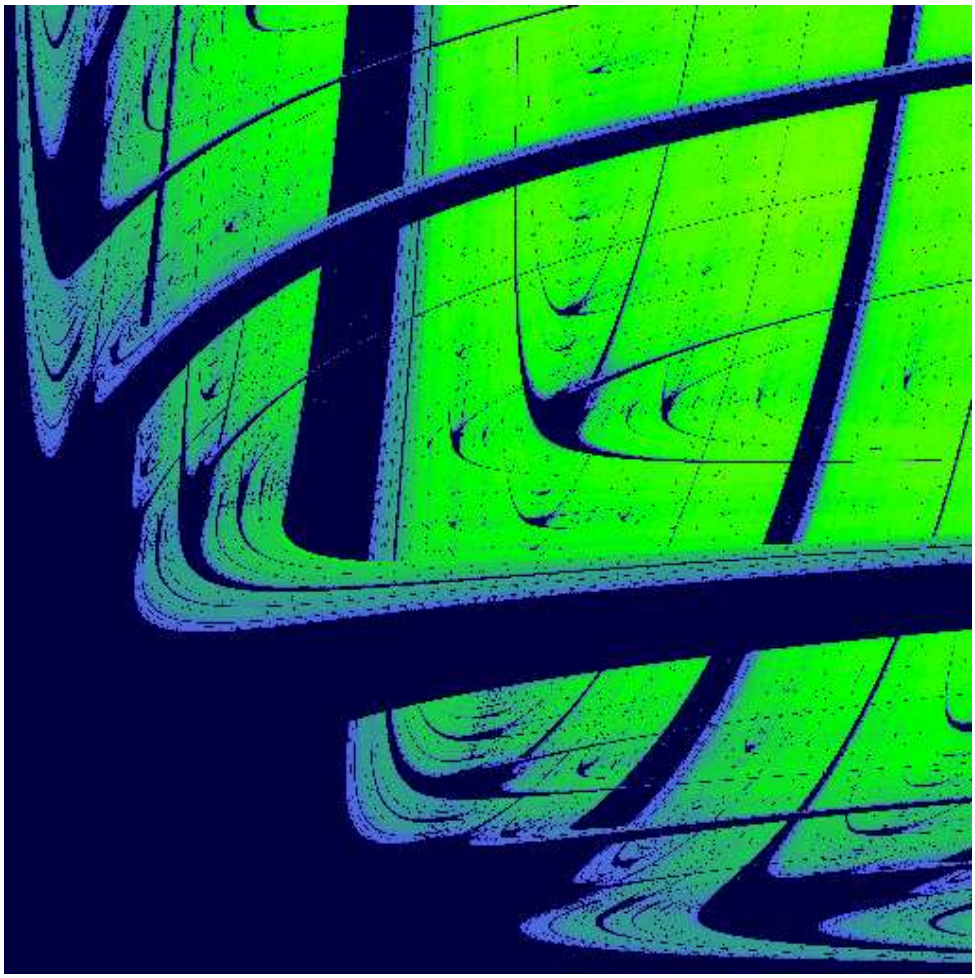

Figure 2. A chaos plot of 2-Ricker-map (5.22) in the parameter plane $(\frac{R_0}{p}, p)$. Black regions corresponds to periodic behaviour, gray regions to chaotic, moreover the larger the Lyapunov exponent the lighter the color of a point. The plot is made with the aid of the package DYNAMICS [Nusse & Yorke: Dynamics].

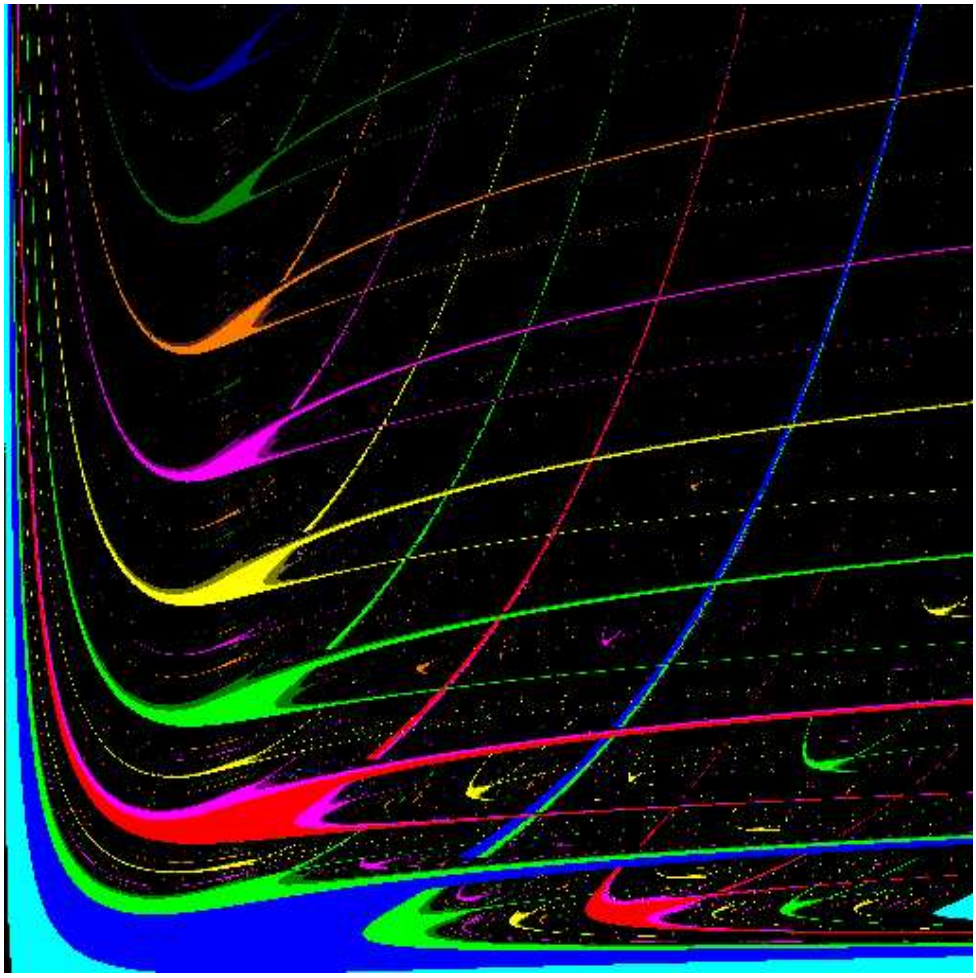

Figure 3. A numerical bifurcation diagram of the 2-Ricker-map (5.22), a period plot, on which windows are shown in which the map has a stable orbit of successive periods $2, 3, 4, 5, \ldots$. The horizontal interval is $p_0 \in [0, 12]$, the vertical interval is $p_1 \in [10, 150]$. Different colours correspond to different periods of attractors: cyan — fixed point (period 1), blue — period 2, red — 3, green — 4, yellow — 5, rose — 6, orange — 7, dark green — 8, dark blue — 9. Black regions are regions with other behaviour, e.g. higher periods, chaos. The bifurcation diagram is produced by using the package DYNAMICS [Nusse & Yorke: Dynamics].

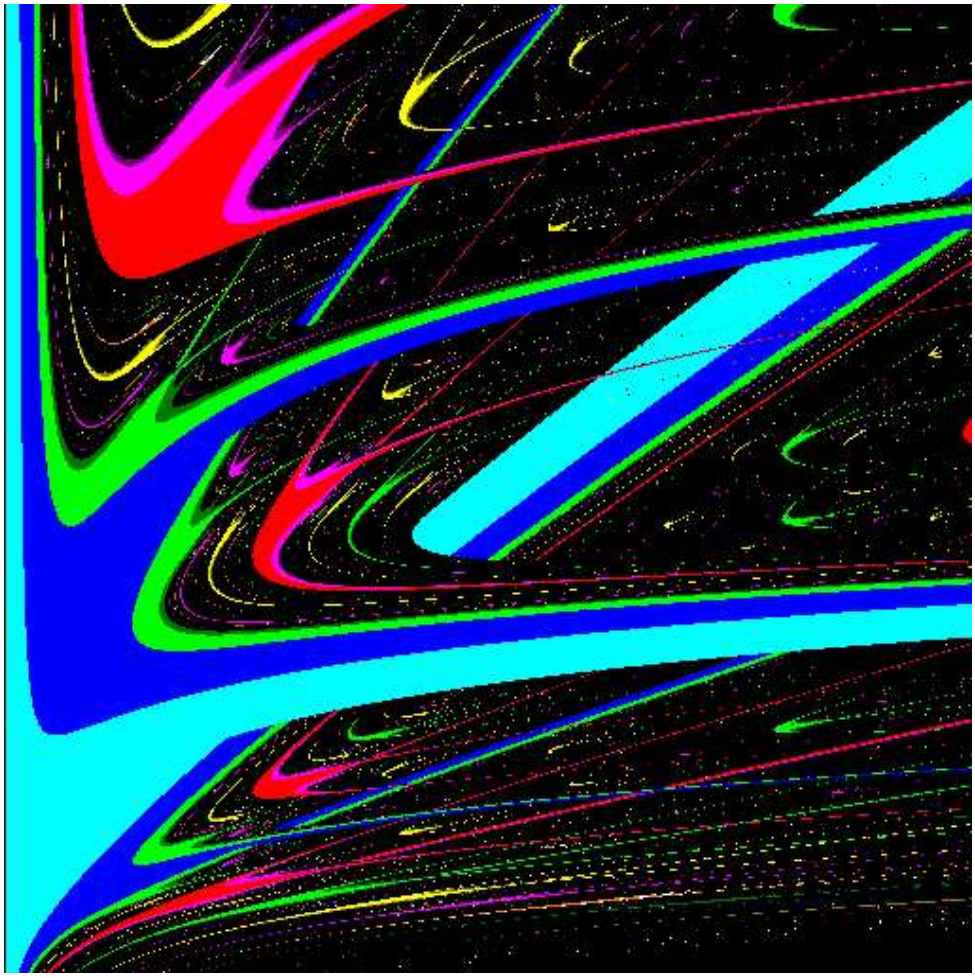

Figure 1. A numerical bifurcation diagram of the 2-Ricker-map (5.22), a so-called period plot. The horizontal interval is $R_0 \in [0, 500]$, the vertical interval is $p \in [0, 40]$. Different colours correspond to different periods of attractors: cyan — fixed point (period 1), blue — period 2, red — 3, green — 4, yellow — 5, rose — 6, orange — 7, dark green — 8. Black regions are regions with other behaviour, e.g. higher periods, chaos. The bifurcation diagram is produced by using the package DYNAMICS [Nusse & Yorke: Dynamics].